Twenty-five-year Trends in the Benthic Community and Sediment Quality of Tampa Bay 1993 - 2017

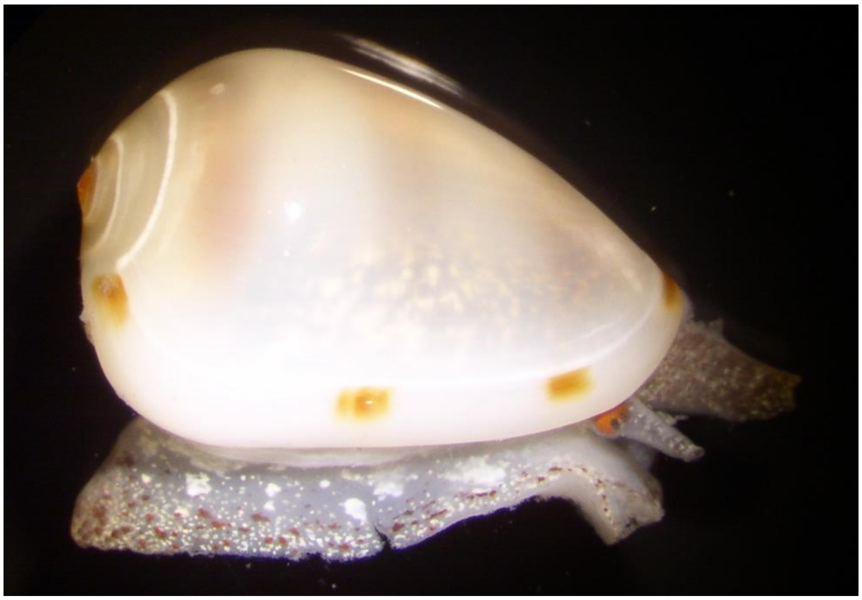

David J. Karlen, Ph.D., Thomas Dix, Ph.D., Barbara K. Goetting, Sara E. Markham, Kevin Campbell, Joette Jernigan, Julie Christian, Kirsti Martinez, Anthony Chacour

Environmental Protection Commission of Hillsborough County

Tampa Bay Benthic Monitoring Program
Interpretive Report
Prepared for: Tampa Bay Estuary Program

May 2020

Corresponding author: David J. Karlen, EPC-HC karlen@epchc.org

Executive Summary

The Tampa Bay Benthic Monitoring Program was initiated in 1993 by the Tampa Bay National Estuary Program as part of a basin-wide monitoring effort to provide data to area managers and to track long-term trends in the Tampa Bay ecosystem. The monitoring program is a cooperative effort between Hillsborough, Manatee and Pinellas Counties, with the Environmental Protection Commission of Hillsborough County managing the biological and sediment contaminant sample processing and data analysis. This report covers the first twenty-five years of monitoring data for the program (1993-2017). A total of 1,791 sites were sampled and analyzed for environmental characteristics, sediment chemistry, and benthic community composition.

The median sample depth bay-wide was 2.7 meters (range 0 – 13.3 meters). Bottom salinities ranged from 0 to 36.3 psu with a bay-wide median salinity of 26 psu and over 66% of the sampling sites were within the polyhaline salinity range (18-30 psu). Salinities were variable between years with the lowest salinities occurring in 1995, 2003, 2010 and 2015 and the highest in 2007. Salinities were significantly different between bay segments with the highest salinities being recorded in Boca Ciega Bay and Lower Tampa Bay, and lowest salinities in the Manatee River. Bottom dissolved oxygen was relatively high bay-wide with a median value of 5.22 mg/L and 78% of the sampling locations had values ≥ 4.0 mg/L. Several areas of hypoxia (<2 mg/L) were found, typically in Hillsborough Bay and portions of Old Tampa Bay, with Hillsborough Bay having the greatest occurrence of bottom hypoxia and anoxia.

Medium-grained sandy sediments predominated in all bay segments, and Hillsborough Bay had the highest percentage of muddy and very fine grain sediments. High percent silt+clay measurements also occurred in Boca Ciega Bay and the Manatee River. Median sediment total organic carbon was 0.55% and ranged from 0.1-9.8% bay wide.

Cadmium (Cd) concentrations tended to be high throughout Tampa Bay, with 40% of the samples exceeding the Threshold Effects Level (TEL); 1.6% of the samples were above the Potential Effects Level (PEL) for toxicity. However, the cadmium:aluminum ratio indicated that the observed Cd concentrations were not elevated above background levels in most samples. Chromium, copper, nickel, lead and zinc were also high at a small percentage of sites, with elevated concentrations primarily found in Hillsborough Bay and the Manatee River.

Polycyclic aromatic hydrocarbons (PAHs) concentrations were generally low with no observed PEL exceedances and only 1.58% of the samples exceeding the TEL for total PAHs. Some individual PAH compounds had higher concentrations, with the low molecular weight PAHs acenaphthene and acenaphthylene exceeding their TELs at 3.78% and 5.78% of the sites respectively, and other Low Molecular Weight PAHs exceeding their TELs at between 1 – 2% of the sites. PEL's for acenaphthene, acenaphthylene, phenanthrene and total low molecular weight PAHs were exceeded at <1% of the sites. Total High Molecular Weight PAHs were above the TEL at 3.65% of the sites. Elevated concentrations of Dibenzo (a,h) anthracene were found at over 13% of the sites, with 1.1% exceeding the PEL. All the measured high molecular weight PAHs exceeded their TELs at a minimum of 3% of the sites and had PEL exceedances at 0.3-1.1% of the sites. The highest overall concentrations of PAHs were observed in Hillsborough Bay followed by the Manatee River and Boca Ciega Bay.

Total Polychlorinated Biphenyls (PCBs) exceeded the TEL in 1.70% of the samples, with highest values found in Hillsborough Bay. Most of the measured pesticides had TEL and PEL exceedances at a few sites. Lindane and the DDT derivative, DDE, exceeded their respective TELs in around 2% of samples. Lindane TEL and PEL exceedances occurred at scattered sites throughout the bay, while DDE concentrations were highest in Hillsborough Bay and the Manatee River.

In order to evaluate sediment contaminant levels, a grading system based on the average PEL ratios for the entire suite of measured sediment contaminants that had established sediment quality guidelines (SQG's). The sediment contaminant level for a given sample was assigned a letter grade (A, B, C. D, F) according to its mean Probable Effects Level (PEL) ratio. The PEL ratio grades were based on the overall distribution of PEL ratios across all samples in our database that included both sediment chemistry and benthic community results, this included samples collected for other programs and special projects (n = 2,682 samples). Sites that fell within the 10th percentile (lowest 10% PEL-ratios, i.e. least contaminated sediments) were assigned an "A"; sites within the 10^{th}-25^{th} percentile were assigned a "B"; sites within the 25^{th}-75^{th} percentile were assigned a "C"; sites within the 75^{th}-90^{th} percentile were assigned a "D"; sites above the 90^{th} percentile were assigned an "F". Most sites fell within the "C" range. The "D" and "F" graded sites were found primarily in Hillsborough Bay, the Manatee River, and Boca Ciega Bay.

About 1600 benthic taxa (approximately 1150 species level ids) were identified over the twenty-five-year monitoring period. The median number of taxa per sample was 36 and ranged from 0 to 176 taxa per sample. There was a general trend of increasing species richness towards the lower bay, with the highest number of taxa being recorded in Lower Tampa Bay and Boca Ciega Bay. There was an overall increasing trend in species richness over time. The abundance of benthic organisms ranged from 0 to 183,425 organisms/m^2, with a median of 6,325 organisms/m^2. Middle Tampa Bay and Old Tampa Bay had the highest abundances while the lowest abundance was observed in Terra Ceia Bay. There was an increasing trend in abundance from 2012-2017. Seven taxa accounted for 25% of the overall benthic abundance. The cephalochordate *Branchiostoma floridae* was the most abundant species, accounting for 5.29% of the total benthic abundance. The other top ranked taxa included the brachiopod *Glottidia pyramidata* (4.23%), the polychaete *Kirkegaardia* sp. (previously identified as *Monticellina cf. dorsobranchialis*)(3.43%), the bivalve *Mysella planulata* (3.91%), unidentified Naididae oligochaetes (3.36%), the amphipod *Ampelisca holmesi* (2.65%), and the gastropod *Caecum strigosum* (2.50%). The Shannon Diversity Index increased towards the lower bay, and was highest in Boca Ciega Bay, Terra Ceia Bay, and Lower Tampa Bay. The lowest median diversity values were in Hillsborough Bay and the Manatee River.

Similarity analysis between sampling years indicated that the Tampa Bay benthic community fell into five temporal groupings: 1993-2002 (Group A); 2004+2006-2009 (Group B); 2003+2005 (Group C); 2012-2017 (Group D); and 2010+2011 (Group E). The 1993-2002 group was characterized by *Branchiostoma floridae*, *Kirkegaardia* sp. and *Caecum strigosum*. The 2004+2006-2009 group was represented by Naididae, *Kirkegaardia* sp., *Mysella planulata* and the polychaete *Fabricinuda trilobata.* The 2003+2005 group was characterized by the bivalve *Amygdalum papyrium*, Naididae, *Kirkegaardia* sp., and *Glottidia pyramidata.* The 2012-2017 group was characterized by *Branchiostoma floridae*, Naididae, *Kirkegaardia* sp., *Caecum pulchellum* and *Ampelisca holmesi;* and the 2010+2011 group was represented by Naididae, the gastropod *Bittiolum varium*, and the polychaetes *Kirkegaardia* sp., *Paraprionospio* sp., and *Aricidea philbinae*.

The Tampa Bay benthic community fell into two main spatial assemblages, according to a species similarity analysis that averaged by bay segment. The lower segments of the bay (Middle and Lower Tampa Bay and Boca Ciega Bay) forming one group and Hillsborough Bay, Old Tampa Bay, Terra Ceia Bay, and the Manatee River forming the second group. The lower bay segments were characterized by *Branchiostoma floridae*, Naididae, the maldanid polychaete ("bamboo worm") *Clymenella mucosa*, the spirorbid polychaete *Neodexiospira steueri*, and *Fabricinuda trilobata*. The other bay segments were characterized by high abundances of *Ampelisca holmesi, Kirkegaardia* sp., *Mysella planulata*, Naididae, and the bivalve *Mulinia lateralis.*

Analysis between the environmental factors and the benthic species composition indicated that the sediment composition was the strongest factor structuring the benthic community, followed by dissolved oxygen.

The Tampa Bay Benthic Index (TBBI) was developed as a measure of the health of benthic habitats in Tampa Bay. The TBBI is scaled from 0-100 with values <73 classified as "Degraded", from 73-87 as "Intermediate", and >87 as "Healthy". Depauperate samples are assigned a TBBI score of 0 and classified as "Empty". The overall TBBI for the 1993-2017 monitoring period had a median value of 84.67, which falls within the "Intermediate" category for benthic habitat health. The highest TBBI values were in the main portion of Tampa Bay (Old Tampa Bay, Middle Tampa Bay, and Lower Tampa Bay), while lower values were found in Hillsborough Bay and the Manatee River. Hillsborough Bay had the highest number of "Empty" samples (4.42%) and one-third of the sites were classified as "Degraded". The Manatee River, Terra Ceia Bay, and Boca Ciega Bay also had many "Degraded" sites (19-30%). Old Tampa Bay, Middle Tampa Bay and Lower Tampa Bay had few empty sites (0-1.5%) and <20% of the sites in each segment were classified as "Degraded", while > 47% of the sites in each of these segments were classified as "Healthy". Bay-wide, 1% of the samples were "Empty", 19.71% were classified as "Degraded," 38.58% as "Intermediate", and 40% as "Healthy". There was an overall increasing trend in the TBBI score over time. The bay-wide median TBBI was continuously in the "Healthy" range from 2013-2017.

The National Estuary Program Coastal Condition Report published in 2007 included an evaluation of the estuarine condition in Tampa Bay based on samples collected by the National Coastal Assessment (NCA) monitoring program (USEPA 2007). The NCA collected sediment samples from 25 sites throughout Tampa Bay in July 2000. These samples were analyzed for benthic invertebrate community structure, and the condition of the benthic community was evaluated at each site using the Gulf Coast Benthic Index (GCBI) developed for the Louisianan Provence EMAP program (Engle et al., 1994; Engle and Summers 1999). The condition of the benthic community at each station was rated as "Good" if the GCBI score was ≥ 5.0, "Fair" if the GCBI score was between 3.0 and 5.0, and "Poor" if the GCBI score was < 3.0 (USEPA 2007). The overall benthic community condition for the estuary was rated based on the following criteria: “Good” if < 10% of the sites had a “Poor” GCBI score and >50% had a “Good: GCBI score; “Fair” if 10% to 20% of the sites had a “Poor” GCBI score or >50% of the sites had a combined “Poor” and “Fair” GCBI score; and “Poor” if >20% of the sites had a “Poor” GCBI score. The overall benthic community condition for Tampa Bay based on these criteria was rated as “Poor” with 36% of the NCA sites having “Poor” GCBI scores, 20% rated as “Fair”, and 44% as “Good” (USEPA 2007).

The benthic community condition of the bay-wide monitoring samples was evaluated applying the same criteria for “Good”, “Fair”, and “Poor” as outlined in the Coastal Condition Report (USEPA 2007), however we utilized the Tampa Bay Benthic Index and its scoring criteria for the individual samples rather than the GCBI used by the EPA. Results from this analysis are presented in the table below by year and bay segment, as well as the overall bay-wide condition. The bay-wide benthic condition was calculated in two ways: 1) by simply evaluating all the samples equally, and 2) by proportionally weighing the samples based on their bay segment area in order to compensate for differing sampling densities in each bay segments. Overall, bay-wide results were consistent with the NCA rating of “Poor” for 12 of the 25 years of monitoring, with 10 years rating as “Fair” and the last three years rating as “Good”. Weighing the samples proportionally by their bay segment area increased the bay-wide rating from “Poor” to “Fair” for 7 of the years, and both 1995 and 2005 increased from “Fair” to “Good”, while 2015-2017 remained rated as “Good” (see Table below).

In addition to the TBBI, this report has attempted a preliminary adaptation of the AZTI Marine Biotic Index (AMBI). The AMBI was developed for European estuarine and coastal soft-bottom environments (Borja et al., 2000, Grall and Glémarec 1997). The AMBI assigns individual taxa to one of five ecological groups (GI, GII, GIII, GIV, GV), with group GI consisting of the most pollution sensitive taxa and GV consisting of the most pollution tolerant taxa. A Biotic Coefficient (BC) is then calculated based on the percent abundance of each ecological group. The BC has a continuous range from 0-6 with empty (“Azoic”) samples assigned a score of 7. The BC scores are further assigned to a site pollution classification using the following BC score ranges:

$0.0 < BC \leq 1.2$ – “Unpolluted”
$1.2 < BC \leq 3.3$ – “Slightly polluted”
$3.3 < BC \leq 5.0$ – “Meanly polluted”
$5.0 < BC \leq 6.0$ – “Heavily polluted”
$BC = 7$ (“Azoic” samples) – “Extremely polluted”

Gillet et al., (2015) adapted the AMBI for the United States coastal waters by assigning the ecological groups to regional species lists, including the Gulf of Mexico. We applied the Gulf of Mexico ecological groups to our Tampa Bay taxa list in order to calculate a regional AMBI Biotic Coefficient and assigned site pollution classifications. We refer to this regional index as the Gulf of Mexico (GoM) AMBI. The GoM_AMBI classified most of the Tampa Bay sites as “Slightly polluted”.

We further attempted to refine the AMBI specifically to our Tampa Bay monitoring dataset by compiling all samples in our database that had both sediment chemistry and benthic species data available (n=2,682 samples). We included samples collected from Special Study locations as part of the Bay-wide Benthic Monitoring program, as well as other projects, to include more freshwater and low salinity sites, as well as areas of high sediment contamination. The compiled samples were assigned to a pollution category based on their bottom dissolved oxygen category and sediment contaminant PEL Grade. The samples were assigned factors based on their PEL-Grade and bottom dissolved oxygen category (i.e. "Normoxic_A, Anoxic_F etc.). The benthic species compositions were averaged within these factors in PRIMER v. 7, and the zero-adjusted Bray-Curtis similarity (Clarke et al., 2006) was calculated on fourth root transformed abundance data. The resulting similarity matrix was used for cluster analysis to group similar species assemblages. These cluster groups were then used to assign individual taxa to the AMBI ecological groups. The final BC value was adjusted using the formula [(7-BC) x (10/7)] to rescale the final index from 0-10 with empty samples scoring as "0" and increasing values towards 10 indicating less polluted sites – hereafter referred to as the "Adjusted Tampa Bay AMBI" (Adj. TB_AMBI). The site pollution BC thresholds were similarly adjusted as follows:

0.00 – 1.39 = "Extremely polluted"
1.40 – 2.89 = "Heavily polluted"
2.90 – 5.29 = "Meanly polluted"
5.30 – 8.29 = "Slightly polluted"
8.30 – 10.00 = "Unpolluted"

The Adj. TB_AMBI results classified most sites as "Unpolluted"; however, the Adj. TB_AMBI is still under development, and the threshold values for the site pollution categories may need to be adjusted.

Tampa Bay has shown tremendous improvements in water quality and seagrass recovery since the early 1980's. The results from this report indicate that the benthic community is now healthier, with increasing trends in overall species richness and abundance. These increases track with improvements in water quality and seagrass coverage. The Tampa Bay Benthic Index also indicates an improving benthic community over time, most notably since 2013, when the median bay-wide TBBI was within the "Healthy" range every year through 2017.

The recommendation of this report is to maintain the current sampling design that has been in place since 2005, with the possibility of increasing the number of special study sites as needed to evaluate areas of special concern to the Tampa Bay Estuary Program and regional bay managers. We also consider including analysis for sediment microplastics as an additional parameter to our monitoring efforts and suggest including the major tributaries as potential special study sites during the next 5-year monitoring cycle.

Condition of Tampa Bay benthic communities based on the TBBI using the EPA's National Coastal Assessment program criteria.

Year	HB	OTB	MTB	LTB	TCB	MR	BCB	Bay-wide	Bay-wide Weighted*
1993	Poor	Poor	Fair	Poor	Fair	Fair		Poor	Poor
1994	Poor	Poor	Poor	Fair	Poor	Poor		Poor	Poor
1995	Poor	Good	Good	Good	Poor	Fair	Fair	Fair	Good
1996	Poor	Good	Fair	Good	Fair/Good*	Fair	Fair	Fair	Fair
1997	Poor	Fair/Good*	Good	Good	Fair/Good*	Poor	Poor	Fair	Fair
1998	Poor	Fair	Fair	Good	Fair	Poor	Poor	Poor	Fair
1999	Fair	Fair	Good	Fair	Poor	Fair	Fair	Fair	Fair
2000	Poor	Good	Fair	Fair	Fair	Poor	Fair	Fair	Fair
2001	Poor	Poor	Fair/Good*	Good	Poor	Fair	Poor	Poor	Fair
2002	Poor	Fair	Good	Fair	Poor	Poor	Poor	Poor	Fair
2003	Poor	Poor	Good	Good	Poor	Poor	Poor	Poor	Poor
2004	Fair	Poor	Good	Good	Good	Poor	Fair	Fair	Fair
2005	Poor	Good	Good	Good	Fair	Fair	Fair/Good*	Fair	Good
2006	Poor	Good	Good	Fair	Fair	Poor	Poor	Poor	Fair
2007	Poor	Good	Good	Fair	Poor	Poor	Fair	Poor	Fair
2008	Poor	Fair	Good	Good	Poor	Fair	Fair	Fair	Fair
2009	Fair	Fair	Good	Fair/Good*	Poor	Fair	Poor	Fair	Fair
2010	Fair	Poor	Poor	Good	Fair/Good*	Fair	Good	Fair	Poor
2011	Poor	Poor	Fair	Poor	Fair	Poor	Fair	Poor	Poor
2012	Poor	Good	Good	Poor	Poor	Poor	Fair	Poor	Fair
2013	Poor	Fair	Good	Good	Good	Poor	Fair	Poor	Fair
2014	Poor	Poor	Good	Good	Good	Poor	Poor	Poor	Poor
2015	Poor	Fair	Good	Good	Good	Fair	Fair	Good	Good
2016	Good	Poor	Good	Good	Good	Fair	Good	Good	Good
2017	Fair	Fair	Good	Good	Fair	Good	Fair	Good	Good

*Weighted by Bay Segment Area

Table of Contents

Executive Summary ii
Table of Contents viii
List of Figures x
List of Tables xviii
Introduction 1
  Program Background 1
Methods 2
  Sampling Design 2
  Field Collection 4
    Hydrographic Measurements 4
    Benthic Macrofauna 4
    Silt+Clay 4
    Sediment Chemistry 4
  Laboratory Procedures 5
    Field data 5
    Sediment Chemistry 5
    Silt+Clay Analysis 5
    Benthic Community Analysis 5
  Data Analysis 6
    Data Categorization 6
    Univariate Statistical Analysis 7
    Multivariate Statistical Analysis 8
    Spatial and Graphical Analysis 8
Results and Discussion 10
  Sampling Locations 10
  Hydrographic and Sediment Characteristics 11
    Depth 13
    Bottom Temperature 17
    Bottom pH 19
    Bottom Salinity 20
    Bottom Dissolved Oxygen 24
    Sediment Composition (%Silt+Clay) 27
    Total Organic Carbon (TOC) 28
    Analysis of Environmental Data 34
  Sediment Contaminants 38
    Metals 38
    Polycyclic Aromatic Hydrocarbons (PAHs) 69
    Polychlorinated biphenyls (PCBs) and Chlorinated Pesticides 106
    Organochlorine Pesticides 107
    PEL Ratio Grade 113
  Benthic Community Structure 137
    Summary Statistics 137
    Dominant Taxa 150
    Benthic Community Similarity Analysis 187

Relating Biological and Environmental data 190
Conclusions and Recommendations 210
Literature Cited 211

List of Figures

Figure 1. Tampa Bay segments and sampling grids. 3
Figure 2. Tampa Bay benthic monitoring sampling sites 1993-2017 by 5-year periods (A-E) and 25-year cumulative data (F). Cumulative total = 1791 sampling sites. Number of sites by year in parenthesis.. 10
Figure 3. Mean sample depth by year. Error bars = 95% confidence interval, dashed line represents bay-wide mean.. 15
Figure 4. Mean sample depth by bay segment. Error bars = 95% confidence interval, dashed line represents bay-wide mean value. 15
Figure 5. Distribution of sample site depth categories 1993-2017 by 5-year periods (A-E) and 25-year composite data (F).. 16
Figure 6. Mean bottom temperature by year. Error bars = 95% confidence interval, dashed line represents bay-wide mean value, solid line indicates 25-year trend.. 18
Figure 7. Mean bottom temperature by bay segment. Error bars = 95% confidence interval, dashed line represents bay-wide mean value. 18
Figure 8. Mean bottom pH by year. Error bars = 95% confidence interval, dashed line represents bay-wide mean value. 19
Figure 9. Mean bottom pH by bay segment. Error bars = 95% confidence interval, dashed line represents bay-wide mean value. 20
Figure 10. Mean bottom salinity by year. Error bars = 95% confidence interval; middle dashed line represents bay-wide mean value; lower and upper dashed lines denote boundaries of high mesohaline/polyhaline (18 psu) and polyhaline/euhaline (30 psu) salinity categories................. 21
Figure 11. Mean bottom salinity by bay segment. Error bars = 95% confidence interval; middle dashed line represents bay-wide mean value; lower and upper dashed lines denote boundaries of high mesohaline/polyhaline (18 psu) and polyhaline/euhaline (30 psu) salinity categories. 22
Figure 12. Spatial analysis of bottom salinity 1993-2017 by 5-year periods (A-E) and 25-year composite data (F).. 23
Figure 13. Mean bottom dissolved oxygen by year in mg/L (black closed circles, solid line; left axis) and as % saturation (blue open circles, dashed line; right axis). Error bars = 95% confidence interval, black dashed line represents bay-wide mean concentration, blue dash line represents bay-wide mean saturation; bottom solid red line represents the critical value for normoxic conditions (> 4 mg/l). 25
Figure 14. Mean bottom dissolved oxygen by bay segment in mg/L (bar graph; left axis) and as % saturation (line graph; right axis). Error bars = 95% confidence interval, black dashed line represents bay-wide mean concentration, blue dash-dot-dot line represents bay-wide mean saturation; bottom solid red line represents the critical value for normoxic conditions (> 4 mg/l). 26
Figure 15. Distribution of bottom dissolved oxygen 1993-2017 by 5-year periods (A-E) and 25-year composite data (F)... 27
Figure 16. Mean percent silt+clay by year. Error bars = 95% confidence interval, dashed line represents bay-wide mean value, lower and upper solid lines denote boundaries of medium/fine (4.51%) and fine/very fine (11.35%) sediment categories. 29
Figure 17. Mean percent silt+clay by bay segment. 95% confidence interval, dashed line represents bay-wide mean value, lower and upper solid lines denote boundaries of medium/fine (4.51%) and fine/very fine (11.35%) sediment categories. 29

Figure 18. Spatial distribution of sediment types in Tampa Bay 1993-2017. 31
Figure 19. Mean total organic carbon by year. Error bars = 95% confidence interval, dashed line represents bay-wide mean. 32
Figure 20. Mean total organic carbon by bay segment. Error bars = 95% confidence interval, dashed line represents bay-wide mean. 32
Figure 21. Spatial distribution of sediment total organic carbon in Tampa Bay 2010-2017. 33
Figure 22. PCO coded by bay segment. 35
Figure 23. PCO by bay segment and year average. 35
Figure 24. PCO by bottom dissolved oxygen classification, bubble size in mg/l. 36
Figure 25. PCO by sediment type, bubble size in % Silt+Clay. 36
Figure 26. PCO by salinity classification, bubble size in psu. 37
Figure 27. PCO by depth classification, bubble size in meters. 37
Figure 28. Mean sediment aluminum concentrations by bay segment. 48
Figure 29. Mean sediment iron concentrations by bay segment. 48
Figure 30. Mean sediment antimony concentrations by bay segment. 49
Figure 31. Tampa Bay Sb:Al ratio with 95% prediction intervals (solid lines). 49
Figure 32. Mean sediment arsenic concentrations by bay segment. Error bars = 95% confidence interval, dashed line represents bay-wide mean. Solid lines represent PEL (upper; red) and TEL (lower; green) values. 50
Figure 33. Tampa Bay As:Al ratio with 95% prediction intervals (solid lines). 50
Figure 34. Spatial distribution of arsenic in Tampa Bay 1993-2017. 51
Figure 35. Mean sediment cadmium concentrations by bay segment. Error bars = 95% confidence interval, dashed line represents bay-wide mean. Solid lines represent PEL (upper; red) and TEL (lower; green) values. 52
Figure 36. Tampa Bay Cd:Al ratio with 95% prediction intervals (solid lines). 52
Figure 37. Distribution of cadmium in Tampa Bay 1993-2017. 53
Figure 38. Mean sediment chromium concentrations by bay segment. Error bars = 95% confidence interval, dashed line represents bay-wide mean. Solid lines represent PEL (upper; red) and TEL (lower; green) values. 54
Figure 39. Tampa Bay Cr:Al ratio with 95% prediction intervals (solid lines). 54
Figure 40. Distribution of chromium in Tampa Bay 1993-2017. 55
Figure 41. Mean sediment copper concentrations by bay segment. Error bars = 95% confidence interval, dashed line represents bay-wide mean. Solid lines represent PEL (upper; red) and TEL (lower; green) values. 56
Figure 42. Tampa Bay Cu:Al ratio with 95% prediction intervals (solid lines). 56
Figure 43. Distribution of copper in Tampa Bay 1993-2017. 57
Figure 44. Mean sediment lead concentrations by bay segment. Error bars = 95% confidence interval, dashed line represents bay-wide mean. Solid lines represent PEL (upper; red) and TEL (lower; green) values. 58
Figure 45. Tampa Bay Pb:Al ratio with 95% prediction intervals (solid lines). 58
Figure 46. Distribution of lead in Tampa Bay 1993-2017. 59
Figure 47. Mean sediment manganese concentrations by bay segment. 60
Figure 48. Tampa Bay Mn:Al ratio with 95% prediction intervals (solid lines). 60
Figure 49. Mean sediment concentrations of nickel by bay segment. Error bars = 95% confidence interval, dashed line represents bay-wide mean. Solid lines represent PEL (upper; red) and TEL (lower; green) values. 61

Figure 50. Tampa Bay Ni:Al ratio with 95% prediction intervals (solid lines). 61
Figure 51. Distribution of nickel in Tampa Bay 1993-2017. 62
Figure 52. Mean sediment selenium concentrations by bay segment. 63
Figure 53. Tampa Bay Se:Al ratio with 95% prediction intervals (solid lines). 63
Figure 54. Mean sediment silver concentrations by bay segment. Error bars = 95% confidence interval, dashed line represents bay-wide mean. Solid lines represent PEL (upper; red) and TEL (lower; green) values. 64
Figure 55. Tampa Bay Ag:Al ratio with 95% prediction intervals (solid lines). 64
Figure 56. Spatial distribution of silver in Tampa Bay 1993-2017. 65
Figure 57. Mean sediment tin concentrations by bay segment. Error bars = 95% confidence interval, dashed line represents bay-wide mean. 66
Figure 58. Tampa Bay Sn:Al ratio with 95% prediction intervals (solid lines). 66
Figure 59. Mean sediment zinc concentrations by bay segment. Error bars = 95% confidence interval, dashed line represents bay-wide mean. Solid lines represent PEL (upper; red) and TEL (lower; green) values. 67
Figure 60. Tampa Bay Zn:Al ratio with 95% prediction intervals (solid lines). 67
Figure 61. Distribution of Zinc in Tampa Bay 1993-2017. 68
Figure 62. Mean sediment acenaphthene concentrations by bay segment. Error bars = 95% confidence interval, dashed line represents bay-wide mean. Solid lines represent PEL (upper; red) and TEL (lower; green) values. 80
Figure 63. Mean sediment acenaphthylene concentrations by bay segment. Error bars = 95% confidence interval, dashed line represents bay-wide mean. Solid lines represent PEL (upper; red) and TEL (lower; green) values. 80
Figure 64. Distribution of acenaphthene in Tampa Bay 1993-2017. 81
Figure 65. Distribution of acenaphthylene in Tampa Bay 1993-2017. 82
Figure 66. Mean sediment anthracene concentrations by bay segment. Error bars = 95% confidence interval, dashed line represents bay-wide mean. Solid lines represent PEL (upper; red) and TEL (lower; green) values. 83
Figure 67. Mean sediment fluorene concentrations by bay segment. Error bars = 95% confidence interval, dashed line represents bay-wide mean. Solid lines represent PEL (upper; red) and TEL (lower; green) values. 83
Figure 68. Distribution of anthracene in Tampa Bay 1993-2017. 84
Figure 69. Distribution of fluorene in Tampa Bay 1993-2017. 85
Figure 70. Mean sediment naphthalene concentrations by bay segment. Error bars = 95% confidence interval, dashed line represents bay-wide mean. Solid lines represent PEL (upper; red) and TEL (lower; green) values. 86
Figure 71. Mean sediment phenanthrene concentrations by bay segment. Error bars = 95% confidence interval, dashed line represents bay-wide mean. Solid lines represent PEL (upper; red) and TEL (lower; green) values. 86
Figure 72. Distribution of naphthalene in Tampa Bay 1993-2017. 87
Figure 73. Distribution of phenanthrene in Tampa Bay 1993-2017. 88
Figure 74. Mean sediment low molecular weight PAH concentrations by bay segment. Error bars = 95% confidence interval, dashed line represents bay-wide mean. Solid lines represent PEL (upper; red) and TEL (lower; green) values. 89
Figure 75. Distribution of total low molecular weight PAHs in Tampa Bay 1993-2017. 90

Figure 76. Mean sediment benzo (a) anthracene concentrations by bay segment. Error bars = 95% confidence interval, dashed line represents bay-wide mean. Solid lines represent PEL (upper; red) and TEL (lower; green) values. 91
Figure 77. Mean sediment benzo (a) pyrene concentrations by bay segment. Error bars = 95% confidence interval, dashed line represents bay-wide mean. Solid lines represent PEL (upper; red) and TEL (lower; green) values. 91
Figure 78. Distribution of benzo(a) anthracene in Tampa Bay 1993-2017. 92
Figure 79. Distribution of benzo(a) pyrene in Tampa Bay 1993-2017. 93
Figure 80. Mean sediment chrysene concentrations by bay segment. Error bars = 95% confidence interval, dashed line represents bay-wide mean. Solid lines represent PEL (upper; red) and TEL (lower; green) values. 94
Figure 81. Mean sediment dibenzo (a,h) anthracene concentrations by bay segment. Error bars = 95% confidence interval, dashed line represents bay-wide mean. Solid lines represent PEL (upper; red) and TEL (lower; green) values. 94
Figure 82. Distribution of chrysene in Tampa Bay 1993-2017. 95
Figure 83. Distribution of dibenzo (a,h) anthracene in Tampa Bay 1993-2017. 96
Figure 84. Mean sediment fluoranthene concentrations by bay segment. Error bars = 95% confidence interval, dashed line represents bay-wide mean. Solid lines represent PEL (upper; red) and TEL (lower; green) values. 97
Figure 85. Mean sediment pyrene concentrations by bay segment. Error bars = 95% confidence interval, dashed line represents bay-wide mean. Solid lines represent PEL (upper; red) and TEL (lower; green) values. 97
Figure 86. Distribution of fluoranthene in Tampa Bay 1993-2017. 98
Figure 87. Distribution of pyrene in Tampa Bay 1993-2017. 99
Figure 88. Mean sediment high molecular weight PAH concentrations by bay segment. Error bars = 95% confidence interval, dashed line represents bay-wide mean. Solid lines represent PEL (upper; red) and TEL (lower; green) values. 100
Figure 89. Mean sediment total PAH concentrations by bay segment. Error bars = 95% confidence interval, dashed line represents bay-wide mean. Solid lines represent PEL (upper; red) and TEL (lower; green) values. 100
Figure 90. Distribution of high molecular weight PAHs in Tampa Bay 1993-2017. 101
Figure 91. Distribution of total PAHs in Tampa Bay 1993-2017. 102
Figure 92. Mean sediment benzo (b) fluoranthene concentrations by bay segment. Error bars = 95% confidence interval, dashed line represents bay-wide mean. 103
Figure 93. Mean sediment benzo (k) fluoranthene concentrations by bay segment. Error bars = 95% confidence interval, dashed line represents bay-wide mean. 103
Figure 94. Mean sediment indeno (1,2,3-c,d) pyrene concentrations by bay segment. Error bars = 95% confidence interval, dashed line represents bay-wide mean. 104
Figure 95. Mean sediment benzo (g,h,i) perylene concentrations by bay segment. Error bars = 95% confidence interval, dashed line represents bay-wide mean. 104
Figure 96. Mean sediment retene concentrations by bay segment. Error bars = 95% confidence interval, dashed line represents bay-wide mean. 105
Figure 97. Mean sediment coronene concentrations by bay segment. Error bars = 95% confidence interval, dashed line represents bay-wide mean. 105

Figure 98. Mean sediment total PCB concentrations by bay segment. Error bars = 95% confidence interval, dashed line represents bay-wide mean. Solid lines represent PEL (upper; red) and TEL (lower; green) values. 115
Figure 99. Distribution of total PCBs in Tampa Bay 1993-2017. 116
Figure 100. Mean sediment aldrin concentrations by bay segment. Error bars = 95% confidence interval, dashed line represents bay-wide mean. 117
Figure 101. Mean sediment dieldrin concentrations by bay segment. Error bars = 95% confidence interval, dashed line represents bay-wide mean. Solid lines represent PEL (upper; red) and TEL (lower; green) values. 117
Figure 102. Distribution of dieldrin in Tampa Bay 1993-2017. 118
Figure 103. Mean sediment p,p'-DDD concentrations by bay segment. Error bars = 95% confidence interval, dashed line represents bay-wide mean. Solid lines represent PEL (upper; red) and TEL (lower; green) values. 119
Figure 104. Mean sediment p,p'-DDE concentrations by bay segment. Error bars = 95% confidence interval, dashed line represents bay-wide mean. Solid lines represent PEL (upper; red) and TEL (lower; green) values. 119
Figure 105. Mean sediment p,p'-DDT concentrations by bay segment. Error bars = 95% confidence interval, dashed line represents bay-wide mean. Solid lines represent PEL (upper; red) and TEL (lower; green) values. 120
Figure 106. Mean sediment total DDT concentrations by bay segment. Error bars = 95% confidence interval, dashed line represents bay-wide mean. Solid lines represent PEL (upper; red) and TEL (lower; green) values. 120
Figure 107. Distribution of p,p'-DDD in Tampa Bay 1993-2017. 121
Figure 108. Distribution of p,p'-DDE in Tampa Bay 1993-2017. 122
Figure 109. Distribution of p,p'-DDT in Tampa Bay 1993-2017. 123
Figure 110. Distribution of total DDT in Tampa Bay 1993-2017. 124
Figure 111. Mean sediment α-BHC concentrations by bay segment. Error bars = 95% confidence interval, dashed line represents bay-wide mean. 125
Figure 112. Mean sediment β-BHC concentrations by bay segment. Error bars = 95% confidence interval, dashed line represents bay-wide mean. 125
Figure 113 Mean sediment lindane (γ-BHC) concentrations by bay segment. Error bars = 95% confidence interval, dashed line represents bay-wide mean. Solid lines represent PEL (upper; red) and TEL (lower; green) values. 126
Figure 114. Mean sediment δ-BHC concentrations by bay segment. Error bars = 95% confidence interval, dashed line represents bay-wide mean. 126
Figure 115. Distribution of lindane in Tampa Bay 1993-2017. 127
Figure 116. Mean sediment endosulfan l concentrations by bay segment. Error bars = 95% confidence interval, dashed line represents bay-wide mean. 128
Figure 117. Mean sediment endosulfan ll concentrations by bay segment. Error bars = 95% confidence interval, dashed line represents bay-wide mean. 128
Figure 118. Mean sediment endosulfan sulfate concentrations by bay segment. Error bars = 1 standard deviation. 129
Figure 119. Mean sediment endrin concentrations by bay segment. Error bars = 95% confidence interval, dashed line represents bay-wide mean. 129
Figure 120. Mean sediment endrin aldehyde concentrations by bay segment. Error bars = 95% confidence interval, dashed line represents bay-wide mean. 130

Figure 121. Mean sediment endrin ketone concentrations by bay segment. Error bars = 95% confidence interval, dashed line represents bay-wide mean. 130
Figure 122. Mean sediment α-chlordane concentrations by bay segment. Error bars = 95% confidence interval, dashed line represents bay-wide mean. 131
Figure 123. Mean sediment γ-chlordane concentrations by bay segment. Error bars = 95% confidence interval, dashed line represents bay-wide mean. 131
Figure 124. Mean sediment total chlordane concentrations by bay segment. Error bars = 95% confidence interval, dashed line represents bay-wide mean. Solid lines represent PEL (upper; red) and TEL (lower; green) values. 132
Figure 125. Distribution of total chlordane in Tampa Bay 1993-2017. 133
Figure 126. Mean sediment heptachlor concentrations by bay segment. Error bars = 95% confidence interval, dashed line represents bay-wide mean. 134
Figure 127. Mean sediment heptachlor epoxide concentrations by bay segment. Error bars = 95% confidence interval, dashed line represents bay-wide mean. 134
Figure 128. Mean sediment methoxychlor concentrations by bay segment. Error bars = 95% confidence interval, dashed line represents bay-wide mean. 135
Figure 129. Mean sediment mirex concentrations by bay segment. Error bars = 95% confidence interval, dashed line represents bay-wide mean. 135
Figure 130. Distribution of Mean PEL ratio Grades 1993-2017. 136
Figure 131. Mean number of benthic taxa by year (black) and Tampa Bay Water Quality Index (blue). Error bars = 95% confidence interval, dashed line represents bay-wide mean. 142
Figure 132. Mean number of benthic taxa by bay segment. Error bars = 95% confidence interval, dashed line represents bay-wide mean. 142
Figure 133. Mean benthic abundance by year. Error bars = 95% confidence interval, dashed line represents bay-wide mean. 143
Figure 134. Mean benthic abundance by bay segment. Error bars = 95% confidence interval, dashed line represents bay-wide mean. 143
Figure 135. Mean Shannon-Wiener Diversity Index ($\log_e$) by year. Error bars = 95% confidence interval, dashed line represents bay-wide mean. 144
Figure 136. Mean Shannon-Wiener Diversity Index ($\log_e$) by bay segment. Error bars = 95% confidence interval, dashed line represents bay-wide mean. 144
Figure 137. Mean Tampa Bay Benthic Index by year. Error bars = 95% confidence interval, dashed line represents bay-wide mean, solid lines indicate cutoffs for "Degraded" (<73; red) and "Healthy" (>87; green) benthic habitats. 145
Figure 138. Mean Tampa Bay Benthic Index by bay segment. Error bars = 95% confidence interval, dashed line represents bay-wide mean, solid lines indicate cutoffs for "Degraded" (<73; red) and "Healthy" (>87; green) benthic habitats. 145
Figure 139. Distribution of Tampa Bay Benthic Index condition 1993-2017 by 5-year periods (A-E) and 25-year composite data (F). 149
Figure 140. Mean abundance of *Branchiostoma floridae* by year. Error bars = 1 standard error, dashed line represents bay-wide mean value. 164
Figure 141. Mean abundance of *Branchiostoma floridae* by bay segment. Error bars = 1 standard error, dashed line represents bay-wide mean value. 164
Figure 142. Late-Summer distribution of *Branchiostoma floridae* in Tampa Bay 1993-2017. 165
Figure 143. Mean abundance of *Glottidia pyramidata* by year. Error bars = 1 standard error, dashed line represents bay-wide mean value. 166

Figure 144. Mean abundance of *Glottidia pyramidata* by bay segment. Error bars = 1 standard error, dashed line represents bay-wide mean value. 166
Figure 145. Late-Summer distribution of *Glottidia pyramidata* in Tampa Bay 1993-2017. 167
Figure 146. Mean abundance of *Kirkegaardia* sp. (=*Monticellina cf. dorsobranchialis)* by year. Error bars = 1 standard error, dashed line represents bay-wide mean value. 168
Figure 147. Mean abundance of *Kirkegaardia* sp. (=*Monticellina cf. dorsobranchialis* by bay segment. Error bars = 1 standard error, dashed line represents bay-wide mean value. 168
Figure 148. Late-Summer distribution of *Kirkegaardia* sp. (= *Monticellina cf. dorsobranchialis*) in Tampa Bay 1993-2017.. 169
Figure 149. Mean abundance of *Mysella planulata* by year. Error bars = 1 standard error, dashed line represents bay-wide mean value. 170
Figure 150. Mean abundance of *Mysella planulata* by bay segment. Error bars = 1 standard error, dashed line represents bay-wide mean value. 170
Figure 151. Late-Summer distribution of *Mysella planulata* in Tampa Bay 1993-2017. 171
Figure 152. Mean abundance of unidentified Naididae (=Tubificinae) by year. Error bars = 1 standard error, dashed line represents bay-wide mean value.. 172
Figure 153. Mean abundance of unidentified Naididae (=Tubificinae) by bay segment. Error bars = 1 standard error, dashed line represents bay-wide mean value. 172
Figure 154. Late-Summer distribution of unidentified Naididae in Tampa Bay 1993-2017...... 173
Figure 155. Mean abundance of *Ampelisca holmesi* (black dots) and *Ampelisca abdita* (blue open triangles) by year. Error bars = 1 standard error, black and blue dashed lines represent bay-wide mean values for *A. holmesi* and *A. abdita* respectively. 174
Figure 156. Mean abundance of *Ampelisca holmesi* and *Ampelisca abdita* by bay segment. Error bars = 1 standard error, black and blue dashed lines represent bay-wide mean values for *A. holmesi* and *A. abdita* respectively. 174
Figure 157. Late-Summer distribution of *Ampelisca holmesi* in Tampa Bay 1993-2017. 175
Figure 158. Late-Summer distribution of *Ampelisca abdita* in Tampa Bay 1993-2017. 176
Figure 159. Mean abundance of *Caecum strigosum* by year. Error bars = 1 standard error, dashed line represents bay-wide mean value. 177
Figure 160. Mean abundance of *Caecum strigosum* by bay segment. Error bars = 1 standard error, dashed line represents bay-wide mean value. 177
Figure 161. Late-Summer distribution of *Caecum strigosum* in Tampa Bay 1993-2017. 178
Figure 162. Mean abundance of *Rudilemboides naglei* by year. Error bars = 1 standard error, dashed line represents bay-wide mean value. 179
Figure 163. Mean abundance of *Rudilemboides naglei* by bay segment. Error bars = 1 standard error, dashed line represents bay-wide mean value. 179
Figure 164. Late-Summer distribution of *Rudilemboides naglei* in Tampa Bay 1993-2017...... 180
Figure 165. Mean abundance of *Fabricinuda trilobata* by year. Error bars = 1 standard error, dashed line represents bay-wide mean value. 181
Figure 166. Mean abundance of *Fabricinuda trilobata* by bay segment. Error bars = 1 standard error, dashed line represents bay-wide mean value. 181
Figure 167. Late-Summer distribution of *Fabricinuda trilobata* in Tampa Bay 1993-2017. 182
Figure 168. Mean abundance of unidentified *Mediomastus* sp. (black circles), *Mediomastus ambiseta* (red squares) and *Mediomastus californiensis* (blue triangles) by year. Error bars = 1 standard error, dashed lines represent bay-wide mean values for each respective taxon. 183

Figure 169. Mean abundance of unidentified *Mediomastus* spp. (solid bars), *Mediomastus ambiseta* (diagonal hash) and *Mediomastus californiensis* (cross hash) by bay segment. Error bars = 1 standard error, dashed lines represent bay-wide mean value for each respective taxon. 183
Figure 170. Late-Summer distribution of unidentified *Mediomastus spp.* in Tampa Bay 1993-2017........ 184
Figure 171. Late-Summer distribution of *Mediomastus ambiseta* in Tampa Bay 1993-2017.... 185
Figure 172. Late-Summer distribution of *Mediomastus californiensis* in Tampa Bay 1993-2017. 186
Figure 173. Cluster Analysis: Benthic community averaged by year. 189
Figure 174. Cluster Analysis; Benthic community averaged by bay segment. 190
Figure 175. MDS plot of benthic species composition by bay segment - all samples shown.... 193
Figure 176. MDS plot of benthic species composition by year and bay segment averaged....... 194
Figure 177. MDS plot data coded by sample depth category - all samples shown. 194
Figure 178. MDS plot data coded by salinity category - all samples shown. 195
Figure 179. MDS plot data coded by dissolved oxygen category - all samples shown. 195
Figure 180. MDS plot data coded by sediment category - all samples shown. 196
Figure 181. MDS plot data coded by PEL grade - all samples shown. 196
Figure 182. MDS plot data coded by TBBI category - all samples shown. 197
Figure 183. MDS plot data coded by Gulf of Mexico AMBI pollution classification. 198
Figure 184. MDS plot data coded by Gulf of Mexico AMBI pollution classification. 198

List of Tables

Table 1. Physical and TBBI descriptors and threshold values.. 9
Table 2. Bay-wide bottom physical characteristics 1993-2017 by year. Top values are medians, lower left= minimum, lower right = maximum. For TOC n = 366. 11
Table 3. Bottom physical parameters (1993-2017) by bay segment. Top values are medians, lower left= minimum, lower right = maximum. For TOC, cumulative n = 366.......................... 13
Table 4. Percentage of sites within depth categories 1993-2017... 16
Table 5. Percentage of samples within salinity categories 1993-2017. 22
Table 6. Percentage of sample sites within dissolved oxygen categories by bay segment 1993-2017... 26
Table 7. Percent sediment categories 1993-2017. 30
Table 8. Percent of total variation explained by principal coordinates....................................... 34
Table 9. Pearson correlations of bottom parameters contributing to principle coordinates. 34
Table 10. Tampa Bay (1993-2017) sediment metals summary statistics and percentage of sites exceeding TEL and PEL values.. 47
Table 11. Tampa Bay (1993-2017) sediment low molecular weight polycyclic aromatic hydrocarbon summary statistics and percentage of sites exceeding TEL and PEL values. 77
Table 12. Tampa Bay (1993-2017) sediment high molecular weight and total polycyclic aromatic hydrocarbon summary statistics and percentage of sites exceeding TEL and PEL values. 78
Table 13. Other measured hydrocarbons without established TEL/PELs 1993-2017................ 79
Table 14. Total PCBs and Pesticide summary statistics 1993-2017.. 113
Table 15. Benthic Community Summary Statistics 1993-2017 by Year.................................. 139
Table 16. Benthic Community Summary Statistics 1993 - 2017 by Bay Segment.................. 141
Table 17. Percentage of sites within TBBI categories by bay segment and bay-wide (1993-2017). 146
Table 18. Condition of Tampa Bay benthic communities 1993-2017 based on the TBBI using the EPA's National Coastal Assessment program criteria by year and segment. 147
Table 19. Condition of Tampa Bay benthic communities 1993-2017 based on the TBBI using the EPA's National Coastal Assessment program criteria by year and combined segments. 148
Table 20. Top ten benthic taxa based on relative abundance by year.. 157
Table 21. Dominant benthic taxa (Relative Abundance) by Bay Segment 1993-2017............. 162
Table 22. Multiple linear regression results of benthic community indices vs. physical parameters... 191
Table 23. Spearman correlation coefficients (ρ) and statistical p-values for benthic community indices vs. environmental parameters and mean sediment PEL ratio....................................... 192
Table 24. SIMPER analysis by depth category; values = percent contribution to similarity. Taxa contributing 50% to similarity within category listed... 202
Table 25. SIMPER analysis by salinity category; values = percent contribution to similarity. Taxa contributing 50% to similarity within category listed.. 203
Table 26. SIMPER analysis by dissolved oxygen category; values = percent contribution to similarity. Taxa contributing 50% to similarity within category listed. 204
Table 27. SIMPER analysis by sediment category; values = percent contribution to similarity. Taxa contributing 50% to similarity within category listed.. 205
Table 28. SIMPER analysis by sediment PEL Grade; values = percent contribution to similarity. Taxa contributing 50% to similarity within category listed.. 206

Table 29. SIMPER analysis by TBBI category; values = percent contribution to similarity. Taxa contributing 50% to similarity within category listed... 207
Table 30. . SIMPER analysis by Gulf of Mexico AMBI Pollution category; values = percent contribution to similarity. Taxa contributing 50% to similarity within category listed............. 208
Table 31. SIMPER analysis by proposed Tampa Bay AMBI Pollution category; values = percent contribution to similarity. Taxa contributing 50% to similarity within category listed............. 209

Introduction

Tampa Bay is the largest open water estuarine system in the state of Florida covering a surface area of over 1,030 km^2 with a surrounding watershed of 5,700 km^2 (Lewis and Estevez 1988). The bay is surrounded by three counties (Hillsborough, Pinellas, and Manatee) which have a combined population of 2,807,023 people (U.S. Census Bureau 2019; estimated population as of July 2019; https://www.census.gov/quickfacts/fact/table/manateecountyflorida,pinellascountyflorida,hillsboroughcountyflorida# accessed 12/30/2019) and includes the cities of Tampa, St. Petersburg, Clearwater, and Bradenton.

Program Background

The Tampa Bay National Estuary Program (TBNEP) [now known as the Tampa Bay Estuary Program (TBEP)] was started in 1991 with the objective of developing a Comprehensive Conservation and Management Plan (CCMP) for Tampa Bay (TBNEP, 1996). As part of the CCMP, the TBNEP developed a basin wide monitoring program to measure the effectiveness of management decisions implemented under the CCMP, and to gather further information to reevaluate and revise the CCMP in the future (Hochberg et al., 1992). During the design phase of the monitoring program, it was recommended that the benthic community should be included in the monitoring effort and that the EPA's Environmental Monitoring and Assessment Program (EMAP) sampling design be adopted (Hochberg et al., 1992).

The bay-wide Tampa Bay Benthic Monitoring Program was initiated in 1993. During the first two years of the program field sampling was conducted by the Environmental Protection Commission of Hillsborough County (EPCHC) and the Manatee County Department of Environmental Management (MCDEM) sampling covered the following bay segments: Hillsborough Bay, Old Tampa Bay, Middle Tampa Bay, Lower Tampa Bay, Manatee River, and Terra Ceia Bay. Starting in 1995, Pinellas County Environmental Management joined the monitoring efforts, initiating annual sampling in Boca Ciega Bay.

The TBNEP finalized the Comprehensive Conservation and Management Plan "Charting the Course" for Tampa Bay in December 1996 (TBNEP, 1996). The CCMP outlined the goals for restoring and protecting Tampa Bay, set restoration targets, and put forth a list of specific action plans for achieving these goals. The benthic monitoring program plays an important role in tracking the progress of these actions and providing important data for management decisions.

The benthic monitoring program's objectives and sampling design were reevaluated in 2003 (Janicki Environmental, 2003). As a result of this assessment, the reporting period was increased from one year to four years, the number of samples collected annually was cut in half (from 124 to 64 samples per year), and the Manatee River and Terra Ceia Bay were combined into a single sampling stratum. These changes were made retroactive to the year 2000 in order to alleviate a backlog in sample processing at that time (Janicki Environmental, 2003). The resulting savings in sampling effort were further redirected towards collecting samples from several areas of concern ("Special Studies") during the 2002-2004 sampling seasons.

The program was again redesigned in 2007 due to budget constraints. The second redesign maintained a total of 64 samples per year divided between 44 samples collected for the bay-wide monitoring design and 20 samples designated for special study sites. The Manatee River and Terra Ceia Bay were maintained as a single sampling stratum and additionally Middle Tampa Bay and Lower Tampa Bay were combined into a single stratum, and the reporting period was increased from four to five years. These changes were made retroactive to 2005. The redesign still allows for the detection of changes bay-wide on an annual basis and within strata between five-year reporting periods.

Methods

Sampling Design

The Tampa Bay Benthic Monitoring Program employs a stratified-random sampling strategy adopted from the EPA's Environmental Monitoring and Assessment Program – Estuaries (EMAP-E) design (Coastal Environmental, 1994). Tampa Bay is divided into seven segments (after Lewis and Whitman, 1985): Hillsborough Bay, Old Tampa Bay, Middle Tampa Bay, Lower Tampa Bay, Boca Ciega Bay, the Manatee River, and Terra Ceia Bay. Each designated segment is treated as a sampling stratum with the Manatee River and Terra Ceia Bay being combined into a single stratum (Coastal Environmental, 1994). Each stratum is overlaid by a hexagonal grid system and a random sampling point is generated within each grid cell. The sampling grid size is variable for each bay segment. A grid size of 13 km^2 is used for Old Tampa Bay, Middle Tampa Bay, and Lower Tampa Bay (Grabe et al., 1996), or a "7x7" grid density meaning a grid density twice enhanced by a factor of 7 from the base EMAP hexagon (40 km^2) (Coastal Environmental, 1994; Grabe et al., 1996). A "7x7x3" grid (4.4 km^2) is used for Hillsborough Bay and Boca Ciega Bay, while a "7x7x7" (1.9 km^2) grid is used for the Manatee River/Terra Ceia Bay stratum (Coastal Environmental, 1994; Grabe et al., 1996). Sampling points within each grid cell are randomized each year, with the exception of the first two years of the program. The sampling for the Manatee River/Terra Ceia Bay stratum used the initial random points generated in 1993 which were resampled in subsequent years until the program redesign in 2003. The Manatee River/Terra Ceia Bay sampling sites have been randomized annually after 2003.

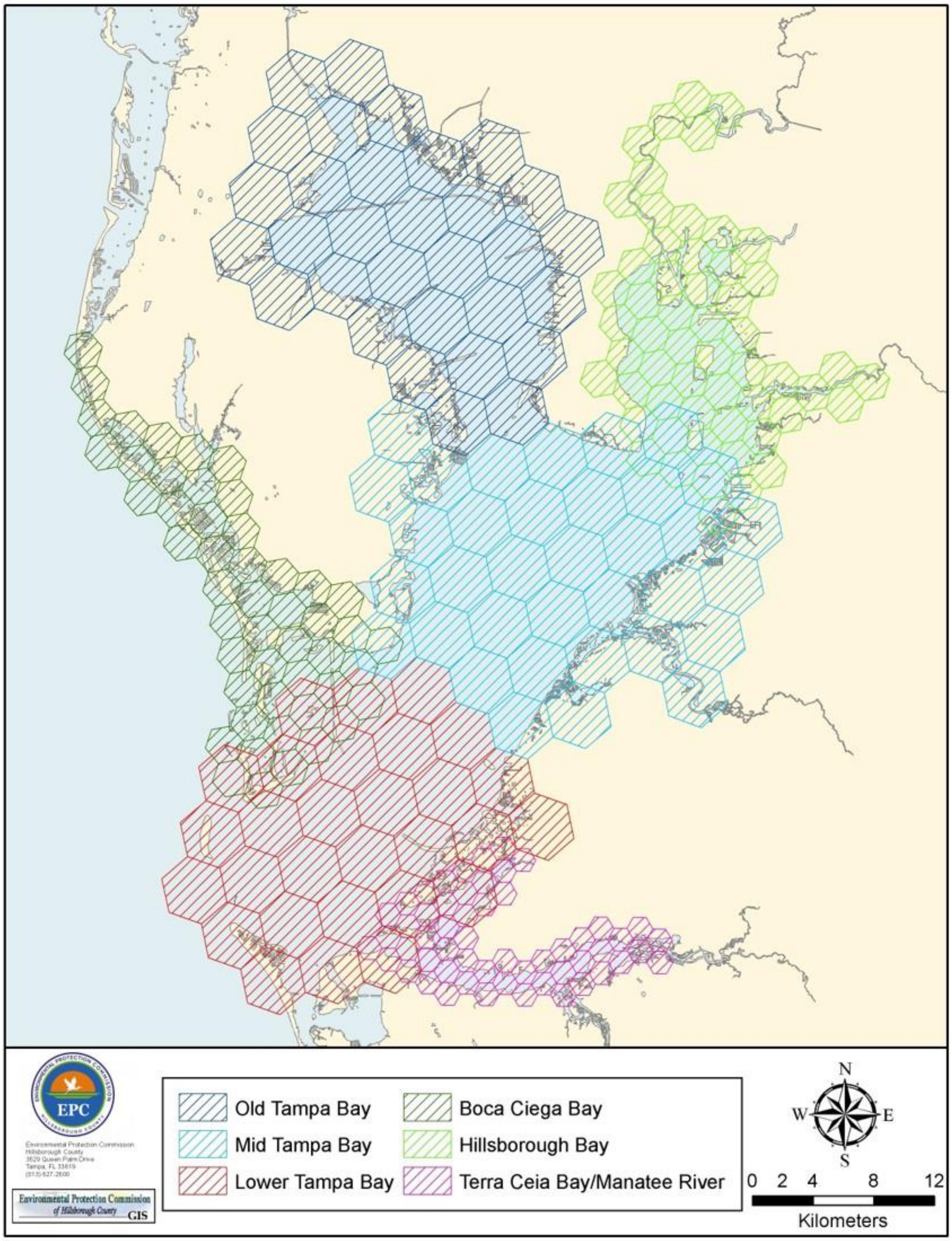

Figure 1. Tampa Bay segments and sampling grids.

Field Collection

Field and laboratory methods were adopted from the EMAP-E Louisianan Province operations manual (Macauley, 1993) and modified for the Tampa Bay monitoring program (Versar, 1993; Courtney et al., 1995). Several modifications to the field sampling routine have been incorporated over the years, as equipment has improved in order to streamline the field sampling and increase efficiency. The following is a brief outline of current field procedures.

Hydrographic Measurements: A hydrographic profile was taken at each station using a Hydrolab® multi-probe sonde. Measurements were taken from the surface (0.1 meters) to the bottom at 1-meter intervals for temperature, salinity, pH, and dissolved oxygen.

Benthic Macrofauna: Sediment samples for benthic macrofaunal community analysis were taken at each site using a Young-Modified Van Veen grab sampler. The grab sample was taken to a sediment depth of 15 cm and covered an area of 0.04 m^2. A 60 cc corer was used to take a subsample for Silt+Clay analysis (see subsection below). The sample was emptied into a plastic bag and residual sediment was washed out of the sampler into the bag with squeeze bottles of ambient seawater. An Epsom salt/seawater solution was added to the sample (equivalent to approximately 1/3 of the sample volume) to relax the organisms. An internal station label was added to the sample; the bag was tied and stored on ice. Samples were sieved through a 0.5 mm mesh sieve and the remaining fraction was rinsed into plastic sample jars. Samples were fixed with 10% buffered formalin for a minimum of 72 hours, and then transferred into 70% isopropyl alcohol for preservation and storage. Rose Bengal was added to the formalin and isopropyl alcohol solutions to stain the organisms. Starting in 2015, samples were fixed using NOTOXhisto™ (Scientific Device Laboratory) for a minimum of 72 hours, then transferred into70% isopropyl alcohol with Rose Bengal for preservation and storage.

Silt+Clay: A 60 cc subsample was removed from the benthic macrofauna sediment grab using a clear plastic syringe corer for Silt+Clay analysis. The apparent Redox Potential Discontinuity (RPD) layer was measured visually with a ruler while the sediment was in the corer. The subsample was then extruded into a HDPE sample jar and stored on ice. An additional sample was taken at 10% of the sites for QA/QC. Samples were stored at 4°C until processing.

Sediment Chemistry: One or more additional sediment grab samples were taken at each site for sediment contaminant analysis depending on the sediment type. The grab sampler and all sampling utensils were field cleaned with Liqui-Nox® detergent (Alconox, Inc. White Plains, NY), rinsed with ambient seawater and decontaminated with 99% pesticide grade isopropyl alcohol (2-Propanol, FisherChemicals, Fisher Scientific Fair Lawn, NJ) prior to sampling. All equipment and samples were handled wearing latex gloves. The top 2 cm layer of sediment was removed from each grab using a stainless steel or Teflon coated spoon and placed in a stainless-steel beaker. If more than one grab was taken, the removed layers of sediment were composited in the stainless-steel beaker and homogenized by stirring. The homogenized sample was then split, with one fraction being placed in a HDPE sample bottle for metals analysis, and the second fraction being placed in a glass sample jar with a Teflon® lined lid for analysis of organic compounds (pesticides, PCBs, PAHs).

Laboratory Procedures

Field data

Hydrographic and other field data were entered into a Microsoft® Access database maintained by the Environmental Protection Commission of Hillsborough County.

Sediment Chemistry

All sediment chemistry samples were analyzed by the EPCHC, except for the initial year of the program (1993) when samples were analyzed by the Skidaway Institute of Oceanography in Savannah, Georgia. Organic samples were not processed for 1994 due to delays in equipment installation and exceedance of sample holding times.

The sediment metal samples were processed using a total digestion method with hydrofluoric acid using a CEM MARS Xpress microwave digester. Analysis was performed on a Perkin Elmer Optima 2000 Optical Emission Spectrometer according to EPA Method 200.7.

The organic samples were extracted using EPA Method 3545A (Accelerated Solvent Extraction), followed by the cleanup methods, EPA 3630C (Silica gel) and EPA 3660B (copper). Analysis was completed using EPA Method 8081 (organochlorine pesticides) and EPA Method 8082 (PCB congeners) on a gas chromatograph equipped with dual Electron Capture Detectors (ECDs). Polycyclic aromatic hydrocarbons (PAHs) were analyzed using EPA Method 8270c on a mass spectrometer.

Silt+Clay Analysis

The Silt+Clay analysis followed procedures outlined in Versar, 1993. This analysis was conducted by Manatee County Department of Environmental Management from 1993-2001 except 1994, when it was done by EPCHC. Analysis was done in-house by EPCHC since 2002.

Benthic Community Analysis

Benthic sorting and identification work were conducted by EPCHC staff for all years excluding 1993 and 1997. In 1993, the identification work was contracted to Mote Marine Laboratory or subcontracted to the Gulf Coast Research Laboratory (crustaceans). Part of the 1997 sample processing was contracted to Versar, Inc. Benthic sediment samples were sorted under a dissecting microscope into general taxonomic categories (Annelids, Mollusks, Crustaceans, and Miscellaneous Taxa). Resorting was done on 10% of the samples completed by each technician for QA/QC. The sorted animals were identified to the lowest practical taxonomic level (species level when possible) and counted. Taxonomic identifications were conducted using available identification keys and primary scientific literature. All identification and count data were recorded on laboratory bench sheets and entered into a Microsoft Access® database maintained by the EPCHC.

Data Analysis

Data Categorization

A Structured Query Language (SQL) routine was used to assign samples to descriptive categories for depth, salinity, dissolved oxygen, sediment type, and Tampa Bay Benthic Index (TBBI) score (Table 1). Ranges for depth categories were based on the median and 1st and 3rd quartile values for all sampling sites collected for the bay-wide benthic monitoring program from 1993-2004. The dissolved oxygen ranges were based on the state water quality standards and salinity category ranges were based on the Venice System (Venice Symposium, 1959). Sediment categories were estimated from percent silt+clay measurements and based on the Wentworth size class system (cf. Percival and Lindsay 1997). Sediment grain size (Φ) was determined by regressing percent silt+clay (% SC) vs. mean grain Φ size for Tampa Bay data collected by Long *et al.*, (1994) using TableCurve 2D ver. 5.0 software (AISN, 2000). These data were used to develop the following relationship between % SC and mean grain size: % SC= 1/ $(0.0097+1.575*e^{\Phi})$ (Adjusted r^2=0.947). Ranges for the Tampa Bay Benthic Index were derived by Janicki Environmental (2005) and Malloy et al., (2007) with the following modifications: Negative TBBI scores, (typically sites with very low abundance dominated by Capitellid polychaetes) were labeled as "Undefined" and removed from analysis; depauperate samples were assigned a TBBI score of 0 and labeled as "Empty".

In addition to the TBBI, this report has attempted a preliminary adaptation of the AZTI Marine Biotic Index (AMBI) developed for European estuarine and coastal soft-bottom environments (Borja et al., 2000, Grall and Glémarec 1997). The AMBI assigns individual taxa to one of five ecological groups (GI, GII, GIII, GIV, GV), with group GI consisting of the most pollution sensitive taxa and GV consisting of the most pollution tolerant taxa. A Biotic Coefficient (BC) is then calculated based on the percent abundance of each ecological group using the following formula proposed by Borja et al., (2000):

Biotic Coefficient = {(0 x %GI) + (1.5 x% GII) + (3 x % GIII) + (4.5 x % GIV) + (6 x %GV)}/100.

The BC has a continuous range from 0-6 with empty ("Azoic") samples assigned a score of 7. The BC scores are further assigned to a site pollution classification with the following BC sores:

$0.0 < BC \leq 1.2$ – "Unpolluted"
$1.2 < BC \leq 3.3$ – "Slightly polluted"
$3.3 < BC \leq 5.0$ – "Meanly polluted"
$5.0 < BC \leq 6.0$ – "Heavily polluted"
BC = 7 ("Azoic" samples) – "Extremely polluted"

Gillet et al., (2015) adapted the AMBI for the United States coastal waters by assigning the ecological groups to regional species lists, including the Gulf of Mexico. We applied the Gulf of Mexico ecological groups to our Tampa Bay taxa list to calculate a regional AMBI Biotic Coefficient and assigned site pollution classification, hereafter referred to as the Gulf of Mexico (GoM) AMBI.

We further attempted to refine the AMBI specifically to our Tampa Bay monitoring dataset by compiling all samples in our database with both sediment chemistry and benthic species data (n = 2,682 samples). To increase sample size, we included samples collected from Special Study locations as part of the Bay-wide Benthic Monitoring program. We likewise utilized samples from other projects including the Tidal Streams study (Sherwood et al 2007), Dredge Hole studies (Grabe et al., 2005; Karlen et al., 2018) and the Hillsborough Independent Monitoring Program (HIMP), in order to include more freshwater and low salinity sites and areas of high sediment contamination. The compiled samples were assigned to a pollution category based on their bottom dissolved oxygen category and sediment contaminant level. The sediment contaminant level for a given sample was assigned a letter grade (A, B, C. D, F) based on the mean Probable Effects Level (PEL) ratio. The PEL ratio grades were based on the overall distribution of PEL ratios across all samples. Sites that fell within the 10th percentile (lowest 10% PEL ratios, i.e. least contaminated sediments) were assigned an "A", sites within the 10^{th}-25^{th} percentile were assigned a "B", sites within the 25^{th}-75^{th} percentile were assigned a "C", sites within the 75^{th}-90^{th} percentile were assigned a "D", and sites above the 90^{th} percentile were assigned an "F". The sites were assigned factors based on their PEL-Grade and bottom dissolved oxygen category (i.e. "Normoxic_A, Anoxic_F etc.). The benthic species compositions were averaged within these factors in PRIMER v. 7, and the zero-adjusted Bray-Curtis similarity (Clarke et al., 2006) was calculated on fourth root transformed abundance data. The resulting similarity matrix was used for running a Cluster Analysis to group the averaged factors by similar species assemblages. These cluster groups were then used to assign individual taxa into the AMBI ecological groups outlined above. The Biotic Coefficient was calculated as with the GoM AMBI. The final BC value was adjusted using the formula [(7-BC) x (10/7)] to rescale the final index from 0-10, with empty samples scoring as "0" and increasing values towards 10 indicating less polluted sites – hereafter referred to as the "Adjusted Tampa Bay AMBI" (Adj. TB_AMBI). The site pollution BC thresholds were similarly adjusted as follows:

0.00 – 1.39 = "Extremely polluted"
1.40 – 2.89 = "Heavily polluted"
2.90 – 5.29 = "Meanly polluted"
5.30 – 8.29 = "Slightly polluted"
8.30 – 10.00 = "Unpolluted"

The Adj. TB_AMBI is still under development and a more detailed description of the methodology will be given in a forthcoming report.

Potential toxicity levels for sediment contaminants followed the sediment quality guidelines established for Florida coastal waters, and utilized the Threshold Effects Levels (TELs) and Probable Effects Levels (PELs) established for individual contaminants (MacDonald 1994; MacDonald et al., 1996). The metal:aluminum ratio was used to determine if individual sediment metals were elevated relative to background levels (Schropp et al., 1990).

Univariate Statistical Analysis

Parametric and non-parametric statistical analysis was done using SigmaStat ® 3.5 (SYSTAT Software, Inc. 2006a). Data were log (n+1) or square root transformed for normality, where needed, for the parametric tests. All percent silt+clay data were arcsine transformed. Analysis of

Variance (ANOVA) with a Holm-Sidak pair-wise post hoc test was used to test for differences between years or between bay segments. Where the assumptions of the ANOVA could not be met by the data transformation, a non-parametric Kruskal-Wallis test was used along with a Dunn's Pairwise Multiple Comparison test. Multiple linear regression and Spearman Correlations were calculated to find associations between the biological metrics, physical parameters, and sediment contaminants.

Multivariate Statistical Analysis

PRIMER v7 (PRIMER-E, Ltd. 2015; Clarke and Gorley 2015) and PERMANOVA+ for PRIMER v7 (Anderson et al., 2008) were used for all multivariate statistical analysis, and for calculating univariate biological metrics (species richness, abundance, Shannon Diversity Index, Pielou's Evenness). Species richness (*S*) was defined as the total number of taxa, while abundance (*N*) as number of individuals per m^2 (calculated as the raw count x 25). The Shannon diversity index (*H'*) calculations employed the natural logarithm opposed to log base 2 (Clarke and Warwick 2001). Principal Components Analysis (PCA) and Principal Coordinates Analysis (PCO) were done on the hydrographic and silt+clay data to search for patterns in the environmental data (Clarke and Warwick 2001; Anderson et al., 2008), the data was normalized and log transformed prior to analysis. The zero-adjusted Bray-Curtis similarity (Clarke et al., 2006) was calculated on fourth root transformed abundance data, and the resulting similarity matrix was used for cluster analysis, Non-metric Multi-Dimensional Scaling (MDS), Similarity Percentage (SIMPER), and Analysis of Similarity (ANOSIM). The BIO-ENV procedure (Clarke and Ainsworth 1993) was used to find correlations between the environmental parameters and benthic community structure.

Spatial and Graphical Analysis

Graphs were generated using SigmaPlot® 10.0 software (Systat Software, Inc. 2006b). Sample location and distributional maps were generated by Pinellas County Department of Environmental Management. Species distributional maps were generated by the Environmental Protection Commission of Hillsborough County using ArcGIS 10.1 (ESRI, 2012).

Table 1. Physical and TBBI descriptors and threshold values.

Depth	
0-0.5 m	Intertidal
>0.5-1.0 m	Shallow subtidal
>1.0-2.0 m	Intermediate Subtidal
>2.0-4.0 m	Deep Subtidal
> 4 m	Deep
Dissolved Oxygen	
0-0.5 ppm	Anoxic
>0.5 – 2.0 ppm	Hypoxic
>2.0-4.0 ppm	Low
> 4.0 ppm	Normoxic
Salinity	
0- 0.5 psu	Tidal Fresh Water
>0.5-5.0 psu	Oligohaline
>5.0-10.0 psu	Low Mesohaline
>10.0 -18.0 psu	High Mesohaline
>18.0-30.0 psu	Polyhaline
> 30.0 psu	Euhaline
Silt+Clay	
0 - 1.70%	Coarse
>1.70-4.51%	Medium
>4.51-11.35%	Fine
>11.35 – 25.95%	Very Fine
> 25.95%	Mud
Tampa Bay Benthic Index	
< 0	Undefined
0	Empty
>0 – 73	Degraded
>73 – 87	Marginal
≥ 87	Healthy

Results and Discussion

Sampling Locations

A total of 1791 random sites were sampled between 1993-2017 throughout the seven bay segments (Figure 2). The numbers of sites (n) are given for each sampling year and bay segment in Tables 2 and 3 respectively, and illustrated in Figure 2. The number of samples collected per year and bay segment decreased after 2000 from the program redesign, although the original sampling effort was maintained in Hillsborough Bay. The sampling effort was further reduced in 2005 across all bay segments. The current sampling design includes approximately 44 bay-wide samples collected across 5 strata: Hillsborough Bay, Old Tampa Bay, Middle + Lower Tampa Bay, Manatee River + Terra Ceia Bay, and Boca Ciega Bay. Additionally, approximately 20 samples are collected at designated special study sites each year to focus sampling efforts in areas of special interest. The special study samples for 2010 were collected in Old Tampa Bay and are included with the 2010 OTB bay-wide samples in the analysis.

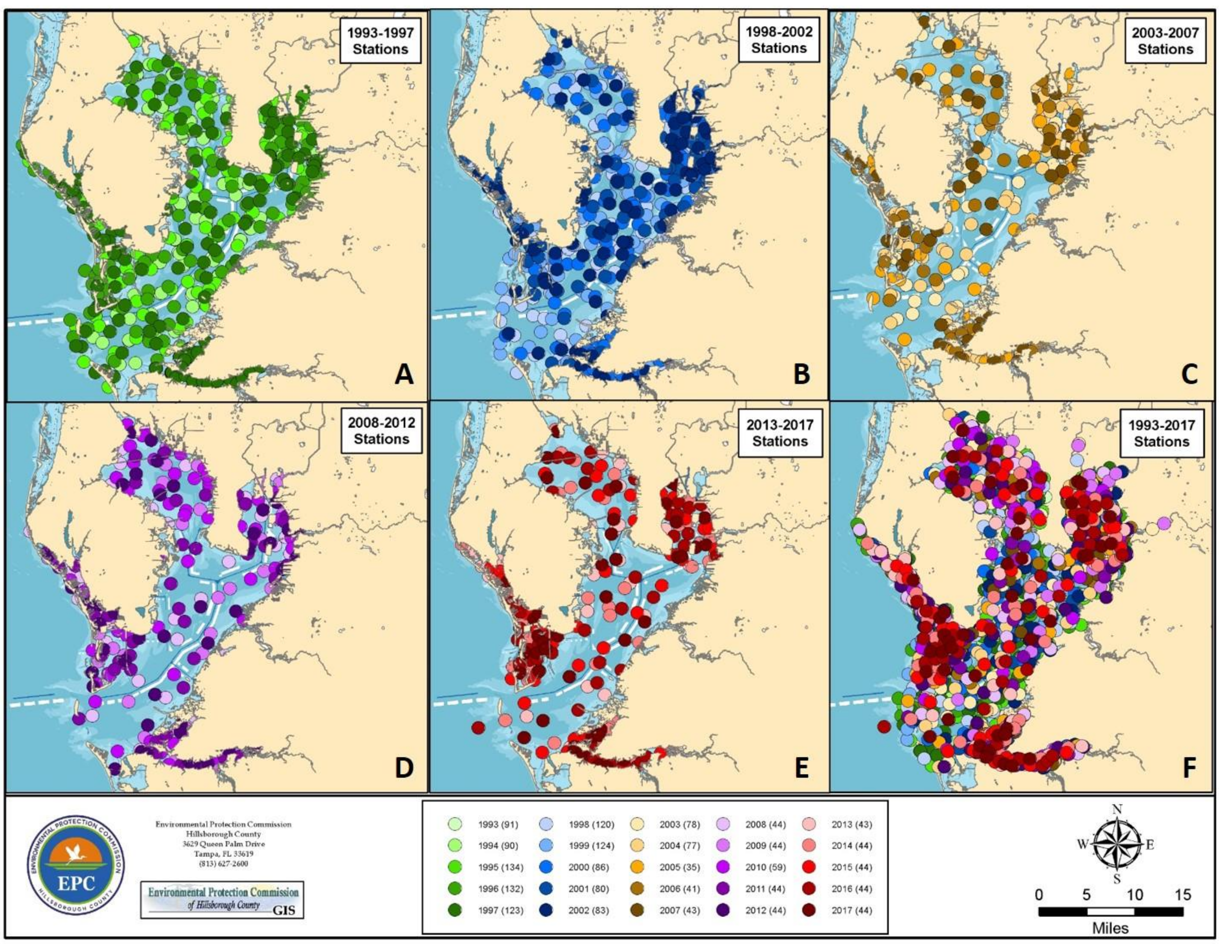

Figure 2. Tampa Bay benthic monitoring sampling sites 1993-2017 by 5-year periods (A-E)

and 25-year cumulative data (F). Cumulative total = 1791 sampling sites. Number of sites by year in parenthesis.

Hydrographic and Sediment Characteristics

Table 2. Bay-wide bottom physical characteristics 1993-2017 by year. Top values are medians, lower left= minimum, lower right = maximum. For TOC n = 366. ND = No Data.

Year	n	Depth (meters)		Temperature (°C)		Salinity (psu)		D.O. (mg/L)		D.O. (% Sat.)		pH		Silt+Clay (%)		TOC (%)	
1993	91	2.8		29.4		25.6		5.4		81.2		7.8		3.4		ND	
		0.1	10.0	25.9	31.2	4.3	34.2	0.3	11.0	4.1	166.5	6.5	8.2	0.0	69.7	ND	ND
1994	90	3.0		28.0		22.7		5.0		74.6		7.9		2.9		ND	
		1.0	8.0	24.9	30.7	7.2	34.8	0.2	10.2	3.0	150.8	7.1	8.3	0.0	86.8	ND	ND
1995	134	2.0		29.0		20.1		5.7		82.7		8.1		3.3		ND	
		0.1	9.0	21.6	33.0	4.3	34.1	0.2	11.3	3.2	157.1	7.1	8.5	0.2	70.3	ND	ND
1996	132	2.9		29.4		26.1		5.0		76.9		8.0		4.4		ND	
		0.1	13.2	22.9	39.2	7.9	34.5	0.3	9.3	4.1	144.1	6.9	8.3	0.8	75.4	ND	ND
1997	123	2.2		28.9		27.6		5.3		80.3		8.0		6.6		ND	
		0.1	11.8	23.9	31.2	0.0	35.9	0.0	14.0	0.5	220.7	6.7	8.7	0.0	81.1	ND	ND
1998	120	2.5		28.2		24.1		5.6		81.7		8.0		3.9		ND	
		0.1	12.5	25.1	33.4	1.8	33.0	0.4	9.5	5.8	135.0	6.8	8.4	1.0	39.4	ND	ND
1999	124	2.8		27.6		25.9		5.6		82.4		8.1		4.3		ND	
		0.1	12.5	25.9	32.0	9.0	35.0	1.0	12.8	15.3	190.5	7.4	8.9	0.8	82.2	ND	ND
2000	86	3.0		28.7		28.7		5.7		84.1		8.0		4.4		ND	
		0.5	8.5	26.1	30.9	5.3	32.9	0.2	9.1	3.4	140.6	7.3	8.4	0.1	91.8	ND	ND
2001	80	3.0		30.2		27.8		4.1		64.9		8.0		4.1		ND	
		0.1	11.0	24.4	32.4	22.0	34.1	0.4	10.7	5.3	162.7	7.5	8.4	1.5	57.8	ND	ND
2002	83	3.1		29.5		27.9		5.1		77.5		8.0		4.6		ND	
		0.5	11.3	27.9	31.3	9.2	34.5	0.3	8.8	4.1	132.2	7.0	8.9	0.0	84.9	ND	ND
2003	78	3.4		29.2		19.5		5.2		73.0		8.0		5.0		ND	
		0.1	9.0	26.3	34.5	0.1	33.4	0.2	9.2	2.7	137.6	7.0	8.6	1.0	71.1	ND	ND
2004	77	3.0		29.7		22.7		5.0		74.5		8.1		3.2		ND	
		0.6	13.0	24.0	31.4	13.9	34.0	0.1	11.0	1.6	165.3	7.4	8.6	0.7	65.7	ND	ND
2005	35	2.2		30.0		23.9		5.3		77.4		8.1		3.6		ND	
		0.5	13.3	27.8	34.2	17.9	34.6	0.1	6.7	1.8	104.4	7.2	8.8	1.1	32.9	ND	ND
2006	41	2.4		29.9		25.6		5.1		77.7		8.1		3.3		ND	
		0.1	7.7	27.2	31.6	1.4	35.4	0.1	7.8	1.8	118.5	7.5	8.4	0.7	94.3	ND	ND

Year	n	Depth (meters)		Temperature (°C)		Salinity (psu)		D.O. (mg/L)		D.O. (% Sat.)		pH		Silt+Clay (%)		TOC (%)	
2007	**43**	3.1		30.7		29.7		4.7		74.5		8.1		4.8		ND	
		0.3	11.7	27.7	33.5	18.3	35.6	0.9	10.8	14.8	181.6	7.5	8.6	1.0	25.1	ND	ND
2008	**44**	2.4		29.1		27.3		5.2		79.3		7.8		4.8		ND	
		0.3	8.3	27.2	31.8	15.7	36.3	2.8	9.2	41.0	136.0	7.2	8.2	1.4	64.1	ND	ND
2009	**44**	2.5		29.7		26.9		4.7		73.1		7.8		5.1		ND	
		0.2	11.0	28.2	33.3	1.9	35.4	0.4	10.1	6.6	166.2	7.0	8.2	1.4	96.0	ND	ND
2010	**59**	2.1		29.2		21.1		5.0		74.9		8.4		4.1		0.4	
		0.1	10.9	26.4	33.1	8.0	34.2	0.2	8.7	2.6	125.0	7.0	9.4	0.9	74.7	0.3	3.8
2011	**44**	2.2		30.8		26.5		4.8		76.3		8.3		5.8		0.5	
		0.5	11.2	21.3	33.6	13.7	34.2	0.1	8.5	1.7	114.8	7.0	8.8	1.1	48.6	0.3	6.8
2012	**44**	2.8		30.1		23.0		4.8		73.6		7.9		5.7		0.4	
		0.3	10.6	28.6	33.3	3.4	34.6	0.5	7.6	7.5	115.5	7.2	8.3	1.0	60.3	0.3	2.9
2013	**43**	2.3		29.9		23.4		5.7		88.4		8.1		4.9		0.6	
		0.4	6.7	23.5	33.9	16.5	33.7	0.3	10.7	5.0	166.2	6.8	8.6	1.1	84.9	0.3	8.3
2014	**44**	2.6		31.1		27.4		4.9		78.1		7.9		4.2		0.7	
		0.5	11.3	30.2	33.8	16.3	35.2	1.3	7.7	20.3	121.4	7.5	8.4	1.2	72.0	0.2	8.3
2015	**44**	2.6		30.1		22.0		4.8		71.2		8.0		3.6		1.3	
		0.5	9.4	27.2	34.1	5.5	31.7	0.2	9.3	2.4	144.6	7.3	8.5	1.2	43.8	0.9	9.8
2016	**44**	2.9		31.4		25.8		5.5		85.6		8.0		4.6		0.4	
		0.3	9.3	27.1	32.4	15.2	33.4	0.1	8.3	1.7	133.5	7.5	8.4	1.2	49.5	0.1	6.8
2017	**44**	2.3		30.8		23.6		4.6		76.1		7.8		4.6		0.4	
		0.8	6.8	27.8	31.9	16.8	32.7	0.1	8.9	2.1	139.5	7.1	8.6	1.6	78.9	0.4	4.5
Cumulative	**1791**	**2.7**		**29.3**		**25.9**		**5.2**		**78.7**		**8.0**		**4.4**		**0.6**	
1993-2017		**0.1**	**13.3**	**21.3**	**39.2**	**0.0**	**36.3**	**0.0**	**14.0**	**0.5**	**220.7**	**6.5**	**9.4**	**0.0**	**96.0**	**0.1**	**9.8**

Table 3. Bottom physical parameters 1993-2017 by bay segment. Top values are medians, lower left= minimum, lower right = maximum. For TOC, cumulative n = 366.

Segment	n	Depth (meters)		Temperature (°C)		Salinity (psu)		D.O. (mg/L)		D.O. (% Sat.)		pH		Silt+Clay (%)		TOC (%)	
Hillsborough Bay	407	2.8		29.7		23.0		3.7		54.0		7.8		7.2		0.7	
		0.1	13.3	25.5	34.5	0.1	30.1	0.0	10.7	0.5	166.2	6.8	8.6	1.0	96.0	0.1	4.8
Old Tampa Bay	269	2.6		29.2		22.1		5.3		78.9		8.1		3.5		0.4	
		0.1	7.5	26.0	33.9	0.0	29.4	0.1	12.8	1.6	190.5	6.7	9.4	0.0	91.8	0.1	3.4
Middle Tampa Bay	303	4.0		29.2		26.8		5.2		79.0		8.0		2.9		0.4	
		0.1	11.1	26.0	39.2	8.1	32.4	0.3	11.0	4.3	165.3	6.9	9.0	0.0	63.0	0.1	4.5
Lower Tampa Bay	221	4.0		28.5		30.6		5.8		87.5		8.1		2.4		0.6	
		0.1	13.0	23.9	31.9	19.3	35.0	3.6	9.3	53.1	137.2	7.2	8.8	0.0	50.7	0.2	6.3
Manatee River	193	2.0		29.0		18.8		5.2		77.3		7.8		5.6		0.9	
		0.1	7.0	22.1	34.1	0.4	31.5	0.3	9.3	4.1	144.6	6.5	8.9	0.7	55.4	0.1	7.3
Terra Ceia Bay	110	2.0		28.5		26.0		6.0		88.4		8.1		4.6		0.6	
		0.1	5.0	21.3	33.3	10.1	33.0	1.8	10.1	26.8	168.7	7.4	8.6	0.0	25.4	0.2	9.8
Boca Ciega Bay	288	1.9		29.7		32.2		5.5		85.8		8.1		6.4		0.6	
		0.1	7.4	21.6	33.5	20.4	36.3	0.9	14.0	15.1	220.7	7.4	8.9	1.1	94.3	0.1	8.3
Cumulative 1993-2017	**1791**	**2.7**		**29.3**		**25.9**		**5.2**		**78.7**		**8.0**		**4.4**		**0.6**	
		0.1	**13.3**	**21.3**	**39.2**	**0.0**	**36.3**	**0.0**	**14.0**	**0.5**	**220.7**	**6.5**	**9.4**	**0.0**	**96.0**	**0.1**	**9.8**

Depth

The median sample depth bay-wide was 2.7 meters (mean = 3.0 meters; Figures 3 & 4), with a maximum depth of 13.3 meters for the shipping channel in Hillsborough Bay (Tables 2 and 3). Sample depths varied significantly between years ($p = 0.019$) with median values ranging from 2 meters in 1995 to 3.4 meters in 2003 (Table 2; Figure 3). The shallower depths observed in 1995 may have been due in part to sampling bias, as there was an asserted effort to collect shallow sites that year. There was an apparent decrease in the average sample depth since 2005 (Figure 3). This can be attributed to fewer samples being collected in the Middle and Lower Tampa Bay segments and an overall decrease in the number of samples collected.

Depth between bay segments were also significantly different (KW; $p < 0.001$) with the shallowest median depth in Boca Ciega Bay, and the deepest median depths in the Middle and Lower Tampa Bay segments (Table 3; Figure 4). Middle and Lower Tampa Bay were not significantly different from each other, but were significantly deeper than the other bay segments. There was a general trend of increasing depth towards the mouth of the bay (Figure 5). However, the deepest sites were recorded in dredged shipping channels and port areas within

Hillsborough Bay. Most of the sampling sites fell within the “Deep Subtidal” range (>2.0 – 4.0 meters) bay-wide and within most bay segments (Table 4). Over half of the sampling sites in the Middle and Lower Tampa Bay segments were categorized as “Deep” with depths exceeding 4 meters (Table 4).

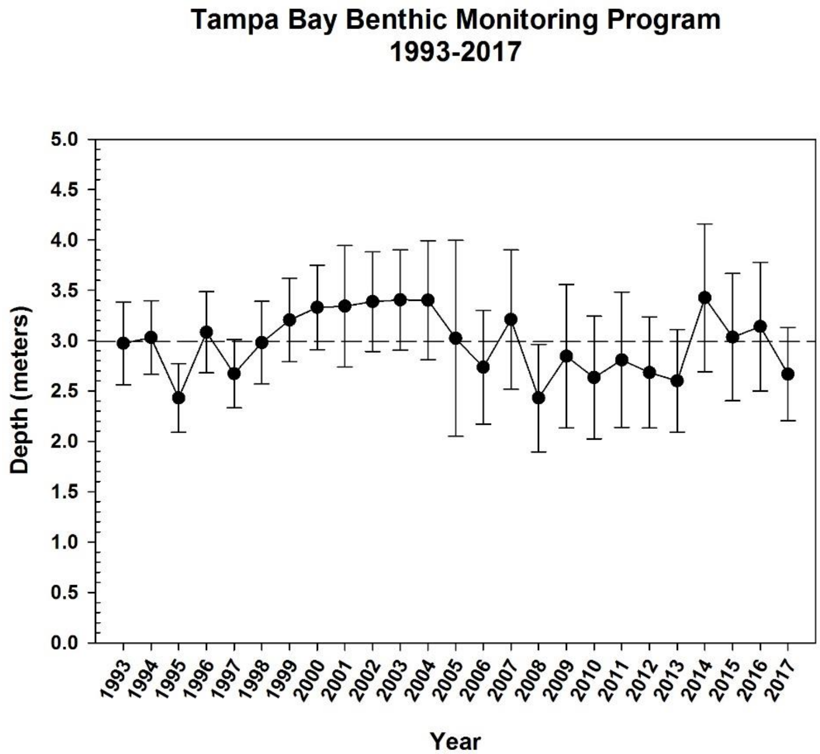

Figure 3. Mean sample depth by year. Error bars = 95% confidence interval, dashed line represents bay-wide mean.

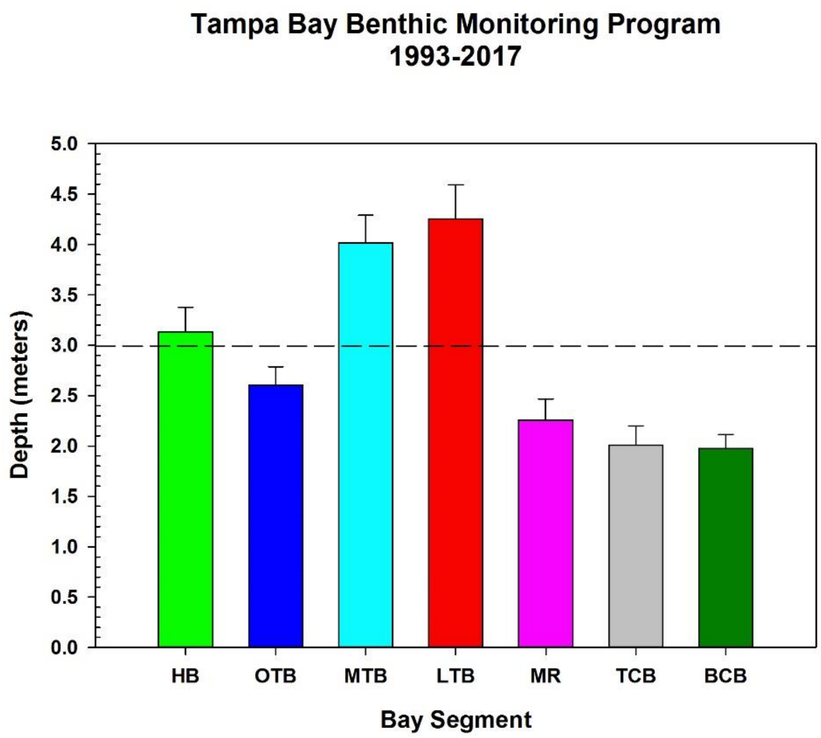

Figure 4. Mean sample depth by bay segment. Error bars = 95% confidence interval, dashed line represents bay-wide mean value.

Table 4. Percentage of sites within depth categories 1993-2017.

	n	Intertidal 0-0.5 m	Shallow Subtidal >0.5-1.0m	Intermediate Subtidal >1.0-2.0m	Deep Subtidal >2.0-4.0m	Deep >4.0m
Hillsborough Bay	407	7.86%	14.50%	16.22%	31.45%	29.98%
Old Tampa Bay	268	8.58%	13.06%	18.66%	37.31%	22.39%
Middle Tampa Bay	303	6.27%	7.59%	10.89%	23.43%	51.82%
Lower Tampa Bay	221	3.17%	8.60%	10.86%	24.89%	52.49%
Manatee River	193	7.25%	20.21%	31.61%	21.76%	19.17%
Terra Ceia Bay	110	5.45%	22.73%	30.91%	37.27%	3.64%
Boca Ciega Bay	288	8.68%	15.97%	31.94%	37.50%	5.90%
Tampa Bay (Total)	1790	7.04%	13.74%	20.11%	30.45%	28.66%

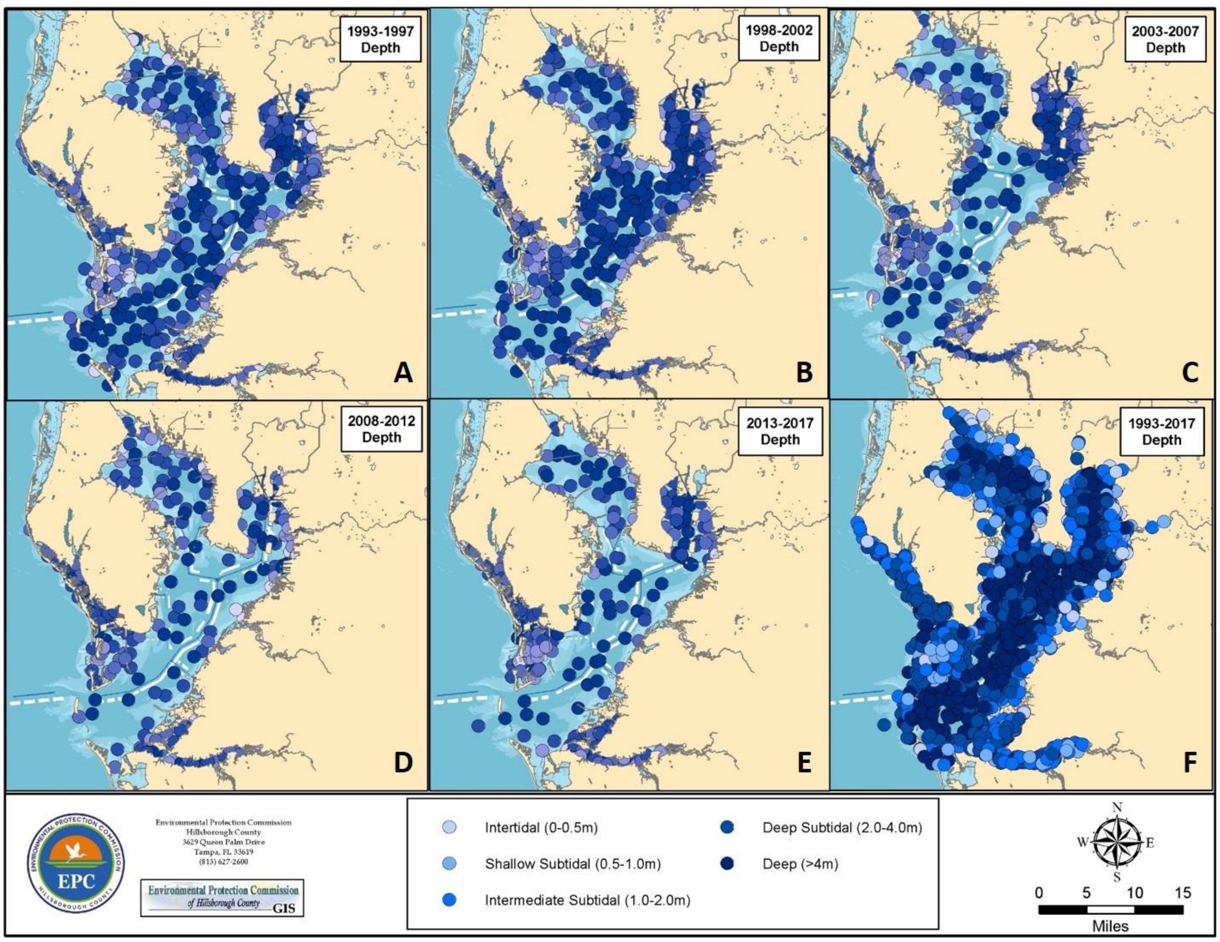

Figure 5. Distribution of sample site depth categories 1993-2017 by 5-year periods (A-E) and 25-year composite data (F).

Bottom Temperature

Increasing water temperature can affect burrowing activity in polychaete worms (*Capitella*), and high temperatures can result in mortality (Przeslawski et al., 2009). Higher water temperatures can also influence benthic community composition and species succession by extending the growing season and recruitment of some organisms, and facilitating invasive species (Dijkstra et al 2011). Higher temperatures have been shown to increase the rates of parasitism in some species resulting in higher mortalities and cascading effects at the community level (Larsen and Mouritsen 2014). Increased sea surface temperatures may directly impact the biogeographic distribution of benthic species, influence shifts in life cycles (timing of reproduction/spawning, increase larval mortality) and alter trophic and competitive interactions between benthic species (reviewed in Birchenough et al., 2015).

Bottom temperatures ranged from 21.3 to 39.2°C with a median temperature of 29.3°C and mean of 29.2 °C (Tables 2 and 3). Temperatures varied significantly between years (KW; $p < 0.001$) with the highest median temperature (31.3°C) occurring in 2016, while the highest mean temperature (31.2°C) was in 2014 (Table 2; Figure 6). There was an apparent trend of increasing temperatures over the 25-year monitoring period. Our previous monitoring report (1993-2012) attributed this trend possibly to a sampling artifact from a shift in the collection period since the start of the program (Karlen et al., 2015). However, this increasing trend has continued since 2012 while the program sampling scheme has remained consistent.

Bottom temperatures were significantly different between bay segments (KW; $p < 0.001$). Hillsborough Bay had the highest median temperature and was significantly higher than the other segments except Boca Ciega Bay (Dunn’s Pairwise Multiple Comparison test). The higher water temperature in Hillsborough Bay may be from the extensive shallow area and restricted flow in this area of the bay. The highest temperature (39.2°C) was recorded in Middle Tampa Bay in 1996 near the discharge of the Big Bend power plant (Table 3). The lowest temperature (21.3 °C) was recorded in Terra Ceia Bay in 2011. This segment was sampled in mid-October that year, which accounts for the lower observed water temperatures relative to the other bay segments and the wider standard error among the data for that year (Figure 7).

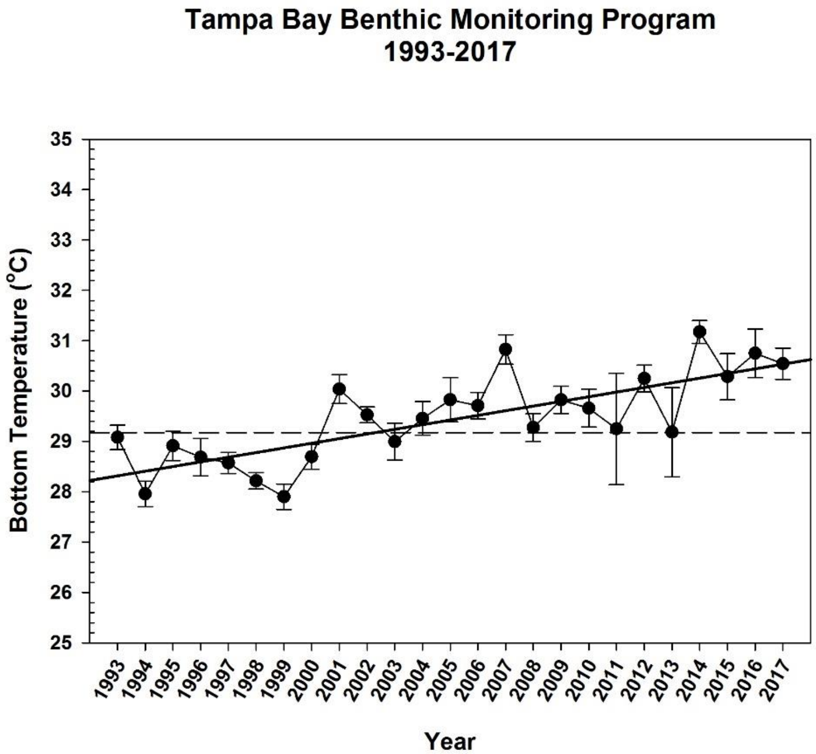

Figure 6. Mean bottom temperature by year. Error bars = 95% confidence interval, dashed line represents bay-wide mean value, solid line indicates 25-year trend.

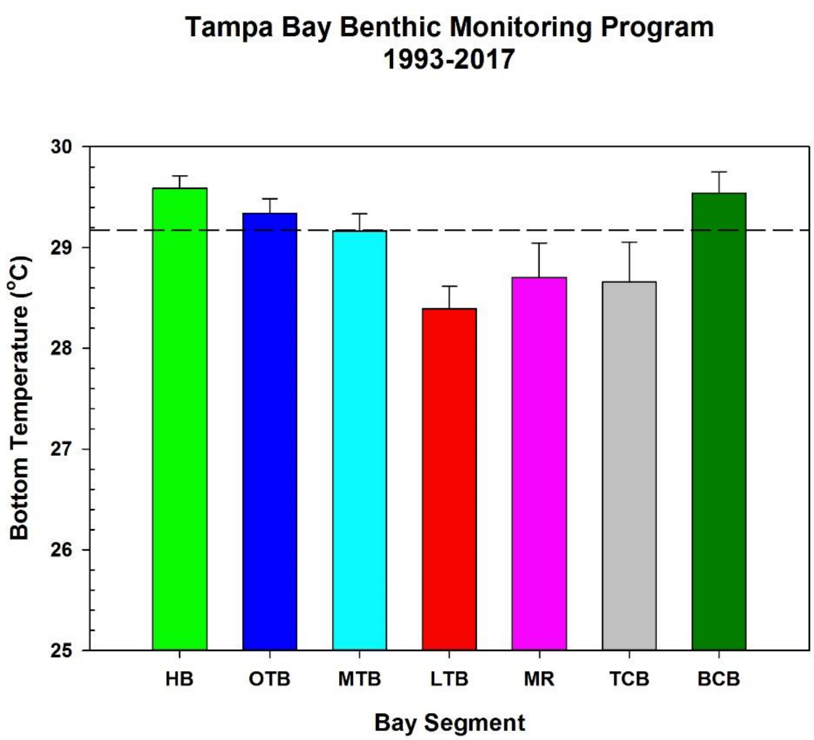

Figure 7. Mean bottom temperature by bay segment. Error bars = 95% confidence interval, dashed line represents bay-wide mean value.

Bottom pH

The median bottom pH was 8.0, and ranged from 6.5 to 9.4. The lowest recorded value and widest range were both in the Manatee River (Table 2 and 3). The highest recorded pH values were in Old Tampa Bay in 2010, due to a bloom of the dinoflagellate *Pyrodinium bahamense* during that year (Karlen 2014). There were significant differences in pH between years (KW; $p < 0.001$, Figure 8), with 1993 recording the overall minimum value. Lowest median pH values were observed in 1993, 2008, and 2009, while the highest median pH was observed in 2010 (Table 2). Although there is a positive correlation between pH and salinity, this did not appear to be a factor in the observed temporal trend in pH. The pH between bay segments also varied significantly, and was lowest in the Manatee River and Hillsborough Bay (KW; $p < 0.001$, Figure 9). This was probably from the greater input of freshwater in these systems. Generally lower pH values are associated with lower salinities due to the presence of acidic compounds in freshwater (tannins) and low concentrations of buffering ions. Higher pH values were observed in Boca Ciega Bay, Terra Ceia Bay and Lower Tampa Bay due in part to higher salinities and possibly to higher seagrass productivity.

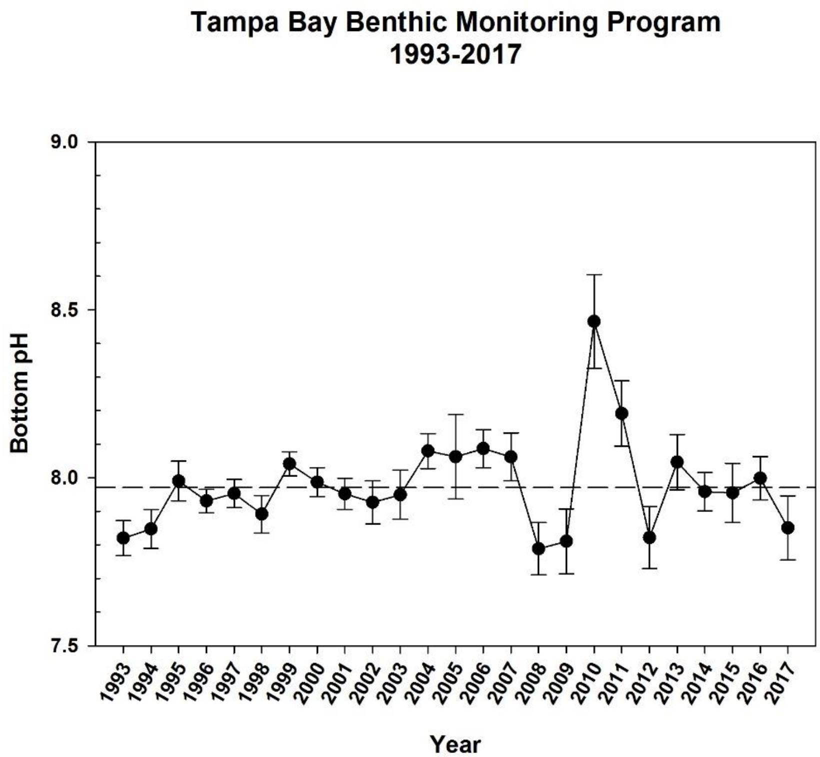

Figure 8. Mean bottom pH by year. Error bars = 95% confidence interval, dashed line represents bay-wide mean value.

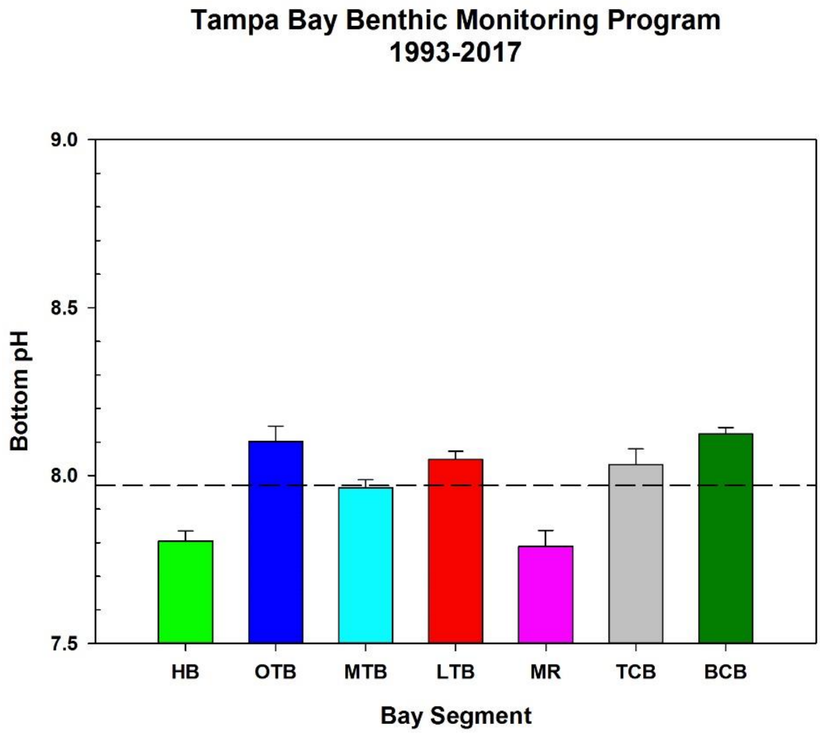

Figure 9. Mean bottom pH by bay segment. Error bars = 95% confidence interval, dashed line represents bay-wide mean value.

Bottom Salinity

Bottom salinities ranged from 0 to 36.3 psu, with a bay-wide median salinity of 26 psu and a mean of 25 psu (Tables 2 and 3). Salinities varied significantly from year to year (KW; $p < 0.001$). Relatively lower salinities occurred in 1995, 2003 and 2015, while 2007 had the highest median salinity (Table 2; Figure 10). Temporal trends generally corresponded with rainfall patterns, with lower salinities observed during years with higher average precipitation and higher salinities observed during periods of drought. Salinities were significantly different between bay segments (KW; $p < 0.001$), with the highest salinities being recorded in Boca Ciega Bay and Lower Tampa Bay, and the lowest median salinity in the Manatee River (Table 3; Figure 11). Most pairwise comparisons (Dunn's method) between bay segments were significant ($p < 0.05$). Boca Ciega Bay had significantly higher salinity than all other bay segments, while the Manatee River has significantly lower salinities than the other bay segments except, for Old Tampa Bay

Most of the sampling sites fell within the polyhaline salinity range, while less than 1% of sites were freshwater or oligohaline (Table 5). The Manatee River had the highest percentage of low salinity sites, while most sites within Boca Ciega Bay and Lower Tampa Bay were euhaline (Table 5). In general, lower salinities were observed in the upper portions of the bay and in the Manatee River, with increasing salinities towards Lower Tampa Bay and Boca Ciega Bay (Table 5; Figures 11 and 12).

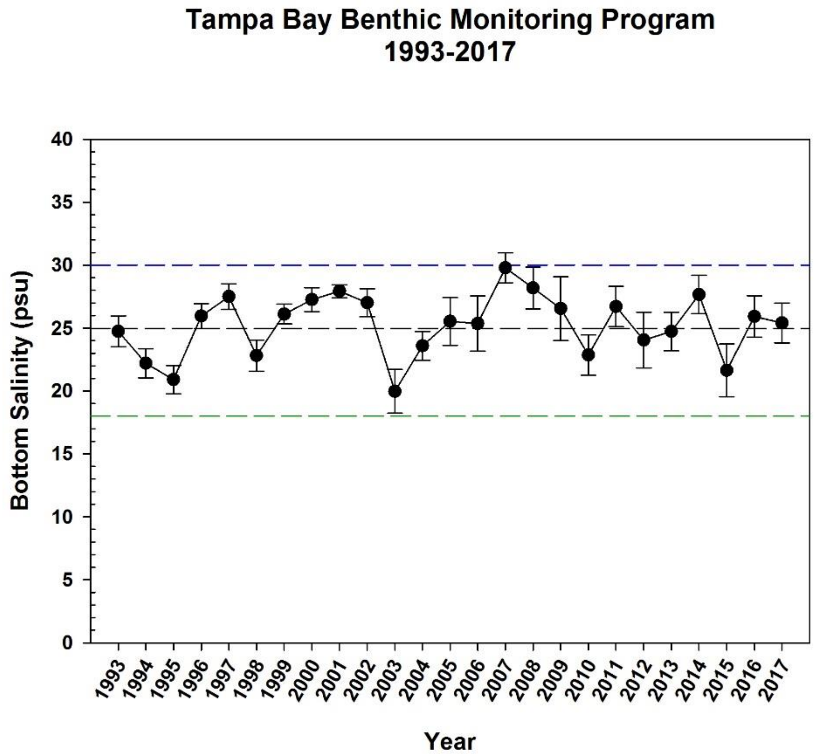

Figure 10. Mean bottom salinity by year. Error bars = 95% confidence interval; middle dashed line represents bay-wide mean value; lower and upper dashed lines denote boundaries of high mesohaline/polyhaline (18 psu) and polyhaline/euhaline (30 psu) salinity categories.

Tampa Bay Benthic Monitoring Program
1993-2017

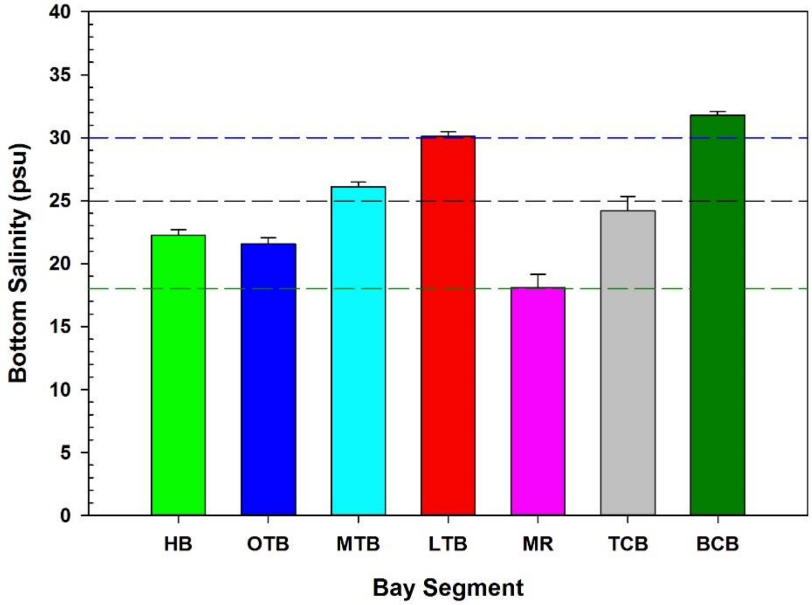

Figure 11. Mean bottom salinity by bay segment. Error bars = 95% confidence interval; middle dashed line represents bay-wide mean value; lower and upper dashed lines denote boundaries of high mesohaline/polyhaline (18 psu) and polyhaline/euhaline (30 psu) salinity categories.

Table 5. Percentage of samples within salinity categories 1993-2017.

	n	Tidal Freshwater 0-0.5 psu	Oligohaline >0.5-5.0 psu	Low Mesohaline >5.0-10.0 psu	High Mesohaline >10.0-18.0 psu	Polyhaline >18.0-30.0 psu	Euhaline >30.0 psu
Hillsborough Bay	407	0.49%	0.74%	0.98%	13.27%	84.28%	0.25%
Old Tampa Bay	269	0.37%	0.00%	0.74%	16.36%	82.53%	0.00%
Middle Tampa Bay	303	0.00%	0.00%	0.33%	1.32%	90.43%	7.92%
Lower Tampa Bay	221	0.00%	0.00%	0.00%	0.00%	41.63%	58.37%
Manatee River	192	0.52%	3.65%	14.06%	25.00%	54.17%	2.60%
Terra Ceia Bay	108	0.00%	0.00%	0.00%	20.37%	67.59%	12.04%
Boca Ciega Bay	288	0.00%	0.00%	0.00%	0.00%	23.61%	76.39%
Tampa Bay (Total)	1788	0.22%	0.56%	1.90%	9.62%	65.77%	21.92%

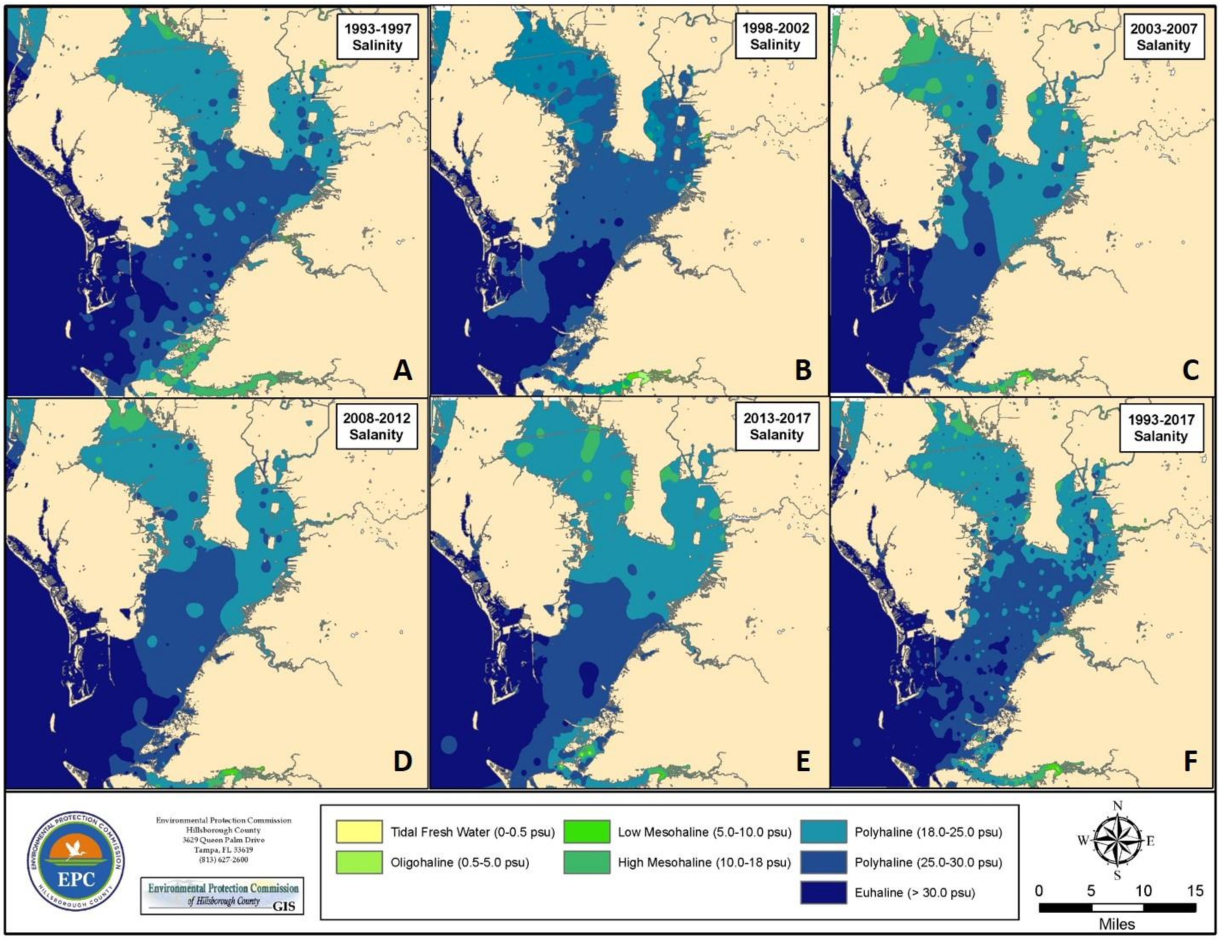

Figure 12. Spatial analysis of bottom salinity 1993-2017 by 5-year periods (A-E) and 25-year composite data (F).

Bottom Dissolved Oxygen

Annual mean bottom dissolved oxygen and percent oxygen saturation measurements over the 25-year monitoring period were consistently above state water quality standards, with a bay-wide median of 5.22 mg/L and 78.2 % saturation (Tables 2 and 3; Figure 13). There were significant differences between years for both parameters (KW; $p < 0.001$), with the lowest median dissolved oxygen in 2001 and highest in 1999 (Figure 13). The maximum dissolved oxygen recorded was in excess of 14 mg/L (>220% saturation) in 1997 at a site in Boca Ciega Bay (Tables 2 and 3). This site (97BCB50) was shallow (0.5 m) and had seagrasses present, therefore the high measurement may have been from these factors. The lower dissolved oxygen levels in 2001 were likely because of a shift in the start of the annual sampling season towards early to mid-August, when water temperatures tended to be higher resulting in lower dissolved oxygen. Mean dissolved oxygen concentrations were generally lower in subsequent years and below the 25-year mean (Figure 13).

Differences between bay segments were also significant (KW; $p < 0.001$). Hillsborough Bay had the lowest mean dissolved oxygen (3.6 mg/l and 53.3% saturation), and was significantly lower than the other bay segments. Terra Ceia Bay had the highest dissolved oxygen, but was not significantly different from Boca Ciega Bay or Lower Tampa Bay (Table 3; Figure 14). Overall, nearly78% of the sites had bottom dissolved oxygen levels within the normoxic range above 4 mg/L (Table 6). Hillsborough Bay had relatively high occurrences of anoxia and hypoxia, while these conditions were nearly absent in the other bay segments (Table 6). The aerial extent of anoxia and hypoxia were also greatest in Hillsborough Bay and in the upper portion of Old Tampa Bay (Table 6; Figure 15). Hillsborough Bay has historically been impacted by hypoxia. Santos and Simon (1980 a&b) documented annual late summer defaunations of the benthic community in Hillsborough Bay from 1975 – 1977 associated with low bottom dissolved oxygen concentrations (< 1 mg/L).

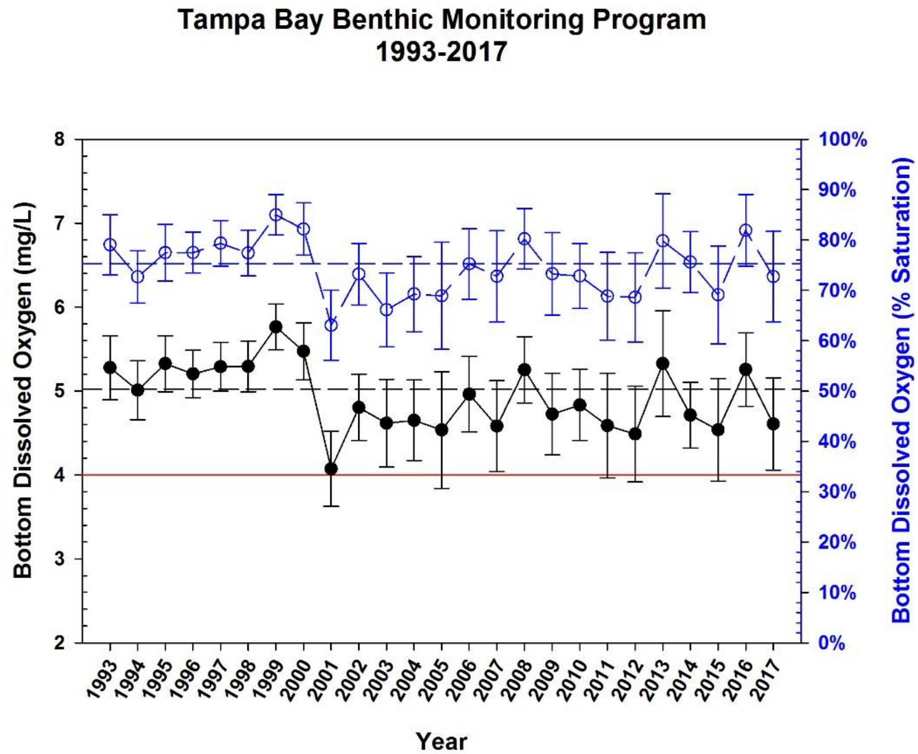

Figure 13. Mean bottom dissolved oxygen by year in mg/L (black closed circles, solid line; left axis) and as % saturation (blue open circles, dashed line; right axis). Error bars = 95% confidence interval, black dashed line represents bay-wide mean concentration, blue dash line represents bay-wide mean saturation; bottom solid red line represents the critical value for normoxic conditions (> 4 mg/l).

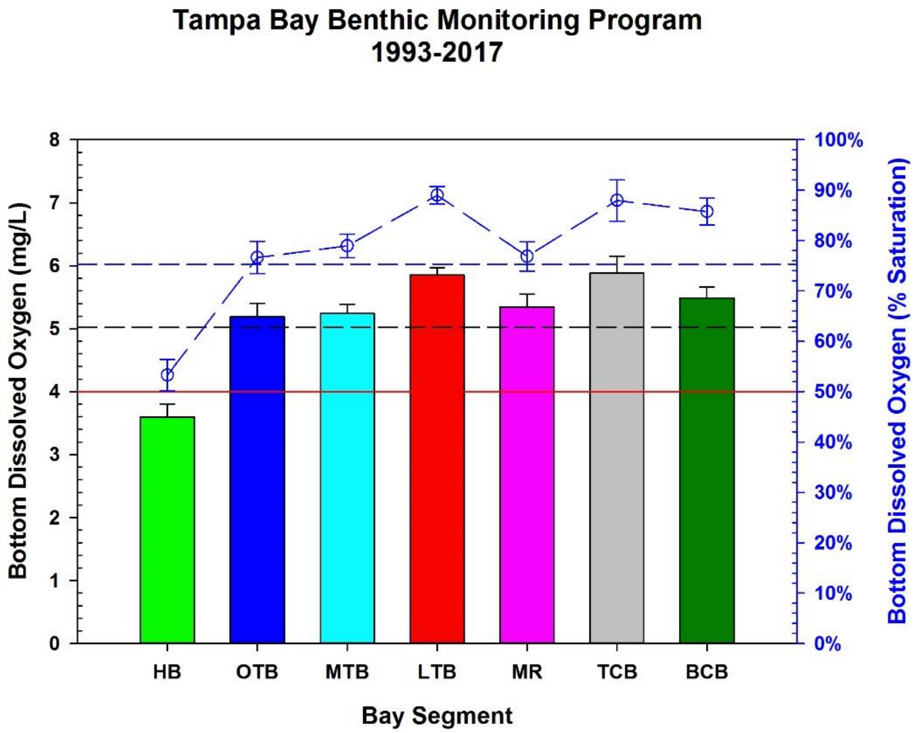

Figure 14. Mean bottom dissolved oxygen by bay segment in mg/L (bar graph; left axis) and as % saturation (line graph; right axis). Error bars = 95% confidence interval, black dashed line represents bay-wide mean concentration, blue dashed line represents bay-wide mean saturation; bottom solid red line represents the critical value for normoxic conditions (> 4 mg/l).

Table 6. Percentage of sample sites within dissolved oxygen categories by bay segment 1993-2017.

	n	Anoxic 0-0.5 mg/l	Hypoxic 0.5-2.0 mg/l	Low >2.0-4.0 mg/l	Normoxic >4.0 mg/l
Hillsborough Bay	405	9.63%	16.79%	27.90%	45.68%
Old Tampa Bay	268	1.49%	2.24%	18.28%	77.99%
Middle Tampa Bay	301	0.33%	0.33%	13.95%	85.38%
Lower Tampa Bay	215	0.00%	0.00%	1.86%	98.14%
Manatee River	191	0.52%	1.57%	8.90%	89.01%
Terra Ceia Bay	109	0.00%	0.92%	8.26%	90.83%
Boca Ciega Bay	285	0.00%	1.05%	11.58%	87.37%
Tampa Bay (Total)	1774	2.54%	4.62%	15.05%	77.79%

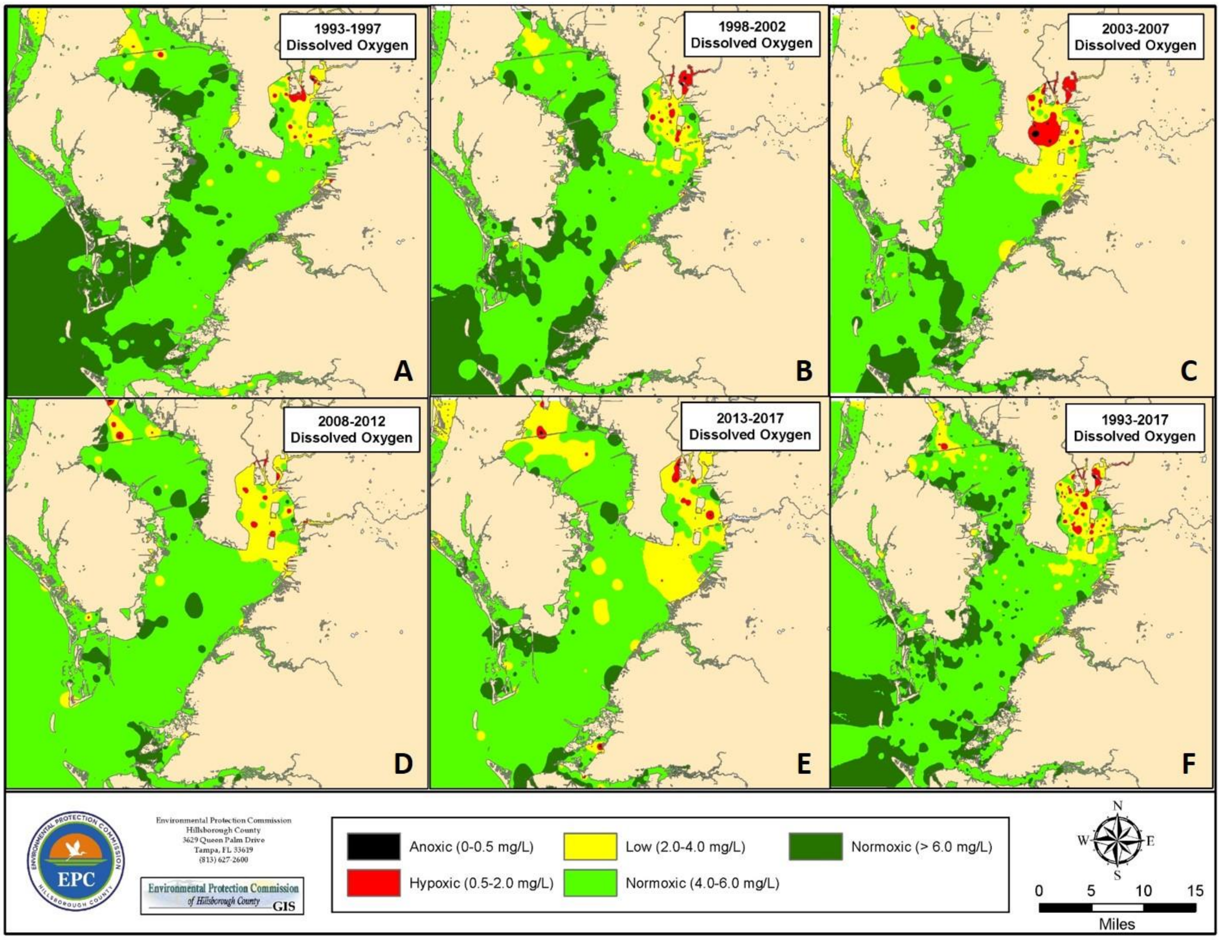

Figure 15. Distribution of bottom dissolved oxygen 1993-2017 by 5-year periods (A-E) and 25-year composite data (F).

Sediment Composition (%Silt+Clay)

The median silt+clay in Tampa Bay was 4.4%, falling within the "medium" grain size classification (Tables 2 and 3), while the mean value was 9.0 %. The maximum recorded silt+clay measurement was 96%, from a sample collected in Seddon Channel in Hillsborough Bay at a depth of 11 meters. There was a significant difference in sediment composition between years (KW; $p < 0.001$), with the highest median silt+clay value being recorded in 1997 (Table 2). However higher mean values were also recorded in 2009, 2011, and 2013 (Figure 16). The higher mean silt+clay values and greater standard errors observed since 2008 (Figure 16) can be attributed to a reduction in the number of samples collected each year, and particularly in the Lower and Middle Tampa Bay segments which tend to have lower silt+clay contents.

Hillsborough Bay had the highest silt+clay values among the bay segments, with high measurements also occurring in Boca Ciega Bay and the Manatee River (Table 3; Figure 17). Medium grained sediments predominated in Old, Middle, and Lower Tampa Bay. Hillsborough Bay had the highest percentage of muddy and very fine grain sediments. Terra Ceia Bay, Boca

Ciega Bay and the Manatee River were predominately medium to fine grained sediments (Table 7). The observed distribution of sediments agreed with previous results by Brooks and Doyle (1991). Several factors contribute to the higher percentage of silty sediments in Hillsborough Bay, including higher sediment input from the Hillsborough and Alafia Rivers, dredged channels which act as sinks for finer grained sediments, and restricted tidal exchange with the rest of Tampa Bay. There was a general trend of decreasing silt+clay from the upper portions of the bay towards the lower end of the bay (Table 7; Figure 18), due in part to less inflow carrying sediment into the lower bay and greater tidal flow between the bay and the Gulf of Mexico (Brooks and Doyle 1991). Brooks and Doyle (1992) mention fine-grained sediments (< 63µm) as a "parameter of concern" which may be considered a pollutant if they are increased by anthropogenic sources. Fine-grained sediments can have adverse effects by increasing turbidity and reducing light penetration through the water column and by accumulating sediment contaminants (Brooks and Doyle 1991, 1992). The accumulation of fine grained sediments can also impact benthic infaunal communities through burial and smothering (Manning et al., 2014).

Total Organic Carbon (TOC)

Total organic carbon (TOC) was incorporated as an additional sediment parameter in 2010, and a total of 366 TOC samples were collected during the 2010-2017 monitoring period. Sources of organic carbon to the bottom sediments include deposition from the water column from plankton blooms (Lesen, 2006), tributaries, and terrestrial runoff. Sediment organics can serve as a food source for deposit feeding benthic fauna, and can structure benthic communities (Magni et al., 2009).

The median TOC was 0.55%, with a mean value of 1.17% and ranging from 0.1 – 9.8%. The highest TOC value was recorded at a Terra Ceia Bay site in 2015 (15TCB12). The mean TOC was significantly different between years with high values in 2014 and 2015 (Figure 19; $p<0.001$). There was no significant difference between bay segments (KW; $p = 0.074$), however lower mean TOC values were found in Old Tampa Bay and Middle Tampa Bay relative to the other bay segments (Figure 20). Sediments with higher TOC content tended to be concentrated in areas of upper Old Tampa Bay, Hillsborough Bay and in the smaller bay segments. However, there were pockets of higher TOC sediments in portions of Middle and Lower Tampa Bay (Figure 21).

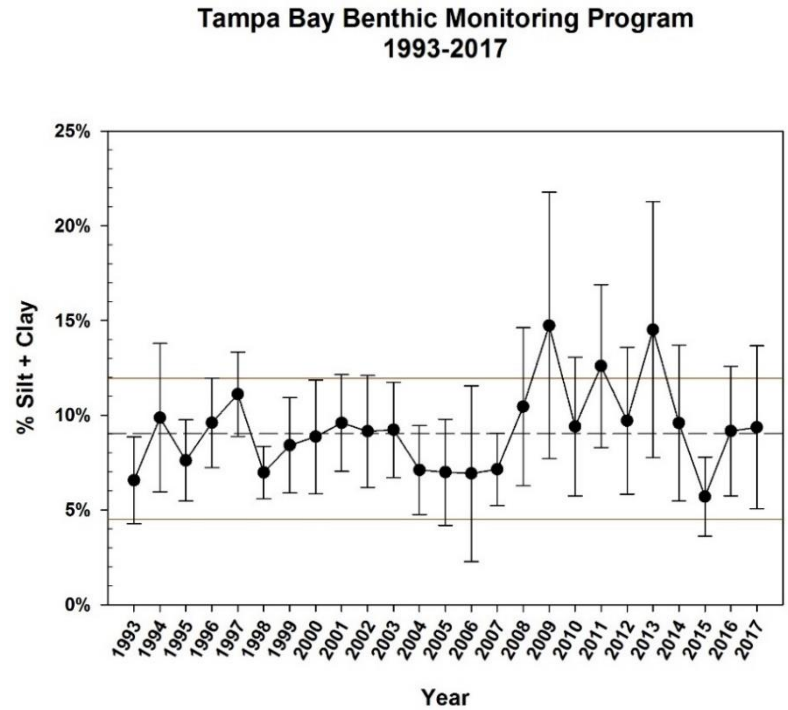

Figure 16. Mean percent silt+clay by year. Error bars = 95% confidence interval, dashed line represents bay-wide mean value, lower and upper solid lines denote boundaries of medium/fine (4.51%) and fine/very fine (11.35%) sediment categories.

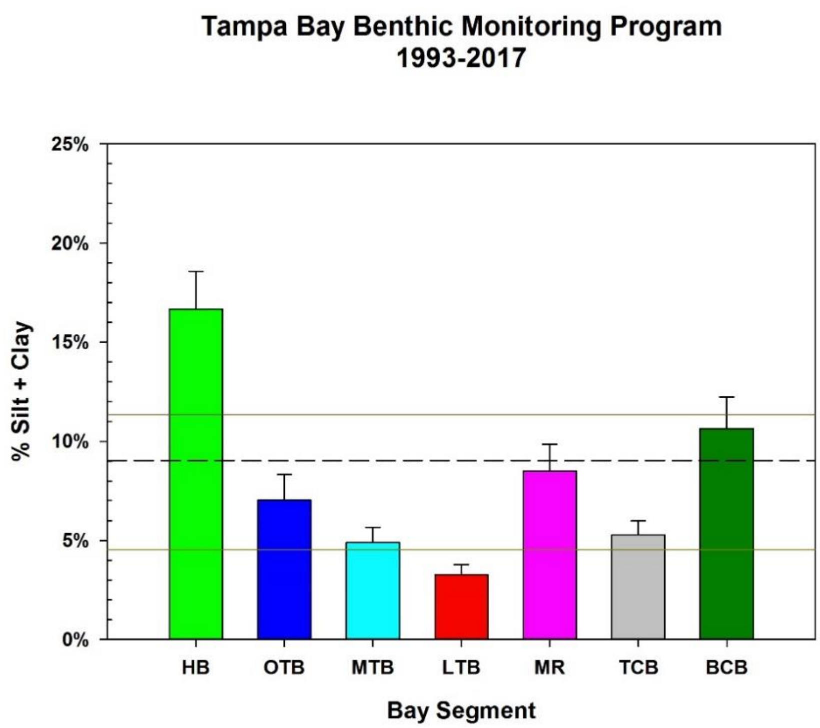

Figure 17. Mean percent silt+clay by bay segment. 95% confidence interval, dashed line represents bay-wide mean value, lower and upper solid lines denote boundaries of medium/fine (4.51%) and fine/very fine (11.35%) sediment categories.

Table 7. Percent silt+clay categories 1993-2017.

	n	Coarse <1.70%	Medium 1.7-4.5%	Fine >4.5-11.3%	Very Fine >11.3-25.95%	Muds >25.95%
Hillsborough Bay	404	5.45%	28.71%	26.49%	17.33%	22.03%
Old Tampa Bay	268	16.79%	43.28%	24.63%	10.07%	5.22%
Middle Tampa Bay	301	22.26%	47.51%	22.59%	5.32%	2.33%
Lower Tampa Bay	219	23.74%	58.90%	15.98%	0.91%	0.46%
Manatee River	191	9.42%	30.37%	43.46%	9.95%	6.81%
Terra Ceia Bay	109	6.42%	43.12%	45.87%	4.59%	0.00%
Boca Ciega Bay	288	4.17%	29.86%	39.58%	18.75%	7.64%
Tampa Bay (Total)	1780	12.53%	39.04%	29.38%	10.84%	8.20%

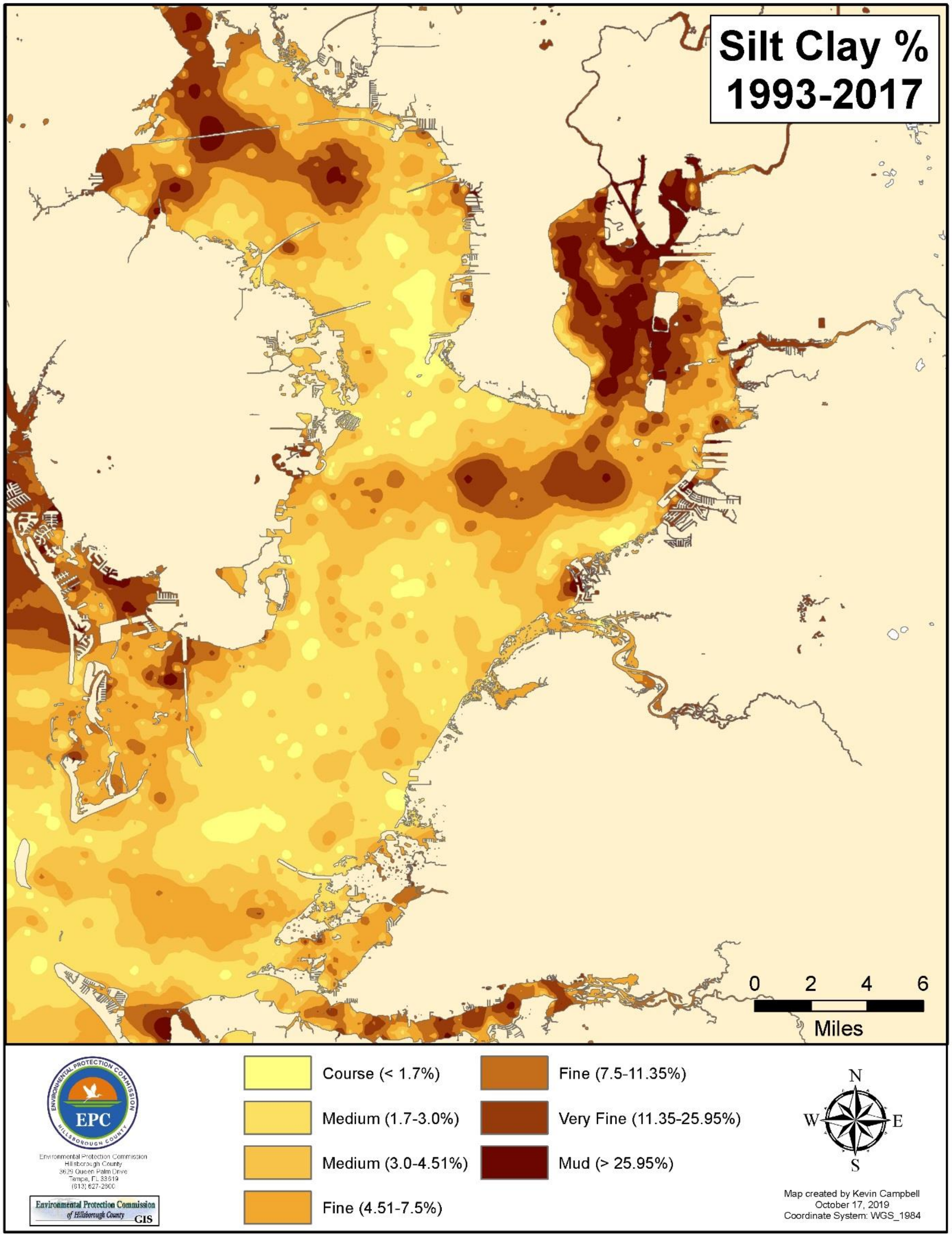

Figure 18. Spatial distribution of sediment types in Tampa Bay 1993-2017.

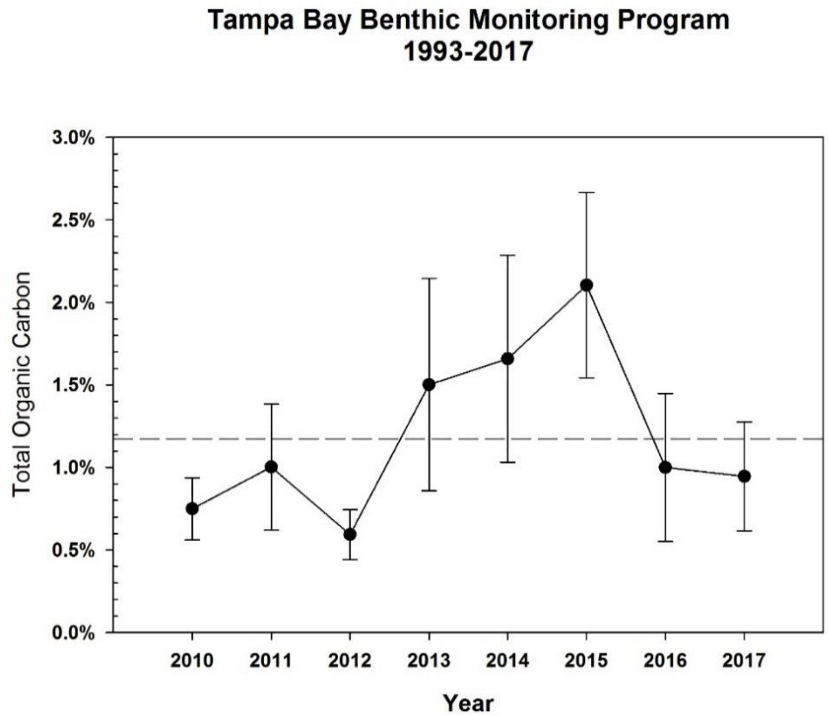

Figure 19. Mean total organic carbon by year. Error bars = 95% confidence interval, dashed line represents bay-wide mean.

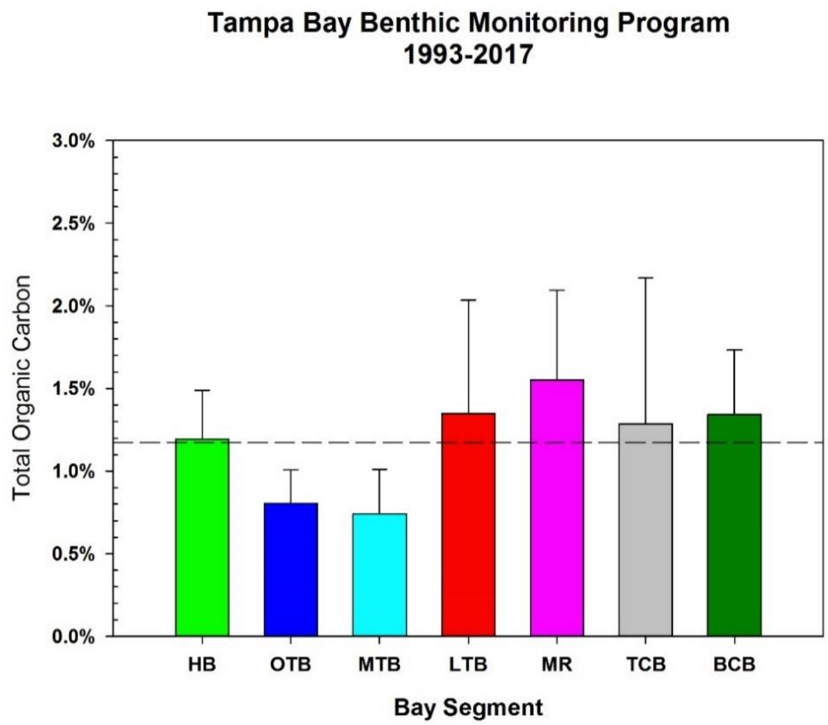

Figure 20. Mean total organic carbon by bay segment. Error bars = 95% confidence interval, dashed line represents bay-wide mean.

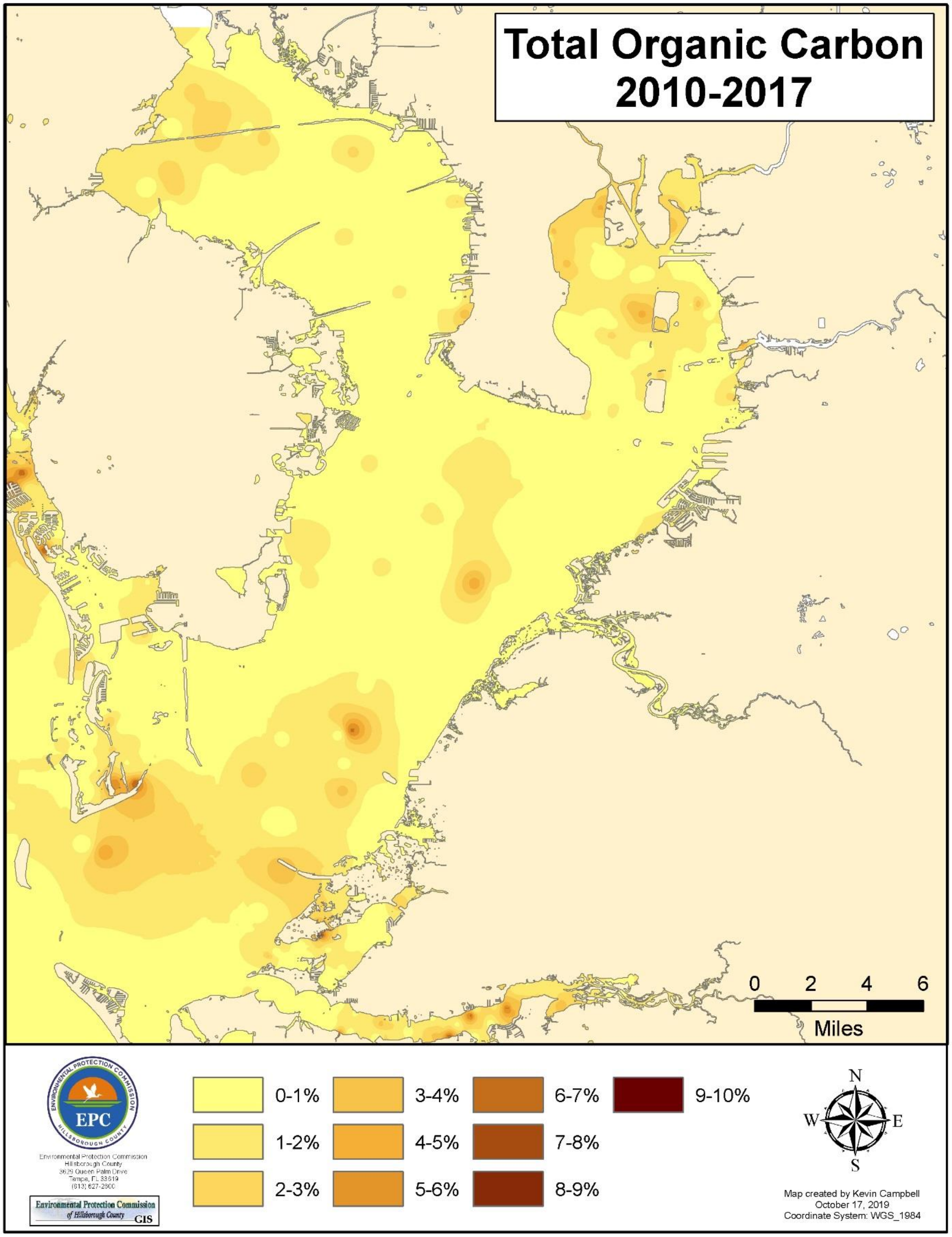

Figure 21. Spatial distribution of sediment total organic carbon in Tampa Bay 2010-2017.

Analysis of Environmental Data

Principal coordinates analysis (PCO) results show that the individual bay segments are defined by unique physical characteristics and spatially adjacent segments overlap in their physical parameters (Figure 22). This pattern is even more apparent when the samples are averaged by year and segment (Figure 23). The first two PCOs cumulatively explaining nearly 59% of the variation (Table 8). The first principal coordinate (PCO1) explained 39.24% of the total variation (Table 8), and was positively correlated with dissolved oxygen, percent DO saturation and pH, and negatively correlated with silt+clay (Table 9; Figures 24 & 25). The second principal coordinate (PCO2) accounts for 19.69% of the total variation (Table 8), and was positively correlated with salinity and depth (Table 9; Figures 26 & 27).

Table 8. Percent of total variation explained by principal coordinates.

PCO	% of Total Variation	% Cumulative Variation
1	39.24	39.24
2	19.69	58.93
3	14.79	73.73
4	10.25	83.97
5	8.39	92.36
6	7.38	99.74
7	0.26	100

Table 9. Pearson correlations of bottom parameters contributing to principle coordinates.

Parameter	PCO 1	PCO 2	PCO 3	PCO 4	PCO 5	PCO 6	PCO 7
Depth	-0.255	0.657	-0.453	0.372	-0.399	-0.019	0.002
Temperature	-0.158	0.255	0.902	0.167	-0.256	0.053	0.006
Dissolved Oxygen	0.941	-0.127	-0.062	-0.082	-0.235	0.154	0.096
% DO Saturation	0.936	-0.076	-0.016	-0.069	-0.248	0.207	-0.093
pH	0.656	0.434	0.089	-0.210	0.026	-0.573	-0.004
Salinity	0.259	0.806	0.035	-0.133	0.389	0.337	0.005
% Silt+Clay	-0.631	0.151	-0.051	-0.691	-0.307	0.073	0.001

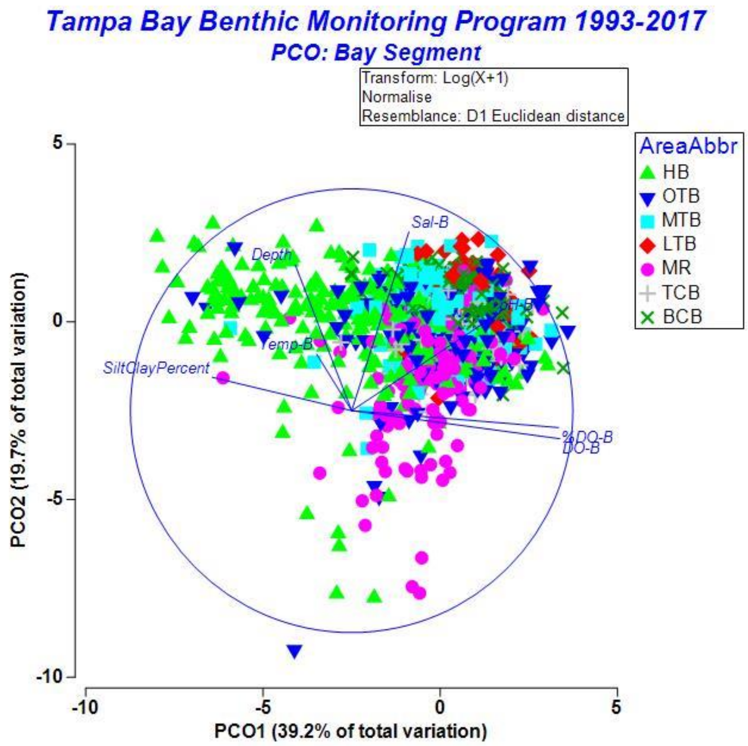

Figure 22. PCO coded by bay segment.

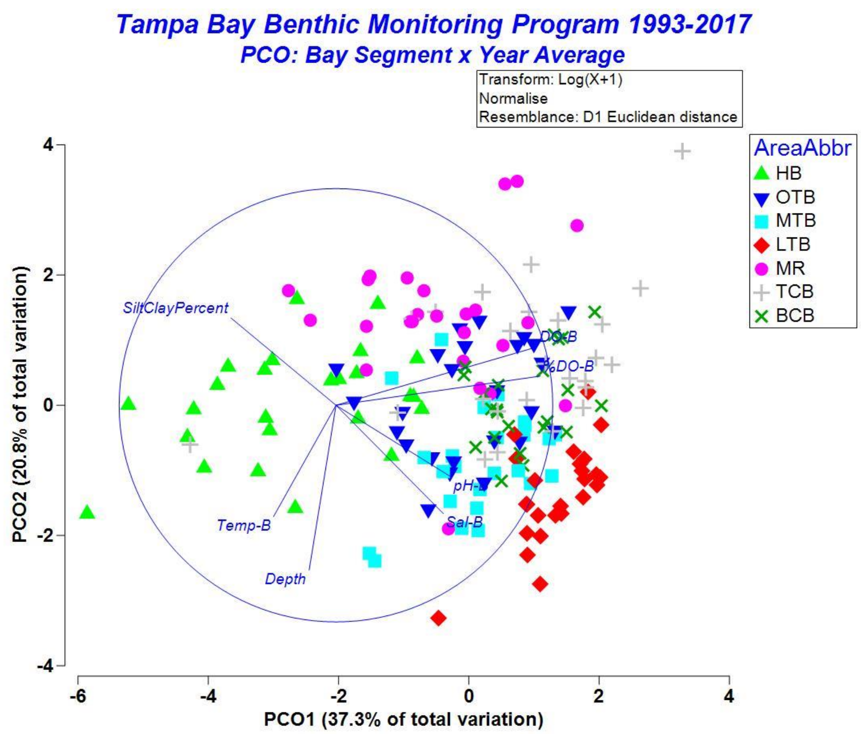

Figure 23. PCO by bay segment and year average.

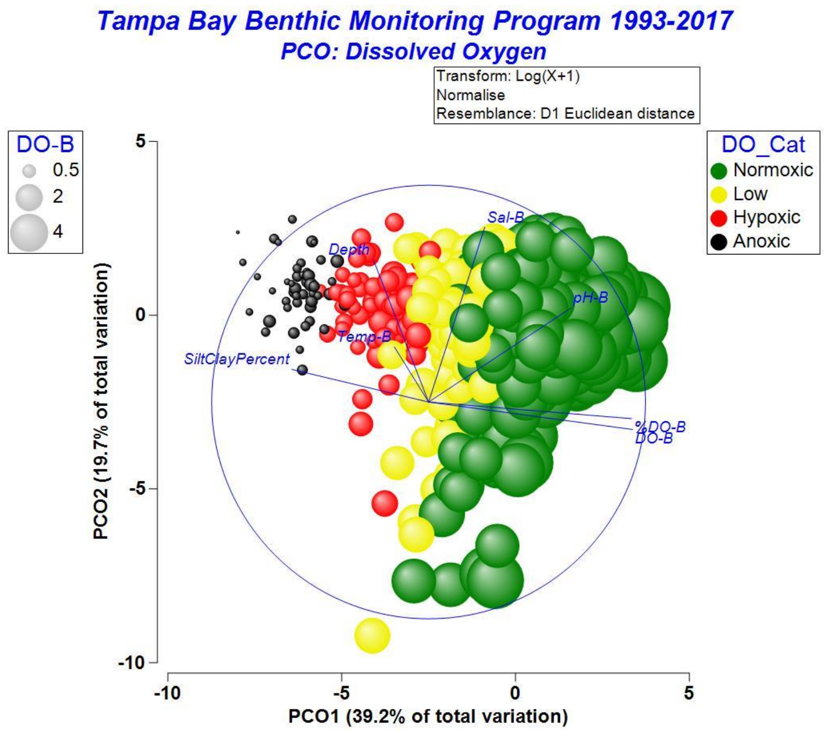

Figure 24. PCO by bottom dissolved oxygen classification, bubble size in mg/l.

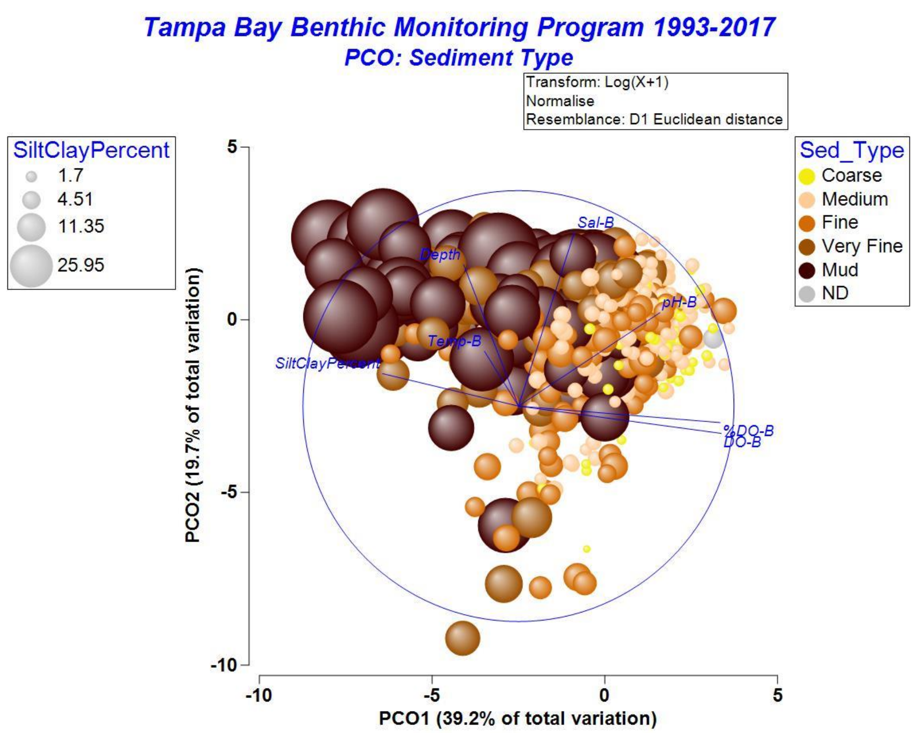

Figure 25. PCO by sediment type, bubble size in % Silt+Clay.

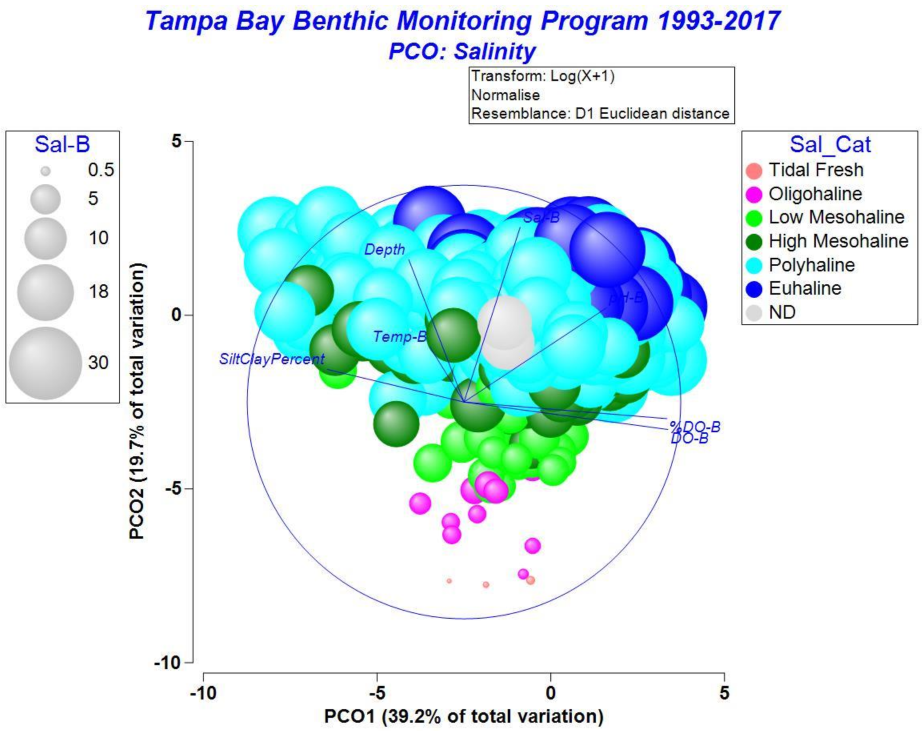

Figure 26. PCO by salinity classification, bubble size in psu.

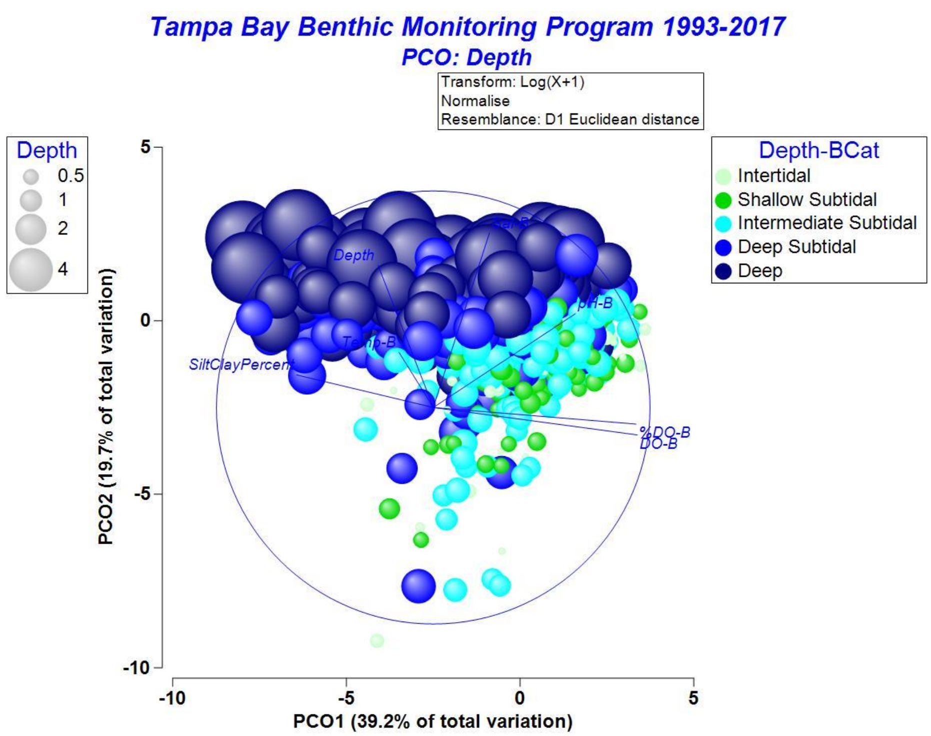

Figure 27. PCO by depth classification, bubble size in meters.

Sediment Contaminants

Metals

Bay-wide sediment metal summary statistics and percent of samples exceeding the sediment toxicity Threshold Effects Level (TEL) and Probable Effects Level (PEL) for each metal (MacDonald 1994) are presented in Table 10 for all years combined. Many of the measurements were below the minimum detectable limit (MDL) resulting in low median values. Results and discussion for individual trace metals are presented below.

Aluminum (Al): Aluminum is among the most common elements in the Earth's crust, and is widely used in many industrial and commercial applications. The concentration of other metals in crustal minerals is proportional to aluminum, hence the metal:aluminum ratio has often been used to normalize metals data for detecting elevated concentrations of a metal above expected background levels (Din, 1992; Pardue et al., 1992; Schropp et al., 1990).

The mean aluminum concentration was 4789 mg/kg (Table 10), with the highest mean concentration in Hillsborough Bay and a decreasing trend towards Lower Tampa Bay (Figure 28). This reflects a greater input of terrestrial sediments into Hillsborough Bay relative to the other bay segments, and a greater proportion of biogenic calcareous sediments in the lower bay.

Iron (Fe): Iron is also among the most common elements in crustal rocks and terrestrial soils. Like aluminum, iron can be used as a normalizing factor for measuring enrichment of other metals in marine sediments (Schiff and Weisberg, 1999). As well as having many industrial uses, such as in the manufacture of steel products, iron is an important micronutrient for organisms. Iron is used by phytoplankton in the production of chlorophyll and in many metabolic pathways involved with photosynthesis and respiration (Street and Paytan, 2005).

Tampa Bay sediments had a mean iron concentration of 2720 mg/kg (Table 10), and were highest in Hillsborough Bay and the Manatee River, decreasing towards Lower Tampa Bay (Figure 29). The higher iron concentrations, as with aluminum, are a result of greater terrestrial inputs from runoff.

Antimony (Sb): Antimony is commonly found in two valance states in the environment; Sb (III) under reducing conditions and Sb (V) under oxidizing conditions (Chen et al., 2003), and is often associated with arsenic compounds (ATSDR, 1992: Filella et al., 2002). Sb (III) is the more soluble and bioavailable form, but can be bound to iron sulfides in the sediment under anoxic conditions (Chen et al., 2003). Sb (V) binds with iron or manganese oxyhydroxides under oxic conditions (Chen et al., 2003). Industrial uses of antimony include antimony oxide which is used as a fire retardant in fabrics and plastics, and alloys with lead and zinc used in batteries, ammunition, pewter, solder, and other metal products (Filella et al., 2002). Sources of antimony to the environment include smelting plants, sewage, and fertilizer facilities (Filella et al., 2002).

Tampa Bay sediment antimony concentrations ranged from <MDL to over 224 mg/kg with a mean of 13.42 mg/kg (Table 10). Mean antimony concentrations were highest in Hillsborough Bay (Figure 30), with the maximum concentration measured at a Hillsborough Bay site located on the east side of the bay segment near a dredge spoil island in 2017 (17HB34). The Sb:Al ratios indicated a few Hillsborough Bay sites may be enriched for antimony above background levels (Figure 31).

Arsenic (As): Arsenic typically exists in two inorganic forms in the environment, the trivalent form As (III) which is more soluble and bioavailable and the pentavalent form As (V) which is often bound with iron compounds in the sediments (Bauer and Blodau, 2006; Guo et al., 1997; Hatje et al., 2010; Masscheleyn et al., 1991). Arsenic is known to be toxic and can accumulate in benthic infauna then transferred to other organisms which feed on them (Barwick and Maher, 2003; Fattorini et al., 2005; Hatje et al., 2010; Neff, 1997; Price et al., 2013; Rainbow et al., 2011). Arsenic is used in several industrial applications including pesticides and as a preservative in pressure treated lumber (ATSDR, 2007a; MacDonald, 1994). Possible sources to the environment may include runoff of pesticides (Pichler et al., 2008; Whitmore et al., 2008), or leaching from treated wood structures such as docks and pilings (Weis et al., 1993).

The bay-wide mean concentration for arsenic was 2.73 mg/kg, with a maximum of over 524 mg/kg (Table 10) measured in 2017 in Hillsborough Bay (17HB34). High concentrations of arsenic (464 mg/kg) were also measured at a site in Old Tampa Bay in 2014 (14OTB18). These two sites were the only PEL exceedances for arsenic, while 5.34% of the samples exceeded the TEL (Table 10). Mean arsenic concentrations were highest in Old Tampa Bay and Hillsborough Bay (Figure 32). The As:Al ratios indicate that the PEL exceedance sites may be from anthropogenic sources (Figure 33). Potentially contaminated sites were scattered in portions of Old, Middle, and Lower Tampa Bay as well as Hillsborough Bay (Figure 34).

Cadmium (Cd): Cadmium has many industrial and agricultural sources including electroplating, paints, plastics, batteries, mining, some pesticides and fertilizers and combustion of fossil fuels (MacDonald, 1994). Cadmium is known to be toxic to aquatic organisms (Long et al., 1994; Lee et al., 2004), and can bioaccumulate in the food chain (Kirby et al., 2001; Seebaugh et al., 2006; Ruelas-Inzunza and Páez-Osuna, 2008). However, several studies have failed to find evidence of trophic effects (Barwick and Maher, 2003), or effects on the colonization of sediments by benthic infauna (Trannum et al., 2004) from elevated cadmium levels in sediment. The toxicity and distribution of cadmium in sediments can be affected by physical factors such as pH and sulfides (Di Toro, 1990; MacDonald, 1994) and bioturbation of the sediments (Rasmussen et al., 1998; Klerks et al., 2007).

Levels of cadmium tended to be high throughout Tampa Bay, with over 40% of the samples above the TEL and 1.56% above the PEL (Table 10). The mean cadmium concentrations were above the TEL threshold in all bay segments except Lower Tampa Bay. The highest concentrations were in Hillsborough Bay and Old Tampa Bay (Figure 35). The Cd:Al ratio (Figure 36), suggests that only a few samples were enriched above background levels for cadmium despite the high percentage of sites above the TEL. This may be from natural sources such as weathering of phosphate enriched soils (MacDonald 1994), or from anthropogenic inputs related to phosphate mining. The elevated cadmium levels were was apparent throughout Tampa

Bay (Figure 37). In contrast to these results, previous surveys (Brooks and Doyle, 1992; Long et al., 1994) found Cd:Al ratios in samples from Tampa Bay suggesting anthropogenic enrichment. Long et al., (1994) further found significant correlations between sediment cadmium concentrations and toxicity bioassays. Frithsen et al., (1995) estimated an annual loading of around 3,500 kg of cadmium to Tampa Bay with Hillsborough Bay receiving the largest loading (39%), followed by Old Tampa Bay (23%). The main sources of cadmium loading were atmospheric deposition (46%), followed by point sources (32%), and urban runoff (21%) (Frithsen et al., 1995).

Chromium (Cr): Chromium is used in the production of chrome plating, chromium metal and chrome alloys, dyes, paints, and paper, among other industrial uses (MacDonald, 1994). Chromium is commonly found in two valence states: Cr(III) and Cr(VI). The Cr (III) form adsorbs to organic particles and can co-precipitate with iron and magnesium oxides, accumulating in the sediment (MacDonald 1994). Cr (III) is considered less toxic to aquatic organisms, while the Cr (VI) form is water soluble, more bioavailable and thus has a greater toxicity than Cr (III) (MacDonald, 1994; McConnell et al., 1996).

Total chromium levels in Tampa Bay were above the TEL at 6.18% of the sites, and exceeded the PEL at 0.72% of the sites (Table 10). The bay-wide mean chromium concentration was 24.98 mg/kg. The highest concentrations occurred in Hillsborough Bay where the mean value exceeded the TEL threshold (Figure 38). Several Hillsborough Bay sites had high Cr:Al ratios, which indicated possible contamination above background concentrations (Figure 39). Areas of highest contamination in Hillsborough Bay were associated with Port Tampa Bay or the shipping channels (Figure 40). The highest recorded chromium concentration (15,320 mg/kg) was found near the mouth of Bullfrog Creek in Hillsborough Bay in 1996 (96HB46). There were additional sites that exceeded the TEL around the periphery of Old Tampa Bay, as well as a few isolated sites in Middle Tampa Bay, Boca Ciega Bay, and the Manatee River (Figure 40).

Previous surveys have likewise found high concentrations of chromium in the upper part of Hillsborough Bay (Brooks and Doyle 1992), and it has been identified as a “Chemical of Concern” for this area of the bay (McConnell et al., 1996; McConnell and Brink 1997). Frithsen et al., (1995) estimated chromium loading to Tampa Bay to be approximately 14,600 kg/yr, primarily from urban runoff (57%) and point sources (27%). Hillsborough Bay and Old Tampa bay receive 43.7% and 24% of the total chromium load respectively, due to the urban development in these areas (Frithsen et al., 1995).

Copper (Cu): Copper is commonly used in biocides for controlling algae and fungi, and in antifouling paints (ATSDR, 2004; MacDonald, 1994). Industrial sources of copper in the environment include wastewater treatment effluents, runoff of copper based biocides, corrosion of copper pipes, and atmospheric deposition from coal burning power plants (ATSDR, 2004; MacDonald, 1994). In Tampa Bay, the estimated annual loading of copper is approximately 12,500 kg with major inputs coming from urban runoff (43%), point sources (35%), and atmospheric deposition (18%) (Frithsen et al., 1995). Copper is known to be toxic to aquatic organisms, and high levels of copper can impede the settlement and colonization of benthic infauna (Olsgard, 1999; Trannum et al., 2004). Elevated sediment copper concentrations can further accumulate in the food chain, particularly in mollusks and crustaceans which utilize copper as a blood pigment (MacDonald, 1994; Barwick and Maher, 2003), and in bottom feeding fishes (Kirby et al., 2001).

Tampa Bay had a mean sediment copper concentration of 6.09 mg/kg and exceeded the TEL in 5.28% of the samples and the PEL in 0.54% of the samples (Table 10). High levels of copper were present in Hillsborough Bay, the Manatee River, and Boca Ciega Bay (Figure 41). The Cu:Al ratios indicated several sites were enriched above background levels in Hillsborough Bay and Boca Ciega Bay (Figure 42). The areas of highest contamination were primarily in Hillsborough Bay near Port Tampa Bay, industrial facilities, and at the mouth of Bullfrog Creek (Figure 43). Brooks and Doyle (1992) found elevated levels of copper in 23% of their samples, with the highest measurement (267 mg/kg) at Bayboro Harbor in Middle Tampa Bay. Copper was identified as a “Chemical of Concern” for upper Hillsborough Bay in past studies (McConnell et al., 1996; McConnell and Brink, 1997).

Lead (Pb): Historically, the mining of lead-silver ore dates back to the Bronze Age over 1000 years BCE (Longman et al., 2018; McConnell et al., 2018) and lead pipes were used for plumbing and transporting potable water dating back to the Roman period (Delile et al., 2014). Lead has many industrial uses including the manufacture of lead batteries and chemical compounds, solder, lead based paints, and ammunition (ATSDR, 2007b; MacDonald, 1994). Lead was used as a gasoline additive until it was phased out in the 1970s, which subsequently resulted in a measurable decrease in lead in the environment (Trefry et al., 1985). Sources of lead in the environment include atmospheric deposition and runoff from contaminated soils (Davis et al., 2001). Lead emissions from automobiles can cause soil contamination along roadways (Hafen, 1996; Newsome, 1997). Legacy contamination from lead based paints can also linger in soils and sediments (Brinkmann, 1994; Rees et al., 2014). Lead bullets and shot have also been responsible for elevated lead levels in soils at shooting ranges, which can leach into the surrounding environment (Bannon et al., 2009; Butkus and Johnson, 2011; Cao et al., 2003; Clausen et al., 2011; Labare et al., 2004). Lead fishing weights can be ingested by waterfowl resulting in lead poisoning (Scheuhammer and Norris, 1996).

Exposure to lead can affect neurological development in children, and affect cognitive functions in adults. Other health effects can include cardiovascular disorders and impaired kidney functions (ATSDR, 2007b; Brown and Margolis, 2012).

The bay-wide mean sediment concentration of lead was 12.6 mg/kg with, a maximum concentration of 638 mg/kg occurring at a site in McKay Bay (Table 10). Sediment lead levels exceeded the TEL at 6% of the sites, and was above the PEL in 0.60% of the samples (Table 10). Hillsborough Bay had the highest mean sediment lead concentrations (Figure 44). The Pb:Al ratio indicated elevated lead levels were present in Hillsborough Bay, as well as in the Manatee River and Old Tampa Bay (Figure 45). The most contaminated sites in Hillsborough Bay were in the upper arm of McKay Bay, in the Hillsborough River and near the Port of Tampa (Figure 44). A few isolated sites in other parts of the bay had high levels of lead, including near Snell Isle in Middle Tampa Bay, the eastern side of Old Tampa Bay near Feather Sound, and the western side of Old Tampa Bay near Culbreath Bayou (Figure 46).

Brooks and Doyle (1992) detected elevated lead concentrations at 93% of their sites, with 12% exceeding the PEL of 112 mg/kg as determined by MacDonald (1994). The highest lead concentration in the Brooks and Doyle survey was 385 mg/kg in McKay Bay. Lead levels in Tampa Bay sediments were also found to be significantly correlated with sediment toxicity tests (Long et al., 1994). Frithsen et al., (1995) estimated annual loading of lead to Tampa Bay at nearly 50,000 kg, primarily from urban runoff (60%), along with atmospheric deposition (20%), point source pollution (11%), and ground water (9%).

Manganese (Mn): Manganese is found naturally in the environment and is an essential nutrient in low concentrations (ATSDR, 2012). However, high concentrations of manganese can impact brain development in children, cause behavioral changes, and affect memory (ATSDR, 2012). The primary industrial use of manganese is in steel production, where it is added to increase hardness and strength (ATSDR, 2012). Other commercial uses include food additives and nutritional supplements, fertilizers, cosmetics, dry-cell batteries, fireworks, paints, and as an additive to gasoline (ATSDR, 2012).

MacDonald (1994) did not establish SQGs for manganese. Manganese concentrations in Tampa Bay ranged from below MDLs to 164 mg/kg with a mean of 20.29 mg/kg (Table 10). The highest concentration was at a Hillsborough Bay site sampled in 2017 near Davis Island (17HB15). Mean manganese concentrations were higher in Hillsborough Bay, Terra Ceia Bay, and Lower Tampa Bay (Figure 47), with a few sites exhibiting high Mn:Al ratios (Figure 48).

Mercury (Hg): Elemental mercury is a liquid at room temperature. It can be found in inorganic compounds such as mercuric sulfide (cinnabar) and mercuric chloride, and in organic compounds such as methylmercury (ATSDR, 1999). Mercury is used in electric switches, thermometers and thermostats, fluorescent light bulbs, as a fungicide, and in dental amalgam fillings (ATSDR, 1999). Anthropogenic sources of mercury are primarily from atmospheric deposition from the combustion of coal and other fossil fuels and the incineration of municipal waste (ATSDR, 1999). Approximately 70% of atmospheric deposition in Florida is estimated to come from the combustion of coal, while 30% is from natural sources such as volcanoes and forest fires (FDEP, 2013). Other potential sources include cement and fertilizer production facilities (ATSDR, 1999; Mirlean, 2008). Mercury, and especially methylmercury, can accumulate in sediments and be ingested by deposit feeding infauna (Sizmur, 2013). Bioaccumulation in fish and birds can occur at higher trophic levels (Adams and Onorato, 2005; Beyer et al., 1997; Cleckner et al., 1998; Julian, 2013). The Florida Department of Environmental Protection established a statewide Total Maximum Daily Load (TMDL) for mercury in 2013. This TMDL was based on the Florida Department of Health's threshold for mercury in fish tissues determined to be unhealthy for human consumption (FDEP 2013). The Tampa Bay watershed is listed as impaired for mercury in fish tissues (FDEP, 2012).

Sediment samples were only analyzed for mercury in 1993 for the four main bay segments. All samples were below the 0.13 mg/kg TEL threshold for mercury (MacDonald, 1994), and the Al:Hg ratios did not indicate that samples were higher than background concentrations. The highest mercury concentration (0.1 mg/kg) was found in Old Tampa Bay in Safety Harbor.

Nickel (Ni): Nickel is primarily used in the manufacturing of stainless steel and nickel plating, and is used as a catalyst for other industrial processes and oil refining (MacDonald, 1994). Other manufacturing uses include batteries, ceramics, and jewelry (ATSDR, 2005a). Potential sources of nickel pollution include the combustion of fossil fuels, electroplating operations, and wastewater treatment facilities (ATSDR, 2005a; MacDonald, 1994; McConnell and Brink, 1997). Exposure to nickel compounds can cause allergic reactions and skin irritation while high-level exposure can be carcinogenic (ATSDR, 2005a). Nickel can accumulate in estuarine sediments, and sediment resuspension can result in the desorption of the solid phase to a more bioavailable water phase (Amezcua-Allieri and Salazar-Coria, 2008).

The mean nickel concentration in Tampa Bay sediments was 11.67 mg/kg, with a maximum concentration of 10,030 mg/kg (Table 10). The highest nickel concentration was recorded at the mouth of Bullfrog Creek in 1996 (site 96HB46). Nickel levels were above the TEL at 7.74% of the sites and exceeded the PEL at 0.54% of the sites (Table 10). Highest levels were in Hillsborough Bay where the mean sediment concentration exceeded the TEL (Figures 49). Only a few sites had Ni:Al ratios which suggested Ni concentrations were above background levels (Figure 50). The potentially contaminated sites were mainly concentrated in Hillsborough Bay and at two sites in Old Tampa Bay (Figure 51).

Brooks and Doyle (1992) found elevated nickel levels at 17% of their sites, with a maximum value of 64.5 mg/kg in Hillsborough Bay. Nickel has been correlated with sediment toxicity (Amezcua-Allieri and Salazar-Coria 2008), although previous sediment toxicity work on Tampa Bay sediments did not find significant correlations between nickel concentrations and amphipod survival bioassays (Long et al., 1994). McConnell et al., (1996), however, identified this metal as a significant environmental risk from potential bioaccumulation and nickel was identified as a contaminant of concern for upper Hillsborough Bay (McConnell and Brink, 1997). Bay-wide loading estimates for nickel were not calculated by Frithsen et al., (1995). McConnell and Brink, (1997) calculated a loading of approximately 753 kg/yr for upper Hillsborough Bay from point source discharges, primarily from the Hooker’s point WWTP (68%) and the Tampa Electric Gannon power plant (32%).

Selenium (Se): Selenium is an essential nutrient in low quantities, and is used as a nutritional supplement in animal feed (ATSDR, 2003). High doses can lead to severe health effects, including pulmonary edema or selenium poisoning (selenosis), characterized by a loss of feeling and control of the victim’s arms and legs (ATSDR, 2003). High levels of selenium can also naturally occur in soils, which can be taken up by agricultural crops and potentially reach toxic concentrations (ATSDR, 2003). Commercially, selenium is used in paints, plastics, glass, nutritional supplements, and as an active ingredient in fungicides and anti-dandruff shampoos (ATSDR, 2003). Selenium from anthropogenic sources can enter the environment through the combustion of coal, disposal of products containing selenium, and agricultural runoff (ATSDR, 2003; Malloy et al., 1999). Selenium can accumulate in marine and freshwater sediments, be taken up by benthic organisms and then accumulate at higher trophic levels (Barwick and Maher, 2003; Kirby et al., 2001; Malloy et al., 1999).

The mean sediment selenium concentration in Tampa Bay was 7.35 mg/kg, with a maximum of 253.41 mg/kg (Table 10). The highest measurement was recorded in 2017 in Hillsborough Bay east of the northern dredge spoil island (17HB34). Mean selenium concentrations were higher in Hillsborough Bay, Old Tampa Bay and Terra Ceia Bay (Figure 52). The Se:Al ratios indicated the highest Hillsborough Bay site was above background levels (Figure 53). Previous studies have documented high levels of selenium in Hillsborough Bay, particularly in the northern area around McKay Bay and the Palm River (Benson et al., 1994; Long et al., 1994).

MacDonald (1994) did not develop SQGs for selenium in Florida coastal sediments. Sediment toxicity thresholds have been proposed for freshwater streams in the western United States of 2.5 µg/g for predicted effects on biota, and 4 µg/g for fish and wildlife toxicity (Van Derveer and Canton, 1997). The median selenium concentration in Tampa Bay (5.48 mg/kg; Table 10) is above these thresholds, however other factors such as sediment organic content, pH and sediment redox potential can affect its bioavailability (Masscheleyn et al., 1990; Van Derveer and Canton, 1997) .

Silver (Ag): Silver can be highly toxic to aquatic organisms, and has a high rate of bioaccumulation (Lee et al., 2004; Luoma et al., 1995). Silver has several industrial uses including the production and processing of photographic materials, electrical contacts, soldering, jewelry and silver plating, and in medicine as an antimicrobial, and in dental fillings (ATSDR, 1990; Purcell and Peters, 1998; MacDonald, 1994). Nanoparticles of silver have increasingly been used in consumer products such as clothing and cosmetics to inhibit bacterial growth (Mühling et al., 2009). Potential sources of silver to the environment include waste incinerators, landfills, wastewater treatment plants, and coal combustion (ATSDR, 1990; MacDonald, 1994).

The mean sediment silver concentration in Tampa Bay was 0.17 mg/kg and ranged from below MDLs to 47.2 mg/kg (Table 10). The highest concentration was found on the east side of Hillsborough Bay in 2017 (17HB34). The second highest concentration (43.01 mg/kg) was recorded in Old Tampa Bay in 2014 near the St. Peter/Clearwater airport (14OTB18). These two samples (0.12%) were the only PEL exceedances for silver, while 1.38% of the sites were above the TEL (Table 10). The highest silver concentrations were in Hillsborough Bay and Old Tampa Bay (Figure 54). The Ag:Al ratio suggests that several samples above the TEL and PEL are from anthropogenic sources (Figure 55). Most of the potentially contaminated sites were in Hillsborough Bay, Old Tampa Bay, and scattered sites in Middle and Lower Tampa Bay (Figures 56). Brooks and Doyle (1991) found silver present at 17% of their Tampa Bay sites concentrated mainly around St. Petersburg and in Hillsborough Bay. Their highest recorded value was 0.5 mg/kg (Brooks and Doyle, 1991), which is below the TEL of 0.73 mg/kg established by MacDonald, (1994) and two orders of magnitude lower than the highest concentrations recorded in this study.

Tin (Sn): Tin has many industrial and commercial applications. Inorganic tin is used in tin-plated food containers and aerosol cans, electroplating, solder, glass production, as an additive to perfumes and soaps, as a food preservative, in metal alloys such as bronze and pewter, and tin(II) fluoride (SnF_2) is added to toothpaste as an anti-cavity ingredient (ATSDR, 2005b). Organic tin compounds are used commercially as heat stabilizers for polyvinyl chlorides (PVCs), in the manufacture of polyurethane foam, as biocides, agrichemicals, wood preservatives, and in antifouling paints (ATSDR, 2005b). Most notably, tributyltin (TBT) was used in antifouling paints, and has been a major source of contamination in the marine environment (ATSDR, 2005b). Sediments contaminated by TBT can cause reproductive deformities (imposex) in gastropods (Balckmore, 2000; Boulajfene et al., 2015; Terlizzi et al., 1999), and negatively impact benthic community structure (Austen and McEvoy, 1997; Dahllof et al., 2001). The use of TBT in antifouling paints has been restricted since 1988 by the Organotin Antifouling Paints Control Act, which limits the types of vessels that can use TBT paints (ATSDR, 2005b). MacDonald (1994) did not establish SQGs for tin in Florida coastal sediments.

The mean sediment tin concentration in Tampa Bay was 2.13 mg/kg, and ranged from below MDLs to 188.72 mg/kg (Table 10). The highest tin concentration was found in Hillsborough Bay in 2017 (17HB34), a site which also had high levels of several other metals. Mean tin concentrations were relatively high in Hillsborough Bay and Old Tampa Bay, and were lowest in Lower Tampa Bay (Figure 57). The Sn:Al ratio suggested that the Hillsborough Bay site was potentially enriched above background levels (Figure 58).

Zinc (Zn): Zinc is a common naturally occurring element and an essential nutrient. Zinc deficiencies can result in decreased immune function, and an increased risk of birth defects for pregnant women (ATSDR, 2005c). High doses of zinc however can cause anemia and damage to the pancreas (ATSDR, 2005c). Zinc has many industrial uses, including galvanization of steel and other metals to prevent corrosion, making alloys such as brass and bronze, and in dry cell batteries (ATSDR, 2005c). Zinc compounds are also used in ceramics, rubber production, in wood preservatives, dietary supplements, cosmetics, sunscreen, and paints (ATSDR, 2005c). Nanoparticles of zinc oxides are used in many products including sunscreens, cosmetics, and in marine antifouling paints (Schultz et al., 2014).

Anthropogenic sources of zinc in the environment include industrial discharges from steel production and electroplating facilities, domestic wastewater treatment plants, atmospheric deposition, and stormwater runoff (ATSDR, 2005c). Sources of zinc in urban runoff include roof and siding materials from buildings, and dust and particles from rubber tire wear along roadways (Davis et al., 2001). Leaching of zinc from antifouling paints can cause contamination in water and sediments (Singh and Turner, 2009a, b; Turner et al., 2009), and antifouling paints used on nets can increase zinc concentrations in farmed fish tissues (Nikolaou et al., 2014). High zinc concentrations can impair growth and fertility in amphipods (Conradi and Depledge, 1999), cause mouthpart deformities in freshwater chironomid larvae (Martinez et al., 2001), damage DNA in polychaetes (Watson et al., 2018), and impact recruitment of benthic organisms (Watzin and Roscigno, 1997). Trophic assimilation of zinc is high in some invertebrates such as barnacles (Rainbow and Wang, 2001; Wang and Rainbow, 2000), which can be further transferred up the food chain (Blackmore, 2000). In contrast, Barwick and Maher (2003) did not find evidence of biomagnifications of zinc at higher trophic levels in a seagrass ecosystem.

The mean sediment zinc concentration in Tampa Bay was 16.98 mg/kg, with a maximum of 522 mg/kg in McKay Bay (97HB10) (Table 10). Zinc levels were above the TEL at 1.86% of the sites and exceeded the PEL at 0.60% of the sites (Table 10). The highest levels were in Hillsborough Bay and the Manatee River (Figure 59). The Zn:Al ratios however did not appear to show elevated zinc levels (Figure 60). Most of the contaminated sites were in Hillsborough Bay at sites within the Hillsborough River, McKay Bay, around the Port of Tampa, and at the mouth of Bullfrog Creek (Figure 61). Brooks and Doyle (1992) found concentrations of zinc as high as 700 mg/kg in McKay Bay, which exceeds the highest value found in our samples (Table 10). Approximately 17% of the sites in the Brooks and Doyle (1992) survey exceeded the PEL value for zinc compared to only 0.69% of our monitoring sites. Frithsen et al., (1995) estimated annual loading of zinc to Tampa Bay at 164,000 tons, with 66% of the input coming from urban runoff.

Table 10. Tampa Bay (1993-2017) sediment metals summary statistics and percentage of sites exceeding TEL and PEL values.

mg/kg	Aluminum Al	Antimony Sb	Arsenic As	Cadmium Cd	Chromium Cr	Copper Cu	Iron Fe	Lead Pb	Manganese Mn	Mercury Hg	Nickel Ni	Selenium Se	Silver Ag	Tin Sn	Zinc Zn
TEL	ND	ND	7.2	0.68	52.3	18.7	ND	30.2	ND	0.13	15.9	ND	0.73	ND	124
PEL	ND	ND	41.6	4.2	160	108	ND	112	ND	0.696	42.8	ND	1.77	ND	271
n	1300	1076	1666	1666	1666	1666	1076	1666	1076	57	1666	1076	1666	1666	1666
Minimum	0.01	0.008	0.004	0.001	0.01	0.01	0.01	0.01	0.01	0.01	0.01	0.01	0.0007	0.009	0.01
Maximum	59540	224.55	524.32	131.63	15320	729.1	29953.45	637.713	164.02	0.1	10030	253.41	47.2	188.72	521.996
Median	1849.115	1.865	1.2615	0.26	7.0775	1.6655	1174.0625	6.7095	12.03	0.01	3.35	5.48	0.041	0.382	5.5925
Mean	4788.96	13.42	2.73	1.05	24.98	6.09	2720.36	12.60	20.29	0.01	11.67	7.35	0.17	2.13	16.98
SD	8354.15	19.18	17.27	4.66	376.31	24.45	4399.99	28.60	22.45	0.02	245.98	11.92	1.57	7.23	41.54
% >TEL;<PEL			**5.34%**	**40.22%**	**6.18%**	**5.28%**		**6.06%**		**0.00%**	**7.74%**		**1.38%**		**1.86%**
% >PEL			**0.12%**	**1.56%**	**0.72%**	**0.54%**		**0.60%**		**0.00%**	**0.54%**		**0.12%**		**0.60%**

ND and diagonal hash lines = SQG Not Determined;

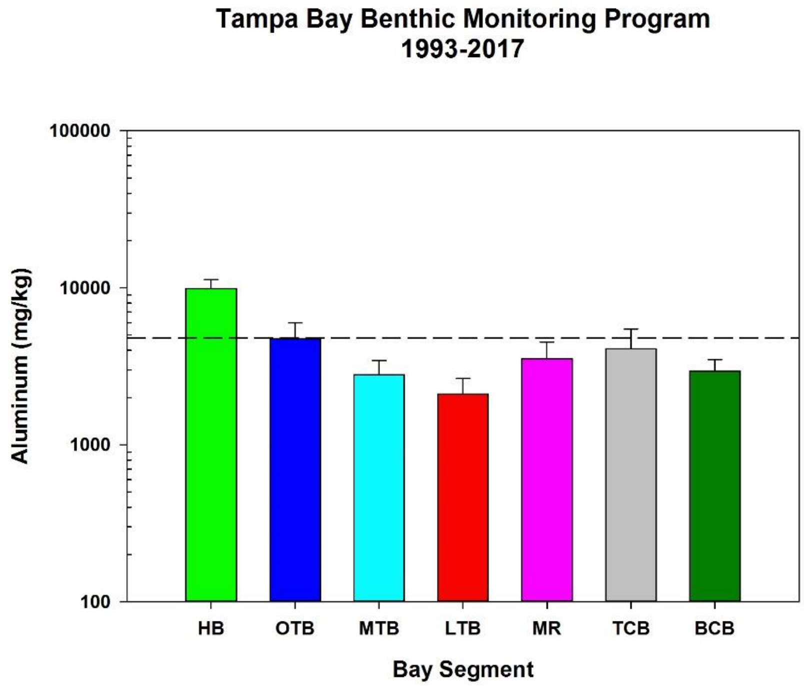

Figure 28. Mean sediment aluminum concentrations by bay segment.
Error bars = 95% confidence interval, dashed line represents bay-wide mean.

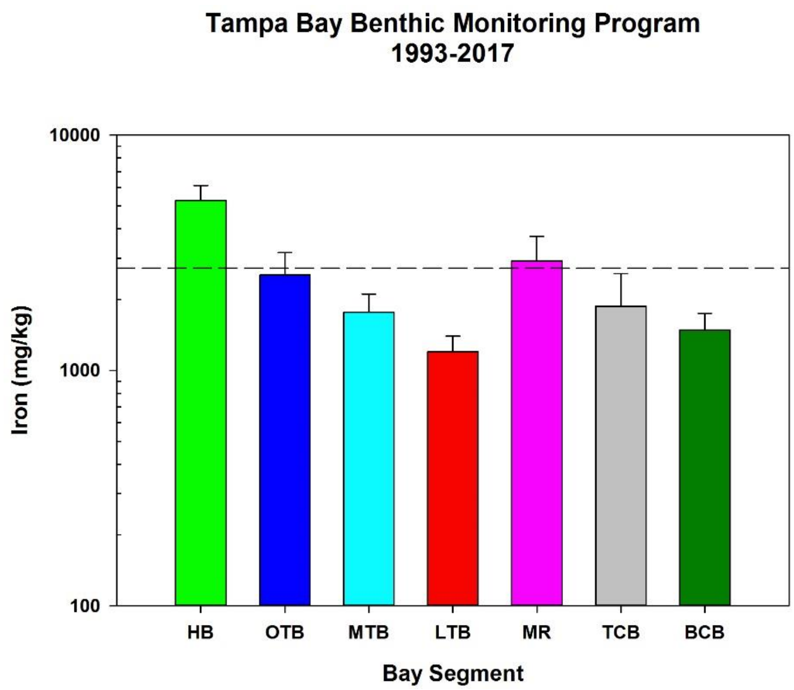

Figure 29. Mean sediment iron concentrations by bay segment.
Error bars = 95% confidence interval, dashed line represents bay-wide mean.

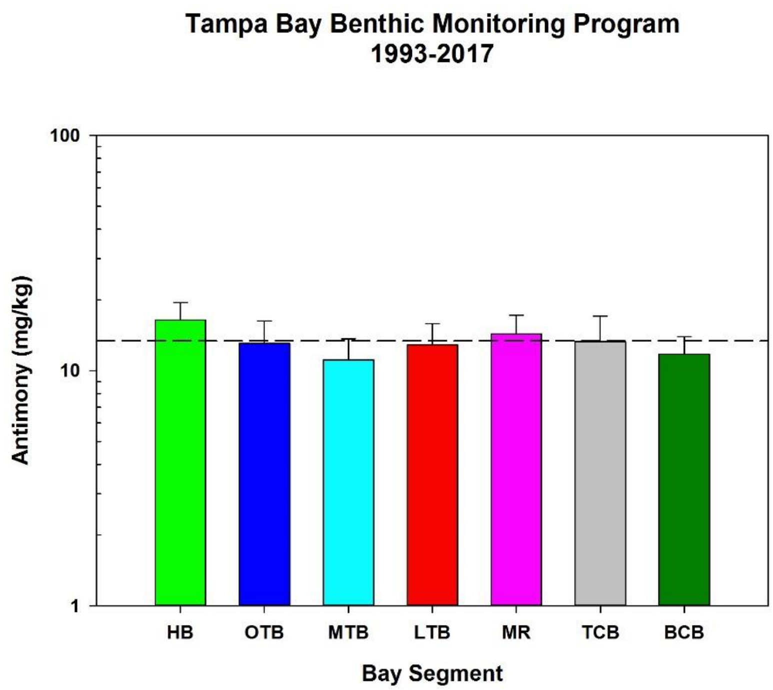

Figure 30. Mean sediment antimony concentrations by bay segment.
Error bars = 95% confidence interval, dashed line represents bay-wide mean.

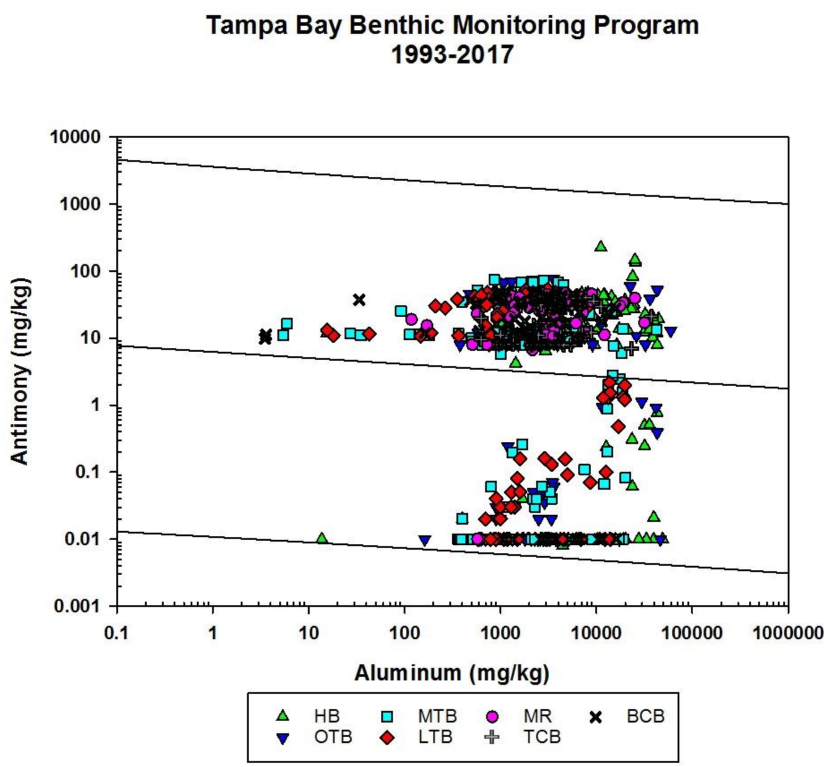

Figure 31. Tampa Bay Sb:Al ratio with 95% prediction intervals (solid lines).

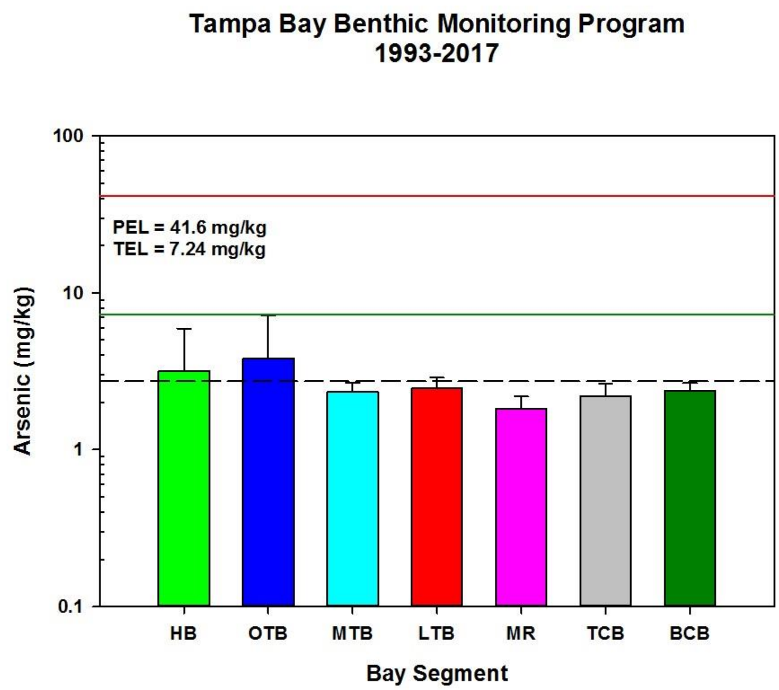

Figure 32. Mean sediment arsenic concentrations by bay segment. Error bars = 95% confidence interval, dashed line represents bay-wide mean. Solid lines represent PEL (upper; red) and TEL (lower; green) values.

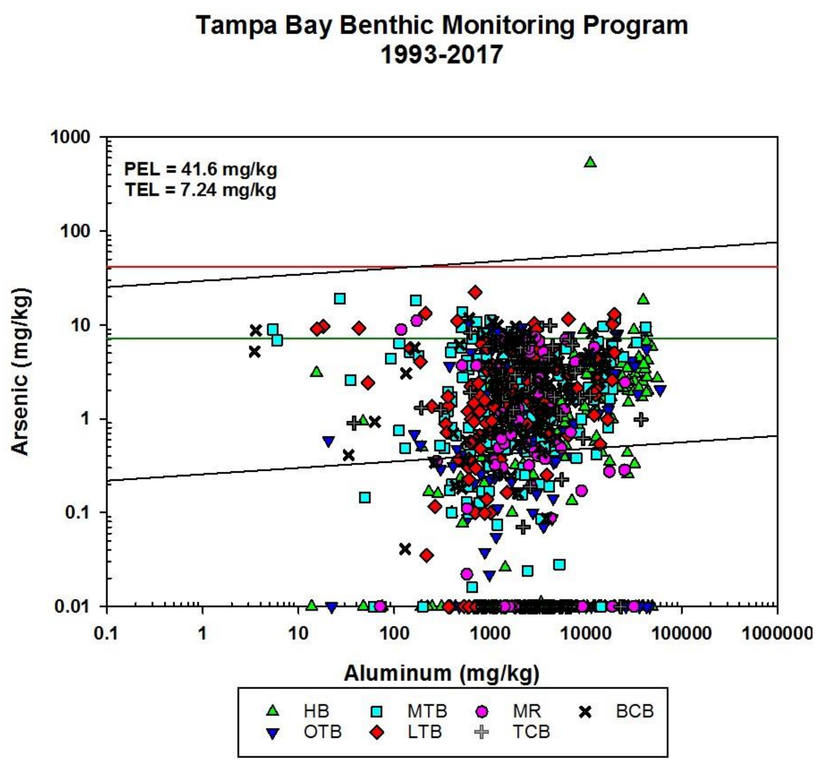

Figure 33. Tampa Bay As:Al ratio with 95% prediction intervals (solid lines). Solid lines represent PEL (upper; red) and TEL (lower; green) values.

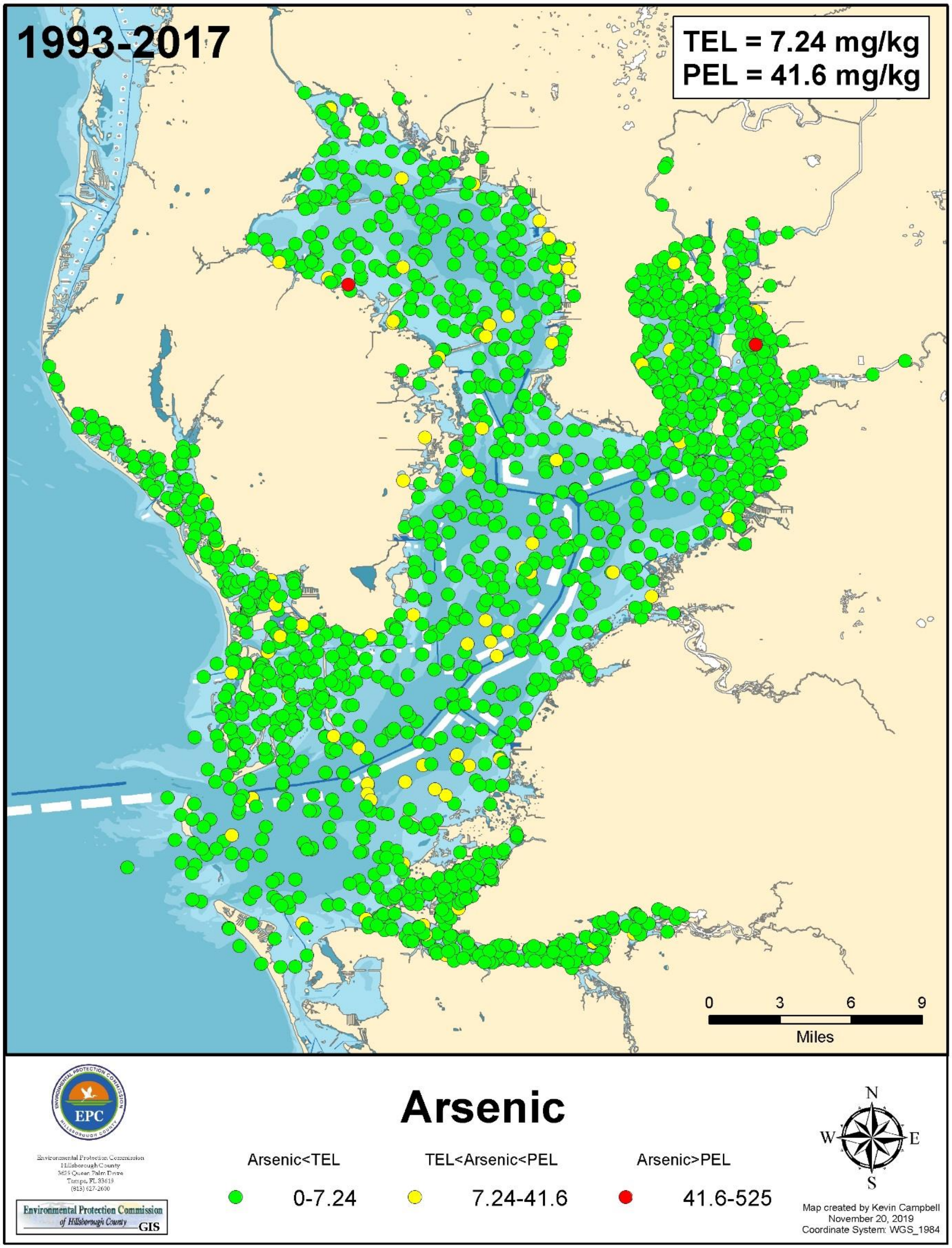

Figure 34. Spatial distribution of arsenic in Tampa Bay 1993-2017.

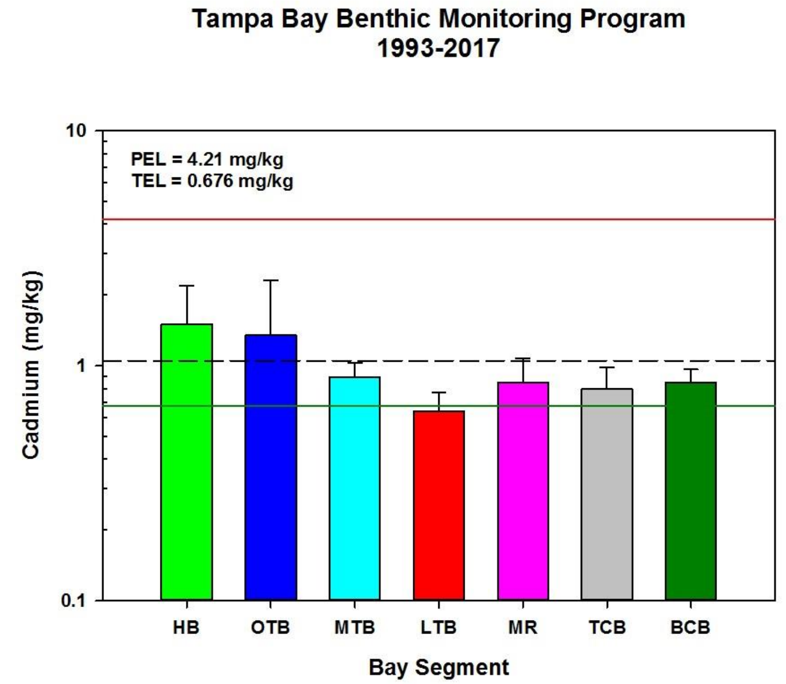

Figure 35. Mean sediment cadmium concentrations by bay segment. Error bars = 95% confidence interval, dashed line represents bay-wide mean. Solid lines represent PEL (upper; red) and TEL (lower; green) values.

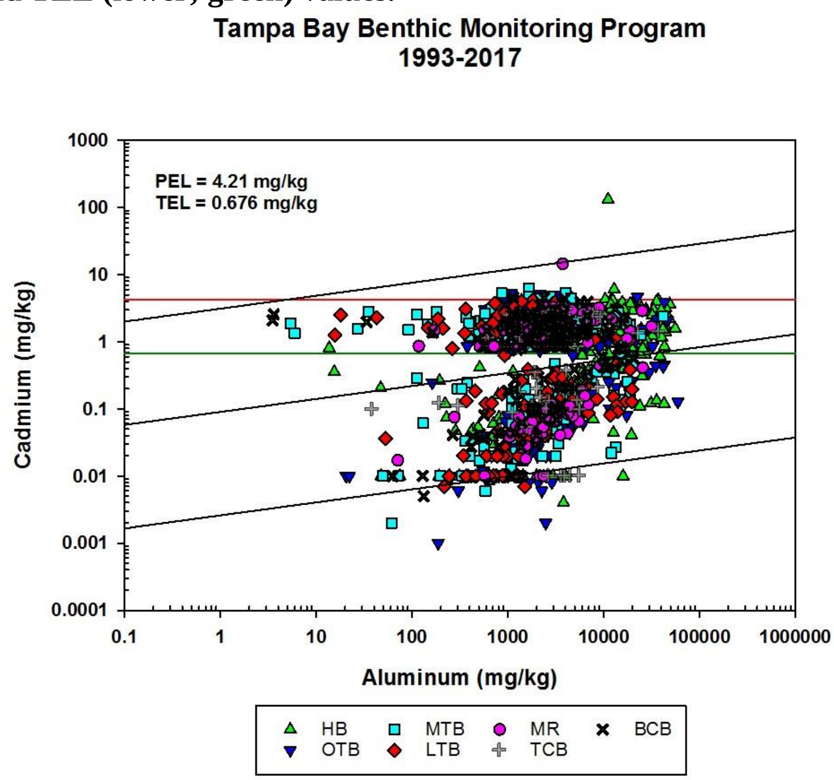

Figure 36. Tampa Bay Cd:Al ratio with 95% prediction intervals (solid lines). Dashed lines represent PEL (upper) and TEL (lower) values.

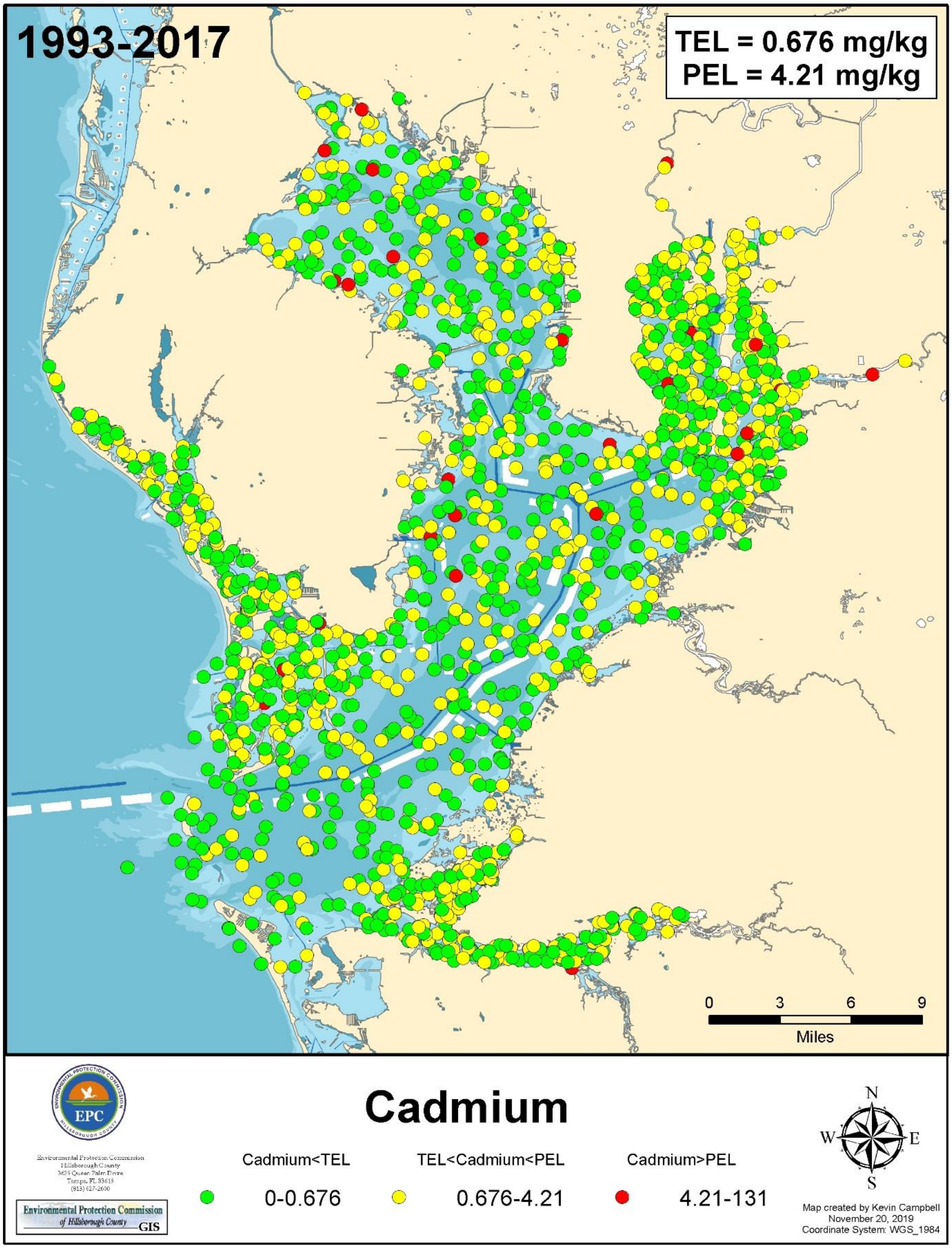

Figure 37. Distribution of cadmium in Tampa Bay 1993-2017.

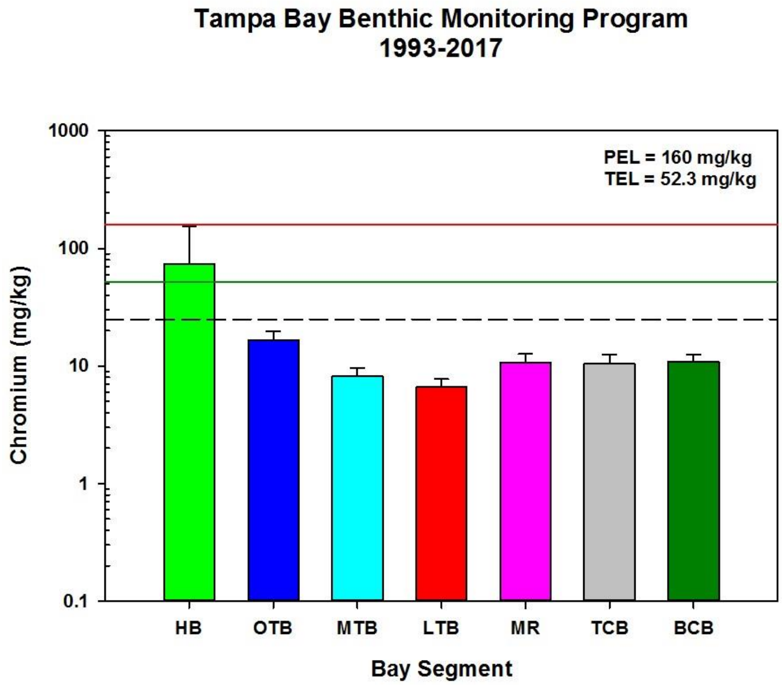

Figure 38. Mean sediment chromium concentrations by bay segment. Error bars = 95% confidence interval, dashed line represents bay-wide mean. Solid lines represent PEL (upper; red) and TEL (lower; green) values.

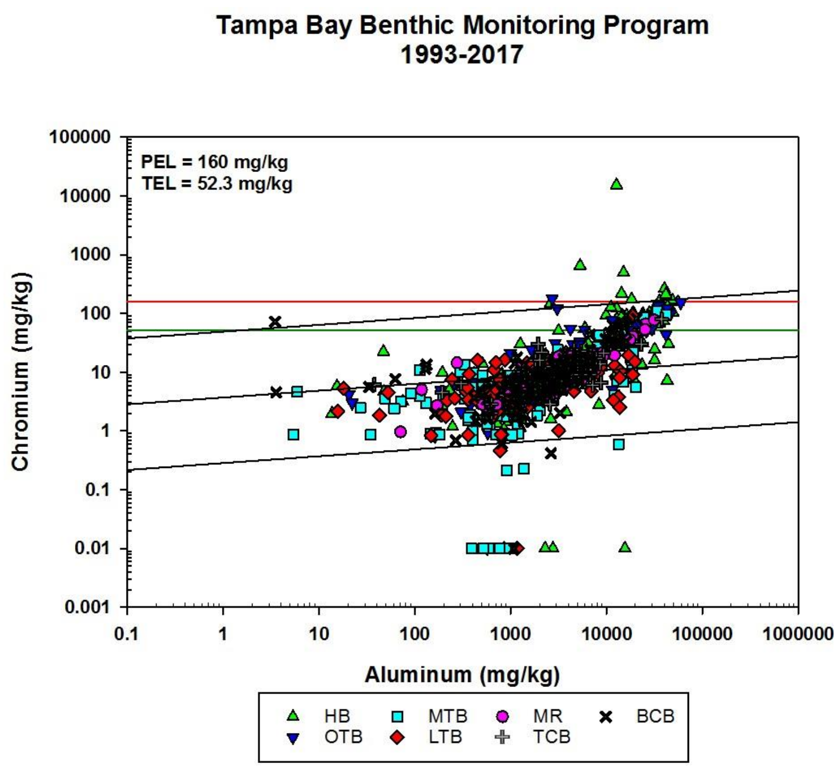

Figure 39. Tampa Bay Cr:Al ratio with 95% prediction intervals (solid lines). Solid lines represent PEL (upper; red) and TEL (lower; green) values.

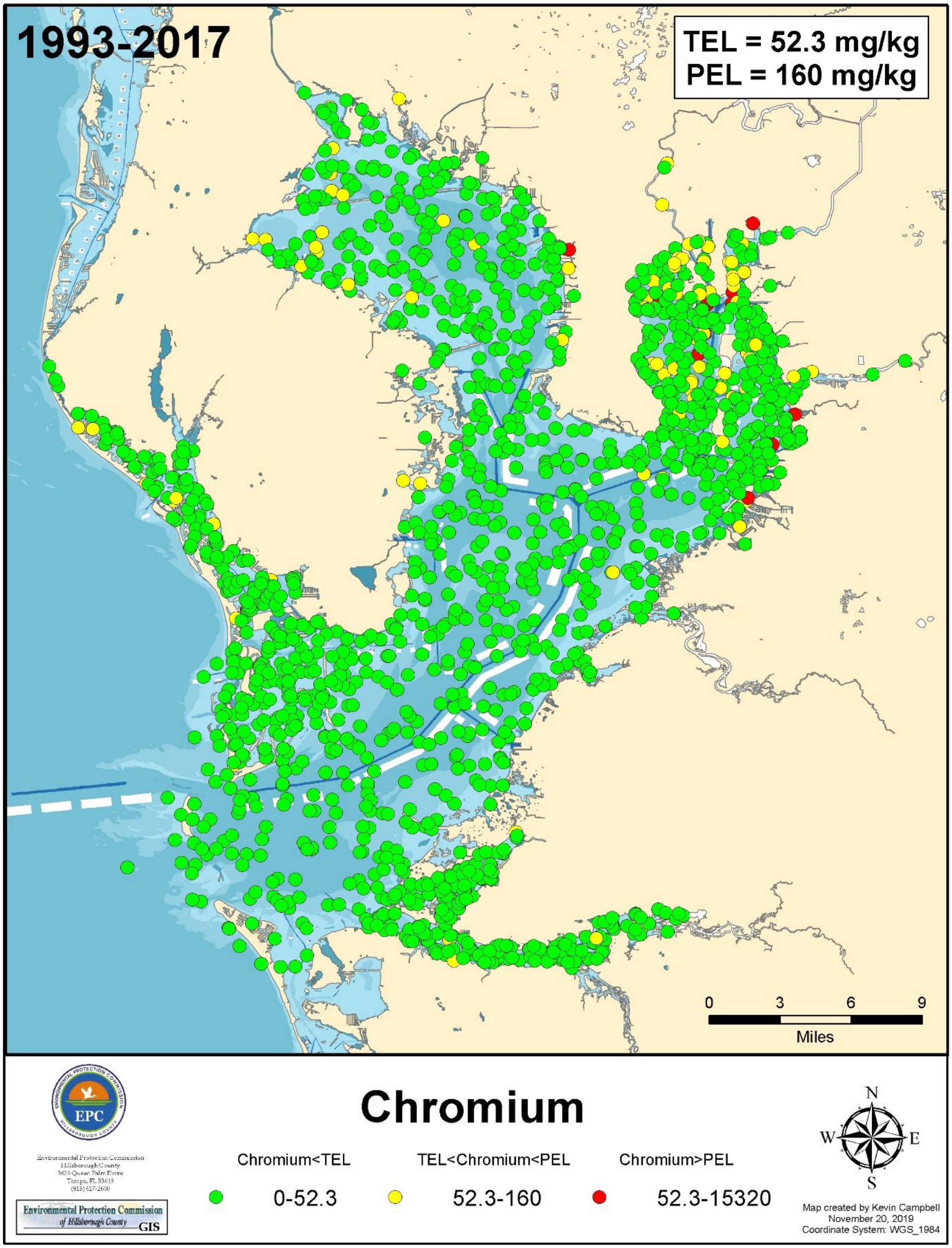

Figure 40. Distribution of chromium in Tampa Bay 1993-2017.

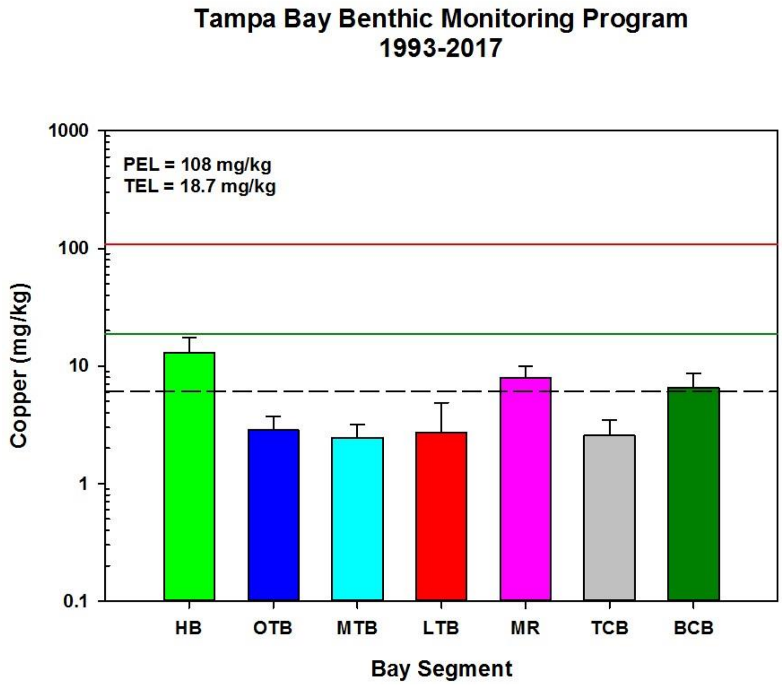

Figure 41. Mean sediment copper concentrations by bay segment. Error bars = 95% confidence interval, dashed line represents bay-wide mean. Solid lines represent PEL (upper; red) and TEL (lower; green) values.

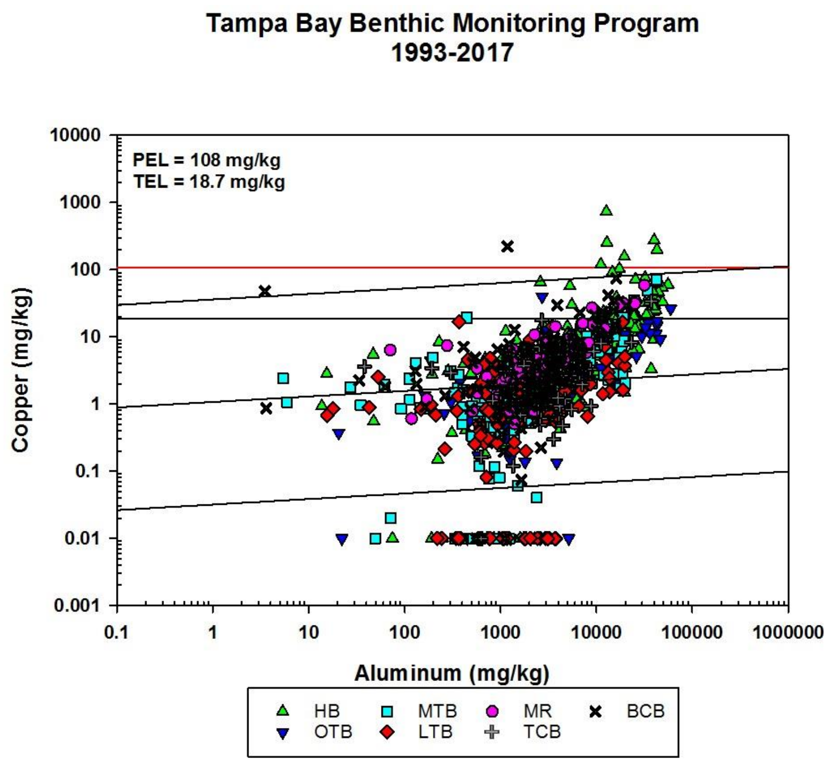

Figure 42. Tampa Bay Cu:Al ratio with 95% prediction intervals (solid lines). Solid lines represent PEL (upper; red) and TEL (lower; green) values.

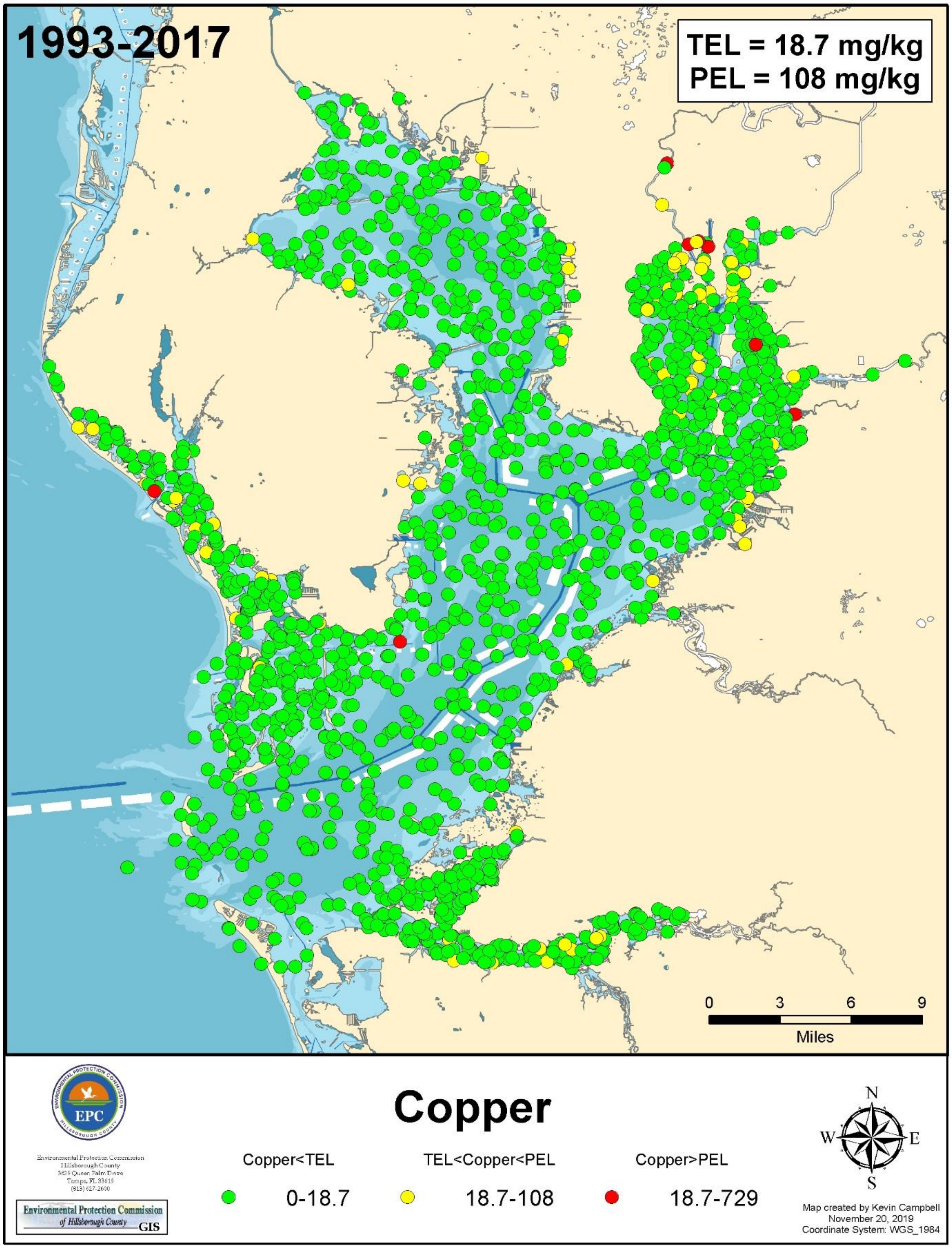

Figure 43. Distribution of copper in Tampa Bay 1993-2017.

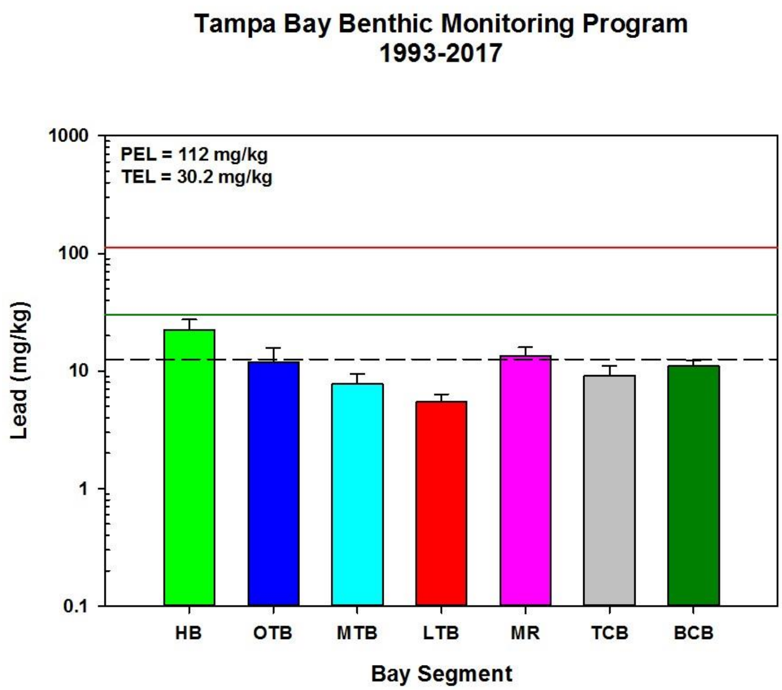

Figure 44. Mean sediment lead concentrations by bay segment. Error bars = 95% confidence interval, dashed line represents bay-wide mean. Solid lines represent PEL (upper; red) and TEL (lower; green) values.

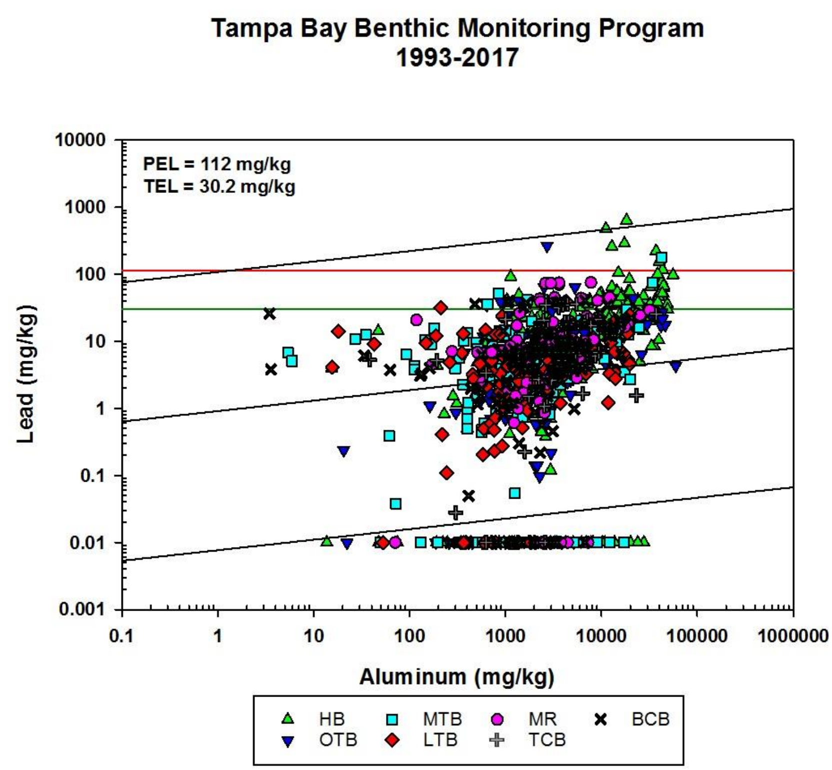

Figure 45. Tampa Bay Pb:Al ratio with 95% prediction intervals (solid lines). Solid lines represent PEL (upper; red) and TEL (lower; green) values.

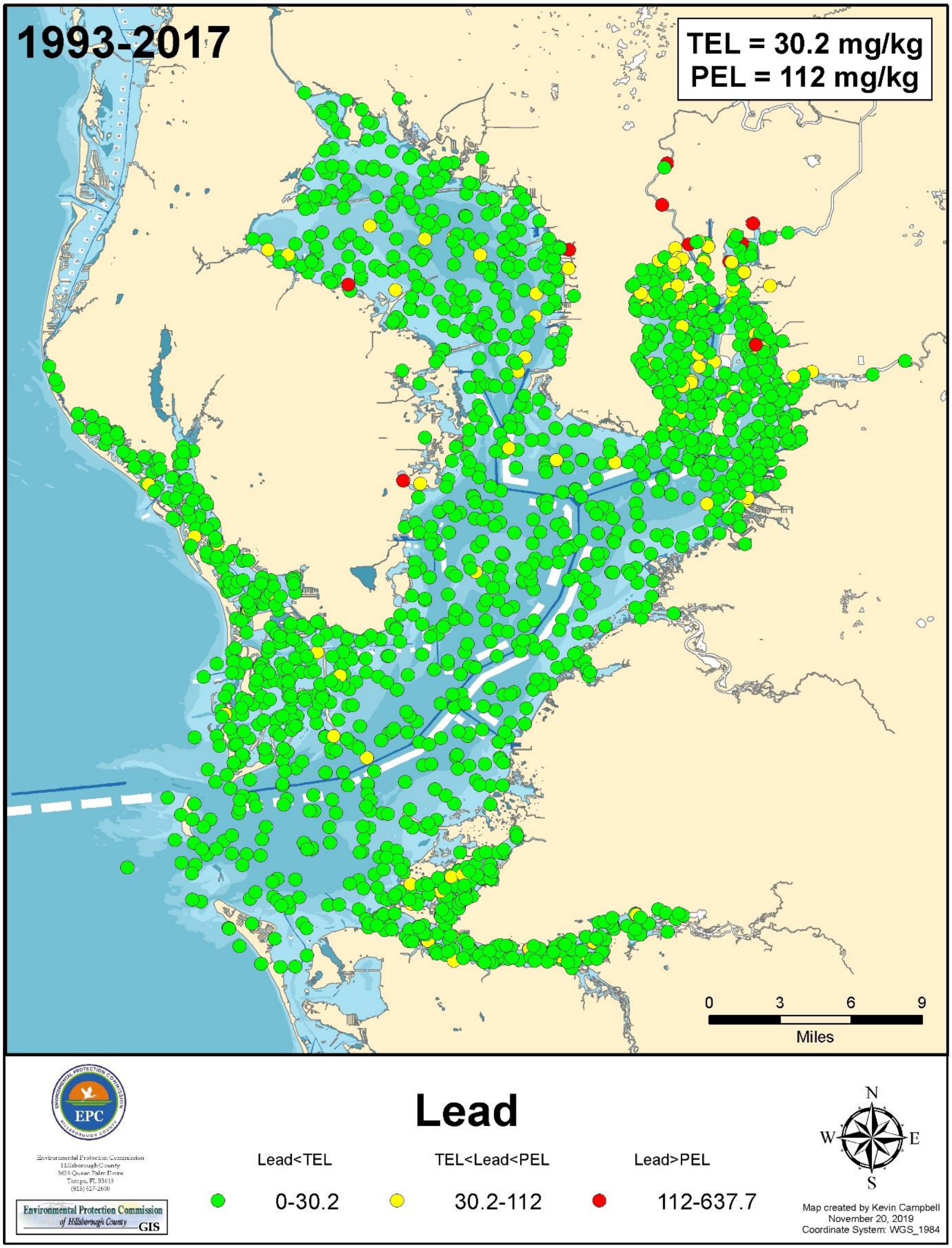

Figure 46. Distribution of lead in Tampa Bay 1993-2017.

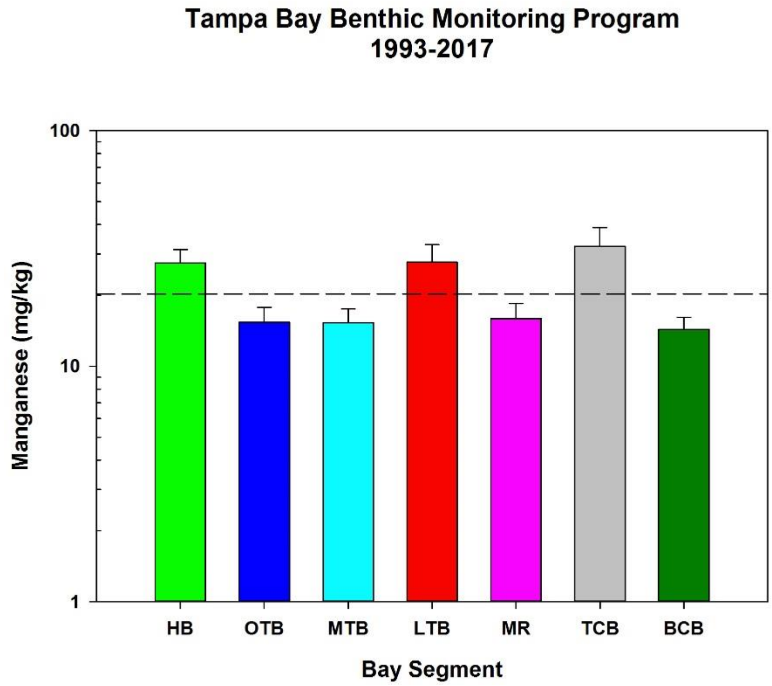

Figure 47. Mean sediment manganese concentrations by bay segment. Error bars = 95% confidence interval, dashed line represents bay-wide mean.

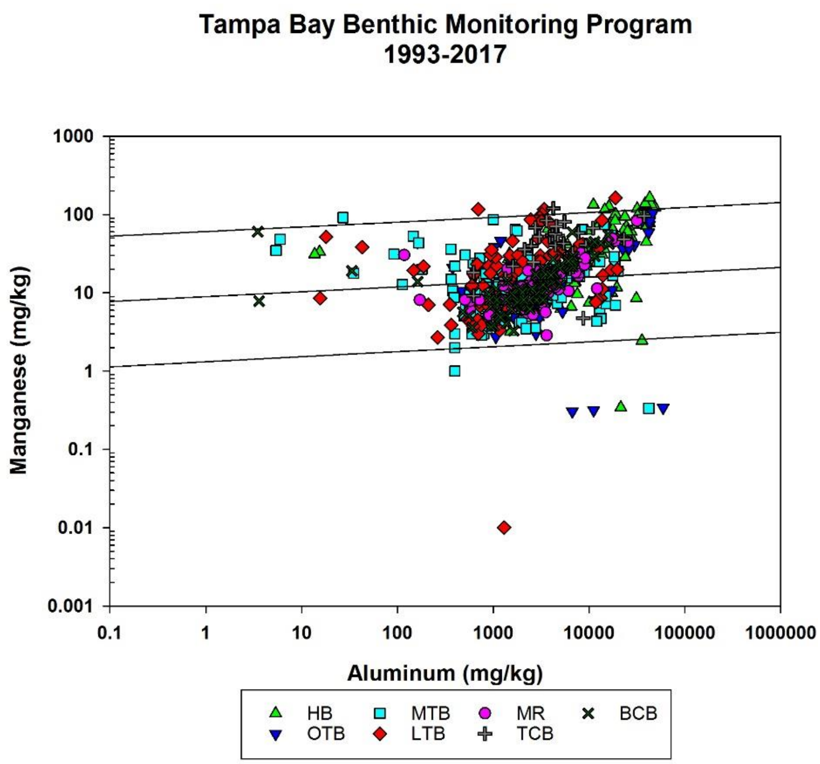

Figure 48. Tampa Bay Mn:Al ratio with 95% prediction intervals (solid lines).

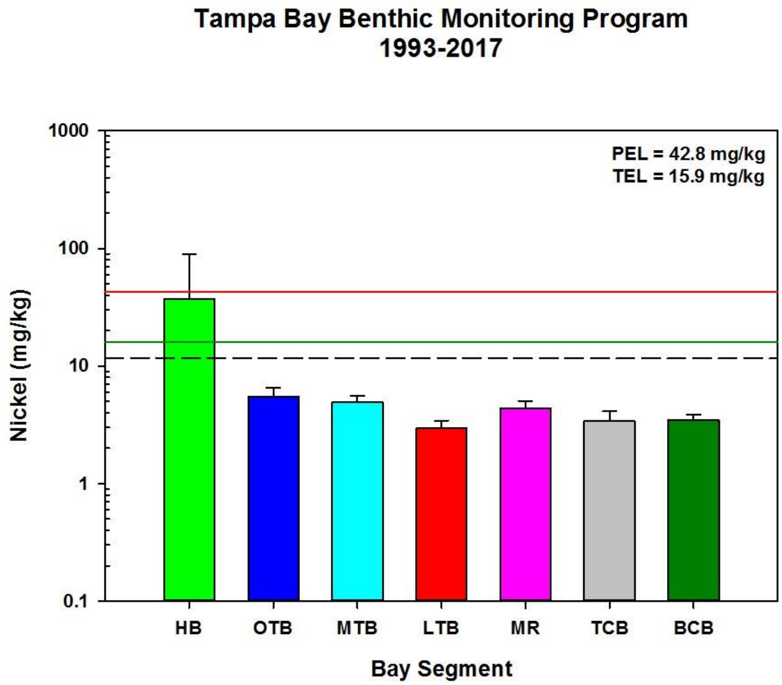

Figure 49. Mean sediment concentrations of nickel by bay segment. Error bars = 95% confidence interval, dashed line represents bay-wide mean. Solid lines represent PEL (upper; red) and TEL (lower; green) values.

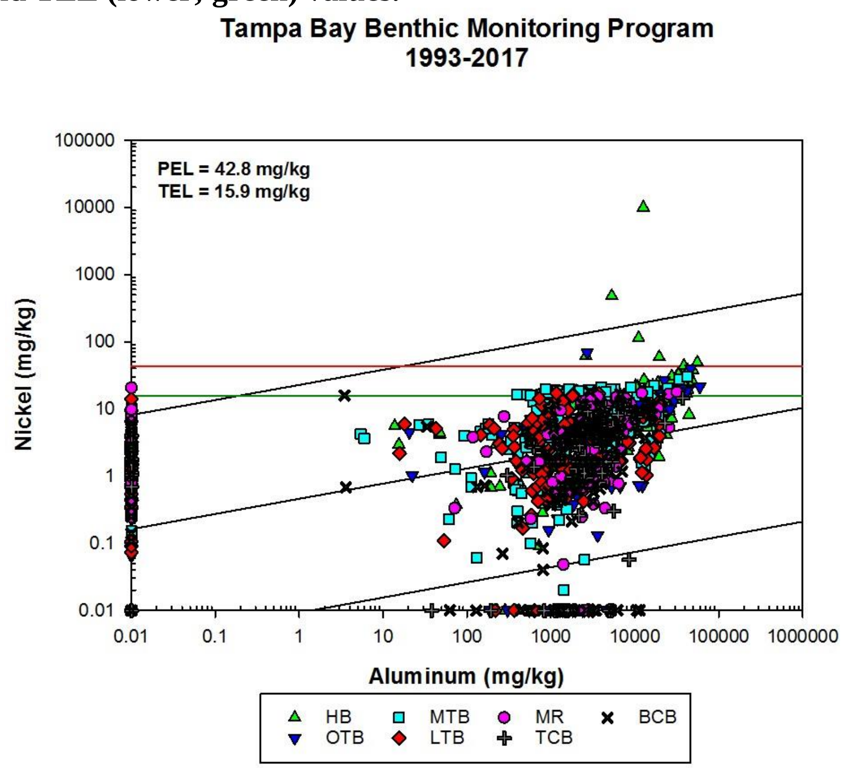

Figure 50. Tampa Bay Ni:Al ratio with 95% prediction intervals (solid lines). Solid lines represent PEL (upper; red) and TEL (lower; green) values.

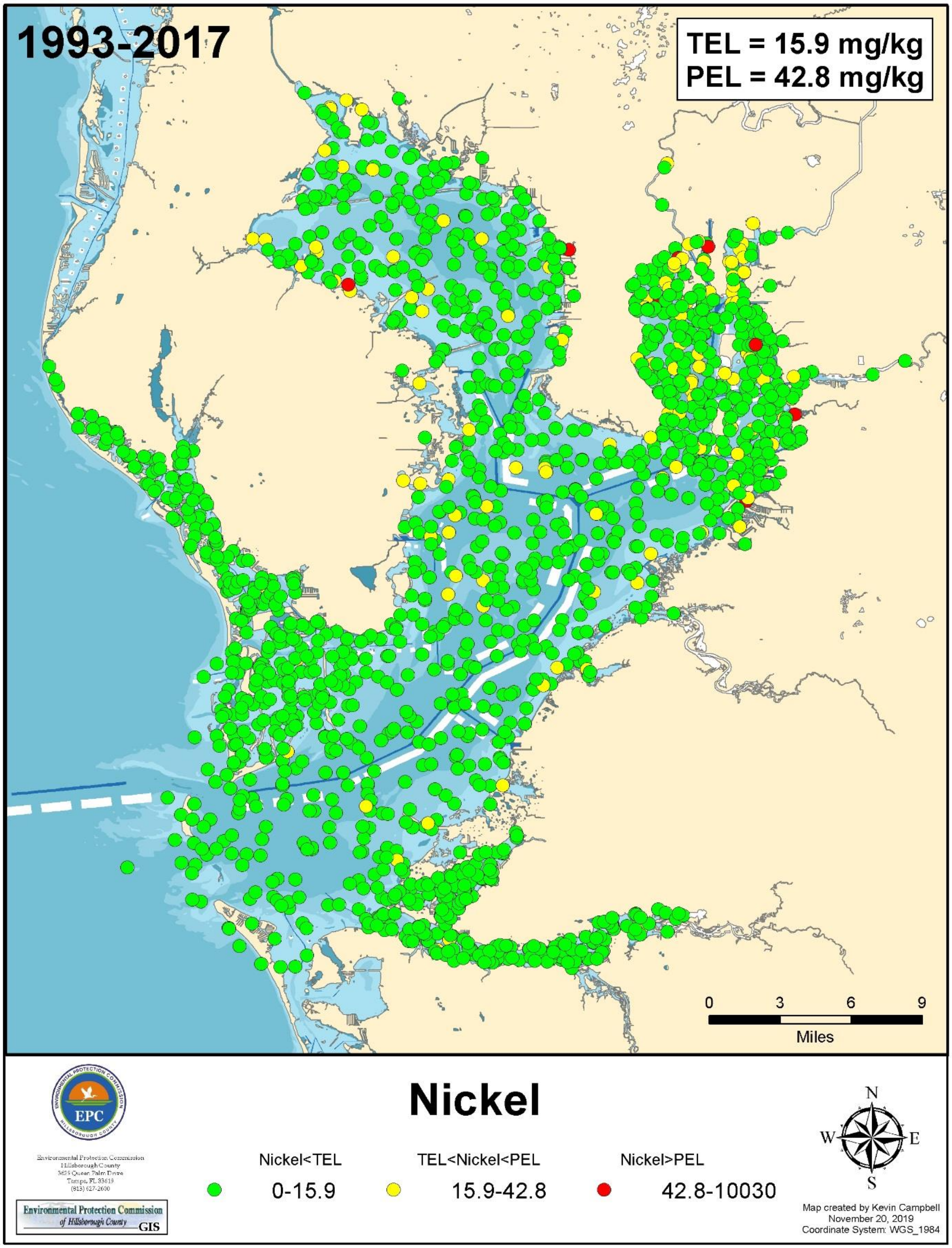

Figure 51. Distribution of nickel in Tampa Bay 1993-2017.

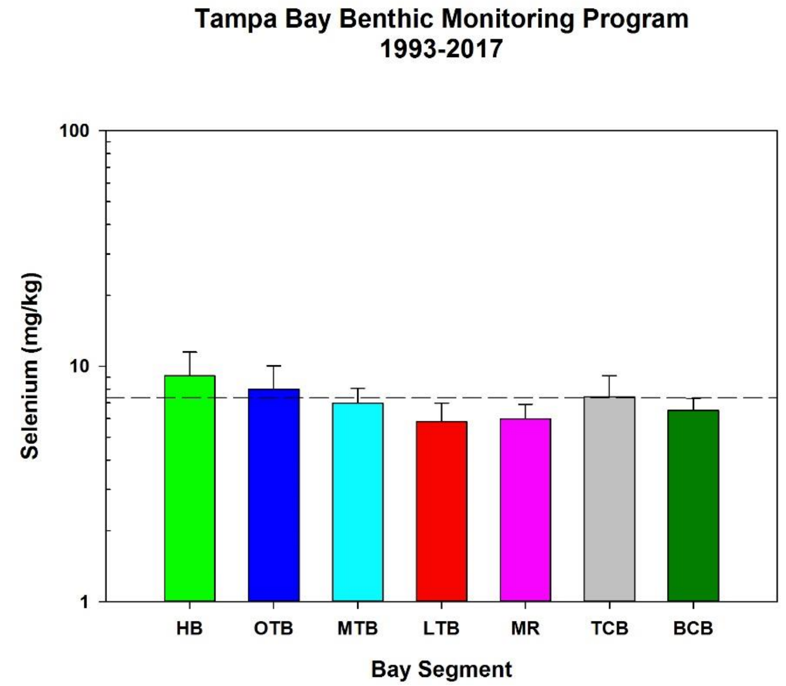

Figure 52. Mean sediment selenium concentrations by bay segment.
Error bars = 95% confidence interval, dashed line represents bay-wide mean.

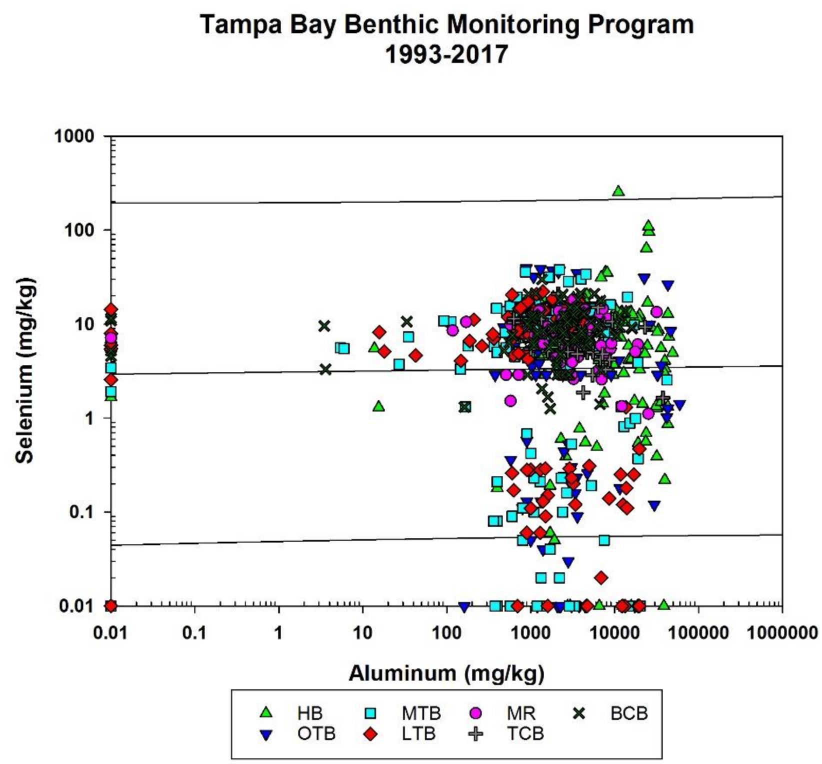

Figure 53. Tampa Bay Se:Al ratio with 95% prediction intervals (solid lines).

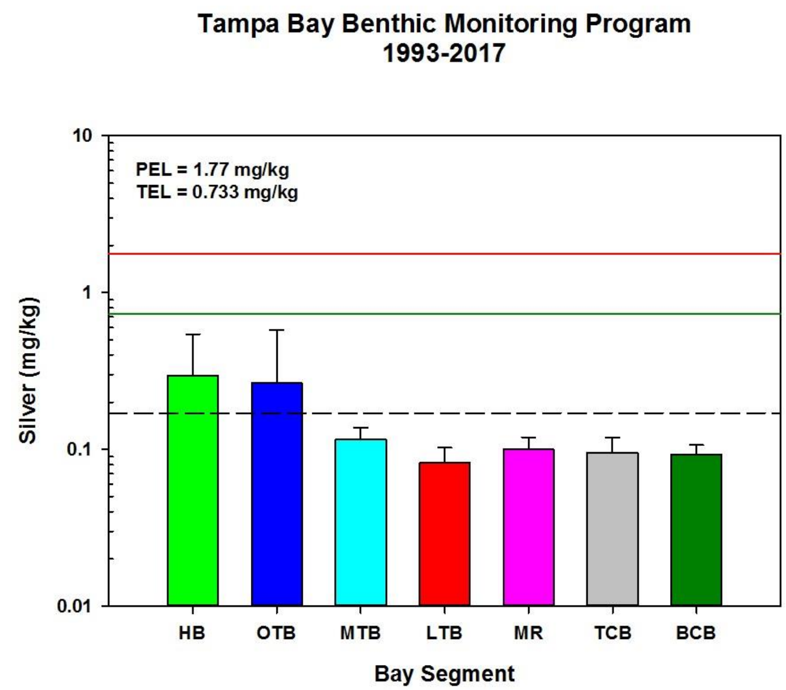

Figure 54. Mean sediment silver concentrations by bay segment. Error bars = 95% confidence interval, dashed line represents bay-wide mean. Solid lines represent PEL (upper; red) and TEL (lower; green) values.

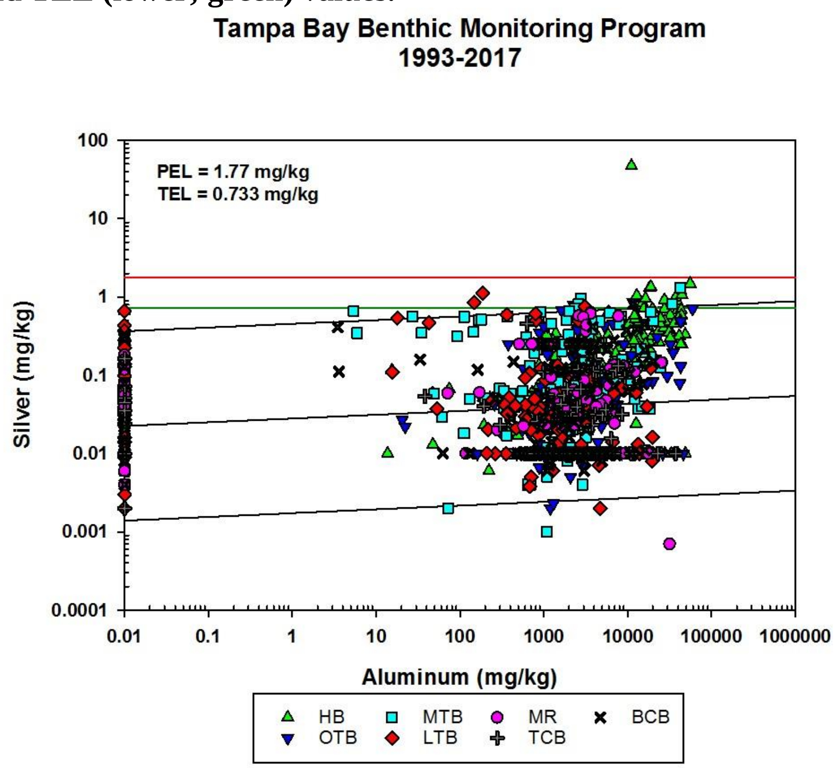

Figure 55. Tampa Bay Ag:Al ratio with 95% prediction intervals (solid lines).

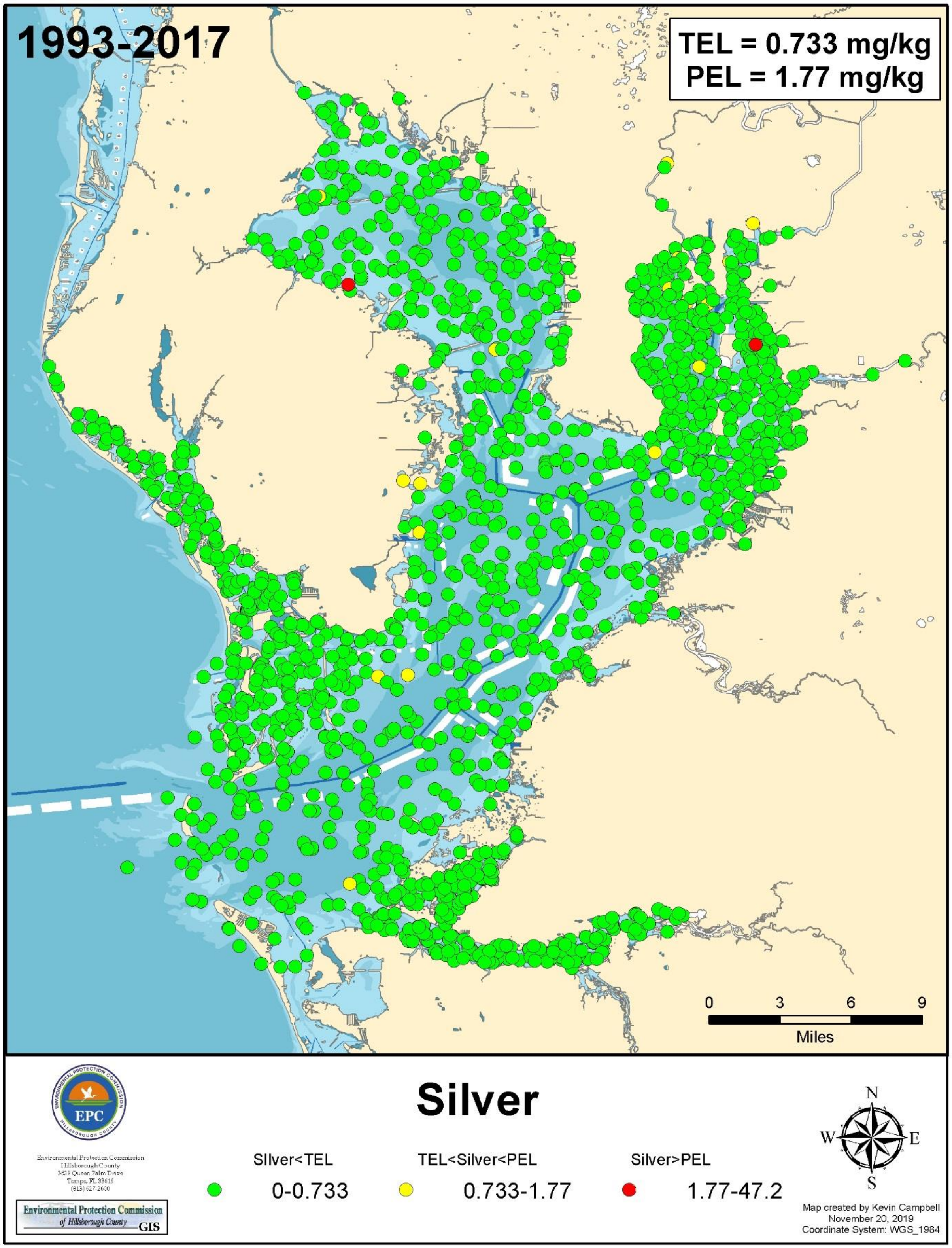

Figure 56. Spatial distribution of silver in Tampa Bay 1993-2017.

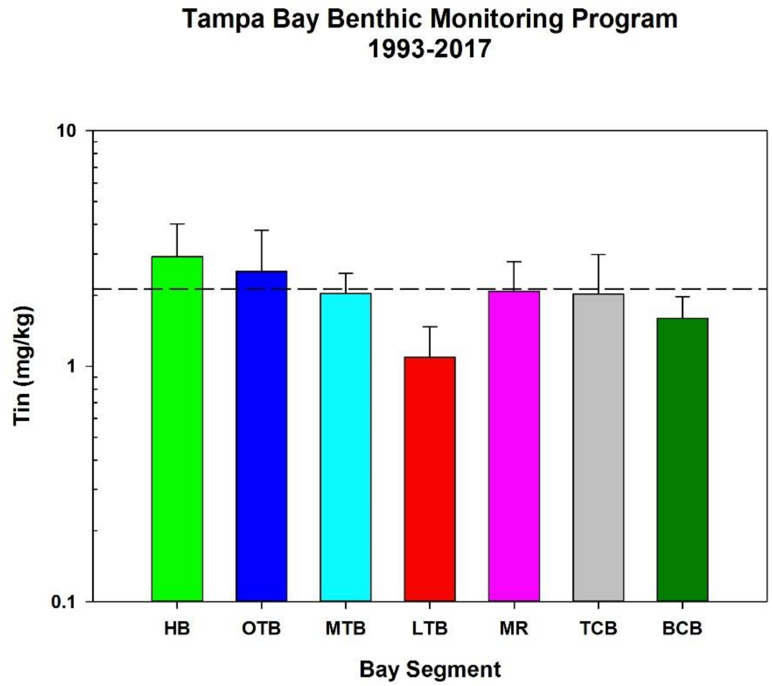

Figure 57. Mean sediment tin concentrations by bay segment. Error bars = 95% confidence interval, dashed line represents bay-wide mean.

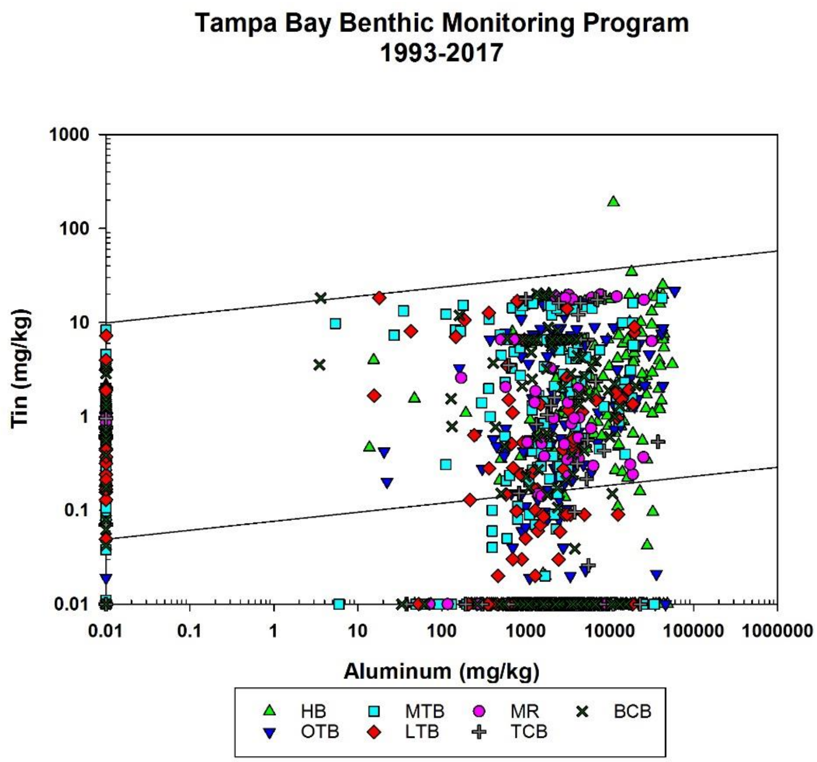

Figure 58. Tampa Bay Sn:Al ratio with 95% prediction intervals (solid lines).

Tampa Bay Benthic Monitoring Program
1993-2017

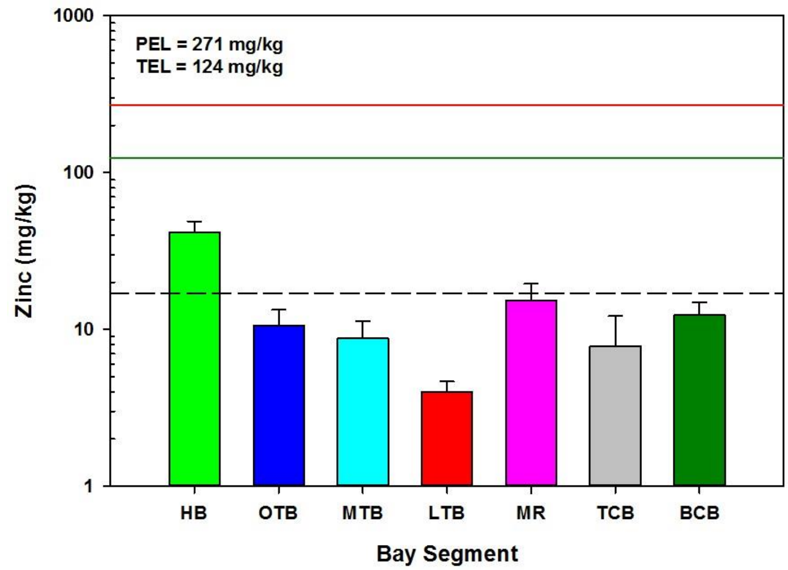

Figure 59. Mean sediment zinc concentrations by bay segment. Error bars = 95% confidence interval, dashed line represents bay-wide mean. Solid lines represent PEL (upper; red) and TEL (lower; green) values.

Tampa Bay Benthic Monitoring Program
1993-2017

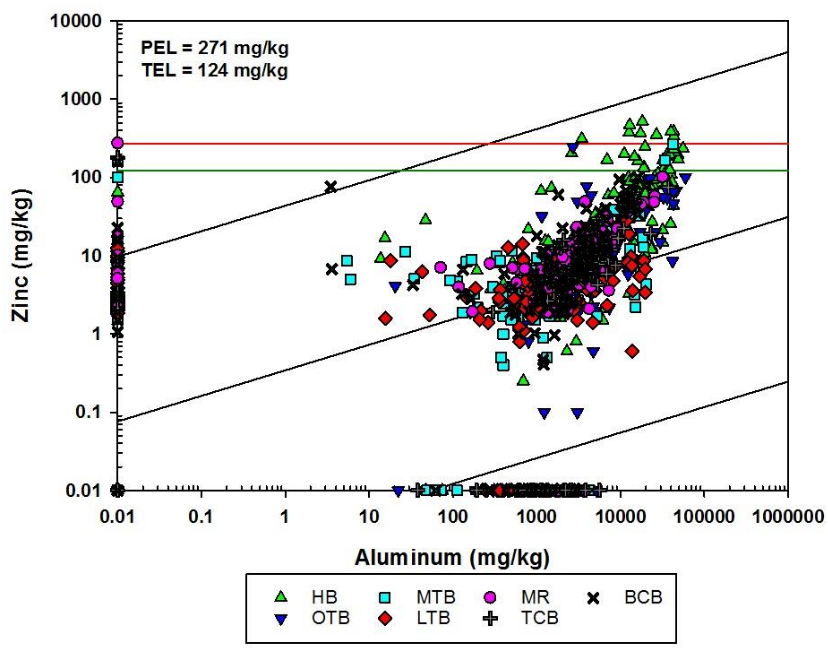

Figure 60. Tampa Bay Zn:Al ratio with 95% prediction intervals (solid lines). Dashed line represents bay-wide mean. Solid lines represent PEL (upper; red) and TEL (lower; green) values.

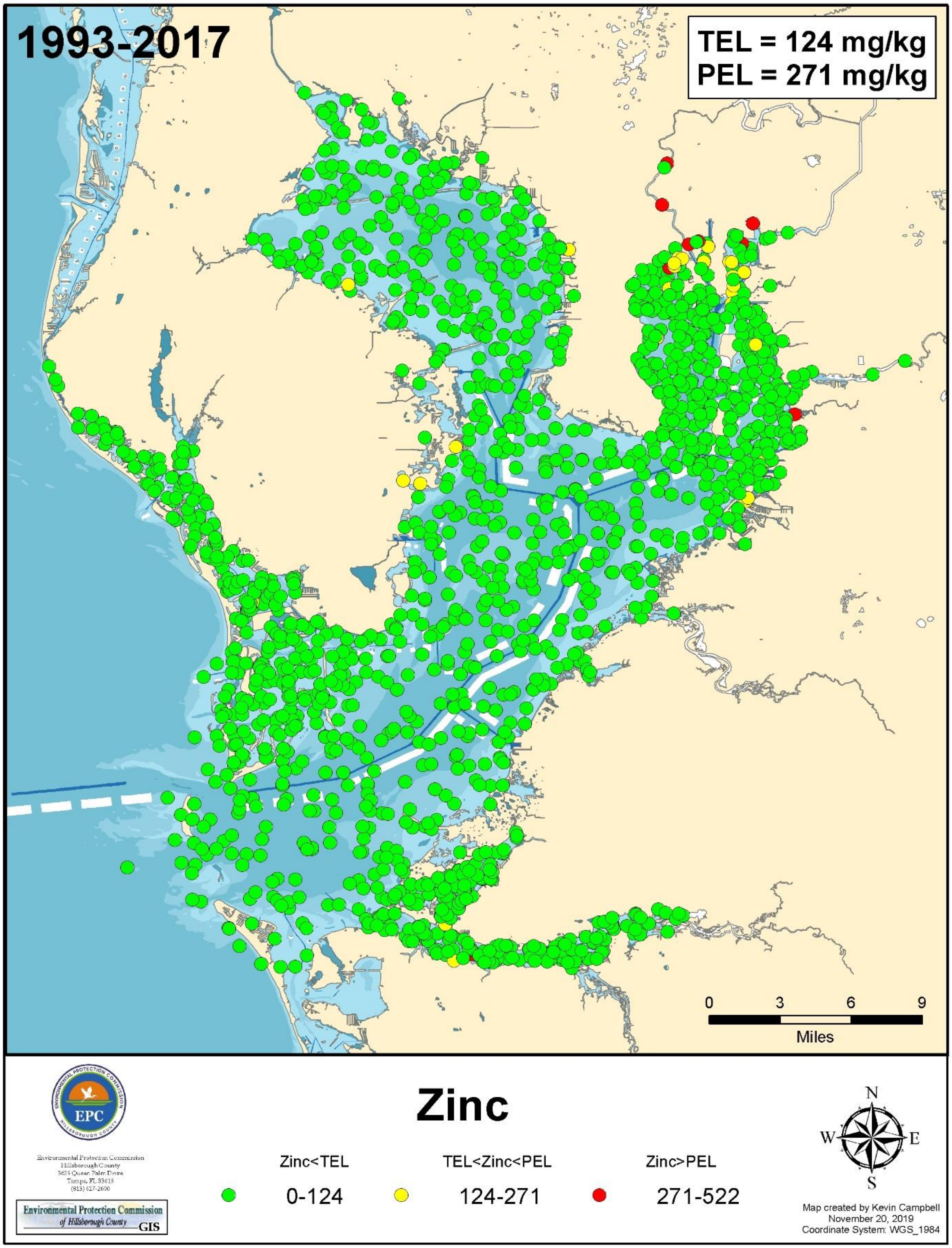

Figure 61. Distribution of Zinc in Tampa Bay 1993-2017.

Polycyclic Aromatic Hydrocarbons (PAHs)

Polycyclic aromatic hydrocarbons (PAHs) are organic compounds formed from carbon and hydrogen atoms arranged in two or more benzene rings (Kennish, 1998). PAHs composed of two to three benzene rings are classified as low molecular weight PAHs (Long et al., 1994). Many of these compounds can have acute toxic effects as well as sublethal effects on marine organisms (Long et al., 1994; Kennish, 1998), which can be enhanced by exposure to UV light (phototoxicity) in the environment (Pelletier et al., 1997). PAHs consisting of four to seven benzene rings are classified as high molecular weight PAHs (Long et al., 1994). These compounds are less toxic to marine organisms, but many can cause cancer (carcinogenic), genetic mutations (mutagenic), or birth defects (teratogenic) (Long et al., 1994; Kennish, 1998).

Natural sources of PAHs include the decomposition or combustion of organic matter and petroleum seeps. PAHs can be introduced into the environment anthropogenically through the combustion of fossil fuels, oil spills, atmospheric deposition, and wastewater effluents (MacDonald, 1994; Frithsen et al., 1995; Kennish, 1998). Stormwater runoff from roads and urban areas is a major route of introduction for PAHs in estuarine systems, with PAH concentrations in water and sediments being highest near roadways and large urban centers (MacDonald, 1994; Ngabe et al., 2000; Van Dolah et al., 2005). Coal tar based seal coats on parking lots and driveways can also be a source of PAHs in stormwater runoff (Mahler et al., 2010; Scoggins et al., 2007; Van Metre and Mahler, 2010; Watts et al., 2010; Witter et al., 2014; Yang et al., 2010).

The primary source of PAHs in Tampa Bay is from the combustion of gasoline via automobile emissions (Grabe and Barron, 2002, 2004), which enters the bay through atmospheric deposition and stormwater runoff (McConnell and Brink, 1997). Earlier analysis of the sediment chemistry samples collected from the Tampa Bay Benthic Monitoring Program indicated that areas of PAH contamination were typically restricted to sites with lower salinities and fine sediments, mainly within in the Hillsborough River and the upper reaches of Hillsborough Bay (Grabe and Barron, 2002; 2004).

Bay-wide sediment PAH summary statistics and percent of samples exceeding the sediment toxicity TEL and PEL for each constituent PAH (MacDonald, 1994) are presented in Tables 11-13 for all years combined. Due to the large number of low measurements, the mean values rather than median values are presented for between-bay segment comparisons.

Low Molecular Weight PAHs

Summary statistics and percentage of samples exceeding toxicity cut-offs for low molecular weight PAHs (LMW-PAHs) are presented in Table 11. Results for individual LMW-PAHs are summarized below.

Acenaphthene ($C_{12}H_{10}$; MW=154.22): Acenaphthene consists of a two-ringed naphthalene molecule bound with an ethylene molecule (Table 11). Commercially, acenaphthene is used as an insecticide and fungicide, and in the production of dyes, pharmaceuticals and plastics (ATSDR, 1995a). The bay-wide mean was 1.29 µg/kg, with a maximum concentration of 129 µg/kg (Table 11). Acenaphthene exceeded the TEL concentrations at 3.78% of the sites and the PEL at 0.14% of the sites (Table 11), with higher concentrations in Hillsborough Bay and Boca Ciega Bay (Figure 62). The sites with the highest levels of acenaphthene were in McKay Bay and near the Port of Tampa (Figure 64).

Acenaphthylene ($C_{12}H_8$; MW = 152.19): Acenaphthylene is similar in structure to acenaphthene but with a double bond in the ethylene molecule (Table 11). It is a component of petroleum products and coal tar, and is released into the environment through the combustion of petroleum and wood (ATSDR, 1995a). Long et al., (1994) found a significant correlation between acenaphthylene concentration and amphipod survival in sediment toxicity tests from Tampa Bay sites. Acenaphthylene sediment concentrations in Tampa Bay ranged from below MDL to 414 µg/kg, with a mean of 1.56 µg/kg (Table 11). Acenaphthylene exceeded its TEL at 5.78% of the sites and its PEL at 0.14% of the sites (Table 11). Mean concentrations were highest in Hillsborough Bay (Figure 63), with the highest levels being recorded in McKay Bay and around the East Bay section of Port Tampa Bay (Figure 65).

Anthracene ($C_{14}H_{10}$; MW = 178.23): Anthracene is a 3-ring PAH used commercially in the production of dyes and synthetic fibers, in wood preservatives, and in the synthesis of some chemotherapeutics (ATSDR, 1995a). Anthracene can be taken up by organisms and can accumulate in the gill tissue of freshwater mussels (Cheney et al., 2009). Exposure to anthracene can reduce the feeding and growth rate in fish (Palanikumar et al., 2013). In Tampa Bay sediments, anthracene was above its TEL at 1.17% of the sites, but there were no recorded PEL exceedances (Table 11). The bay-wide mean concentration was 2.78 µg/kg with a maximum value of 169 µg/kg (Table 11). The highest concentrations were in Hillsborough Bay (Figure 66), particularly in McKay Bay and in the vicinity of the Port of Tampa (Figure 68).

Fluorene ($C_{13}H_{10}$; MW = 166.22): Fluorene is a 3-ring PAH that is a component of diesel emissions and coal tar, is an intermediate compound in many chemical processes, and is used in the manufacture of dyes (ATSDR, 1995a). Fluorene had a mean bay-wide concentration of 1.80 µg/kg, and a maximum recorded concentration of 123 µg/kg (Table 11). Fluorene exceeded its TEL at 1.58% of the sites, but there were no recorded PEL exceedances (Table 11). Sites with fluorene concentrations above the TEL threshold were primarily in Hillsborough Bay around the Port of Tampa, McKay Bay, and the Hillsborough River (Figure 69).

Naphthalene ($C_{10}H_8$; MW = 128.17): Naphthalene is a 2-benzene ring PAH and a constituent of petroleum and coal tar (ATSDR, 2005d). It is used in the production of phthalic anhydride which is used in the production of phthalic plasticizers, resins, dyes, pharmaceuticals, and insect repellents (ATSDR, 2005d). Naphthalene crystals are also used as a moth repellent (i.e. moth balls), and as a deodorizer (ATSDR, 2005d). Exposure to high doses of naphthalene can cause lysis of red blood cells (hemolytic anemia) and cataracts (ATSDR, 2005d). High concentrations are lethal; while lower concentrations can reduce feeding rates in marine copepods, which can further affect egg production (Calbet et al., 2007). Uptake of naphthalene in freshwater mussels can be incorporated in gill tissues causing reduction in gill cilia activity (Cheney et al., 2009).

Mean sediment naphthalene concentrations were 2.58 µg/kg, with a maximum of 358 µg/kg (Table 11). Naphthalene was above the TEL at 1.31% of the sites, while no sites exceeded the

PEL (Table 11). Mean naphthalene levels were highest in Hillsborough Bay and lowest in Middle Tampa Bay (Figure 70). Most sites with TEL exceedances were in Hillsborough Bay around the Port of Tampa, McKay Bay and the Hillsborough River (Figure 72).

Phenanthrene ($C_{14}H_{10}$; MW = 178.23): Phenanthrene has the same chemical formula and molecular weight as anthracene, but differs in the configuration of its 3-ring chain structure (Table 11). Commercially, phenanthrene is used in the manufacture of explosives and in dyes (ATSDR, 1995a). Potential sources to the environment include diesel emissions, coal tar pitch, and fly ash from waste incinerators (ATSDR, 1995a). Addition of phenanthrene to estuarine waters can enhance primary productivity in phytoplankton, possibly by reducing grazing pressure from zooplankton or by stimulating photosynthetic pathways (Kelly et al., 1999). Uptake of phenanthrene by blue mussels (*Mytilus edulis*) was enhanced by higher concentrations of particulate organic carbon in the water from adsorption of PAHs to food particles and greater feeding rate of mussels (Bjork and Gilek, 1996). Phenanthrene can adsorb onto polyethylene microplastic particles, which may serve as a transport vector in estuarine systems (Bakir et al., 2014). Phenanthrene in sediments is toxic to macrofaunal oligochaetes and meiofaunal copepods, lower concentrations can reduce reproduction success in benthic organisms (Lotufo and Fleeger, 1996; Lotufo and Fleeger, 1997).

The mean sediment concentration of phenanthrene in Tampa Bay was 10.87 µg/kg, with a maximum concentration of 863 µg/kg (Table 11). Phenanthrene was above the TEL at 1.65% of the sites and exceeded the PEL at 0.28% of the sites (Table 11). Mean concentrations were highest in Hillsborough Bay (Figure 71). The sites above the PEL were in Hillsborough Bay near the Port of Tampa, the Hillsborough River, and McKay Bay (Figure 73).

Total LMW-PAHs (ΣLMW-PAH): The total Low Molecular Weight PAH (ΣLMW-PAH) concentration is calculated from the sum of the six individual low molecular weight PAHs discussed above. The mean ΣLMW-PAH concentration in Tampa Bay was 20.88 µg/kg, with a maximum concentration of 1928 µg/kg (Table 11). ΣLMW-PAHs exceeded the TEL at 0.96 % of the sites and exceeded the PEL at 0.07% (Table 11). Hillsborough Bay had the highest mean concentration with elevated levels also in the Manatee River and Boca Ciega Bay (Figure 74). The sites with the highest concentrations of ΣLMW-PAH were around the Port of Tampa in Hillsborough Bay and the single site exceeding the PEL was in McKay Bay (Figure 75).

High Molecular Weight PAHs

Summary statistics and percentage of samples exceeding toxicity cut-offs for high molecular weight PAHs (HMW-PAHs) are presented in Table 12. Results for individual HMW-PAHs are summarized below.

Benzo(a) anthracene ($C_{18}H_{12}$; MW=228.29): Benzo(a) anthracene is composed of a four-benzene ring chain (Table 12). It has no commercial uses, but is a component of many hydrocarbon mixtures, and is classified as a probable carcinogen (ATSDR, 1995a). There is evidence that benzo(a) anthracene in estuarine sediments can bioaccumulate in polychaetes (Ferguson and Chandler, 1998).

The benzo(a) anthracene concentrations in Tampa Bay sediments had a mean value of 17.58 µg/kg, with a maximum of 1,564 µg/kg (Table 12). The TEL was exceeded at 3.85% of the sites and concentrations were above the PEL at 0.41% of the sites (Table 12). Mean benzo(a) anthracene concentrations were highest in Hillsborough Bay, and elevated in the Manatee River and Boca Ciega Bay (Figure 76). The maximum concentration was recorded in McKay Bay, and other sites above the PEL were found in the Hillsborough River and around the Port of Tampa, as well as a single location in Boca Ciega Bay (Figure 78).

Benzo(a) pyrene ($C_{20}H_{12}$; MW=252.31): Benzo(a) pyrene has a 5-benzene ring structure (Table 12). It is not produced commercially, but is a product of incomplete combustion; its primary source to the environment is through the atmospheric deposition of particles (ATSDR, 1995a). Benzo(a) pyrene is a known carcinogen, and can cause birth defects and sterility in mice as well as chromosome damage (ATSDR, 1995a). High concentrations of benzo(a) pyrene in an algal food source fed to oysters reduced reproductive output and larval survival (Eun Jung et al., 2007), and exposure to sub-lethal doses caused reduced feeding and growth in fish (Palanikumar et al., 2013). Bioaccumulation of benzo(a) pyrene by infaunal invertebrates is influenced by the feeding mode of the organism, and is higher in deposit feeders which directly ingest contaminated sediments (Kane Driscoll and McElroy, 1996; Leppanen and Kukkonen, 2000). However, high total organic carbon content in the sediment and longer sediment-chemical contact time can bind benzo(a) pyrene and reduce its bioavailability to infaunal invertebrates (Kukkonen and Landrum, 1998; Leppanen and Kukkonen, 2000).

Tampa Bay sediments had a mean concentration of 25.28 µg/kg, with a maximum value of over 2100 µg/kg (Table 12). Benzo(a) pyrene exceeded its TEL at 4.33% of the sites and was above the PEL at 0.48% of the sites (Table 12). Higher concentrations were in Hillsborough Bay, the Manatee River, and Boca Ciega Bay (Figure 77). The highest concentrations of benzo(a) pyrene were in the Hillsborough River, McKay Bay, and other locations within Hillsborough Bay (Figure 79). Other sites that exceeded the PEL were found in Boca Ciega Bay, the Manatee River and in a residential canal near Riviera Bay in Middle Tampa Bay (Figure 79).

Chrysene ($C_{18}H_{12}$; MW= 228.29): Chrysene has the same molecular weight and formula as benzo(a) anthracene, but a different configuration of its 4-benzene ring structure (Table 12). Chrysene is carcinogenic, and causes skin tumors in mice (ATSDR, 1995a). Chrysene is not produced for commercial purposes, but is a product of combustion. Environmental sources include particulate emissions from waste incinerators and burning of natural gas (ATSDR, 1995a).

Chrysene had a mean concentration of 22.53 µg/kg in Tampa Bay sediments, and exceeded its TEL at 3.30% of the sampling sites and its PEL at 0.55% of the sites (Table 12). Concentrations were higher in Hillsborough Bay, Boca Ciega Bay, and the Manatee River (Figure 80). The highest levels of chrysene were found in the Hillsborough River, McKay Bay, and around the Port of Tampa. Several other sites exceeding the PEL in Boca Ciega Bay, the Manatee River, and at one site in Middle Tampa Bay within a residential canal near Riviera Bay (Figure 82).

Dibenzo(a,h) anthracene ($C_{22}H_{14}$; MW = 278.35): Dibenzo(a,h) anthracene is composed of a chain of 5 benzene rings (Table 12). It can be carcinogenic, causing skin tumors in mice and fetal death in pregnant rats (ATSDR, 1995a).

The mean sediment concentration was 8.21 µg/kg, above the TEL of 6.2 µg/kg (Table 12). Dibenzo(a,h) anthracene has a lower TEL and PEL than the other high molecular weight PAHs, and was above its TEL at 13.15% of the sampling sites and exceeded the PEL at 1.10% of the sites (Table 12). Mean sediment concentrations were highest in Hillsborough Bay, with Old Tampa Bay, the Manatee River, and Boca Ciega Bay also having mean concentrations exceeding the TEL (Figure 81). Sites above the PEL were in McKay Bay, the Hillsborough River, and in the vicinity of the Port of Tampa in Hillsborough Bay (Figure 83). Other sites above the PEL were in Boca Ciega Bay, the Manatee River, two sites in Old Tampa Bay, and Riviera Bay in Middle Tampa Bay (Figure 83).

Fluoranthene ($C_{16}H_{10}$; MW = 202.25): Fluoranthene has a 4-ring structure, and along with pyrene, has the smallest molecular mass of the HMW-PAHs (Table 12). Commercially, fluoranthene is used in lining material to protect the interior of steel and iron water pipes and storage tanks (ATSDR, 1995a). Sources to the environment include particulate exhaust from diesel combustion, waste incinerators, and natural gas appliances (ATSDR, 1995a). It is not considered carcinogenic, but has been linked to liver, kidney and hematological effects in mice (ATSDR, 1995a). Fluoranthene toxicity to invertebrates (crustaceans) in water and sediments is enhanced by exposure to UV light (Boese et al., 1997; Wilcoxen et al., 2003) and increasing organic carbon (Swartz et al., 1990).

Fluoranthene in Tampa Bay sediments had a mean concentration of 33.19 µg/kg, with a maximum of 3015 µg/kg (Table 12). Sediment concentrations were above the TEL at 4.61% of the sampling sites and exceeded the PEL at 0.34% of the sites (Table 12). Mean fluoranthene concentrations were higher in Hillsborough Bay, the Manatee River, and Boca Ciega Bay relative to the other bay segments (Figure 84). Sites with the highest concentrations were in the Hillsborough River, McKay Bay, in the vicinity of the Port of Tampa, and Boca Ciega Bay (Figure 86).

Pyrene ($C_{16}H_{10}$; MW = 202.25): Pyrene is a 4-ring PAH with the same molecular weight and formula as fluoranthene, but differs in its structural arrangement (Table 12). It is not considered carcinogenic, but may enhance the effects of other cancer-causing PAHs such as benzo(a) pyrene (ATSDR, 1995a). Pyrene is not produced commercially. Sources of pyrene to the environment include automobile exhaust, particulates from diesel exhaust, emissions from natural gas appliances, and as a component of coal tar pitch (ATSDR, 1995a). Exposure to high levels of pyrene can delay molting and reproduction in grass shrimp (*Palaemonetes pugio*), and reduce survivorship of offspring (Oberdorster et al., 2000). Reduced production of offspring was also observed in oligochaetes exposed to pyrene spiked sediments (Lotufo and Fleeger, 1996). Sediment associated pyrene can bioaccumulate in deposit feeding oligochaetes after ingesting contaminated sediments (Leppanen et al., 2000). Metabolism of ingested contaminated sediments by polychaete worms (*Nereis diversicolor*) and bioturbation of sediments by burrowing polychaetes, such as *Arenicola marina,* can also transfer pyrene from sediments to the overlying water column (Christensen et al., 2002).

In Tampa Bay sediments the mean pyrene concentration was 36.11 µg/kg, with a maximum of 4890 µg/kg (Table 12). Pyrene exceeded its TEL in 3.37% of the samples and was above its PEL in 0.48%. Mean pyrene concentrations were higher in Hillsborough Bay, the Manatee River, and Boca Ciega Bay (Figure 85). Sites with sediment pyrene concentrations above the PEL were found in the Hillsborough River, McKay Bay, in the vicinity of the Port of Tampa, and at one location in Boca Ciega Bay (Figure 87).

Total HMW PAHs (ΣHMW-PAHs): The total high molecular weight PAHs (ΣHMW-PAHs) is the summation of the six individual HMW-PAHs discussed above. The mean ΣHMW-PAHs was 148.89 µg/kg, with a maximum concentration of 14,455 µg/kg (Table 12). Sediment ΣHMW-PAHs were above the TEL at 3.65% of the sites and exceeded the PEL at 0.34% (Table 12). Highest mean concentrations were in Hillsborough Bay, the Manatee River, and Boca Ciega Bay (Figure 88). Five sites exceeded the PEL; four within Hillsborough Bay including sites in the Hillsborough River, McKay Bay, around the Port of Tampa, and one site in Boca Ciega Bay (Figure 90).

Total PAHs (ΣPAHs): Total PAHs (ΣPAHs) is the summation of the six LMW-PAHs and six HMW-PAHs. The mean ΣPAHs concentration was 163.78 µg/kg, with a maximum concentration of 15,562 µg/kg (Table 12). Total PAHs were above the TEL at 1.75% of the sites, but there were no PEL exceedances recorded (Table 12). Mean ΣPAHs were highest in Hillsborough Bay, the Manatee River, and Boca Ciega Bay (Figure 89). Sites exceeding the TEL were primarily located in Hillsborough Bay around the Port of Tampa, the Hillsborough River, and McKay Bay, and sites in the Manatee River, Boca Ciega Bay and Old Tampa Bay (Figure 91).

Other Polycyclic Aromatic Hydrocarbons

Several additional PAHs that do not have established sediment quality guidelines were measured as part of the monitoring program. Summary statistics for these are presented in Table 13 and are summarized below.

Benzo(b) fluoranthene ($C_{20}H_{12}$; MW = 252.31): Benzo(b) fluoranthene is a high molecular weight PAH with a 5-ring structure, and has the same formula and molecular weight as benzo(a) pyrene (Table 13). It is known to be carcinogenic, causing skin tumors in mice (ATSDR, 1995a). Benzo(b) fluoranthene can reduce the activity of the enzyme isocitrate dehydrogenase (IDH), which functions in the aerobic energy production in fish muscle tissue (Oliva et al., 2012).

The mean benzo(b) fluoranthene concentration in Tampa Bay sediments was 33.63 µg/kg, with a maximum of 3382 µg/kg (Table 13). Highest concentrations were in Hillsborough Bay, the Manatee River, and Boca Ciega Bay (Figure 92).

Benzo(k) fluoranthene ($C_{20}H_{12}$; MW = 252.31): Benzo(k) fluoranthene has the same formula and molecular weight as benzo(b) fluoranthene but a different configuration of its 5-ring structure (Table 13). It is classified as being carcinogenic, but is less potent then benzo(a) fluoranthene in causing skin tumors in mice (ATSDR, 1995a). It can also increase antioxidant enzyme activity in scallops as a response to high dose exposure (Pan et al., 2005).

The mean sediment benzo(k) fluoranthene concentration in Tampa Bay sediments was 18.08 µg/kg, with a maximum level of 1808 µg/kg (Table 13). The highest concentrations were in Hillsborough Bay, the Manatee River, and Boca Ciega Bay (Figure 93).

Indeno(1,2,3-c,d) pyrene ($C_{22}H_{12}$; MW = 276.33): Indeno(1,2,3-c,d) pyrene is a six-ring PAH (Table 13). Sources to the environment include waste incineration and automobile exhaust (ATSDR, 1995a). It can be mutagenic and carcinogenic in mice (ATSDR, 1995a).

The mean concentration of indeno(1,2,3-c,d) pyrene in Tampa Bay sediments was 21.04 µg/kg, with a maximum value of 2161 µg/kg (Table 13). Sediment concentrations were significantly higher in Hillsborough Bay, the Manatee River, and Boca Ciega Bay relative to Middle and Lower Tampa Bay (Figure 94).

Benzo(g,h,i) perylene ($C_{22}H_{12}$; MW = 276.33): Benzo(g,h,i) perylene is composed of six benzene rings and has the same chemical formula and molecular weight as Indeno(1,2,3-c,d) pyrene (Table 13). It can be mutagenic and a co-carcinogen in combination with other PAHs (ASTDR, 1995a). Sources to the environment include automobile exhaust and fly-ash from waste incinerators (ATSDR, 1995a).

The mean concentration of benzo(g,h,i) perylene in Tampa bay sediments was 23.86 µg/kg, with a maximum of 2500 µg/kg (Table 13). Sediment concentrations were significantly higher in Hillsborough Bay, the Manatee River, and Boca Ciega Bay relative to Middle and Lower Tampa Bay (Figure 95).

Retene ($C_{18}H_{18}$; MW = 234.34): Retene is composed of a 3-ring phenanthene with attached methyl and isopropyl groups, and is also known as 1-methyl-7-isopropylphenanthene (Table 13). Sources to the environment include the combustion of resin in pine wood (Ramdahl, 1983), and effluent from paper and pulp mills (Oikari et al., 2002). Retene exposure can cause defects in fish embryos (Billiard et al., 1999). High sediment levels from paper mill discharges can be bioavailable to fish (rainbow trout) in freshwater sysems (Oikari et al., 2002).

Analysis for retene in the Tampa Bay Benthic Monitoring samples started in 2001. The mean concentration of retene in Tampa Bay sediments was 5.96 µg/kg, with a maximum of 260.45 µg/kg at a site in Boca Ciega Bay (Table 13). The highest retene concentrations were in Hillsborough Bay, Old Tampa Bay, the Manatee River, and Boca Ciega Bay; while the lowest were in Lower Tampa Bay (Figure 96) .

Coronene ($C_{24}H_{12}$; MW = 300.35): Coronene is a large PAH composed of a six benzene rings in a larger ring structure (Table 13). It is a component of coal tars and is not considered carcinogenic (ATSDR, 1995a).

Tampa Bay monitoring samples were analysed for coronene from 2001-2008, and resumed in 2013. The mean coronene concentraion in Tampa Bay sediments was 10.22 µg/kg, with a maximum of 1262.48 (Table 13). The highest concentration was found at a site in the Hillsborough River. Hillsborough Bay had the highest mean concentration of coronene, with elevated levels also in the Manatee River (Figure 97).

Table 11. Tampa Bay (1993-2017) sediment low molecular weight polycyclic aromatic hydrocarbon summary statistics and percentage of sites exceeding TEL and PEL values.

µg/kg	Acenaphthene	Acenaphthylene	Anthracene	Fluorene	Naphthalene	Phenanthrene	Total LMW PAHs
MW	154.22	152.19	178.23	166.22	128.17	178.23	
Formula	$C_{12}H_{10}$	$C_{12}H_8$	$C_{14}H_{10}$	$C_{13}H_{10}$	$C_{10}H_8$	$C_{14}H_{10}$	
Structure	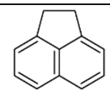	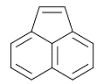	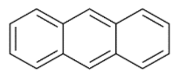	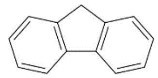	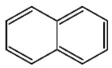	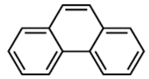	
TEL	6.7	5.9	46.9	21.2	34.6	86.7	312
PEL	88.9	128	245	144	391	544	1440
n	1454	1454	1454	1454	1454	1454	1454
Minimum	0.01	0.01	0.01	0.01	0.01	0.01	0.06
Maximum	129	414	169	123	358	862.93	1928
Median	0.01	0.01	0.01	0.01	0.01	0.01	0.06
Mean	1.29	1.56	2.78	1.80	2.58	10.87	20.88
SD	6.10	12.71	11.97	7.06	14.41	51.98	89.64
% >TEL;<PEL	**3.78%**	**5.78%**	**1.17%**	**1.58%**	**1.31%**	**1.65%**	**0.96%**
% >PEL	**0.14%**	**0.14%**	**0.00%**	**0.00%**	**0.00%**	**0.28%**	**0.07%**

Table 12. Tampa Bay (1993-2017) sediment high molecular weight and total polycyclic aromatic hydrocarbon summary statistics and percentage of sites exceeding TEL and PEL values.

µg/kg	Benzo (a) anthracene	Benzo (a) pyrene	Chrysene	Dibenzo(a,h) anthracene	Fluoranthene	Pyrene	Total HMW PAHs	TOTAL PAHs
MW	228.29	252.31	228.29	278.35	202.25	202.25		
Formula	$C_{18}H_{12}$	$C_{20}H_{12}$	$C_{18}H_{12}$	$C_{22}H_{14}$	$C_{16}H_{10}$	$C_{16}H_{10}$		
Structure	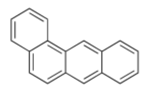	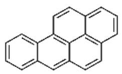	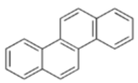	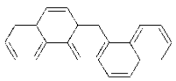	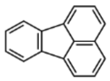	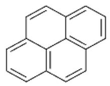		
TEL	74.8	88.8	108	6.2	113	153	655	1680
PEL	693	763	846	135	1490	1400	6680	16800
n	1454	1454	1454	1453	1454	1454	1454	1454
Min.	0.01	0.01	0.01	0.01	0.01	0.01	0.06	0.12
Max.	1564	2103.88	2326.89	830	3014.98	4890	14455.03	15562.48
Median	0.01	0.01	0.01	0.01	0.01	0.01	4.455	8.86
Mean	17.58	25.28	22.53	8.21	33.19	36.11	142.89	163.78
SD	82.21	116.70	109.45	42.72	165.77	207.46	710.16	789.63
% >TEL;<PEL	**3.85%**	**4.33%**	**3.30%**	**13.15%**	**4.61%**	**3.37%**	**3.65%**	**1.58%**
% >PEL	**0.41%**	**0.48%**	**0.55%**	**1.10%**	**0.34%**	**0.48%**	**0.34%**	**0.00%**

Table 13. Other measured hydrocarbons without established TEL/PELs 1993-2017.

µg/kg	Benzo(b) fluoranthene	Benzo(k) fluoranthene	Indeno(1,2,3, c,d) pyrene	Benzo(g,h,i) perylene	Retene	Coronene
MW	252.31	252.31	276.33	276.33	234.34	300.35
Formula	$C_{20}H_{12}$	$C_{20}H_{12}$	$C_{22}H_{12}$	$C_{22}H_{12}$	$C_{18}H_{18}$	$C_{24}H_{12}$
Structure	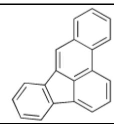	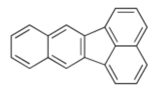	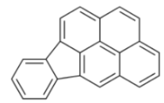	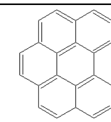	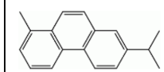	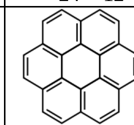
n	1454	1454	1454	1453	819	671
Min.	0.01	0.01	0.01	0.01	0.01	0.01
Max.	3382.50	1808.00	2161.00	2500.01	260.45	1262.48
Median	0.01	0.01	0.01	0.01	0.01	0.01
Mean	33.63	19.94	21.04	23.86	5.96	10.22
SD	167.71	92.92	103.78	111.27	16.22	60.92

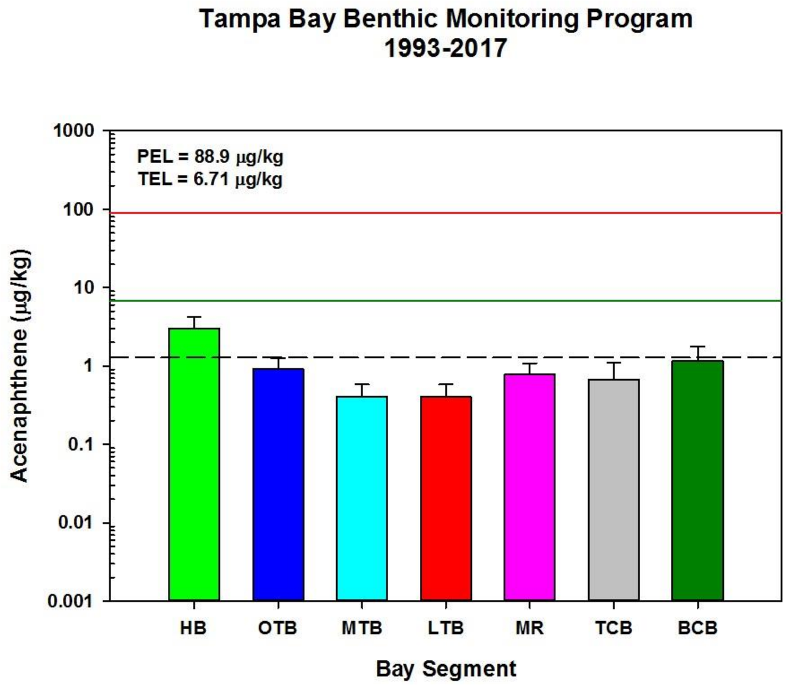

Figure 62. Mean sediment acenaphthene concentrations by bay segment. Error bars = 95% confidence interval, dashed line represents bay-wide mean. Solid lines represent PEL (upper; red) and TEL (lower; green) values.

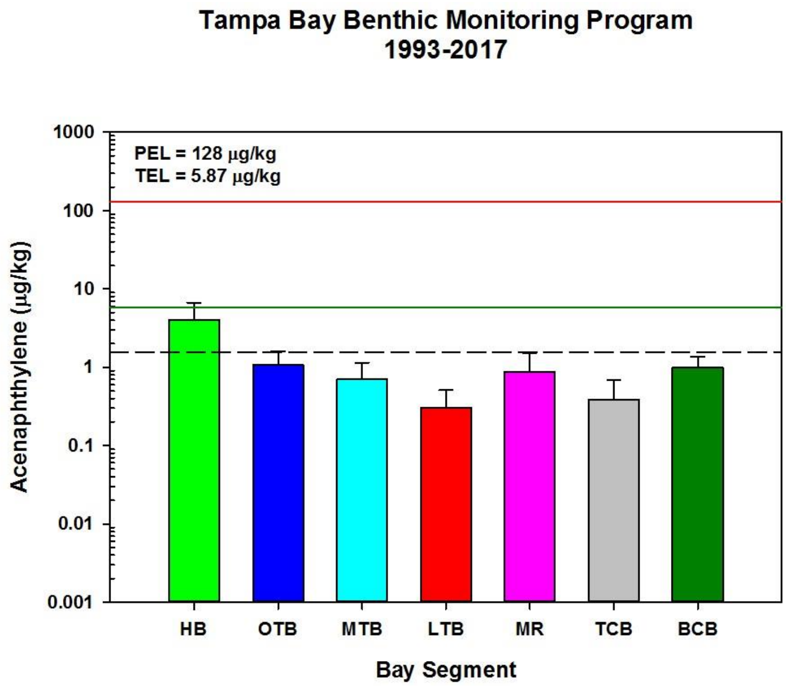

Figure 63. Mean sediment acenaphthylene concentrations by bay segment. Error bars = 95% confidence interval, dashed line represents bay-wide mean. Solid lines represent PEL (upper; red) and TEL (lower; green) values.

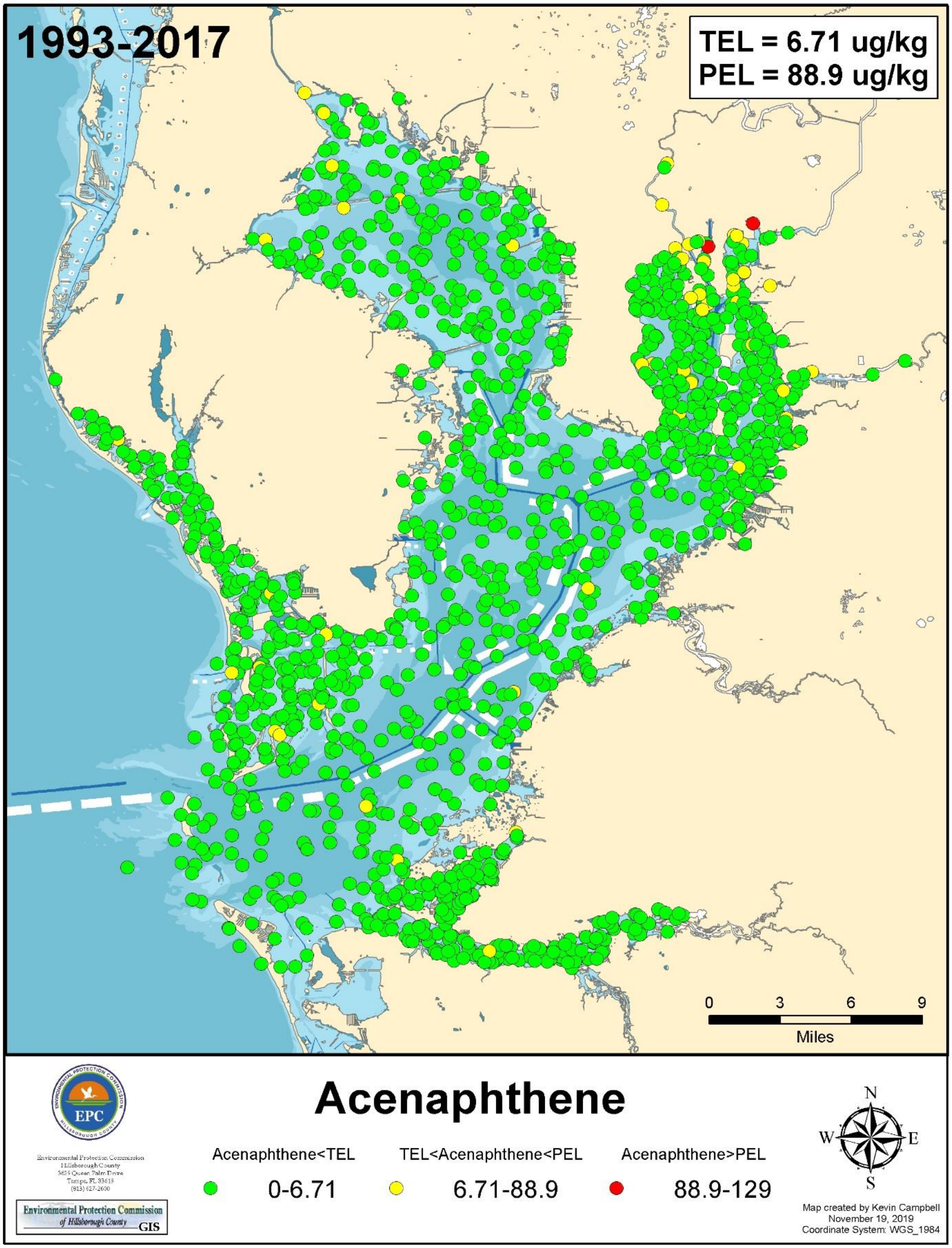

Figure 64. Distribution of acenaphthene in Tampa Bay 1993-2017.

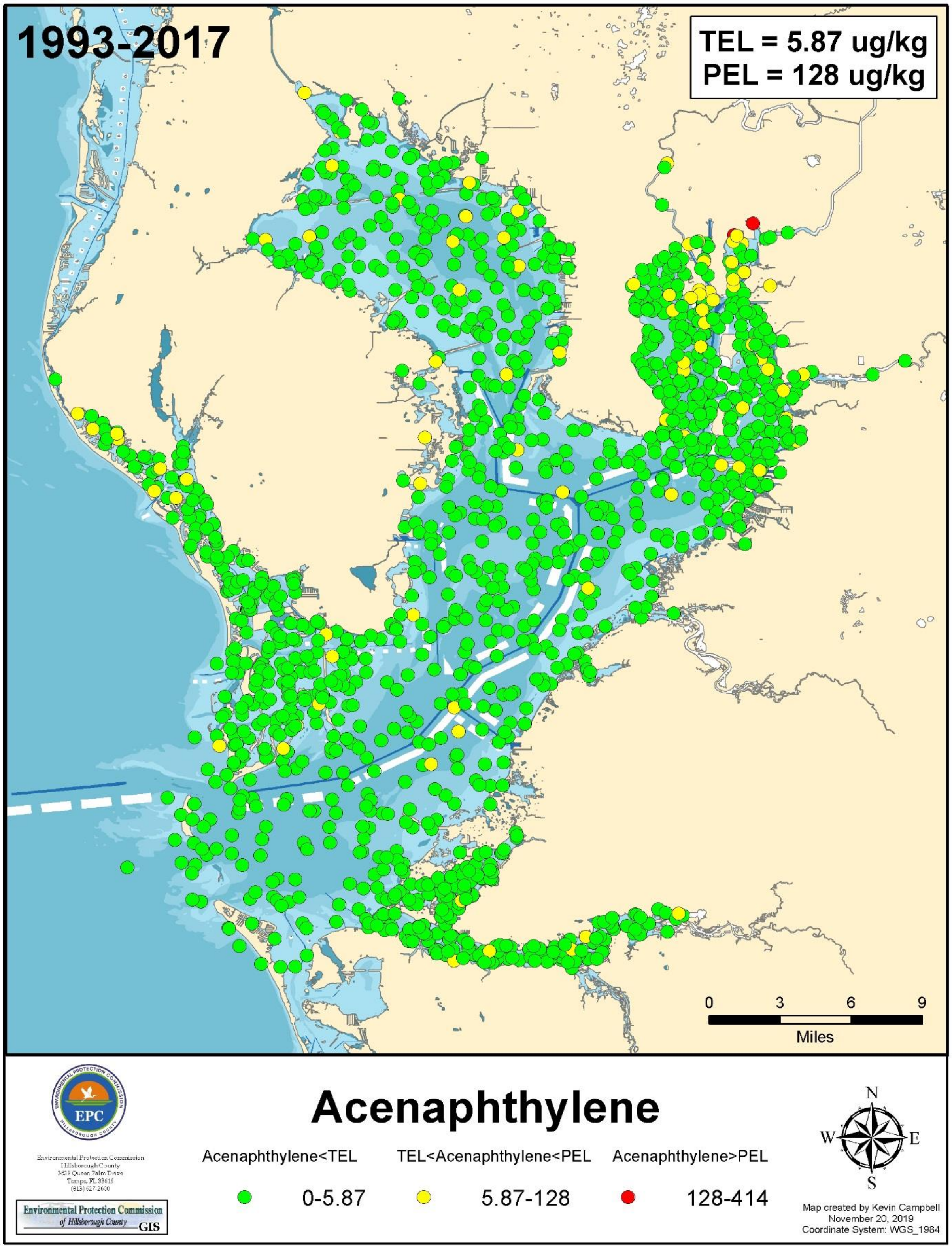

Figure 65. Distribution of acenaphthylene in Tampa Bay 1993-2017.

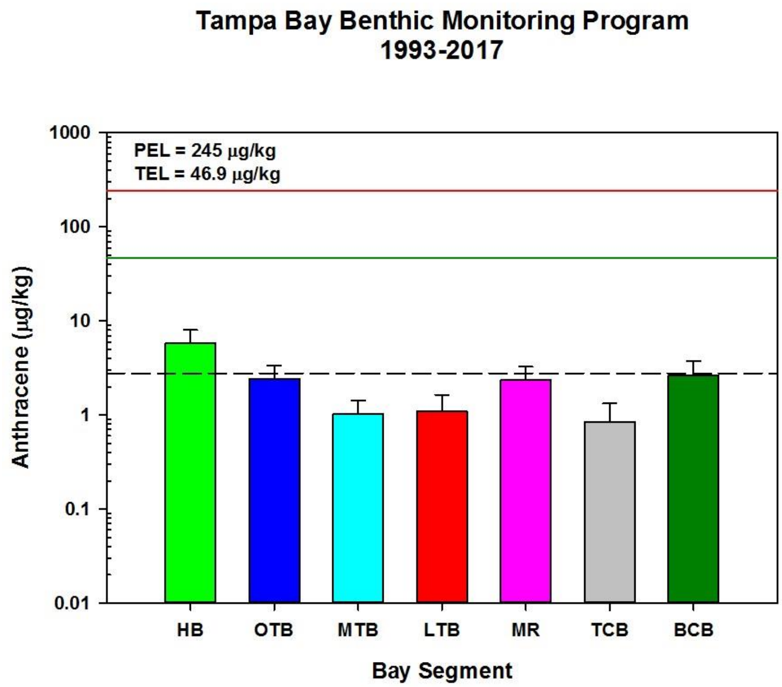

Figure 66. Mean sediment anthracene concentrations by bay segment. Error bars = 95% confidence interval, dashed line represents bay-wide mean. Solid lines represent PEL (upper; red) and TEL (lower; green) values.

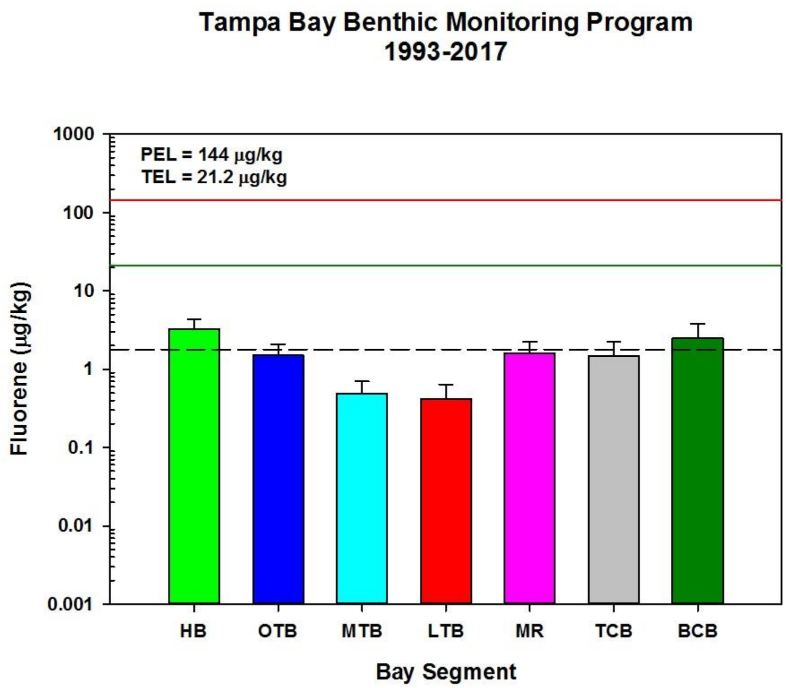

Figure 67. Mean sediment fluorene concentrations by bay segment. Error bars = 95% confidence interval, dashed line represents bay-wide mean. Solid lines represent PEL (upper; red) and TEL (lower; green) values.

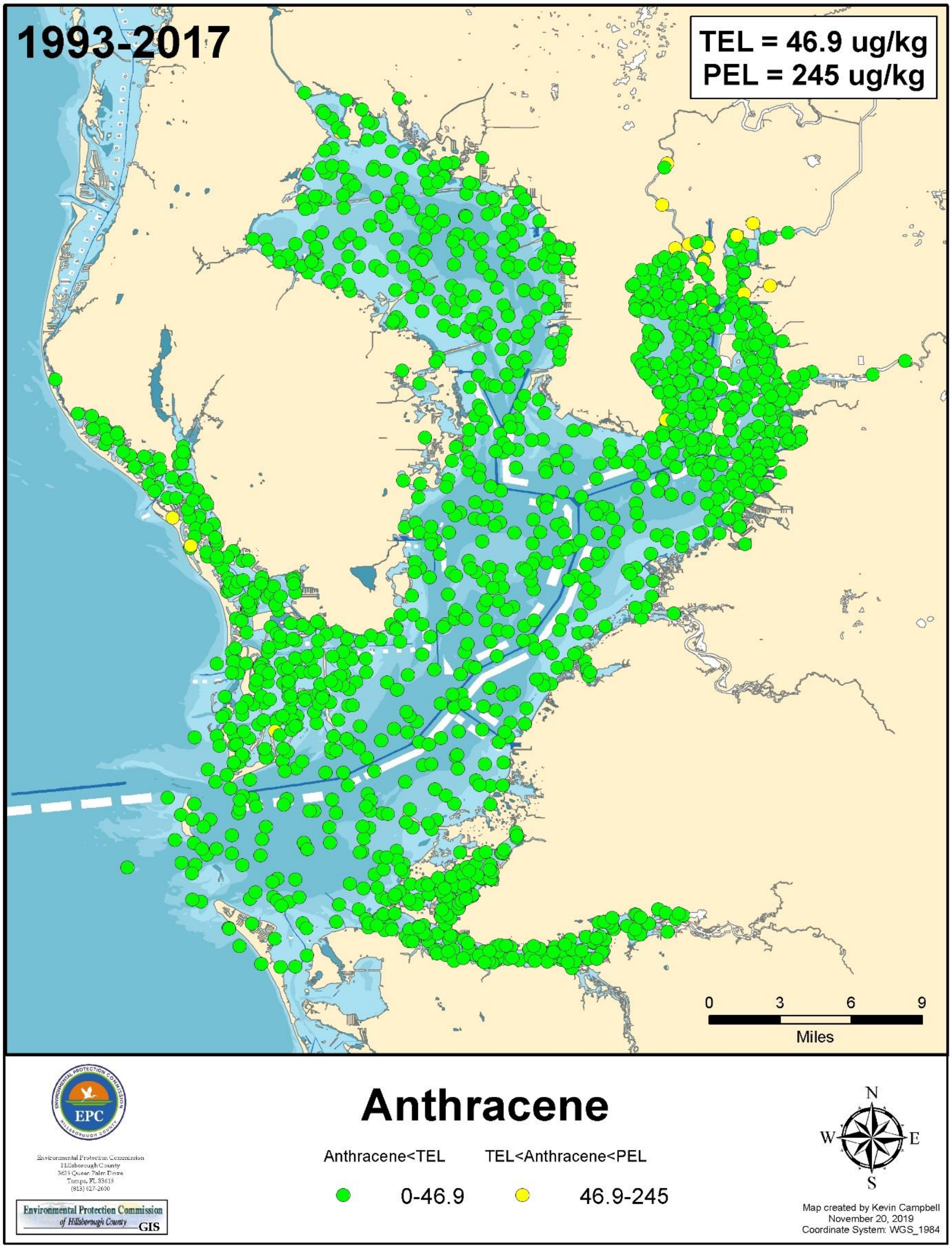

Figure 68. Distribution of anthracene in Tampa Bay 1993-2017.

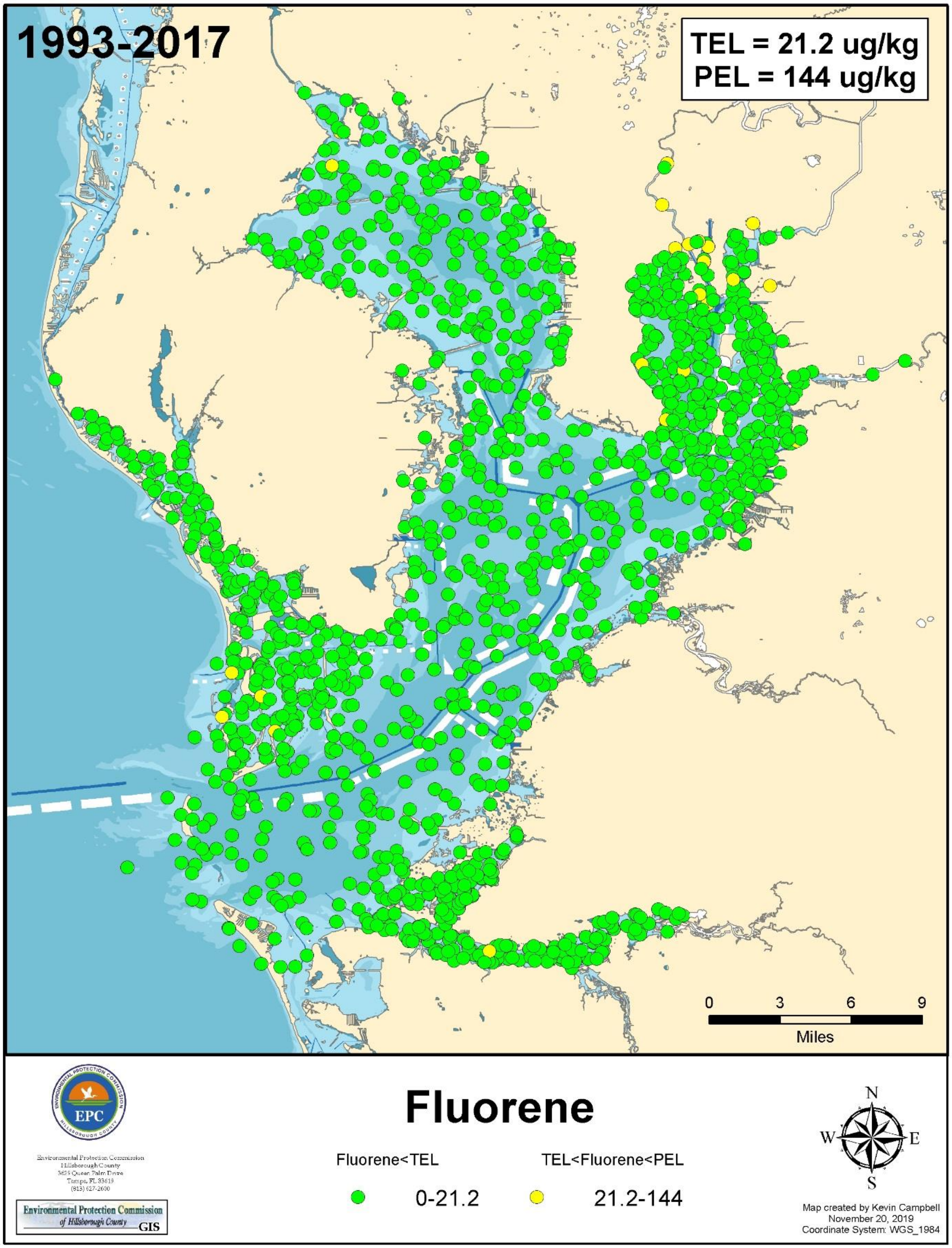

Figure 69. Distribution of fluorene in Tampa Bay 1993-2017.

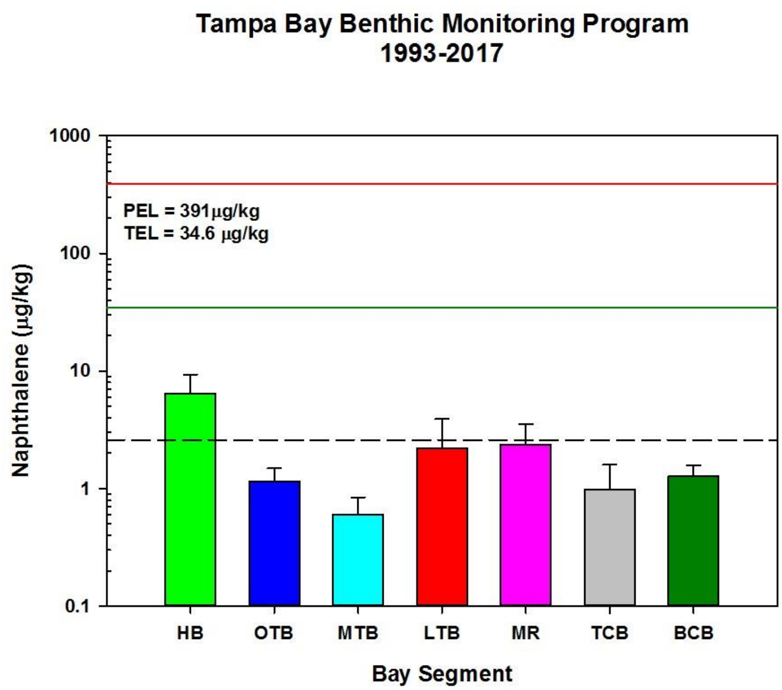

Figure 70. Mean sediment naphthalene concentrations by bay segment. Error bars = 95% confidence interval, dashed line represents bay-wide mean. Solid lines represent PEL (upper; red) and TEL (lower; green) values.

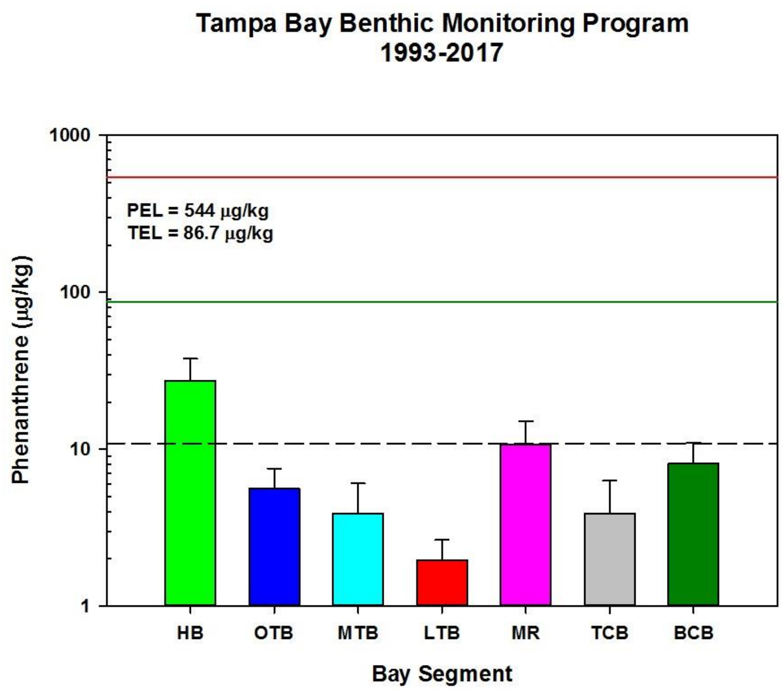

Figure 71. Mean sediment phenanthrene concentrations by bay segment. Error bars = 95% confidence interval, dashed line represents bay-wide mean. Solid lines represent PEL (upper; red) and TEL (lower; green) values.

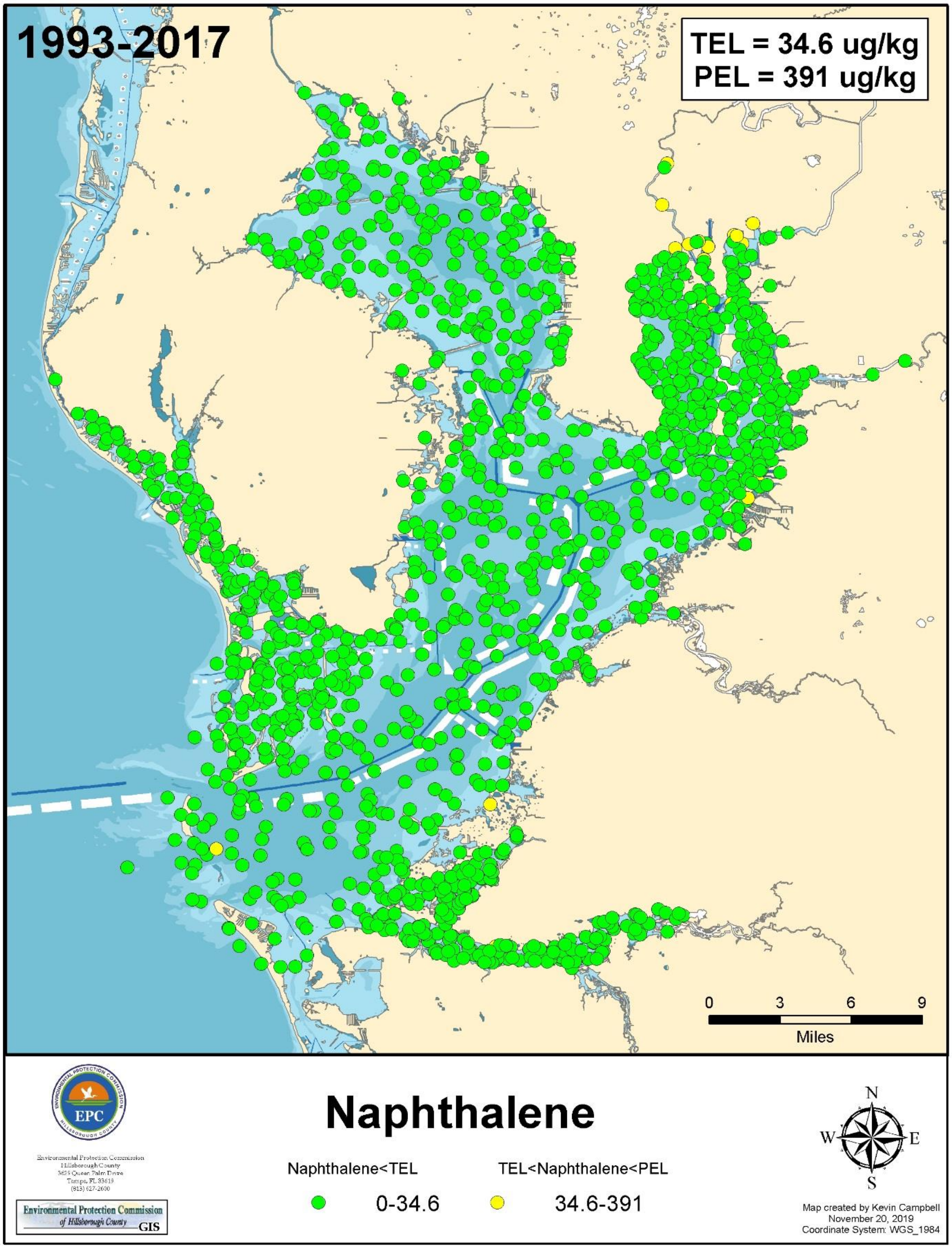

Figure 72. Distribution of naphthalene in Tampa Bay 1993-2017.

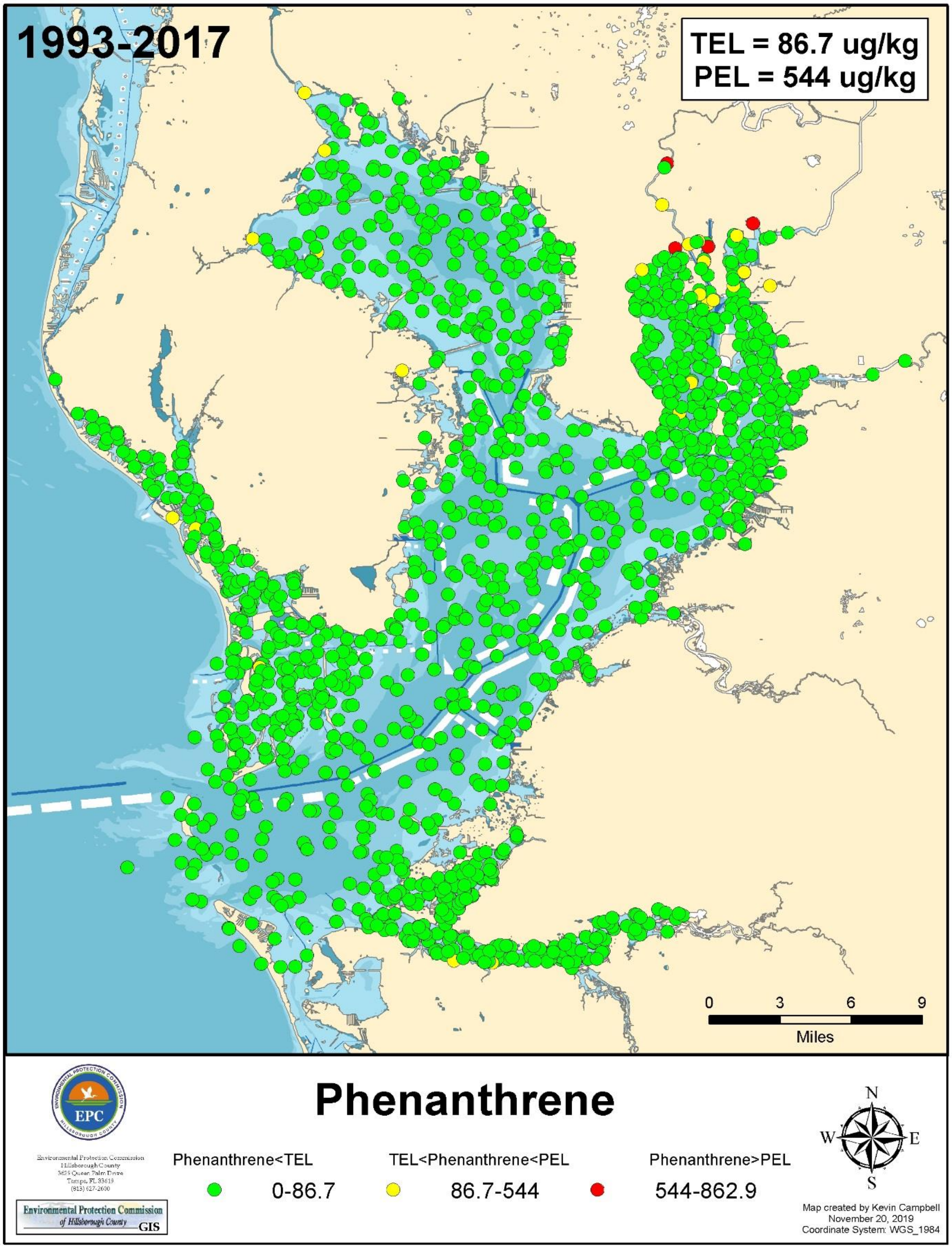

Figure 73. Distribution of phenanthrene in Tampa Bay 1993-2017.

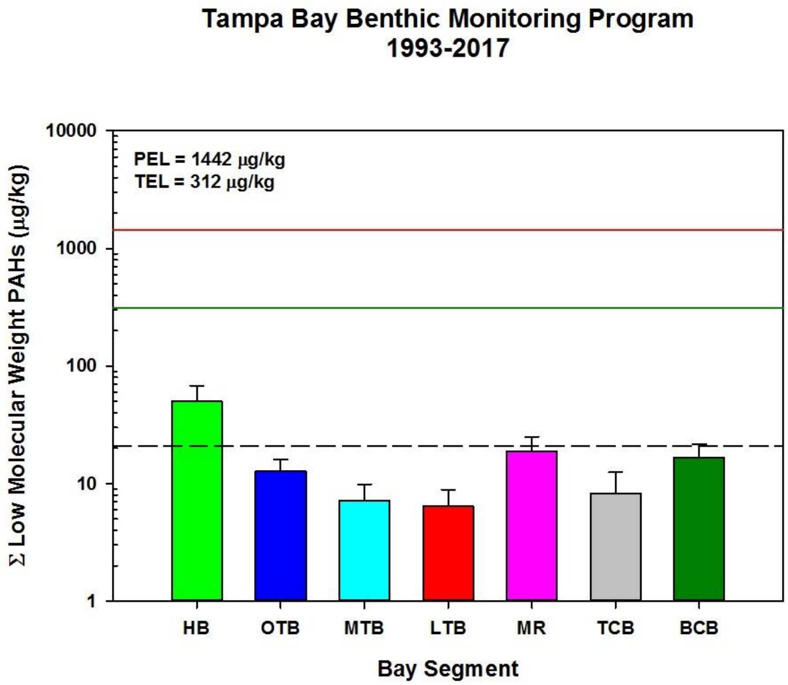

Figure 74. Mean sediment low molecular weight PAH concentrations by bay segment. Error bars = 95% confidence interval, dashed line represents bay-wide mean. Solid lines represent PEL (upper; red) and TEL (lower; green) values.

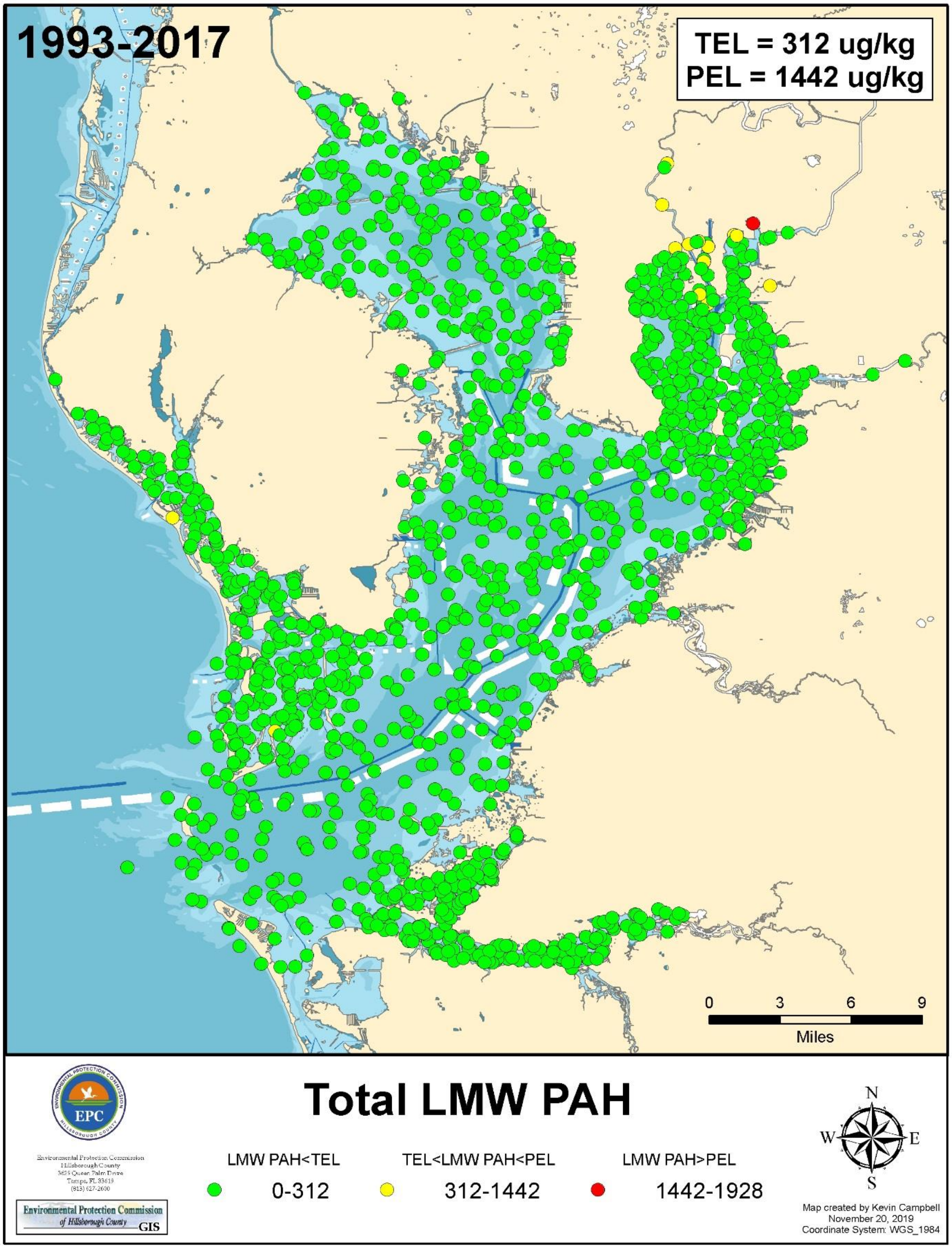

Figure 75. Distribution of total low molecular weight PAHs in Tampa Bay 1993-2017.

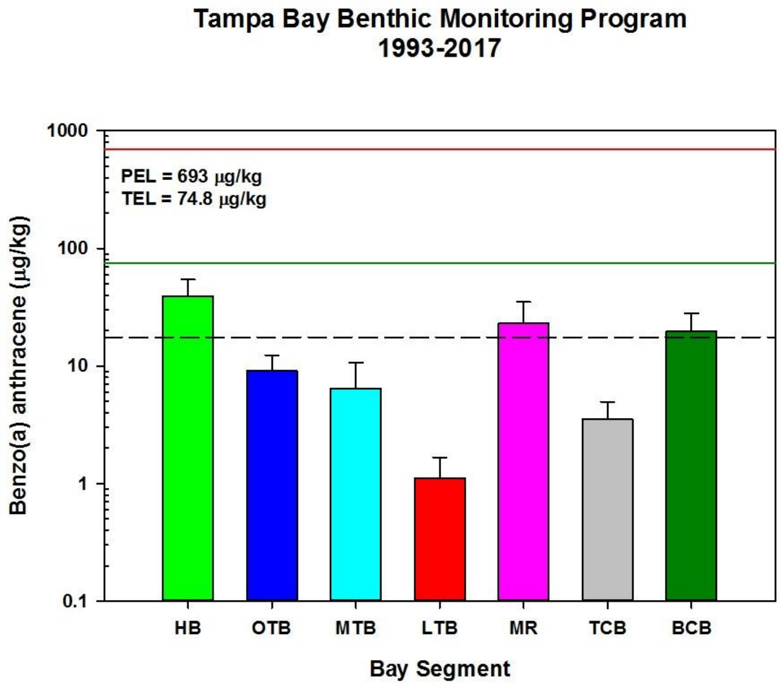

Figure 76. Mean sediment benzo(a) anthracene concentrations by bay segment. Error bars = 95% confidence interval, dashed line represents bay-wide mean. Solid lines represent PEL (upper; red) and TEL (lower; green) values.

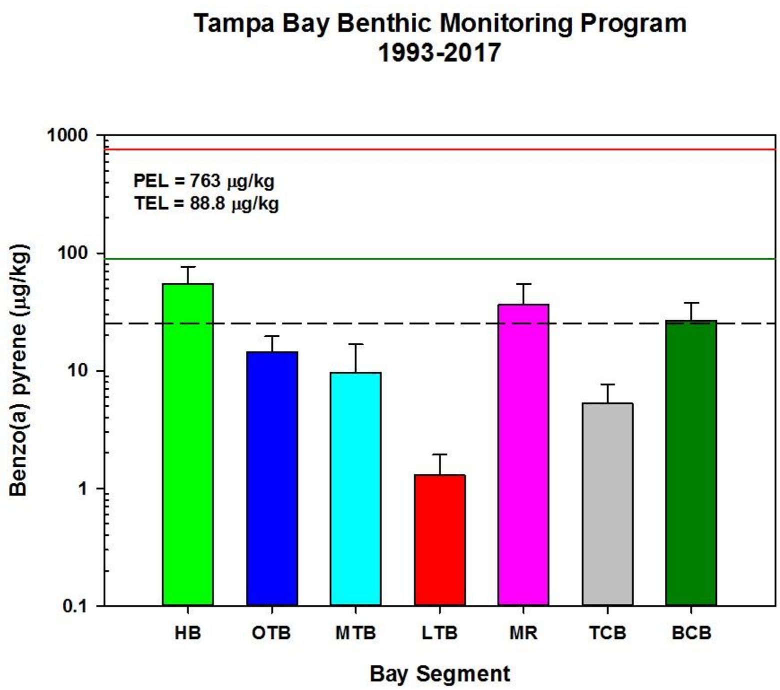

Figure 77. Mean sediment benzo(a) pyrene concentrations by bay segment. Error bars = 95% confidence interval, dashed line represents bay-wide mean. Solid lines represent PEL (upper; red) and TEL (lower; green) values.

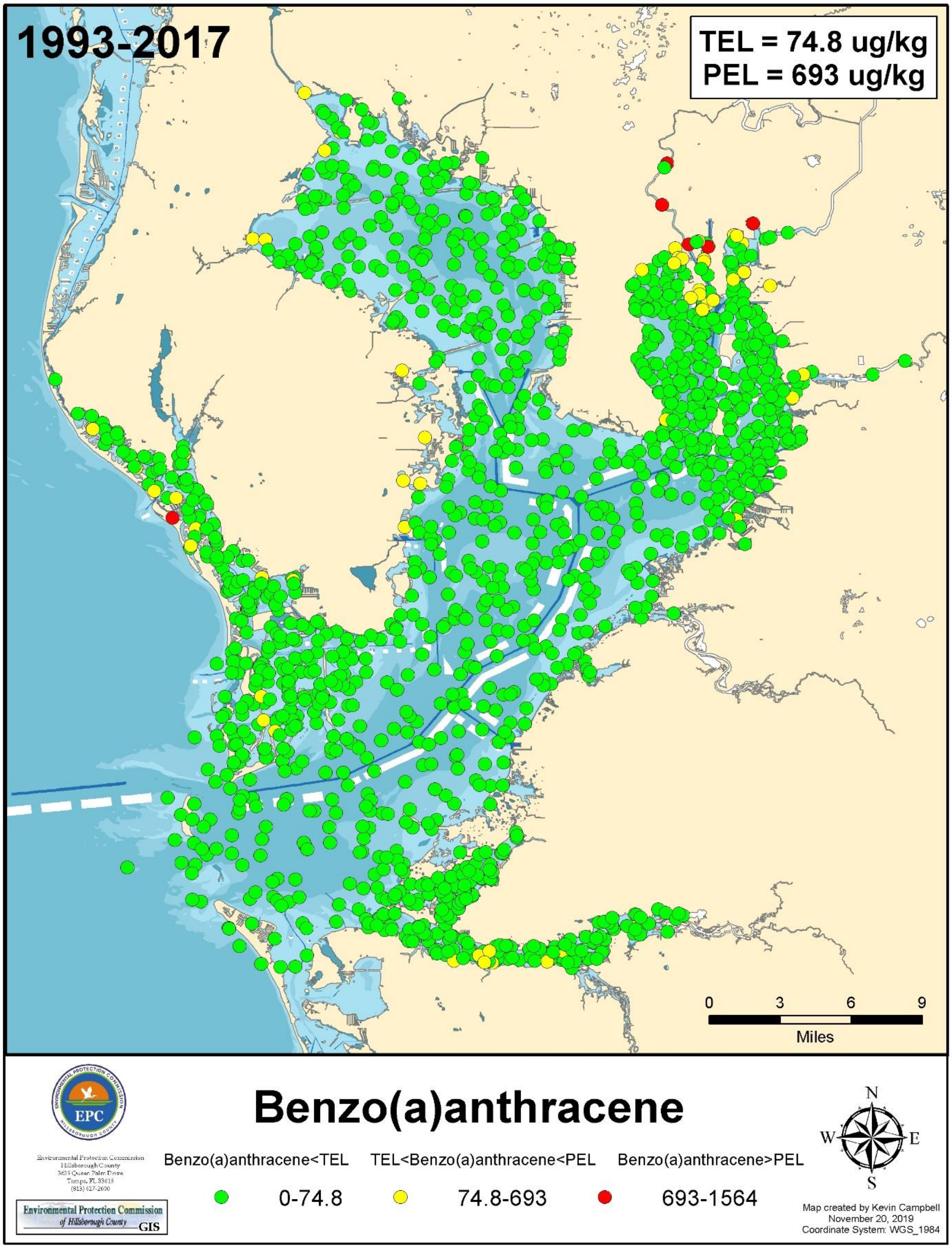

Figure 78. Distribution of benzo(a) anthracene in Tampa Bay 1993-2017.

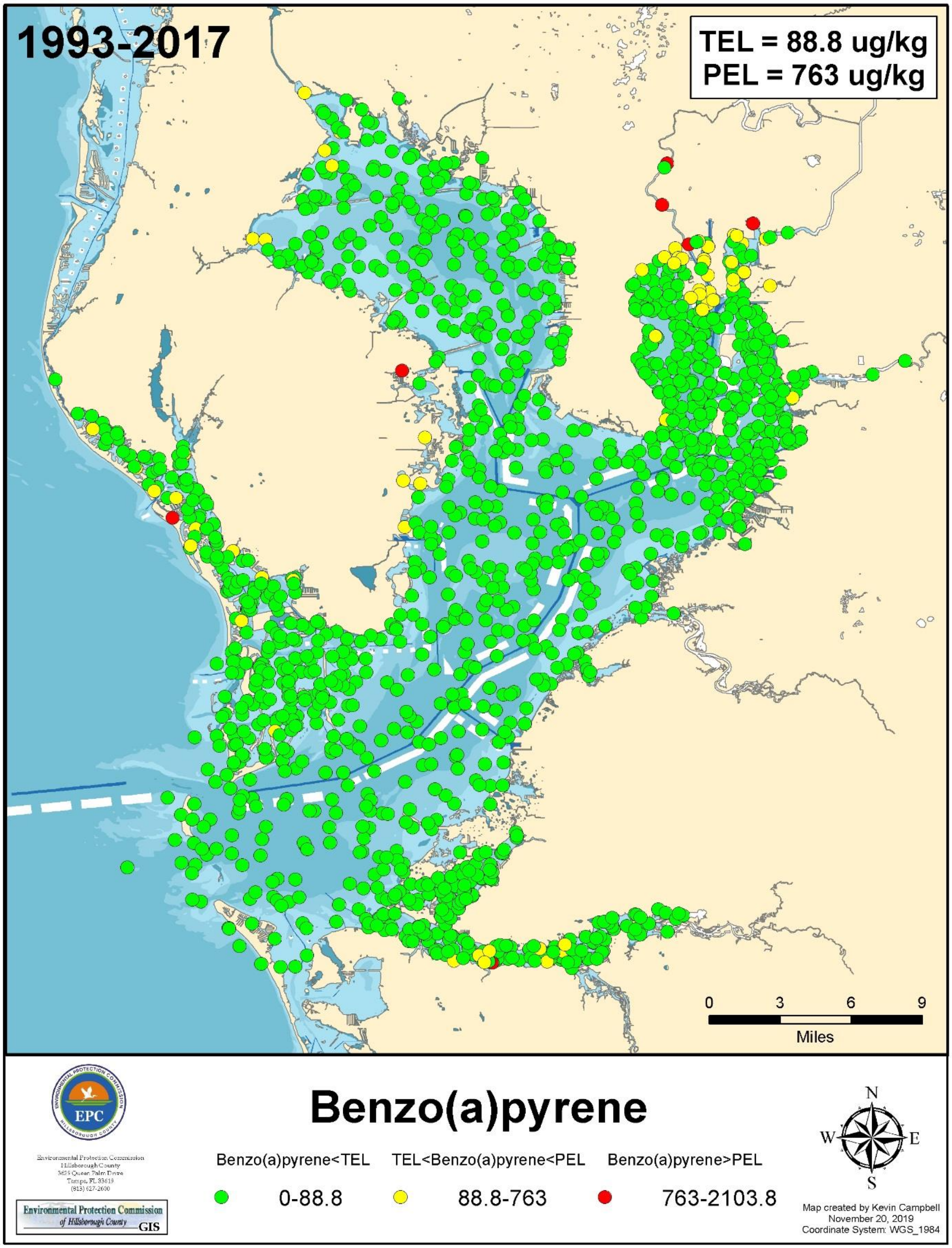

Figure 79. Distribution of benzo(a) pyrene in Tampa Bay 1993-2017.

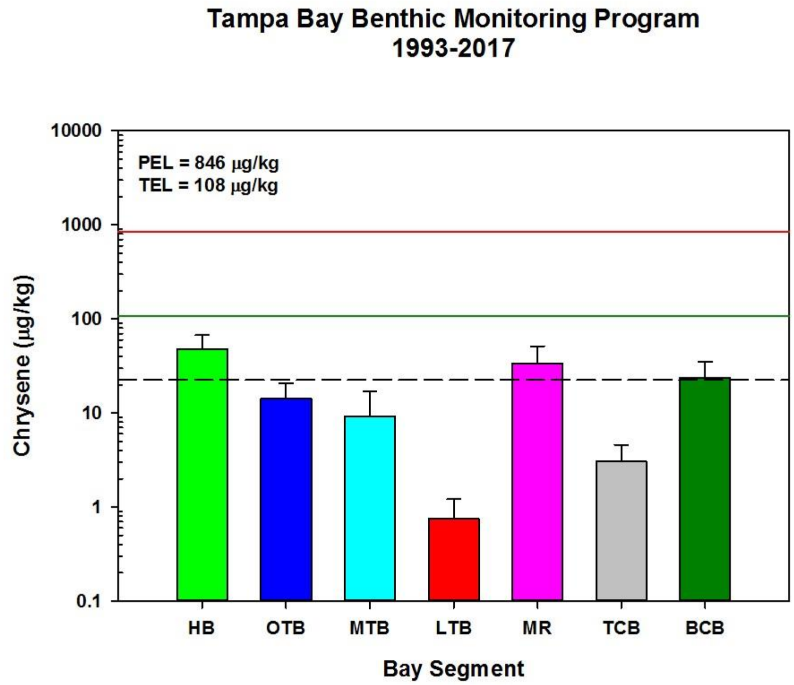

Figure 80. Mean sediment chrysene concentrations by bay segment. Error bars = 95% confidence interval, dashed line represents bay-wide mean. Solid lines represent PEL (upper; red) and TEL (lower; green) values.

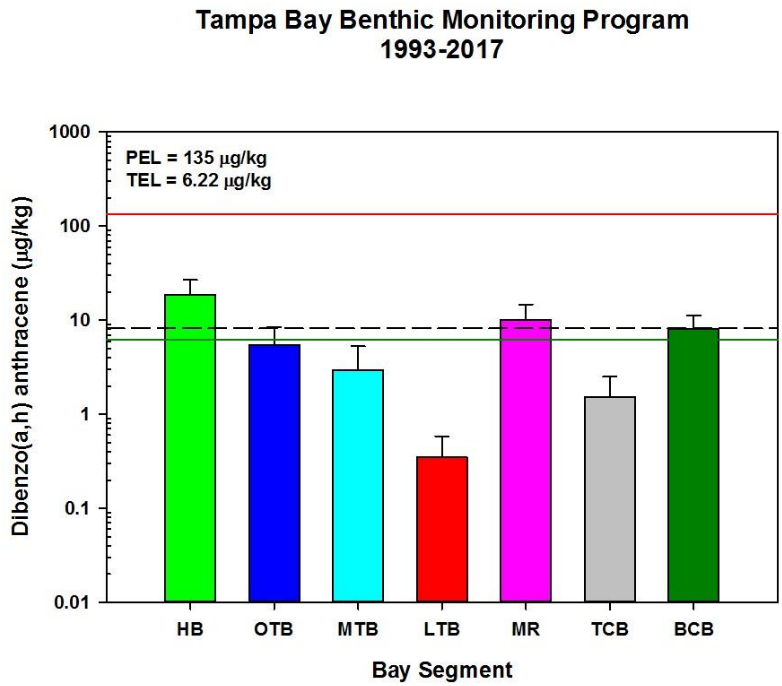

Figure 81. Mean sediment dibenzo(a,h) anthracene concentrations by bay segment. Error bars = 95% confidence interval, dashed line represents bay-wide mean. Solid lines represent PEL (upper; red) and TEL (lower; green) values.

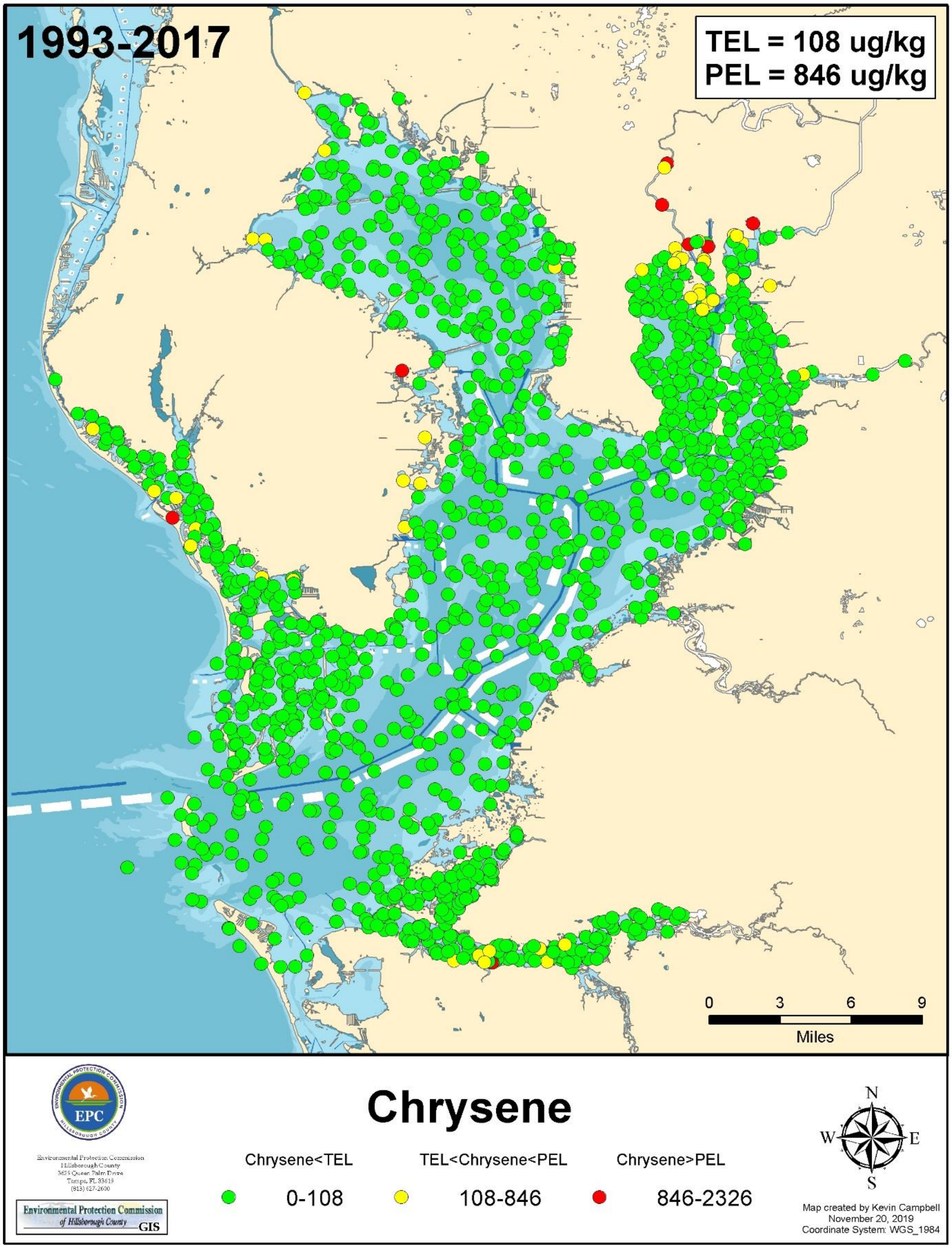

Figure 82. Distribution of chrysene in Tampa Bay 1993-2017.

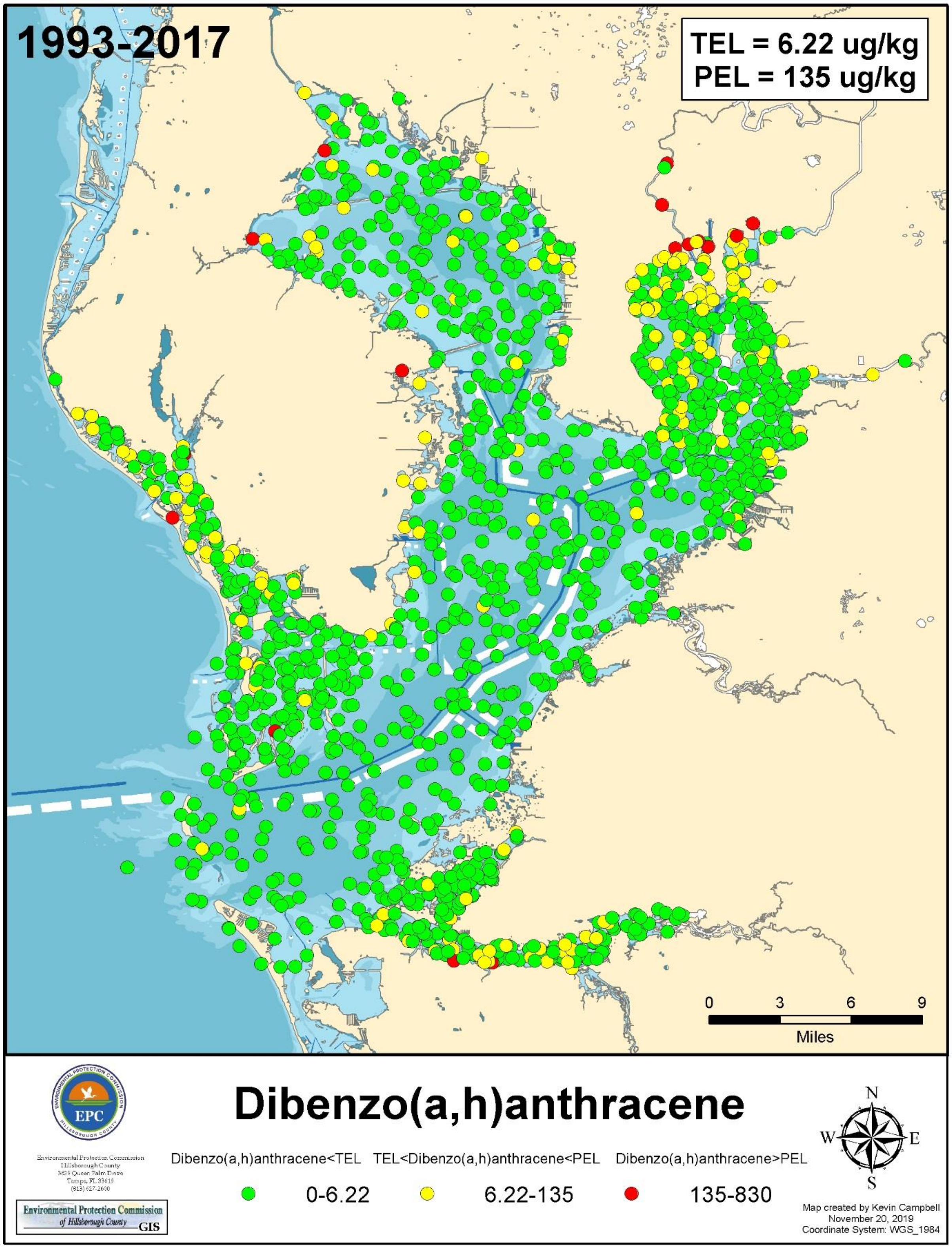

Figure 83. Distribution of dibenzo(a,h) anthracene in Tampa Bay 1993-2017.

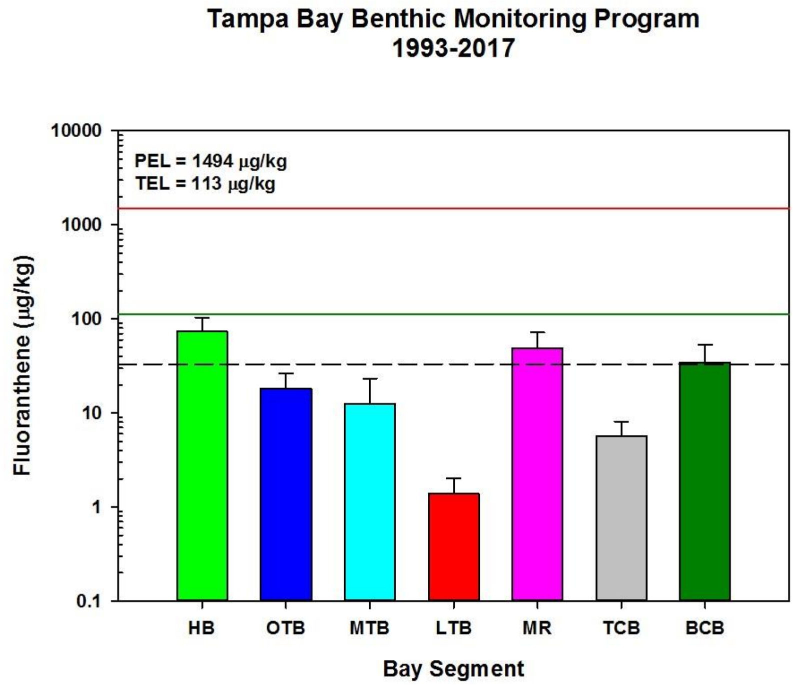

Figure 84. Mean sediment fluoranthene concentrations by bay segment. Error bars = 95% confidence interval, dashed line represents bay-wide mean. Solid lines represent PEL (upper; red) and TEL (lower; green) values.

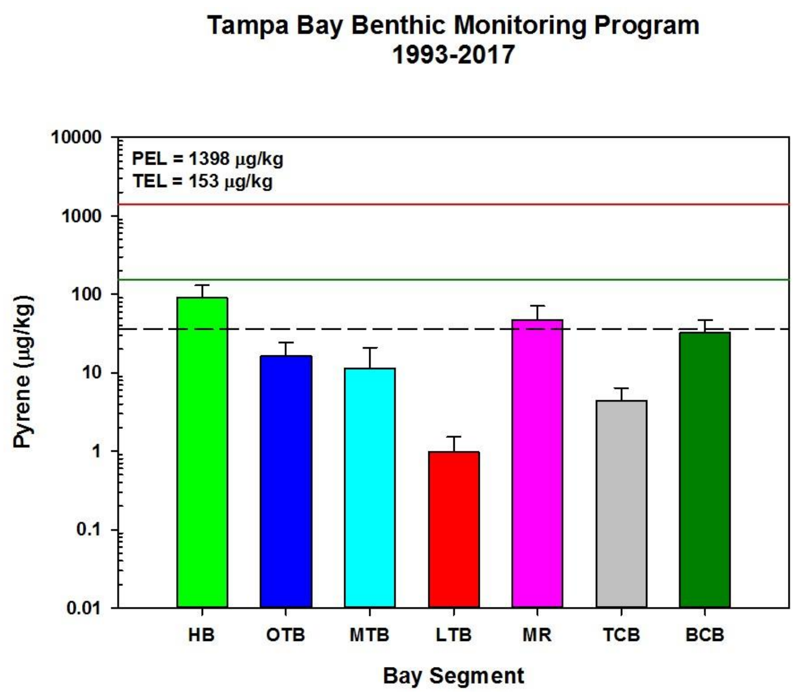

Figure 85. Mean sediment pyrene concentrations by bay segment. Error bars = 95% confidence interval, dashed line represents bay-wide mean. Solid lines represent PEL (upper; red) and TEL (lower; green) values.

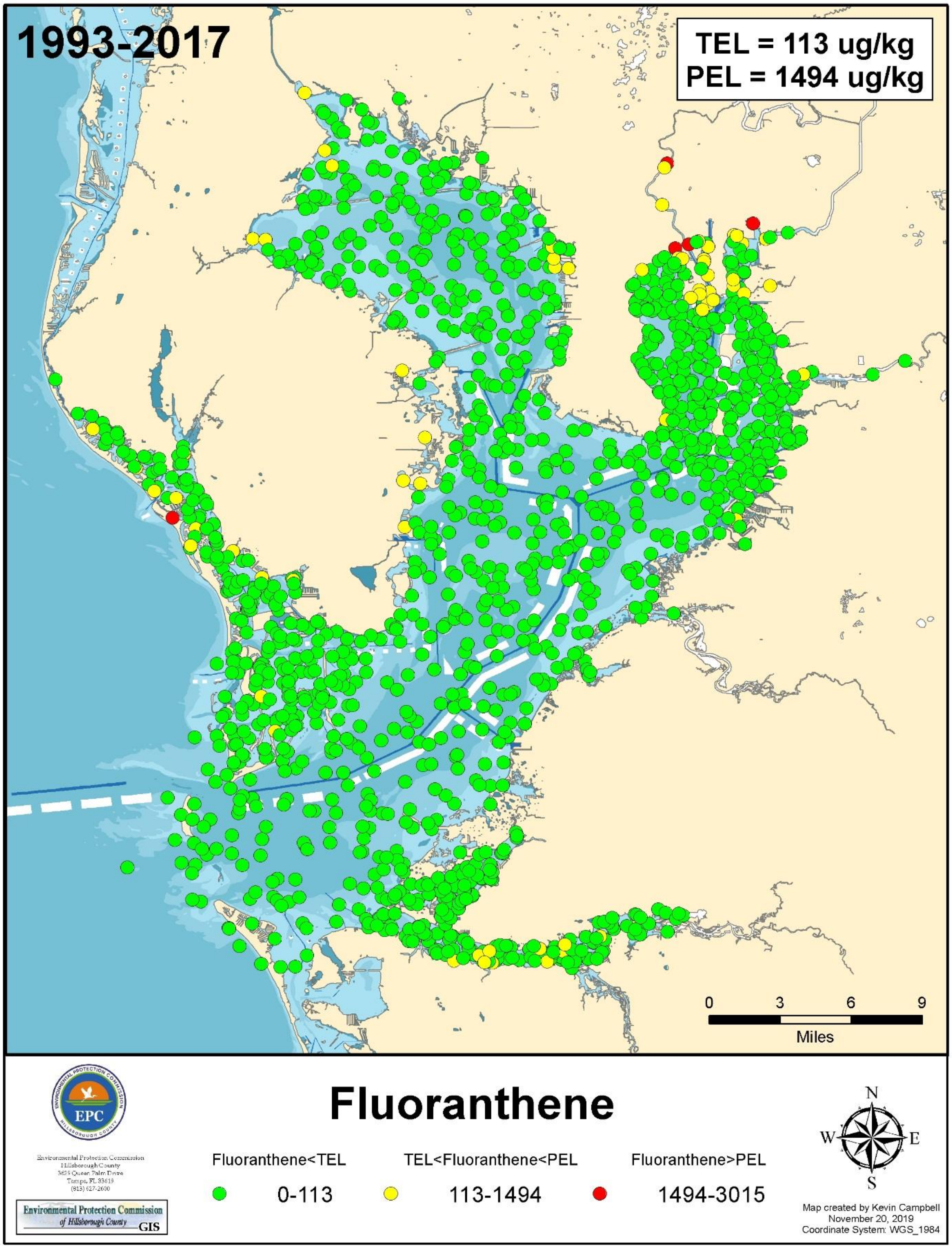

Figure 86. Distribution of fluoranthene in Tampa Bay 1993-2017.

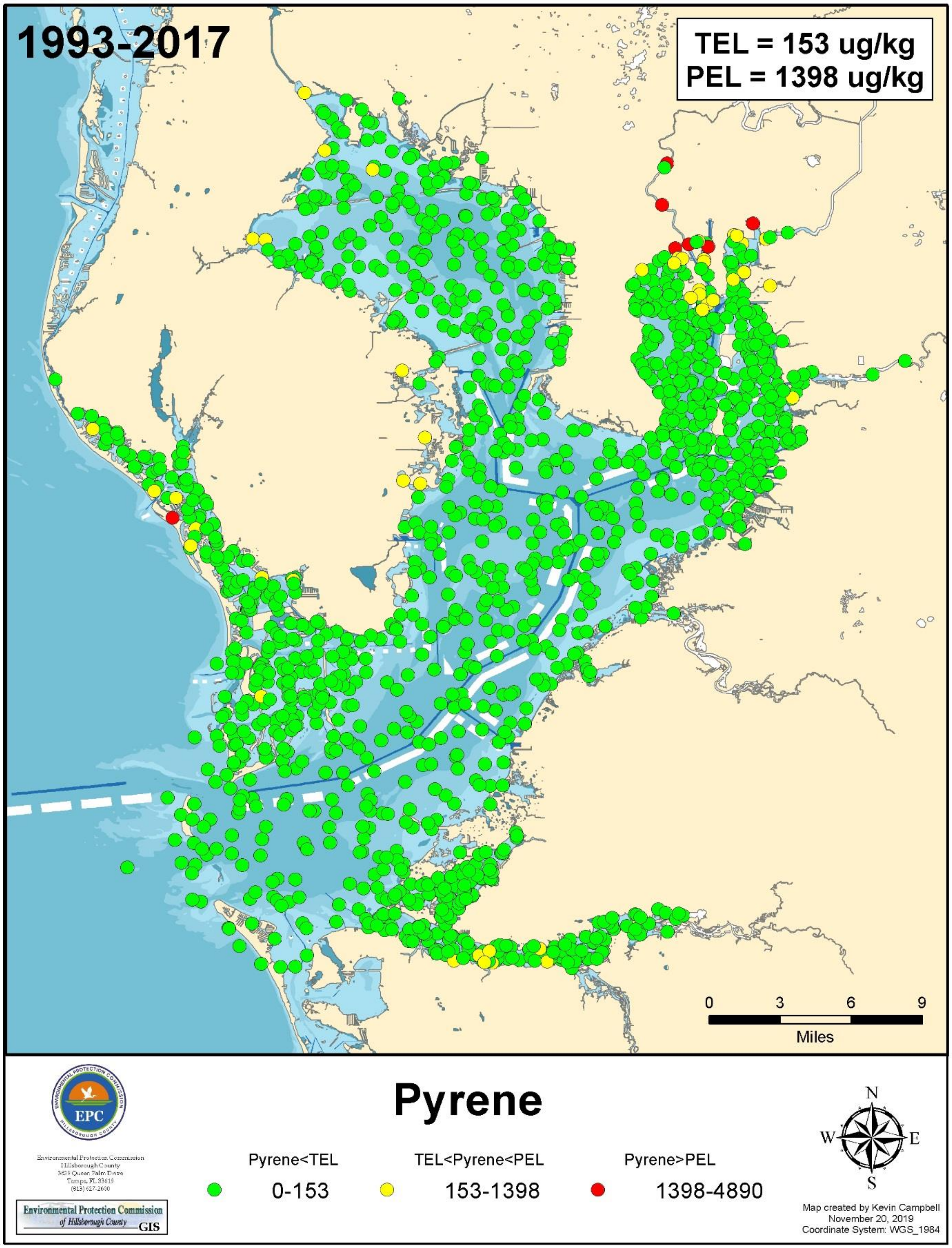

Figure 87. Distribution of pyrene in Tampa Bay 1993-2017.

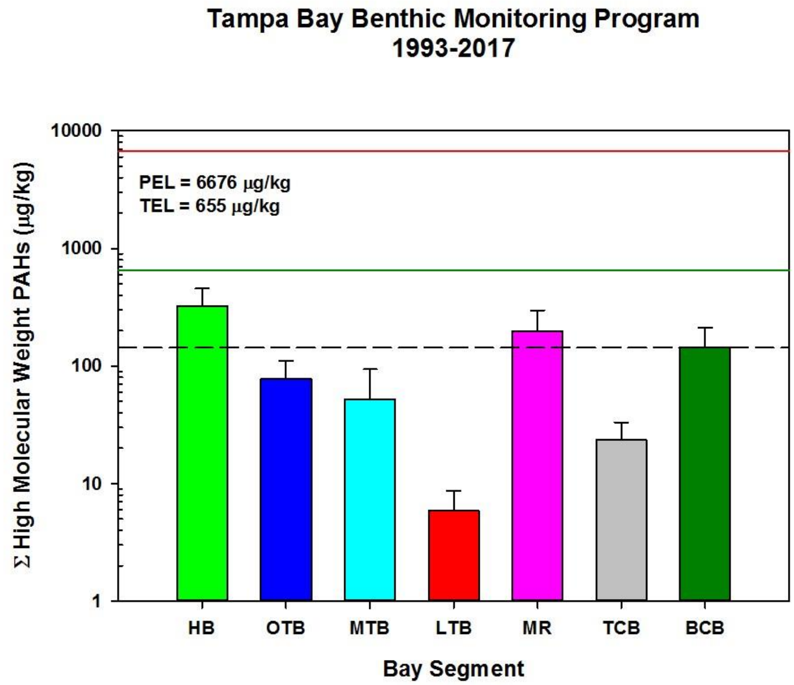

Figure 88. Mean sediment high molecular weight PAH concentrations by bay segment. Error bars = 95% confidence interval, dashed line represents bay-wide mean. Solid lines represent PEL (upper; red) and TEL (lower; green) values.

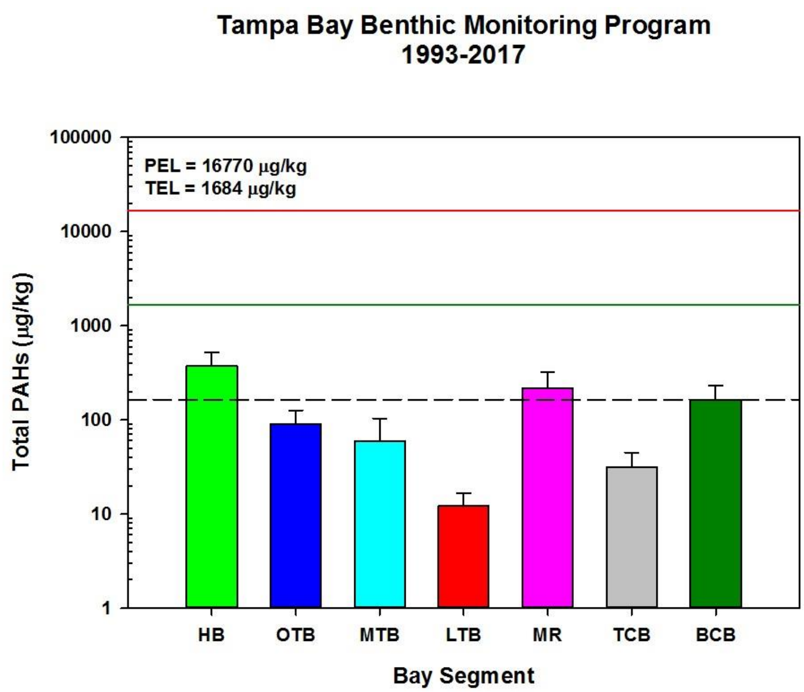

Figure 89. Mean sediment total PAH concentrations by bay segment. Error bars = 95% confidence interval, dashed line represents bay-wide mean. Solid lines represent PEL (upper; red) and TEL (lower; green) values.

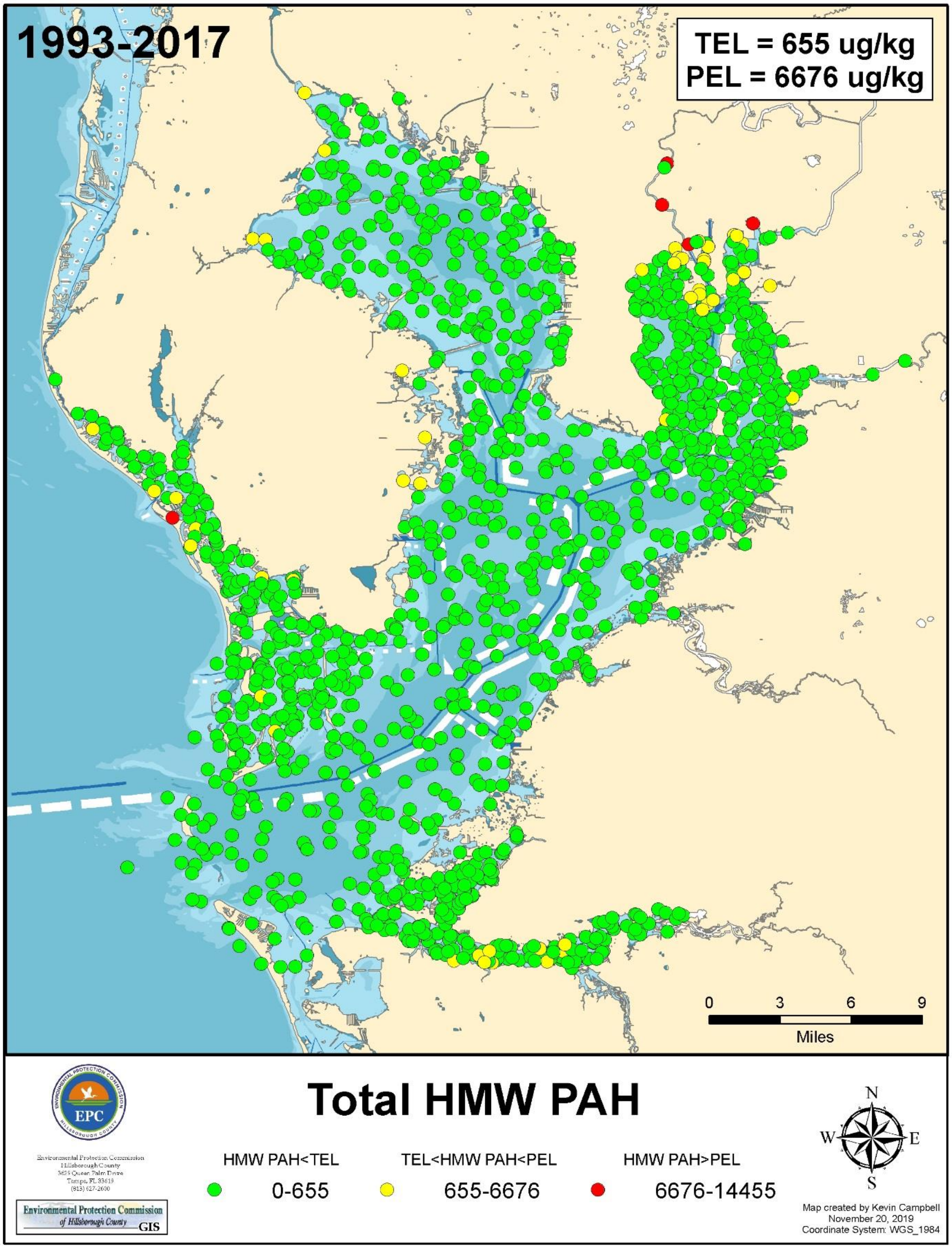

Figure 90. Distribution of high molecular weight PAHs in Tampa Bay 1993-2017.

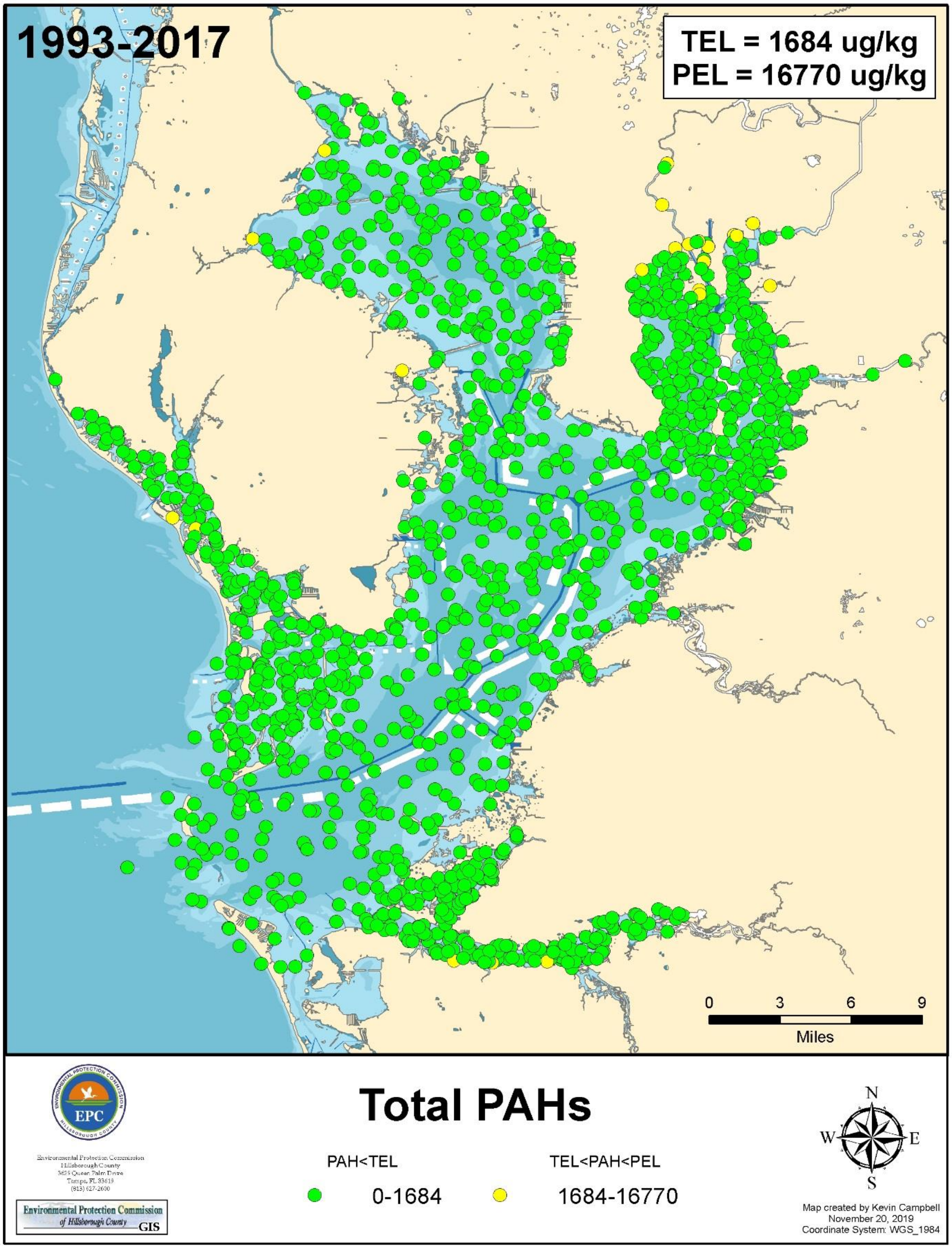

Figure 91. Distribution of total PAHs in Tampa Bay 1993-2017.

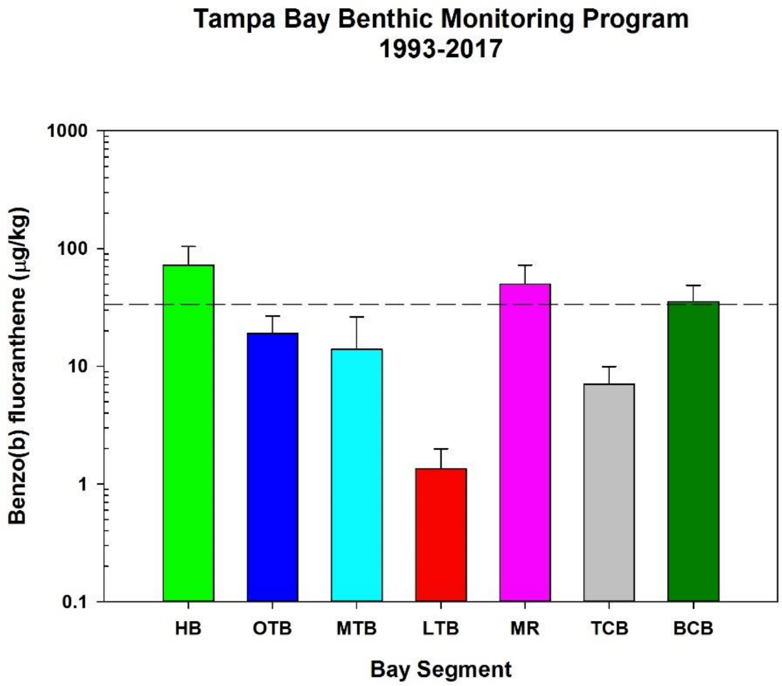

Figure 92. Mean sediment benzo(b) fluoranthene concentrations by bay segment. Error bars = 95% confidence interval, dashed line represents bay-wide mean.

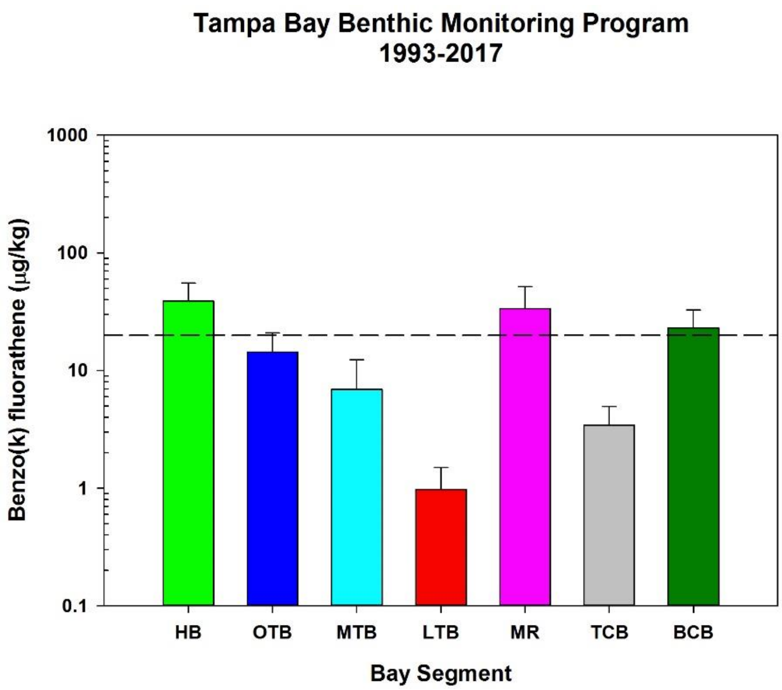

Figure 93. Mean sediment benzo(k) fluoranthene concentrations by bay segment. Error bars = 95% confidence interval, dashed line represents bay-wide mean.

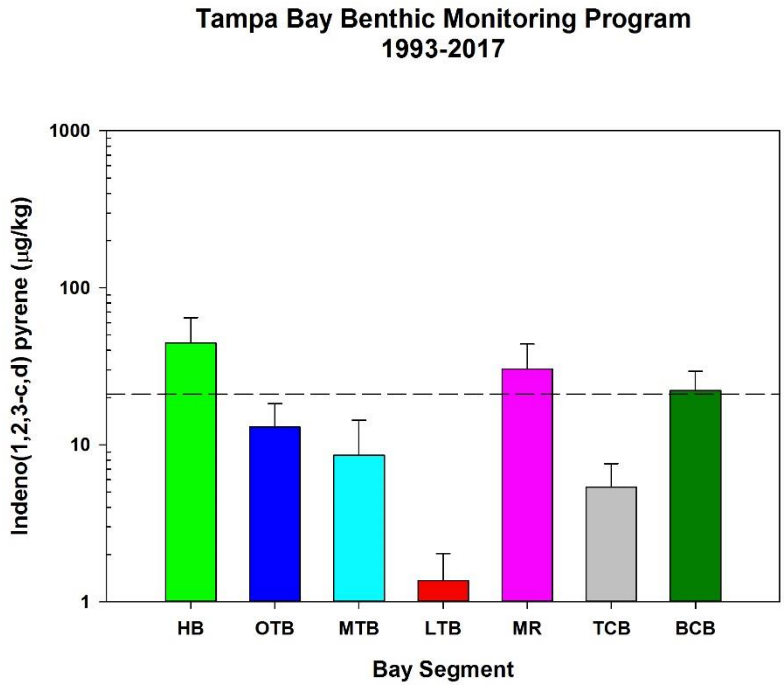

Figure 94. Mean sediment indeno(1,2,3-c,d) pyrene concentrations by bay segment. Error bars = 95% confidence interval, dashed line represents bay-wide mean.

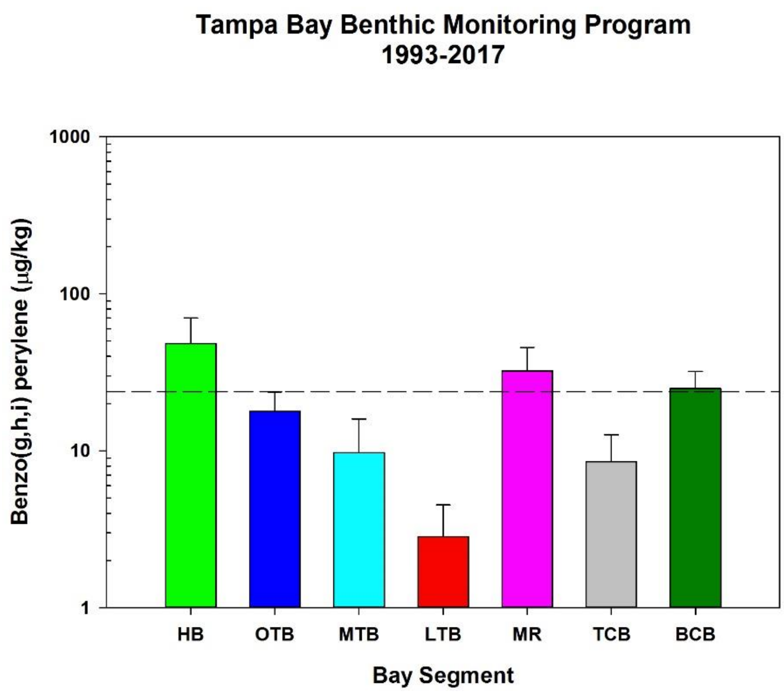

Figure 95. Mean sediment benzo(g,h,i) perylene concentrations by bay segment. Error bars = 95% confidence interval, dashed line represents bay-wide mean.

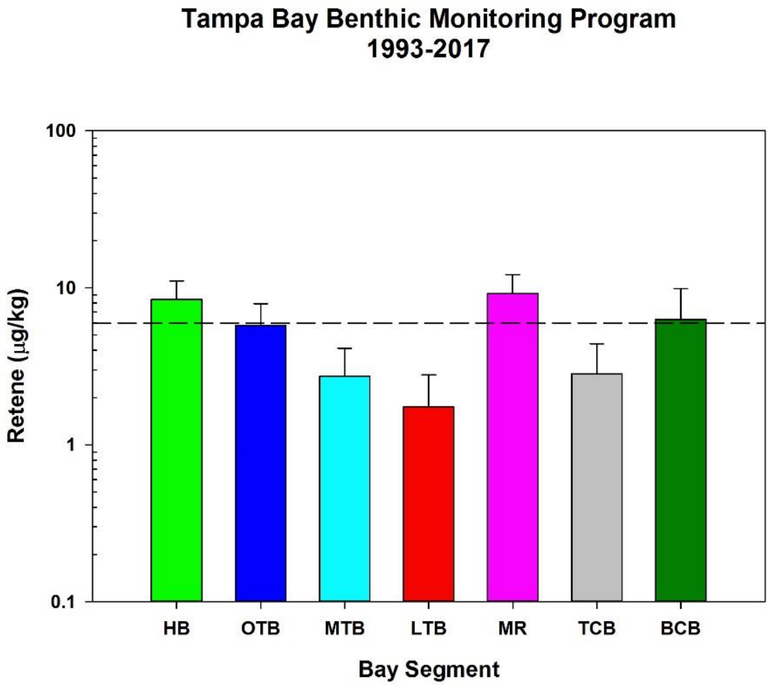

Figure 96. Mean sediment retene concentrations by bay segment. Error bars = 95% confidence interval, dashed line represents bay-wide mean.

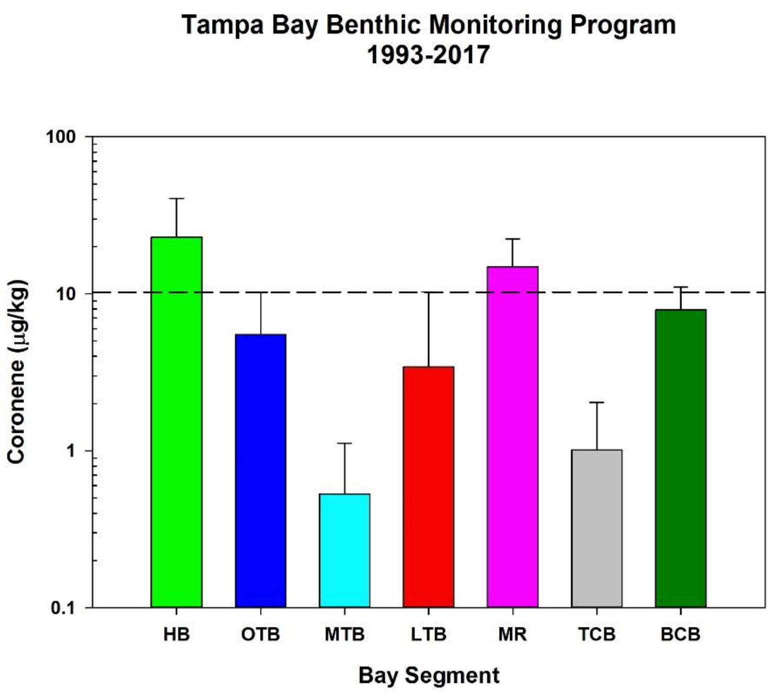

Figure 97. Mean sediment coronene concentrations by bay segment. Error bars = 95% confidence interval, dashed line represents bay-wide mean.

Polychlorinated biphenyls (PCBs) and Chlorinated Pesticides

Bay-wide summary statistics for Total PCBs and pesticides are presented in Table 14.

Polychlorinated biphenyls (PCBs) ($C_{12}H_xCl_x$; MW = 188.65 – 498.66): Polychlorinated biphenyls (PCBs) are organic compounds composed of a biphenyl polycyclic aromatic hydrocarbon ($C_{12}H_{10}$) with one (monochlorobiphenyl; $C_{12}H_9Cl$) to ten (decachlorobiphenyl; $C_{12}Cl_{10}$) attached chlorine atoms (Frithsen et al., 1995). PCBs can have 209 possible isomers (congeners), which are grouped based on the number of attached chlorine atoms (Frithsen et al., 1995). PCBs were commonly used for numerous industrial applications including; as dielectric fluids in transformers and capacitors, lubricants, hydraulic fluids, flame retardants, adhesives, and plasticizers among other uses (MacDonald, 1994; Frithsen et al., 1995). The manufacture of PCBs in the United States was banned in 1976, but production in other countries continued through the 1980's (Frithsen et al., 1995). PCBs are known to be carcinogenic, and can cause numerous developmental, endocrine, and immunological defects (ATSDR, 2000, 2011). Sources of PCB contaminants in the environment include waste discharges from industry, leaching from disposal sites, leaks and spills of PCB containing products, and vaporization from plastics (Frithsen et al., 1995; Kennish, 1998). Recent contaminants of concern such as microplastics and carbon nanoparticles, can adsorb PCBs and potentially serve as a transport vector in the marine environment (Velzboer et al., 2014).

Because PCBs are stable compounds and insoluble in water, they tend to accumulate in fine grained sediments with high organic content. PCBs further can accumulate in macroalgae and fat tissues, and bioaccumulate in organisms, then get biomagnified at higher trophic levels in the food web (Kennish, 1998; Fair et al., 2010; Cheney et al., 2019). However, other studies suggest that bioaccumulation of PCBs may be more a factor of size and age of the individual organism, rather than its trophic level (Burreau et al., 2006; Magnusson et al., 2006). Concentrations of PCBs in marine and freshwater organisms have been shown to be related to sediment concentrations and proximity of known areas of contamination (Kuzyk et al., 2005; Straub et al., 2007; Cheney et al., 2019). However, accumulation of PCBs and other organic contaminants have been found in benthic organisms (amphipods) even at the deepest ocean depths (Jamieson et al., 2017).

Bay-wide, the mean total PCB concentration was 2.28 µg/kg, with a maximum of 197.87 µg/kg (Table 14). PCBs exceeded the TEL in 1.70% of the samples and were above the PEL at 0.07% of the sites (Table 14). The highest mean concentration was in Hillsborough Bay (Figure 98). The only PEL exceedance was at one site in the Hillsborough River, which had elevated concentrations of Aroclors 1254 and 1232 (Figure 99).

Frithsen et al., (1995) estimated annual loading of PCBs to Tampa Bay at 11 kg/year, with the primary input from atmospheric deposition. Grabe and Barron (2002; 2004) found PCB contamination in Tampa Bay was primarily in the tributaries and the Palm River.

Organochlorine Pesticides

Chlorinated pesticides or organochlorines are composed of one or more hydrocarbon rings with attached chlorine atoms (Kamrin, 1997). This group of organic compounds was widely used as pesticides for agriculture and mosquito control, but most uses have been reduced or eliminated in the United States since the 1970's due to their adverse effects on non-target organisms (Kamrin, 1997; Kennish, 1998). However, these pesticides are still used in other parts of the world. Chlorinated pesticides work by attacking the central nervous system. They affect the sodium/potassium balance along nerves causing continuous transmission of impulses along the nerve fiber, which can result in nervousness, tremors, or convulsions ultimately causing paralysis and death (Kamrin, 1997; Kennish, 1998). Chlorinated pesticides are lipid soluble and can accumulate in fat tissues, as well as adsorb to organic sediments. These compounds bioaccumulate, and high tissue concentrations can be found in predatory species at the top trophic levels (Kamrin, 1997; Kennish, 1998).

Aldrin ($C_{12}H_8Cl_6$; MW = 364.91) and Dieldrin ($C_{12}H_8Cl_6O$; MW = 380.91): Aldrin and dieldrin were used as pesticides on agricultural crops during the 1950's until the US Department of Agriculture suspended their use in 1970. However, they were still used for termite control until 1987 (MacDonald, 1994; ATSDR, 2002a). Both pesticides can cause neurological damage resulting in convulsions, and have been found to cause liver tumors and kidney damage in animal studies (ATSDR, 2002a). Aldrin converts to dieldrin in the environment from bacterial action and when exposed to sunlight (ATSDR, 2002a). Dieldrin is more stable in the environment, and persists in soil and sediments (ATSDR, 2002a). High dieldrin sediment concentrations can be toxic to amphipods (Swartz et al., 1994), and it can bioaccumulate in fish tissue (Muller et al., 2004). Frithsen et al., (1995) estimated the annual loading of dieldrin to Tampa Bay at 775 kg, with agricultural runoff accounting for 99% of the input.

The mean concentration of aldrin in Tampa Bay sediments was 0.06 µg/kg, and dieldrin had a mean concentration of 0.08 µg/kg (Table 14). Maximum concentrations for both aldrin and dieldrin (12.58 and 10.65 µg/kg respectively) occurred in Hillsborough Bay in 2016, and both contaminants had highest mean concentrations in Hillsborough Bay (Figures 100 & 101). Aldrin does not have established sediment quality guidelines, but dieldrin was above its TEL concentration in 1.70% of the samples and exceeded its PEL in 0.20% of the samples, with PEL exceedances occurring in Hillsborough Bay (Table 14; Figure 102).

Total DDT and metabolites

Dichlorodiphenylethane (DDT) was widely used as an agricultural pesticide and for mosquito control through the 1960s (Kamrin, 1997). While DDT has been banned in the United States for nearly 50 years, total DDT and it's breakdown compounds p,p'-DDD, p,p'-DDE and p,p'-DDT are still detectable in Tampa Bay sediments (Table 14). Frithsen et al., (1995) estimated annual loadings of DDT to Tampa Bay of approximately 1,660 kg with 95% coming from agricultural runoff. One of the most notorious effects of DDT is the breakdown of the hormones that regulate calcium mobilization and eggshell formation in birds, which historically had led to the reproductive failure and population decline of several bird species (Kennish, 1998). DDT can also accumulate in aquatic food webs (Wang and Wang, 2005). DDT has been associated with decreasing abundance of amphipods (Swartz et al., 1994), and can have effects on the overall benthic community structure (Ferraro and Cole, 1997). Exposure to DDT can affect the nervous system and cause liver damage, and all its metabolites are classified as possible carcinogens (ATSDR, 2002b). Results for the three DDT metabolites and total DDT are highlighted below.

Dichlorodiphenyldichoroethane (p,p'-DDD; $C_{14}H_{10}Cl_4$; MW = 320.04): P,p'-DDD in Tampa Bay sediments had a mean concentration of 0.14 µg/kg, with a maximum of 29.98 µg/kg (Table 14). It was above its TEL at 1.06% of the sites and exceeded its PEL at 0.28% of the sites (Table 14). P,p'-DDD levels were highest in Hillsborough Bay, elevated in Boca Ciega Bay, and levels were lowest in Lower Tampa Bay (KW; $p<0.001$; Figure 103). The site with the highest concentration was in the Hillsborough River (03HB09, 4x above the PEL); other sites above the PEL were in the Hillsborough and Alafia Rivers and McKay Bay (Figure 107).

Dichlorodiphenyldichloroethylene (p,p'-DDE; $C_{14}H_8Cl_4$; MW = 318.02): The mean sediment concentration of p,p'-DDE in Tampa Bay was 0.39 µg/kg, with a maximum value of 117.35 µg/kg, which is 3x higher than the PEL (Table 14). The TEL for p,p'-DDE was exceeded at 1.98% of the sites, whereas no sites were above the PEL (Table 14). P,p'-DDE was highest in Hillsborough Bay and the Manatee River, with lower levels in Middle Tampa Bay (Figure 104). The highest recorded concentration was at site 03HB09 in the Hillsborough River, several other sites in Hillsborough Bay were above the TEL (Figure 108).

Dichlorodiphenyltrichoroethane (p,p'-DDT; $C_{14}H_9Cl_5$; MW = 354.49): The bay-wide mean concentration for p,p'-DDT was 0.13 µg/kg, with a maximum of 43.06 µg/kg (Table 14). Concentrations were above the TEL at 1.13% of the sites and above the PEL at 0.28% (Table 14). Hillsborough Bay had the highest mean concentration, but elevated levels were also present in the Manatee River (Figure 105). The highest concentration was found in a sample collected in the sea plane basin at Davis Island in Hillsborough Bay (07HB21), which was 9x greater than the PEL. The other sites exceeding the PEL were in the Hillsborough River, including sample 03HB09 which was 4x above the PEL (Figure 109).

Total DDT (ΣDDT): Total DDT is the sum of the three DDT metabolites (p,p'-DDD, p,p'-DDE and p,p'-DDT), and is symbolized as ΣDDT. The mean ΣDDT in Tampa bay was 0.66 µg/kg with a maximum concentration of 166.36 µg/kg (Table 14). ΣDDT was above the TEL at 1.70% of the sites and exceeded the PEL at 0.14% of the sites (Table 14). Mean ΣDDT was highest in Hillsborough Bay, with elevated concentrations also recorded in the Manatee River (Figure 106). The sites that exceeded the PEL were in Hillsborough Bay and the Hillsborough River (Figure 110).

Lindane (gamma-BHC) and Benzene hexachloride isomers ($C_6H_6Cl_6$; MW = 290.83): Benzene hexachloride (BHC), also known as hexachlorocyclohexane (HCH), is a six-carbon ring structure with six attached chlorine atoms (Table 14). Four isomers of BHC, commonly found in technical grade mixtures of this chemical (ATSDR, 2005e), are presented in Table 14. These include α-BHC, β-BHC, γ-BHC, and δ-BHC. Of these, γ-BHC is commonly known as the pesticide lindane, used as an insecticide on crops and to control insect-borne diseases, as well as in shampoo and lotions to control lice in humans (ATSDR, 2005e, Kamrin, 1997). Production of lindane in the United States ended in 1976, however it can still be imported for insecticide use (ATSDR, 2005e). Lindane is highly toxic to aquatic invertebrates and fish (Kamrin, 1997), and affects phytoplankton and zooplankton abundances (Fliedner and Klein, 1996). Like other organochlorines, lindane accumulates in organic sediments and bioaccumulates in organisms living and feeding in the sediments. Egeler et al., (1997) found tubificid oligochaetes bioaccumulate lindane from sediments in microcosm studies. Frithsen et al., (1995) did not include lindane in their loading estimates for Tampa Bay.

The mean concentration of α-BHC bay-wide was 0.04 µg/kg, with a maximum of 4.61 µg/kg (Table 14). Mean concentrations were higher in Hillsborough Bay, Middle Tampa Bay, Terra Ceia Bay, and Boca Ciega Bay (Figure 111). The mean sediment concentration of β-BHC was 0.89 µg/kg, with a maximum of 152.23 (Table 14). The highest level was recorded in 2014 in Middle Tampa Bay near Piney Point on the east side of the bay (14MTB63). Mean sediment concentrations were highest in Hillsborough Bay, Middle Tampa Bay, the Manatee River, and Boca Ciega Bay (Figure 112).

Lindane (γ-BHC) had a mean sediment concentration of 0.07 µg/kg, with a maximum of 23.08 µg/kg (Table 14). Lindane was above the TEL concentration at 2.27% of the sites and exceeded the PEL at 0.50% of the sites (Table 14). Mean lindane concentrations were high in Hillsborough Bay (Figure 113). Sites that exceeded the PEL were present in Hillsborough Bay, Lower Tampa Bay, Boca Ciega Bay, and Middle Tampa Bay in Cockroach Bay (Figure 115). The site with the highest lindane concentration was collected near Pendola Point in Hillsborough Bay in 2016 (16HB28) and was 23x higher than the PEL (Figure 115).

The mean concentration of δ-BHC was 0.09 µg/kg, with a maximum of 24.83 µg/kg (Table 14). The maximum concentration was from Hillsborough Bay near Pendola Point (16HB28). Mean concentrations were highest in Hillsborough Bay (Figure 114).

Endosulfan ($C_6H_6Cl_6O_3S$; MW = 406.93) and Endosulfan sulfate ($C_6H_6Cl_6O_4S$; MW = 422.92): Endosulfan is found in two isomeric forms; endosulfan 1 (or α-endosulfan), and endosulfan 2 (or β-endosulfan). Endosulfan sulfate is a breakdown product of endosulfan and is more persistent in the environment (ATSDR, 2013). The use of endosulfan in the United States had been restricted to certain crops and was scheduled to be phased out in 2016 (ATSDR, 2013). Exposure to high doses of endosulfan can cause neurological effects such as seizures, death in humans, and kidney damage (ATSDR, 2013). It is not known to be carcinogenic (Kamrin, 1997; ATSDR, 2013).

MacDonald, (1994) did not establish SQGs for endosulfan or endosulfan sulfate. The USEPA did recommend a level of 62 µg/L for endosulfan sulfate in freshwater lakes, rivers, and streams (ATSDR, 2013). A toxicity study on grass shrimp (*Palaemonetes pugio*) determined an endosulfan LC_{50} of 0.92 µg/L for males and 1.99 µg/L for females while mixed populations had a LC_{50} of 0.62 µg/L (Wirth et al., 2001). Endosulfan exposure also delayed reproduction in female grass shrimp and significantly reduced the number of gravid individuals (Wirth et al., 2002). They further found that embryos exposed to endosulfan had a significantly longer hatch time (Wirth et al., 2001). You et al., (2004) determined LC_{50} values for the freshwater amphipod, *Hyalella Azteca,* and chironomid, *Chironomus tentans,* for α-endosulfan, β-endosulfan, and endosulfan sulfate in freshwater sediments. They found LC_{50} values of 51.7, >1000, and 873 $\mu g/g_{oc}$ for *H. azteca*, and 0.96, 3.24, and 5.22 $\mu g/g_{oc}$ for *C. tentans* for α-endosulfan, β-endosulfan, and endosulfan sulfate respectively (You et al., 2004). McLeese et al., (1982) determined an LC_{50} of 0.34 mg/kg for the polychaete, *Nereis virens,* after 288 hours of exposure to endosulfan contaminated sediments. Endosulfan has been found to cause reduced growth rates in some freshwater snails and delay the release of brooding hatchlings in streams near coffee plantations in Jamaica (Ellis-Tabanor and Hyslop, 2005). Endosulfan was found to reduce fertilization success and cause tail and spinal deformation in zebrafish *(Danio rerio*) embryos (Teta and Naik, 2018). Embryos of the Oriental Fire-Bellied Toad (*Bombina orientalis*) exposed to endosulfan had decreased survival and increases in developmental abnormalities (Kang et al., 2008). Endosulfan can bioaccumulate and potentially be transferred up the food chain. In freshwater crabs, endosulfan initially accumulated in the hepatopancreas tissues (digestive gland), then transferred to the gonads which served as a sink for the pesticide (Negro et al., 2012). Exposure to sublethal concentrations can reduce the levels of total proteins and carbohydrates in muscle tissues of commercially important penaeid shrimp (*Metapenaeus monoceros*), decreasing its nutritional value (Suryavanshi et al., 2009).

The mean sediment concentration for endosulfan 1 in Tampa Bay was 0.05 µg/kg, with a maximum value of 10.83 µg/kg recorded in Hillsborough Bay in 2016 near Pendola Point (Table 14). Elevated mean concentrations were found in Hillsborough Bay, Middle Tampa Bay, the Manatee River, Terra Ceia Bay, and Boca Ciega Bay (Figure 116). The mean endosulfan 2 sediment concentration was 0.05 µg/kg, with a maximum of 3.76 µg/kg (Table 14). The maximum concentration was recorded in Hillsborough Bay in 2007 (07HB21), within the Davis Island Sea plane basin. Endosulfan 2 mean concentrations were high in Hillsborough Bay, Middle Tampa Bay, and the Manatee River (Figure 117). Mean sediment concentrations for endosulfan sulfate were 0.05 µg/kg, with a maximum value of 5.14 µg/kg (Table 14). Endosulfan sulfate had the highest sediment concentrations in Hillsborough Bay and the Manatee River (Figure 118), with the maximum concentration occurring at a site in Hillsborough Bay in 2004 (04HB13).

Endrin, Endrin aldehyde and Endrin ketone ($C_{12}H_8Cl_6O$); MW = 380.91): Endrin is a stereoisomer of dieldrin and was used as a pesticide for insects, rodents, and birds (ATSDR, 1996). Endrin aldehyde and endrin ketone are degradation products of endrin formed through exposure to heat and light (ATSDR, 1996). All three compounds have the same formula and molecular weight, but differ in their oxygen bond. Production of endrin in the United States ended in 1986, although it is still used in other countries (ATSDR, 1996). Exposure to endrin in humans primarily affects the central nervous system, causing convulsions and possible mortality at high exposures (ATSDR, 1996). It is not considered to be carcinogenic, but has been found to cause liver damage in animal studies, and can accumulate in fat tissues (ATSDR, 1996). MacDonald (1994) did not develop SQGs for endrin, endrin aldehyde, or endrin ketone. Bioassays on freshwater chironomid larvae (*Chironomus tentans*) have reported a 10-day LC_{50} of 4.22 ng/g_{oc} corrected for organic content (You et al., 2004). Endrin spiked sediments were found to affect bioturbation by the freshwater oligochaetes, *Limnodrilus hoffmeisteri,* and *Stylodrilus heringianus*, reducing activity at high concentrations (Keilty et al., 1988). This study also reported bioaccumulation of endrin in the body tissues and a decrease in body mass, assumed to be caused by decreased feeding and increased stress from endrin exposure (Keilty et al., 1988).

In Tampa Bay sediments, the mean concentration of endrin was 0.04 µg/kg, with a maximum value of 3.32 µg/kg (Table 14). The maximum concentration was recorded in Terra Ceia Bay in 2008 (08TBC26). Mean sediment concentrations were highest in Terra Ceia Bay and elevated in Hillsborough Bay, Middle Tampa Bay, the Manatee River, and Boca Ciega Bay (Figure 119). The mean endrin aldehyde concentration was 0.06 µg/kg, with a maximum value of 4.67 µg/kg (Table 14). The maximum concentration was found in 2004 in Hillsborough Bay in the East Bay area of Port Tampa Bay (04HB10). Mean concentrations were highest in Hillsborough Bay, the Manatee River, and Boca Ciega Bay (Figure 120). The mean sediment concentration for endrin ketone was 0.04 µg/kg, with a maximum of 5.1 µg/kg (Table 14). Endrin ketone concentrations were highest in the Manatee River (Figure 121), with the maximum level found in 1998 in the Manatee River near Bradenton (98MR20).

Chlordane ($C_{10}H_6Cl_8$; MW = 409.78): Total chlordane (ΣChlordane) is a composite of several isomers, primarily consisting of α-chlordane, (*cis*-chlordane), and γ-chlordane, (*trans*-chlordane) (ATSDR, 1994; MacDonald, 1994). Chlordane was formally used for several applications including as a home and garden pesticide, a treatment for termites, and a wood preservative (ATSDR, 1994, MacDonald, 1994; Frithsen et al., 1995). After 1983, it was only approved for termite control (ATSDR, 1994). The use of chlordane has been banned in the U.S. since 1988, after it was classified as a probable carcinogen by the EPA, although production and export are still allowed (ATSDR, 1994; Kamrin, 1997). In addition to cancer, exposure to chlordane can also cause neurological symptoms and liver damage (ATSDR, 1994). This pesticide is highly toxic to marine and aquatic organisms, particularly crustaceans and aquatic insects (Kamrin, 1997; Moore et al., 1998). It has been shown to accumulate in the fatty tissues of commercially and recreationally important fish and shellfish (Kennish and Ruppel, 1996, 1997). Annual inputs of chlordane to Tampa Bay were estimated at 1,050 kg, with 77% coming from agricultural runoff and 21% from urban runoff (Frithsen et al., 1995).

The mean sediment concentration for α-chlordane was 0.16 µg/kg, with a maximum of 76.35 µg/kg (Table 14). Mean concentrations were highest in Hillsborough Bay (Figure 122), with the maximum level being recorded in the Hillsborough River (03HB09). The mean sediment concentration of γ-chlordane was 0.18 µg/kg, with a maximum of 90.40 µg/kg. Mean concentrations were highest in Hillsborough Bay (Figure 123), with maximum levels recorded in the Hillsborough River (03HB09; 98HB006), and Seddon Channel, near the mouth of the Hillsborough River. The mean ΣChlordane concentration was 0.45 µg/kg, with a maximum of 166.75 µg/kg. Mean concentrations were highest in Hillsborough Bay and Old Tampa Bay (Figure 124). The maximum concentration was recorded at site 03HB09 in the Hillsborough River. Total chlordane exceeded its TEL at 0.78% of the sites and 0.99% of the sites were above the PEL (Table 14). Locations exceeding the PEL were primarily in Hillsborough Bay, including sites within the Hillsborough River, Alafia River, and McKay Bay. Other areas with PEL exceedances included a single location in Old Tampa Bay, the Manatee River, and Coffeepot Bayou in Middle Tampa Bay (Figure 125). Two sites with exceedingly high ΣChlordane levels were in the Hillsborough River (03HB09), which was 35x higher than the PEL and in Old

Tampa Bay (95OTB15), which was 28x higher than the PEL. Both sites were near the shoreline of Tampa urban residential areas.

Heptachlor ($C_{10}H_5Cl_7$; MW = 373.32) and Heptachlor epoxide ($C_{10}H_5Cl_7O$): Heptachlor is a component and breakdown product of chlordane, and has a similar chemical structure. Heptachlor epoxide is a metabolite produced from the bacterial breakdown of heptachlor in the environment, or from the metabolism of heptachlor in animals [Kamrin, 1997; Syracuse Research Corporation (SRC), 2007]. Heptachlor was used as a pesticide on crops and in homes to control ants, termites, and soil insects; it was phased out in 1988, however it is still approved by the EPA to control fire ants in underground power transformers (Kamrin, 1997; SRC, 2007). Exposure to high levels of heptachlor can damage the liver, kidneys, and red blood cells, and can have neurotoxic effects such as convulsions and coma (Kamrin, 1997; SRC, 2007). Both heptachlor and heptachlor epoxide are toxic to birds, fish, and aquatic invertebrates. It can bioconcentrate in fatty tissues and biomagnify in the food chain (SCR, 2007). MacDonald (1994) did not establish SQGs for either heptachlor or heptachlor epoxide.

The mean concentration of heptachlor in Tampa Bay sediments was 0.38 µg/kg, with a maximum level of 212 µg/kg (Table 14). The maximum concentrations were recorded in 2015 in Hillsborough Bay (15HB09) and the Manatee River (15MR42). Mean concentrations were also highest in Hillsborough Bay and the Manatee River (Figure 126). Heptachlor epoxide had a mean concentration of 0.06 µg/kg, with a maximum level of 12.15 µg/kg (Table 14). The two highest concentrations (12.15 and 10.28 µg/kg) were recorded in 2016 at sites in Hillsborough Bay (16HB32 and 16HB28 respectively). Mean concentrations were highest in Hillsborough Bay and Terra Ceia Bay (Figure 127).

Methoxychlor ($C_{16}H_{15}Cl_3O_2$; MW = 345.65): Methoxychlor has a similar structure to DDT, but is considered to be less toxic to humans and mammals. Methoxychlor is still manufactured and used in the United States (Kamrin, 1997). It is used to control insects on agricultural crops and livestock, and in formulations for use on ornamental gardens and on pets (ATSDR, 2002c). There are few recorded health effects from human studies; it has not been found to be carcinogenic, however animals exposed to high doses have exhibited neurological symptoms such as convulsions (ATSDR, 2002c). Several methoxychlor metabolites are similar to estrogen, and can reduce fertility, alter mating cycles, and affect reproductive organs in rats (Kamrin, 1997; ATSDR 2002c). Exposure to methoxychlor was found to inhibit testosterone production in ovarian tissues in freshwater bass (Borgert et al., 2004). Methoxychlor has a low toxicity to birds, but is highly toxic to aquatic invertebrates and some fish (Kamrin, 1997). MacDonald (1994) did not establish SQGs for Methoxychlor, however You et al., (2004) determined a 10-day LC_{50} of 36.7 µg/g_{oc} for aquatic insects (*Chironomus tentans*), and 85 µg/g_{oc} for the freshwater amphipod, *Hyalella azteca,* in spiked sediments. Methoxychlor can bioaccumulate in invertebrates, however most fish can metabolize and excrete it, and it is not believed to accumulate in the food web (Kamrin, 1997;ATSDR 2002c).

The mean concentration of methoxychlor in Tampa Bay sediments was 0.17 µg/kg, with a maximum level of 55.94 µg/kg (Table 14). The maximum concentration was found at a site in Hillsborough Bay located in the Davis Island seaplane basin (07HB21). Mean concentrations were highest in Hillsborough Bay and the Manatee River (Figure 128).

Mirex ($C_{10}Cl_{12}$; MW = 545.54): Mirex was manufactured and used as a pesticide in the United States during the 1960s and 1970s until production was stopped in 1976 (ATSDR, 1995b). It was used primarily for the control of fire ants, and as a fire retardant under the trade name Dechlorane® in plastics, rubber, paper, and electrical products (ATSDR, 1995b). Mirex is classified as a possible carcinogen, and exposure can cause damage to the digestive system, liver, kidneys, and affect the nervous and reproductive systems (ATSDR, 1995b). Mirex reacts when exposed to light to form photomirex, which also has harmful health effects and is more toxic than mirex (ATSDR, 1995b). Mirex is toxic to aquatic invertebrates (Naqvi and de la Cruz, 1973), and can bioaccumulate in fish and marine mammals (ATSDR, 1995; Yougui et al., 2003).

The mean concentration of mirex in Tampa Bay sediments was 0.11µg/kg, with a maximum recorded level of 41.1 µg/kg (Table 14). The highest concentration was at a site in Hillsborough Bay near Ballast Point in 2008 (08HB13). Mean concentrations were highest in Hillsborough Bay and the Manatee River (Figure 129).

PEL Ratio Grade

Figure 130 shows the overall distribution of sediment contaminants in Tampa Bay based on the average PEL ratio across all measured sediment contaminants with established SQLs. The sites were assigned a letter grade (A, B, C. D, F) based on the mean PEL ratio. Most sites fell within the "C" range, while the "D" and "F" graded sites were found primarily in Hillsborough Bay, the Manatee River, and Boca Ciega Bay.

Table 14. Total PCBs and Pesticide summary statistics 1993-2017.

µg/kg	ΣPCBs	Aldrin	Dieldrin	p,p'-DDD	p,p'-DDE	p,p'-DDT	ΣDDT
MW	188.65 – 498.66	364.91	380.91	320.04	318.02	354.49	
Formula	$C_{12}H_xCl_x$	$C_{12}H_8Cl_6$	$C_{12}H_8Cl_6O$	$C_{14}H_{10}Cl_4$	$C_{14}H_8Cl_4$	$C_{14}H_9Cl_5$	
Structure	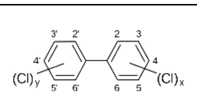	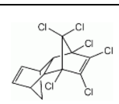	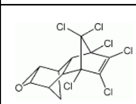	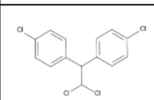	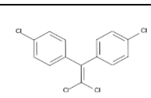	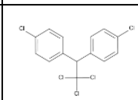	
TEL	21.6	ND	0.72	1.2	2.1	1.2	3.89
PEL	189	ND	4.3	7.8	374	4.8	51.7
n	1411	1411	1411	1411	1411	1411	1411
Minimum	0.09	0.01	0.01	0.01	0.01	0.01	0.03
Maximum	197.87	12.58	10.65	29.975	117.347	43.06	166.363
Median	0.19	0.01	0.01	0.01	0.01	0.01	0.03
Mean	2.28	0.06	0.08	0.14	0.39	0.13	0.66
SD	9.48	0.44	0.43	0.98	3.65	1.29	5.38
% >TEL;<PEL	**1.70%**		**1.70%**	**1.06%**	**1.98%**	**1.13%**	**1.70%**
% >PEL	**0.07%**		**0.21%**	**0.28%**	**0.00%**	**0.28%**	**0.14%**

Table 14. Continued

μg/kg	α- BHC	β-BHC	γ-BHC (Lindane)	δ-BHC	Endosulfan 1	Endosulfan 2	Endosulfan sulfate	Endrin	Endrin aldehyde	Endrin ketone
MW	290.83	290.83	290.83	290.83	406.93	406.93	422.92	380.91	380.91	380.91
Formula	$C_6H_6Cl_6$	$C_6H_6Cl_6$	$C_6H_6Cl_6$	$C_6H_6Cl_6$	$C_6H_6Cl_6O_3S$	$C_6H_6Cl_6O_3S$	$C_6H_6Cl_6O_4S$	$C_{12}H_8Cl_6O$	$C_{12}H_8Cl_6O$	$C_{12}H_8Cl_6O$
Structure	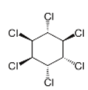	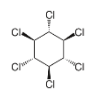	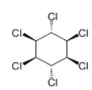	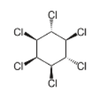	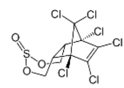	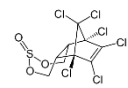	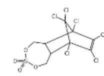	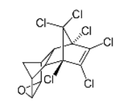	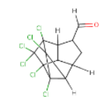	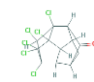
TEL	ND	ND	0.32	ND	ND	ND	ND	ND	ND	ND
PEL	ND	ND	0.99	ND	ND	ND	ND	ND	ND	ND
n	1411	1411	1411	1411	1411	1411	1411	1411	1411	1411
Minimum	0.01	0.01	0.01	0.01	0.01	0.01	0.01	0.01	0.01	0.005
Maximum	4.61	152.23	23.08	24.83	10.83	3.76	5.14	3.32	4.67	5.1
Median	0.01	0.01	0.01	0.01	0.01	0.01	0.01	0.01	0.01	0.01
Mean	0.04	0.89	0.07	0.09	0.05	0.05	0.05	0.04	0.06	0.04
SD	0.17	7.20	0.63	0.89	0.36	0.18	0.19	0.15	0.26	0.18
% >TEL;<PEL			**2.27%**							
% >PEL			**0.50%**							

Table 14. Continued.

μg/kg	α-Chlordane	γ-Chlordane	ΣChlordane	Heptachlor	Heptachlor Epoxide	Methoxychlor	Mirex
MW	409.78	409.78	409.78	373.32	389.32	345.65	545.54
Formula	$C_{10}H_6Cl_8$	$C_{10}H_6Cl_8$	$C_{10}H_6Cl_8$	$C_{10}H_5Cl_7$	$C_{10}H_5Cl_7O$	$C_{16}H_{15}Cl_3O_2$	$C_{10}Cl_{12}$
Structure	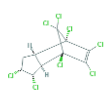	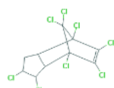		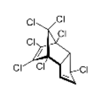	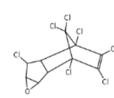	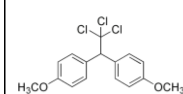	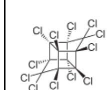
TEL	ND	ND	2.3	ND	ND	ND	ND
PEL	ND	ND	4.8	ND	ND	ND	ND
n	1318	1318	1411	1411	1411	1411	1411
Minimum	0.01	0.01	0.01	0.01	0.01	0.01	0.01
Maximum	76.35	90.40	166.75	212	12.15	55.94	41.1
Median	0.01	0.01	0.02	0.01	0.01	0.01	0.01
Mean	0.16	0.18	0.45	0.38	0.06	0.17	0.11
SD	2.20	2.59	5.90	8.00	0.45	1.63	1.40
% >TEL;<PEL			**0.78%**				
% >PEL			**0.99%**				

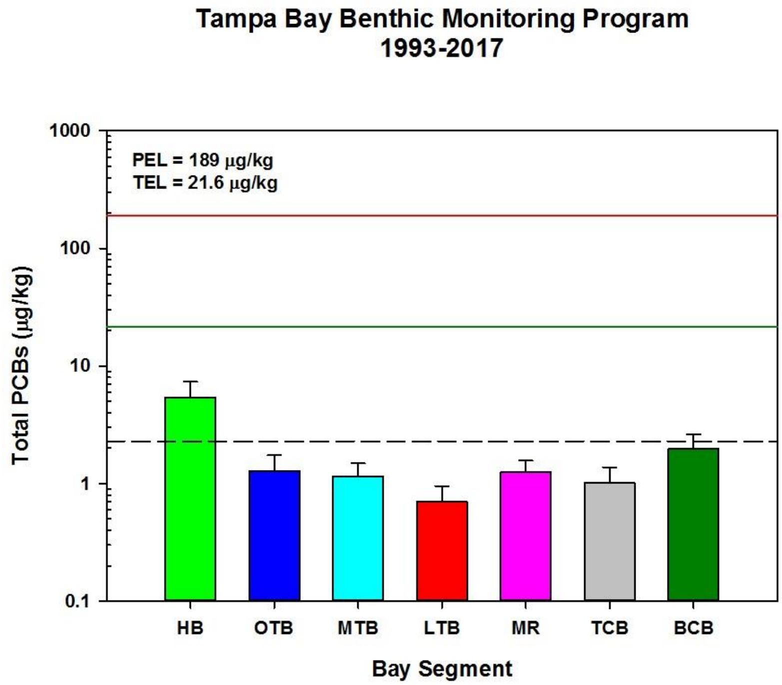

Figure 98. Mean sediment total PCB concentrations by bay segment. Error bars = 95% confidence interval, dashed line represents bay-wide mean. Solid lines represent PEL (upper; red) and TEL (lower; green) values.

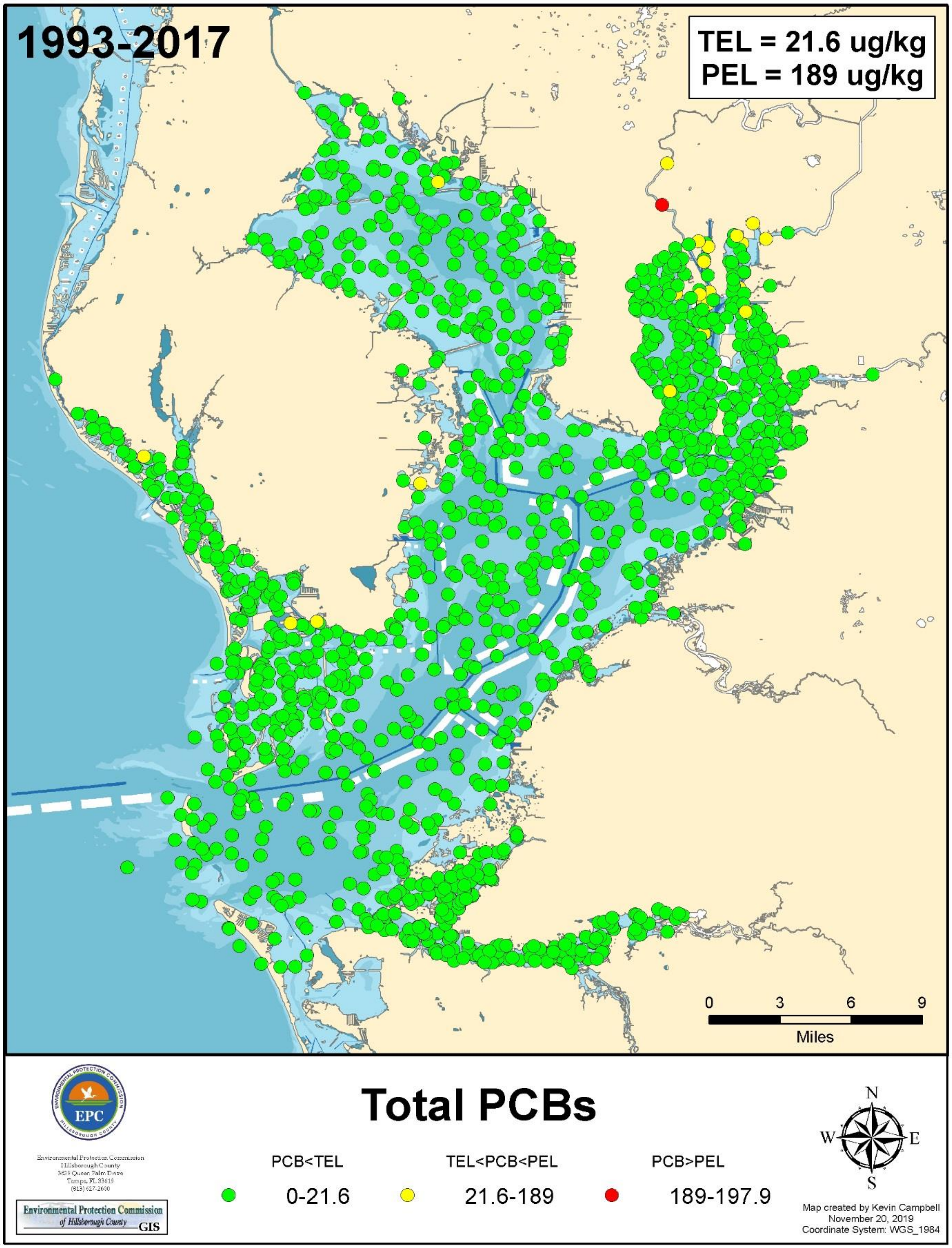

Figure 99. Distribution of total PCBs in Tampa Bay 1993-2017.

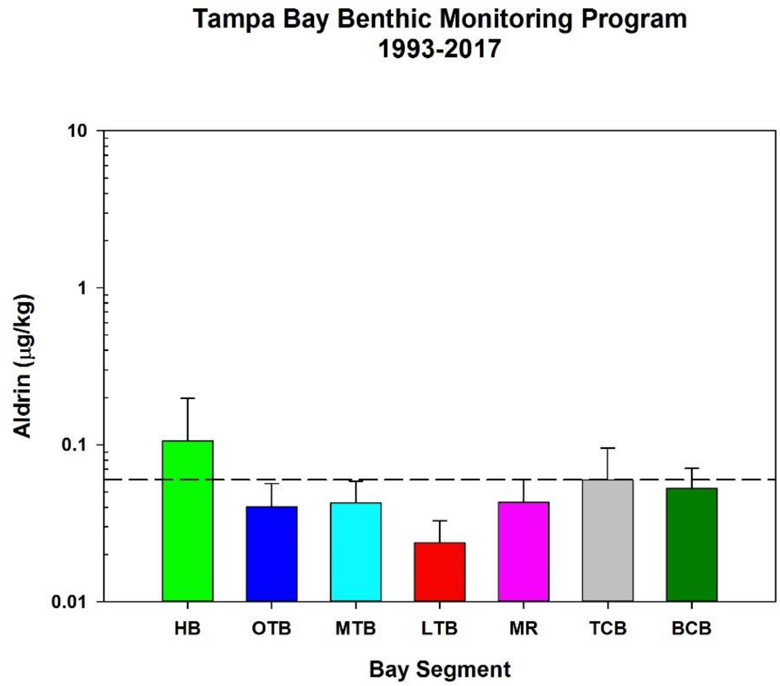

Figure 100. Mean sediment aldrin concentrations by bay segment. Error bars = 95% confidence interval, dashed line represents bay-wide mean.

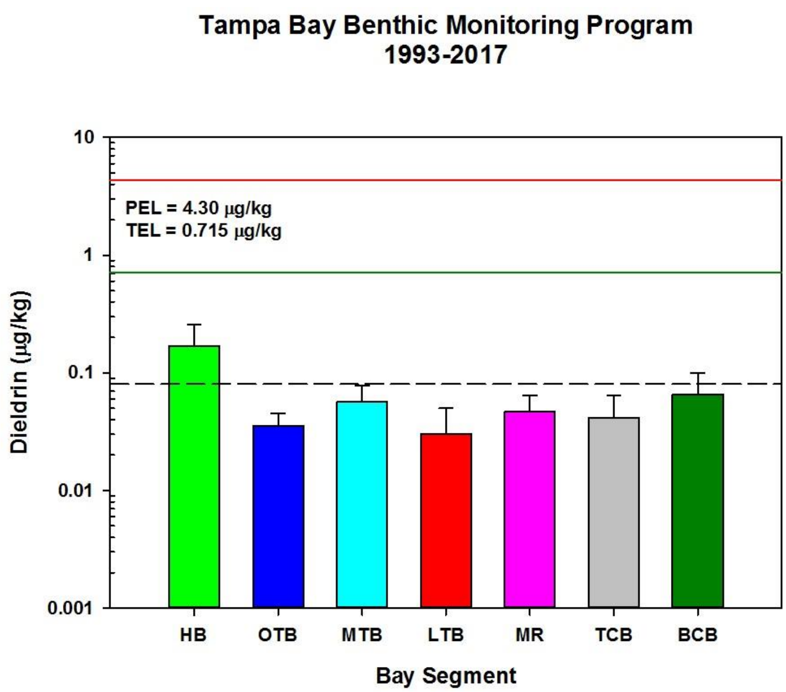

Figure 101. Mean sediment dieldrin concentrations by bay segment. Error bars = 95% confidence interval, dashed line represents bay-wide mean. Solid lines represent PEL (upper; red) and TEL (lower; green) values.

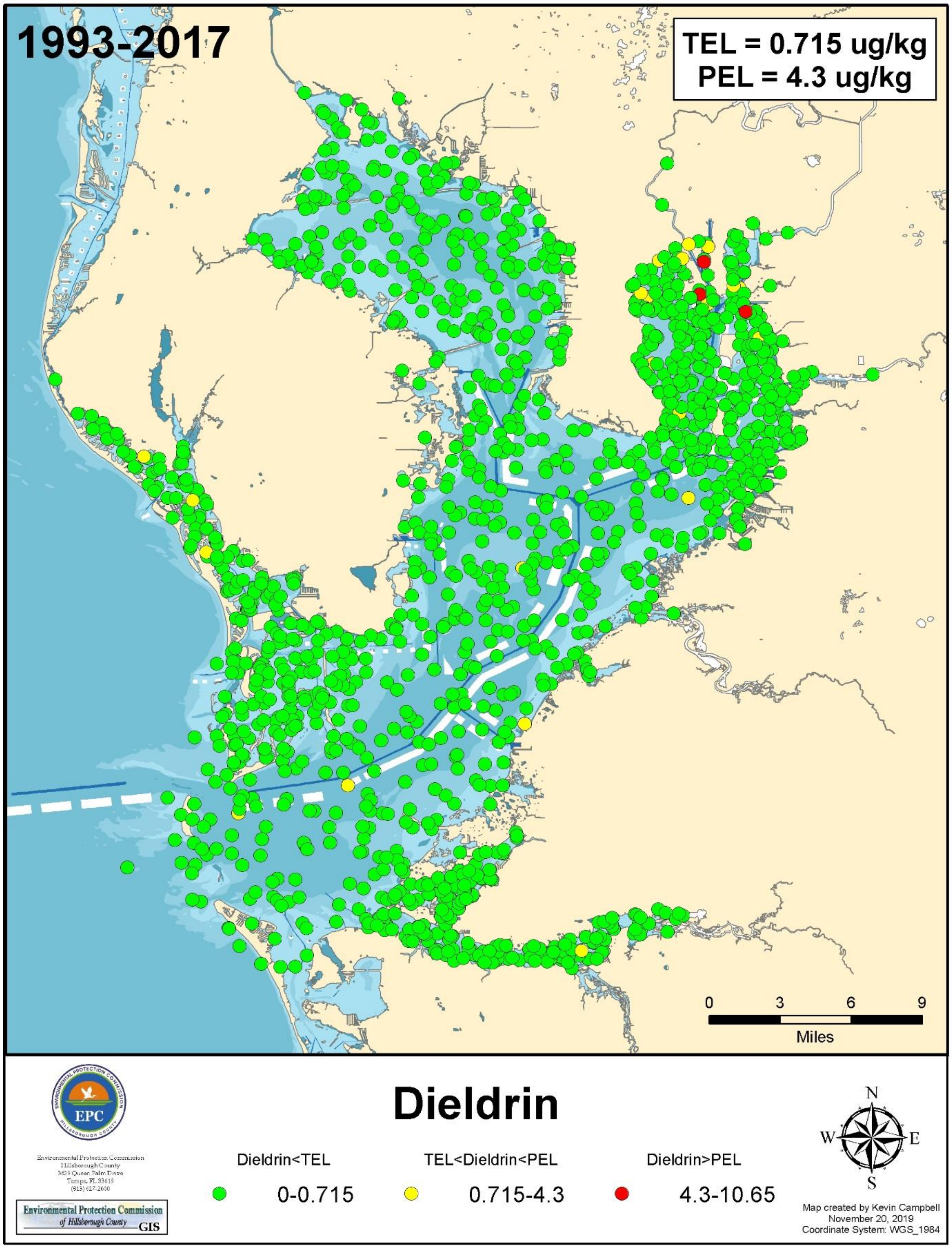

Figure 102. Distribution of dieldrin in Tampa Bay 1993-2017.

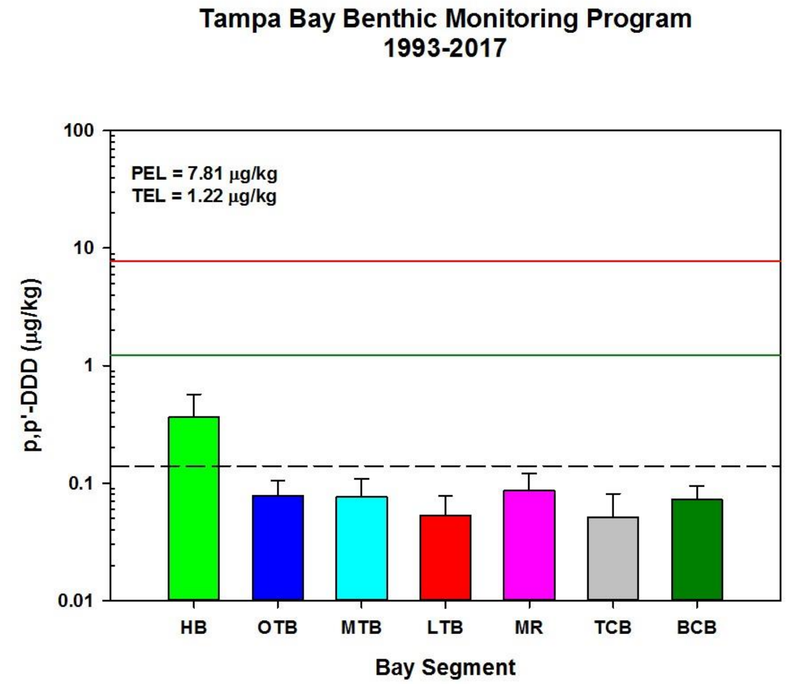

Figure 103. Mean sediment p,p'-DDD concentrations by bay segment. Error bars = 95% confidence interval, dashed line represents bay-wide mean. Solid lines represent PEL (upper; red) and TEL (lower; green) values.

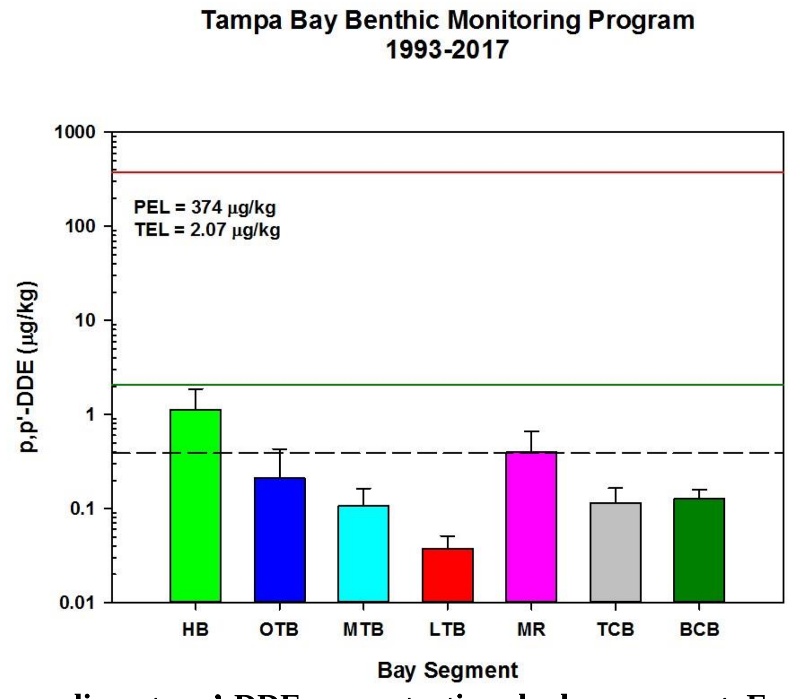

Figure 104. Mean sediment p,p'-DDE concentrations by bay segment. Error bars = 95% confidence interval, dashed line represents bay-wide mean. Solid lines represent PEL (upper; red) and TEL (lower; green) values.

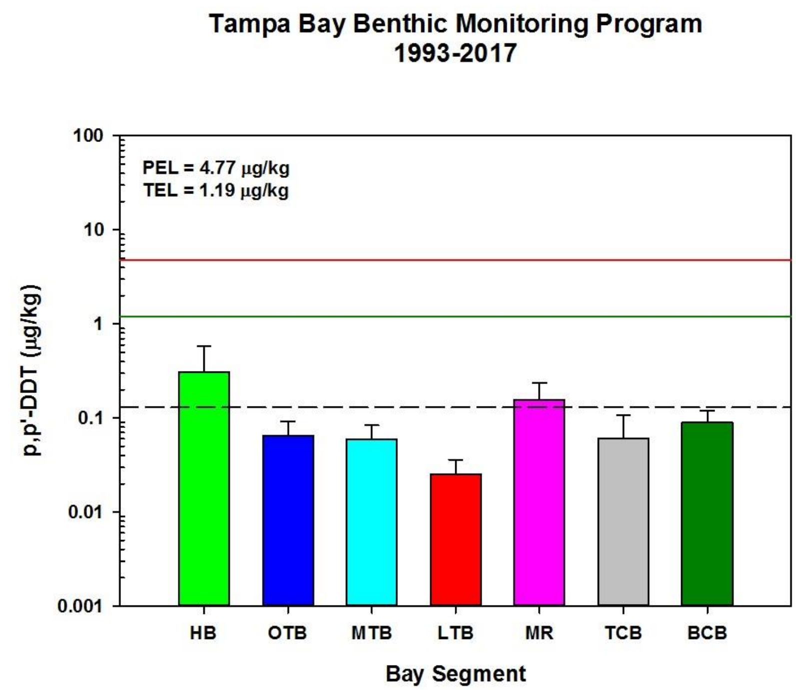

Figure 105. Mean sediment p,p'-DDT concentrations by bay segment. Error bars = 95% confidence interval, dashed line represents bay-wide mean. Solid lines represent PEL (upper; red) and TEL (lower; green) values.

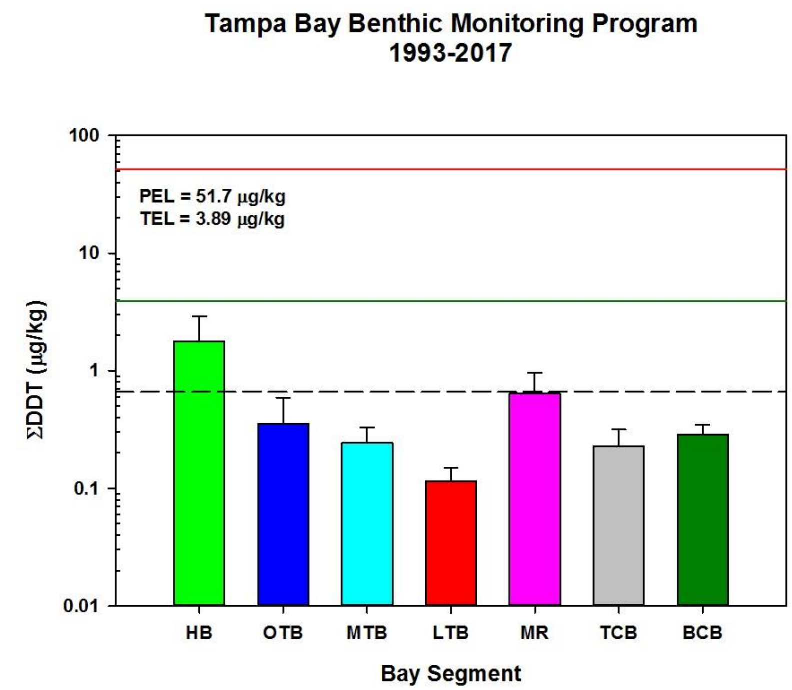

Figure 106. Mean sediment total DDT concentrations by bay segment. Error bars = 95% confidence interval, dashed line represents bay-wide mean. Solid lines represent PEL (upper; red) and TEL (lower; green) values.

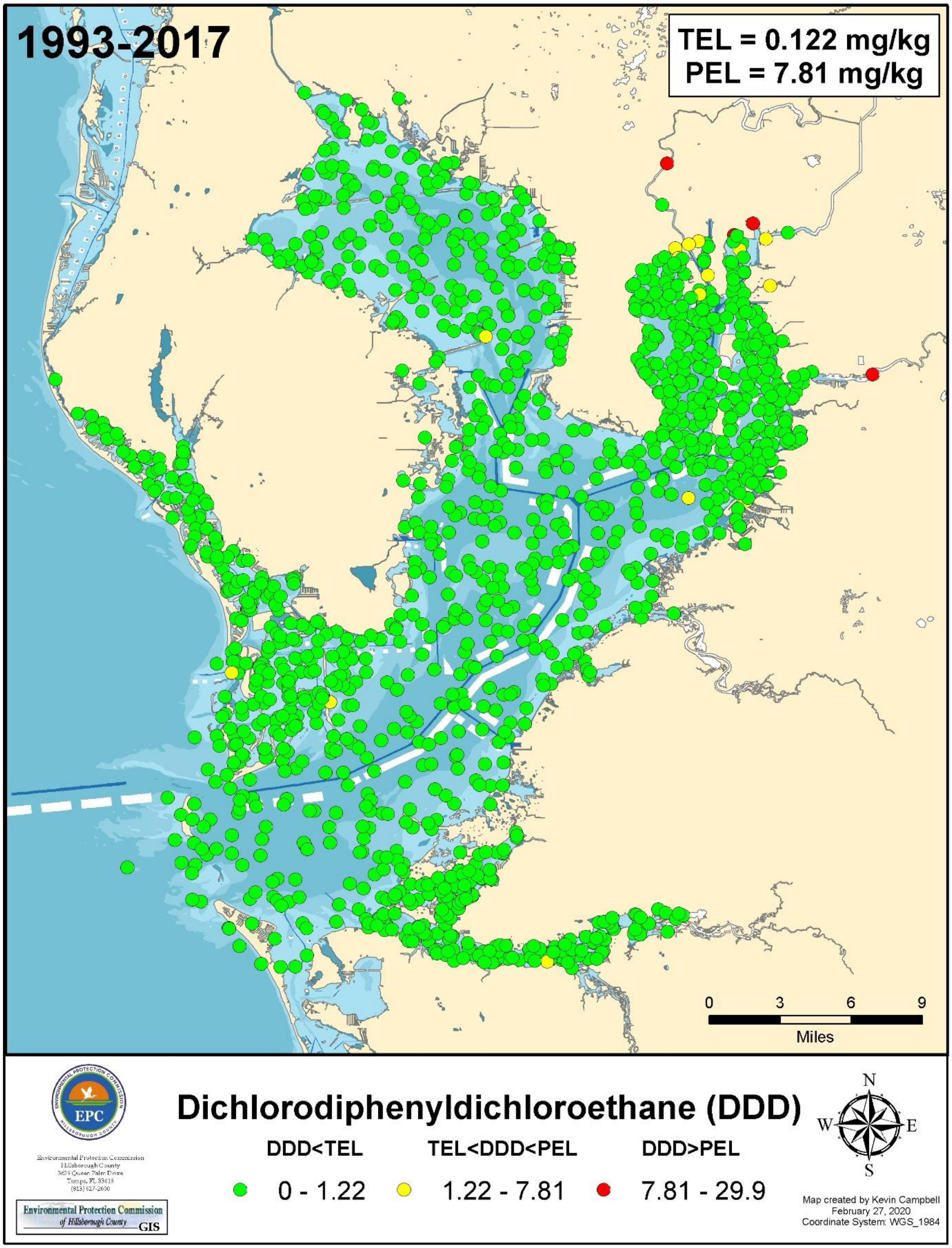

Figure 107. Distribution of p,p'-DDD in Tampa Bay 1993-2017.

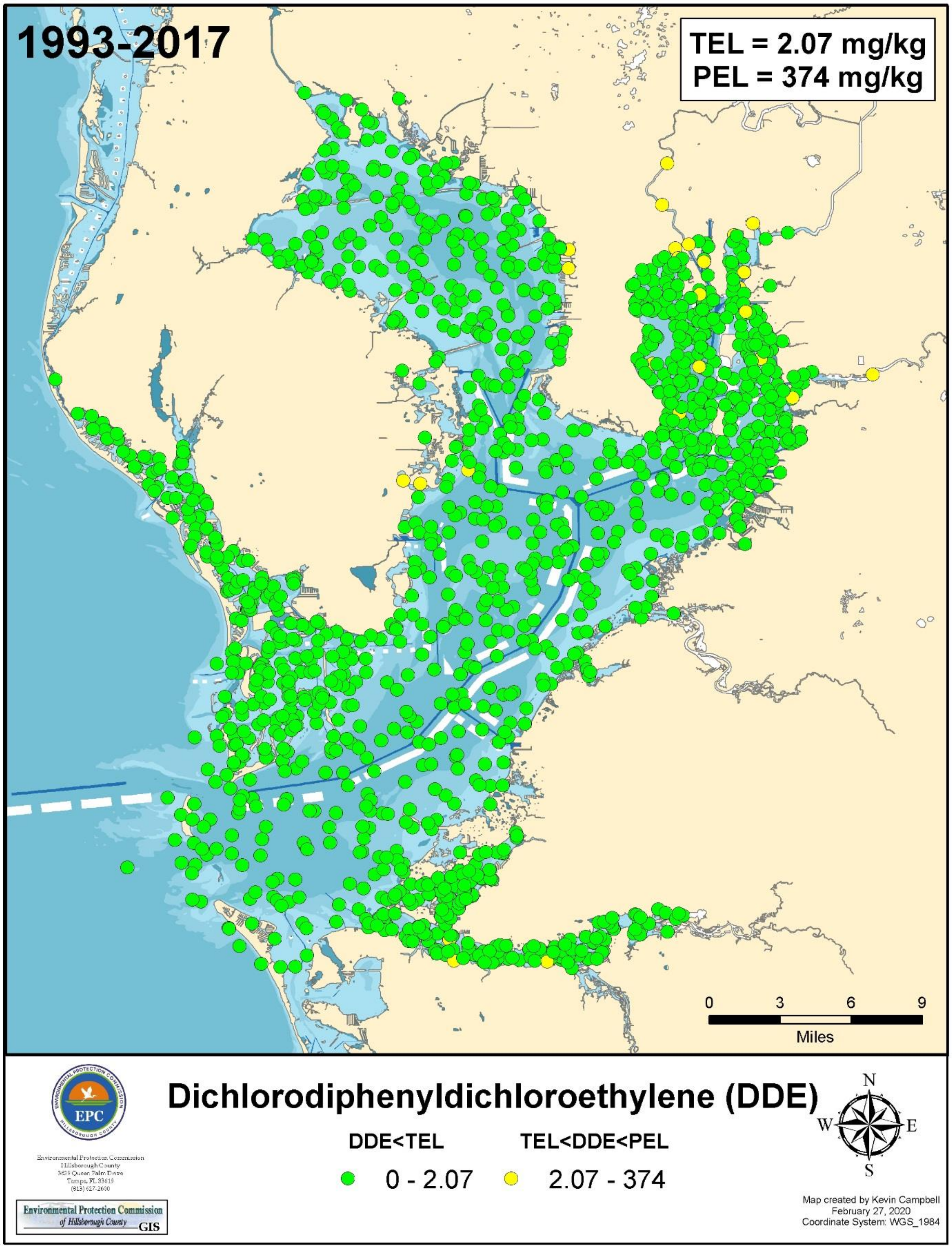

Figure 108. Distribution of p,p'-DDE in Tampa Bay 1993-2017.

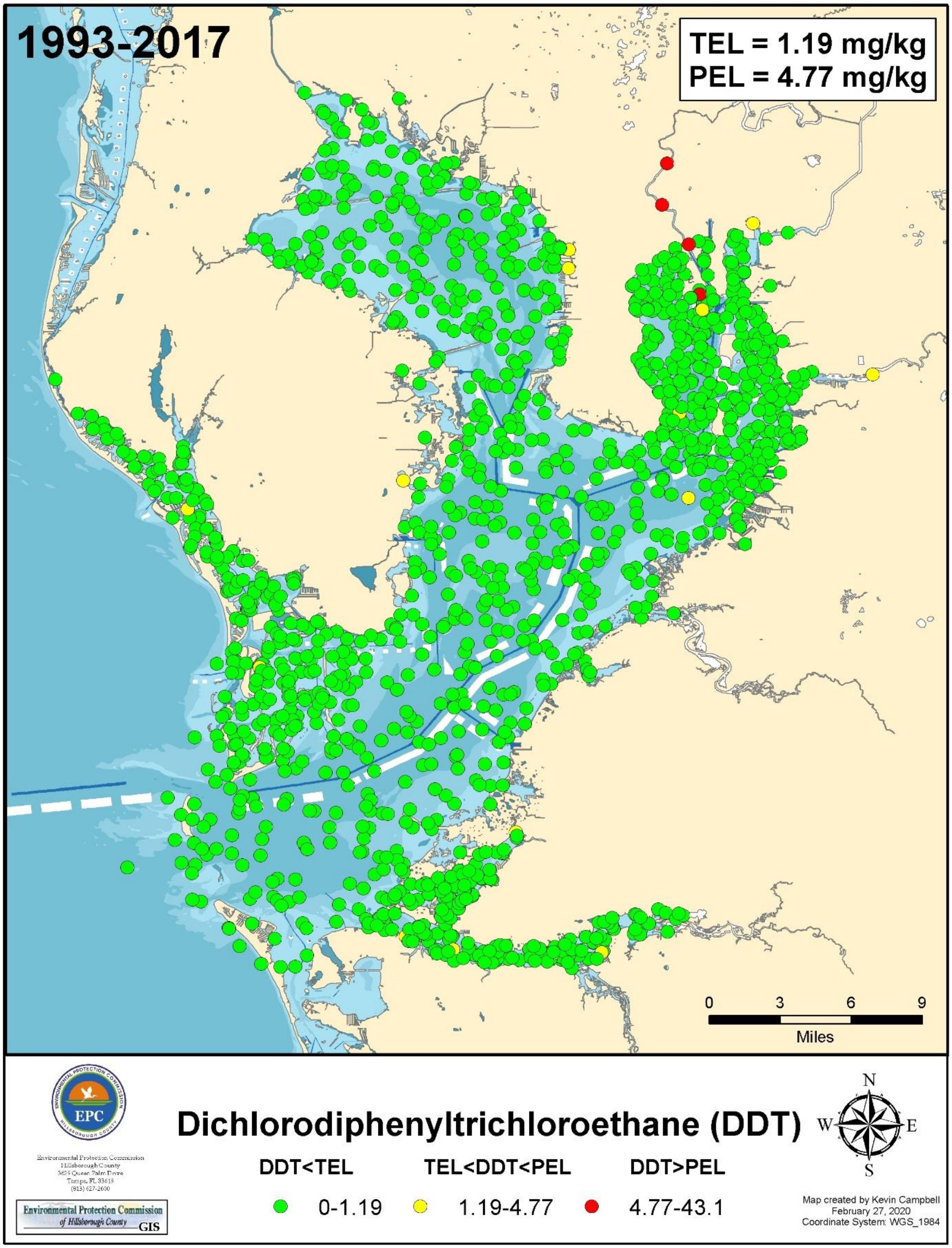

Figure 109. Distribution of p,p'-DDT in Tampa Bay 1993-2017.

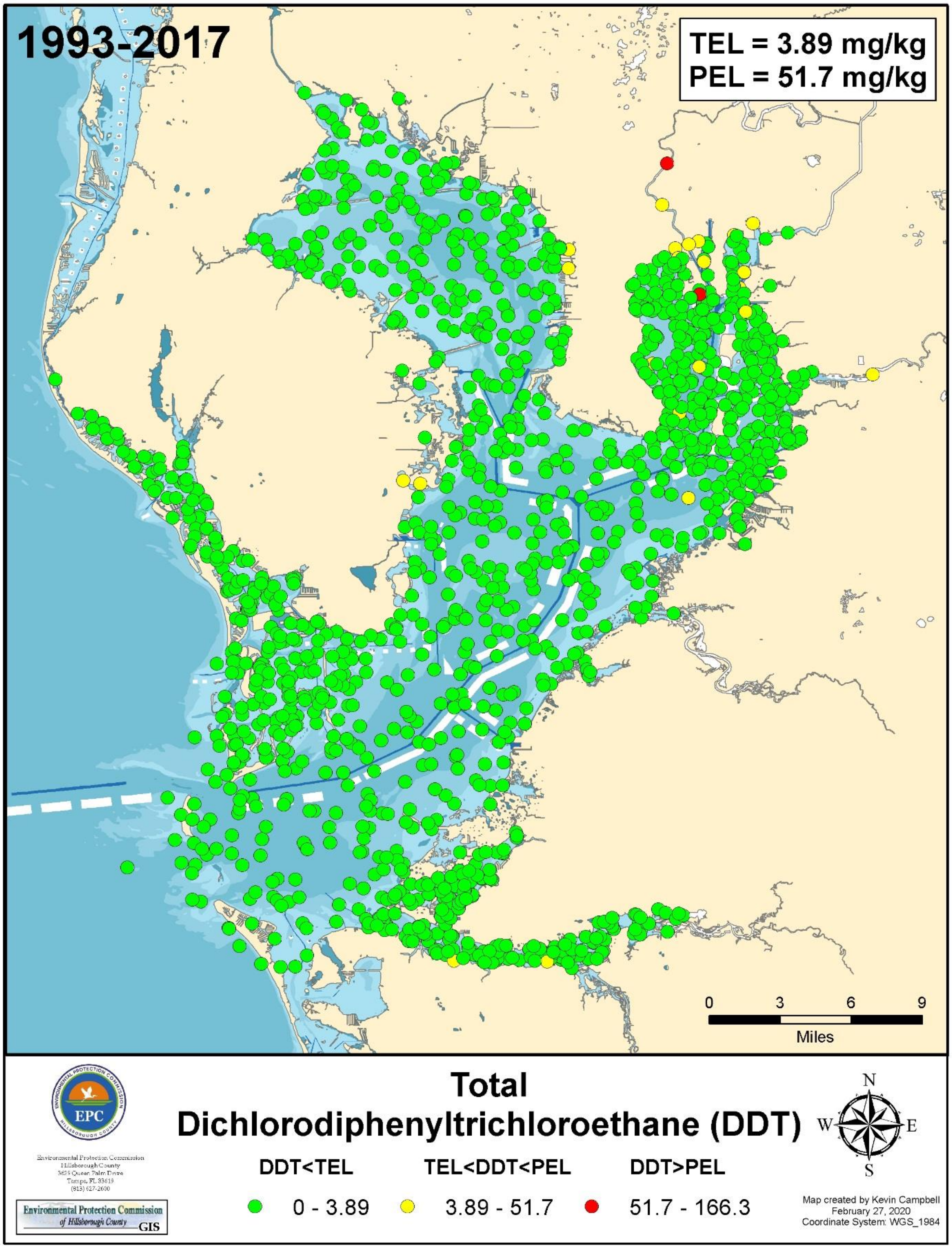

Figure 110. Distribution of total DDT in Tampa Bay 1993-2017.

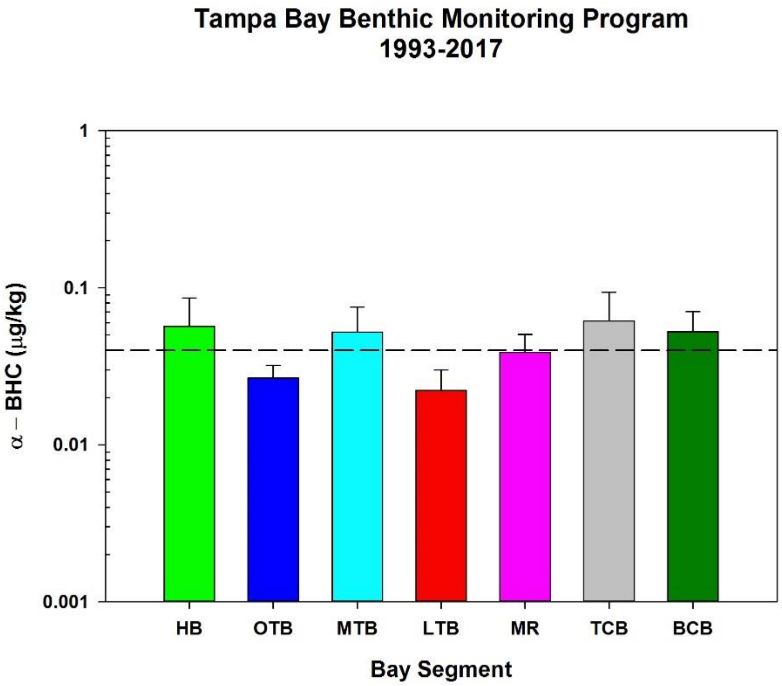

Figure 111. Mean sediment α-BHC concentrations by bay segment. Error bars = 95% confidence interval, dashed line represents bay-wide mean.

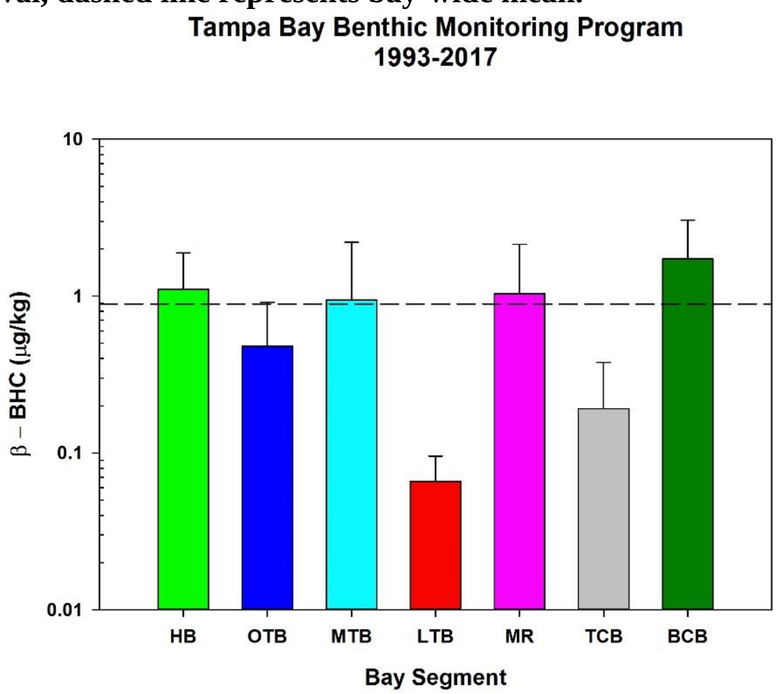

Figure 112. Mean sediment β-BHC concentrations by bay segment. Error bars = 95% confidence interval, dashed line represents bay-wide mean.

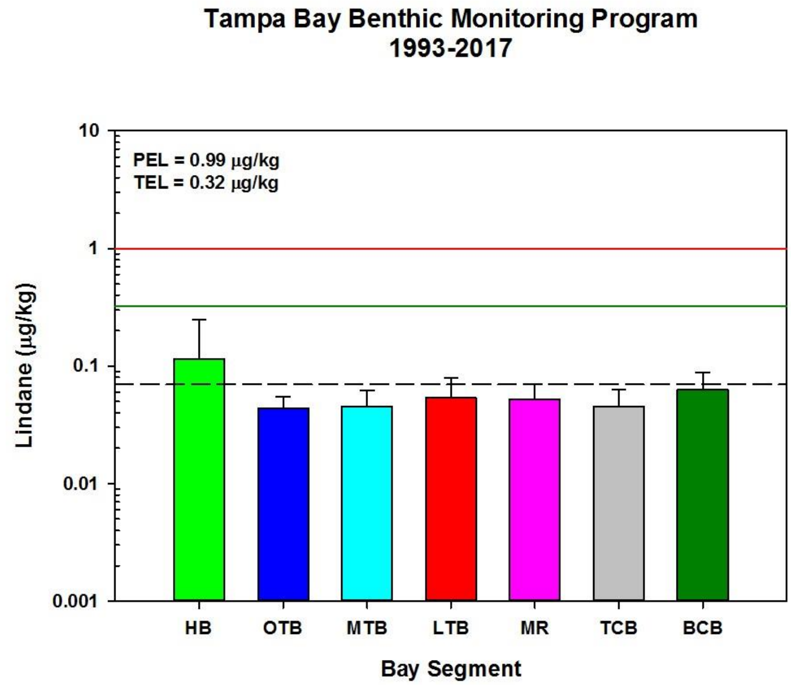

Figure 113 Mean sediment lindane (γ-BHC) concentrations by bay segment. Error bars = 95% confidence interval, dashed line represents bay-wide mean. Solid lines represent PEL (upper; red) and TEL (lower; green) values.

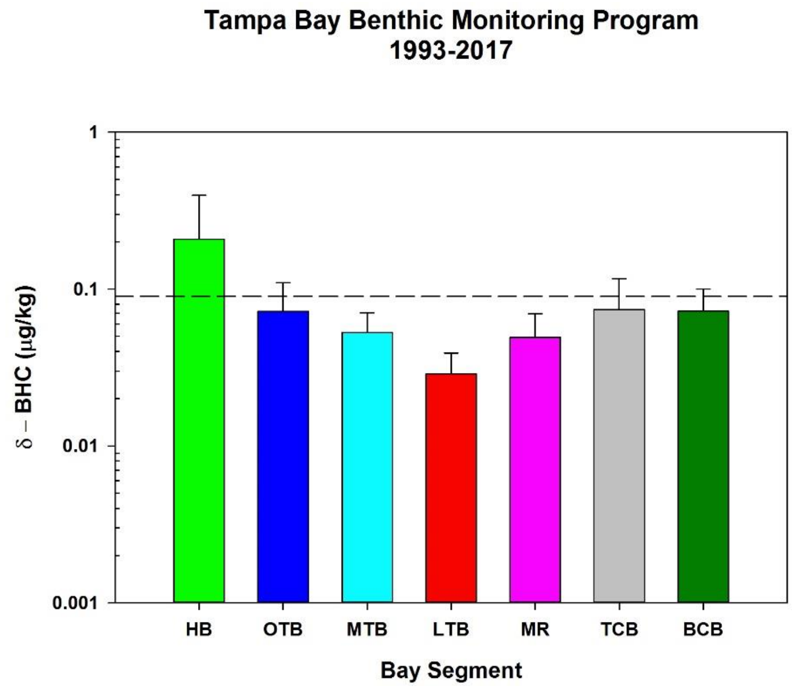

Figure 114. Mean sediment δ-BHC concentrations by bay segment. Error bars = 95% confidence interval, dashed line represents bay-wide mean.

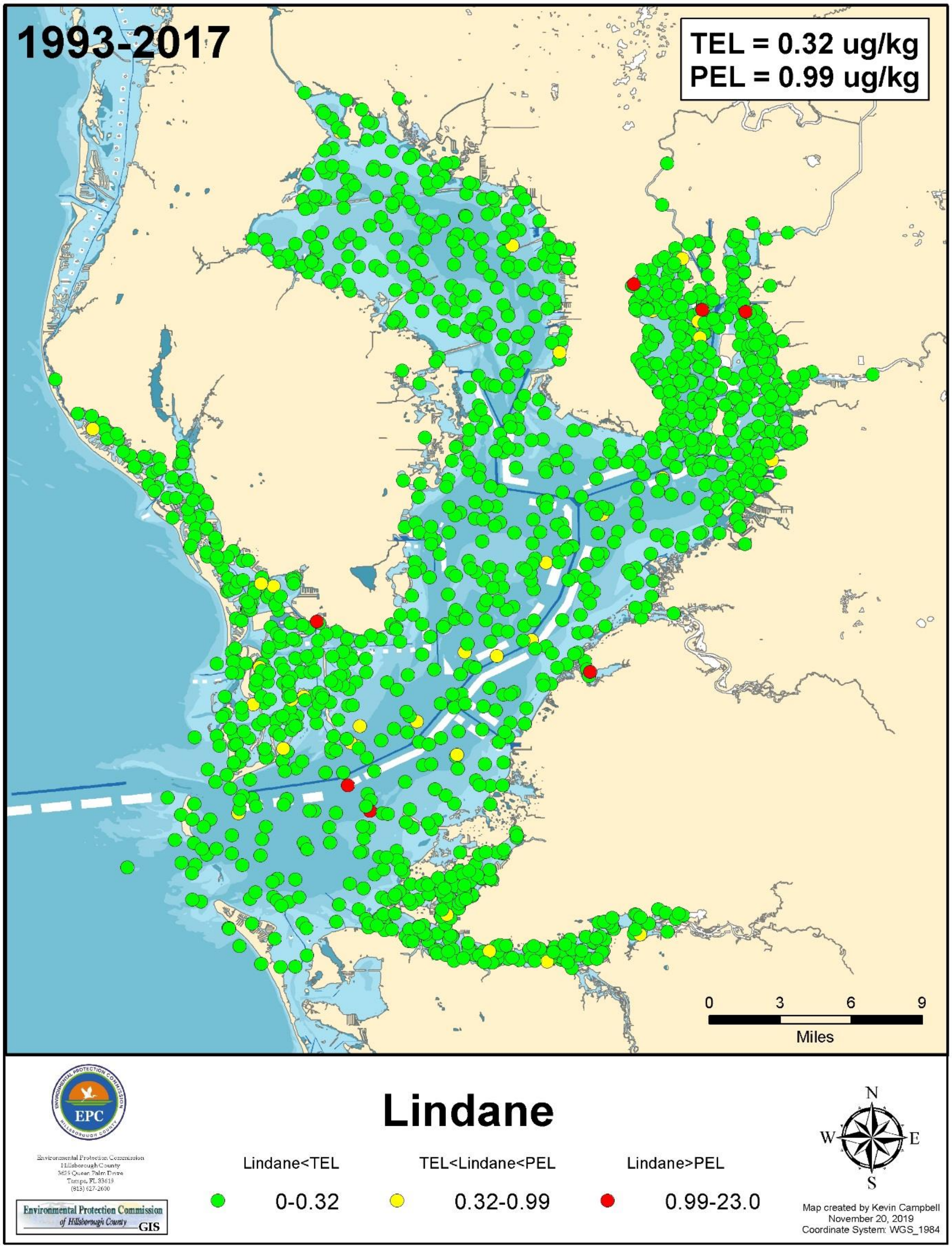

Figure 115. Distribution of lindane in Tampa Bay 1993-2017.

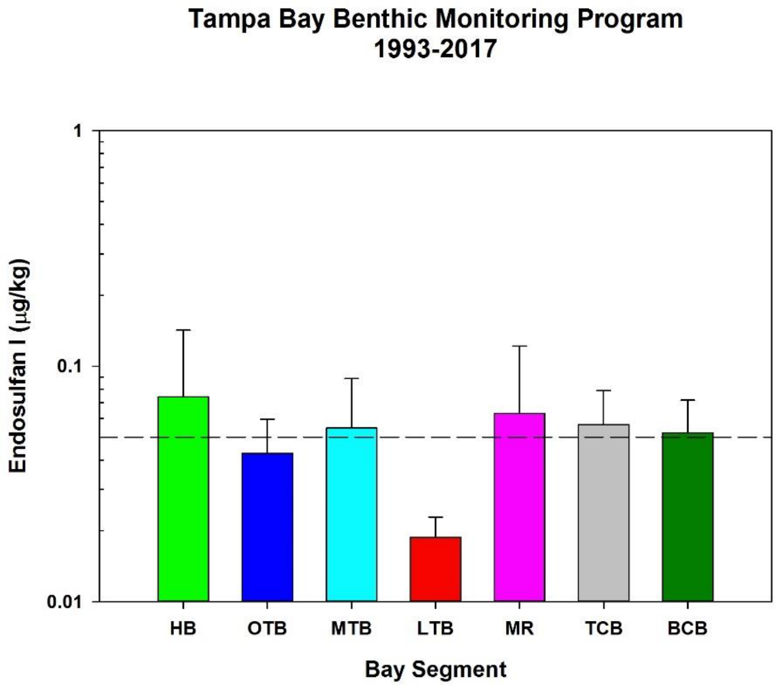

Figure 116. Mean sediment endosulfan l concentrations by bay segment. Error bars = 95% confidence interval, dashed line represents bay-wide mean.

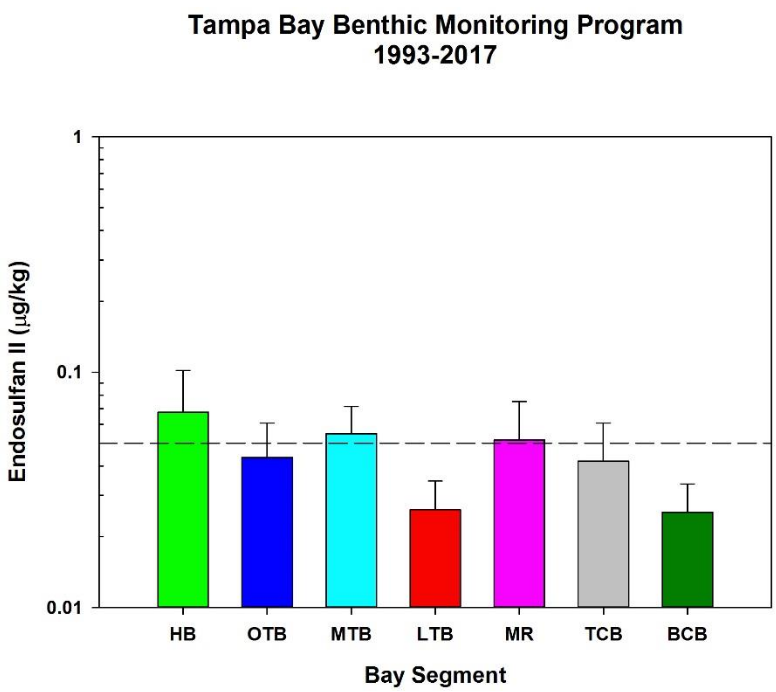

Figure 117. Mean sediment endosulfan ll concentrations by bay segment. Error bars = 95% confidence interval, dashed line represents bay-wide mean.

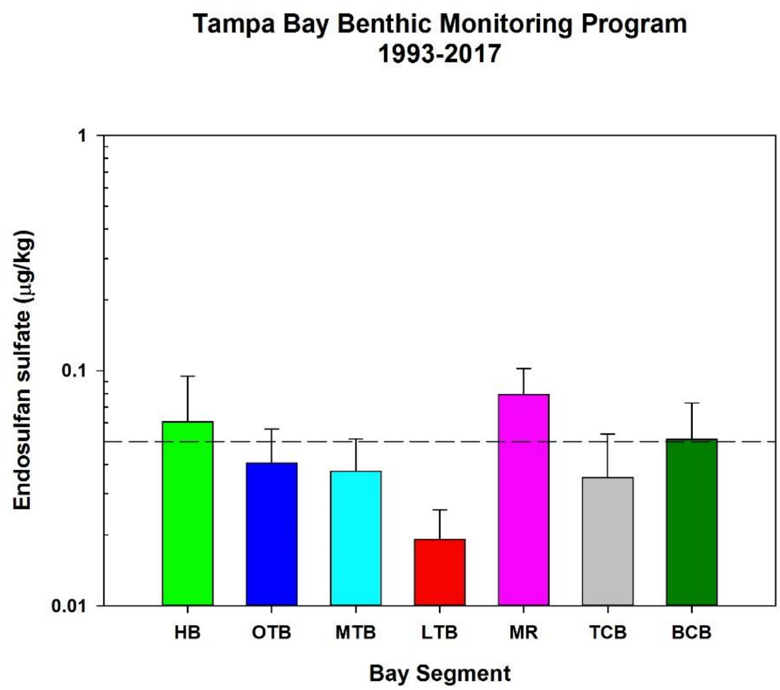

Figure 118. Mean sediment endosulfan sulfate concentrations by bay segment. Error bars = 1 standard deviation.

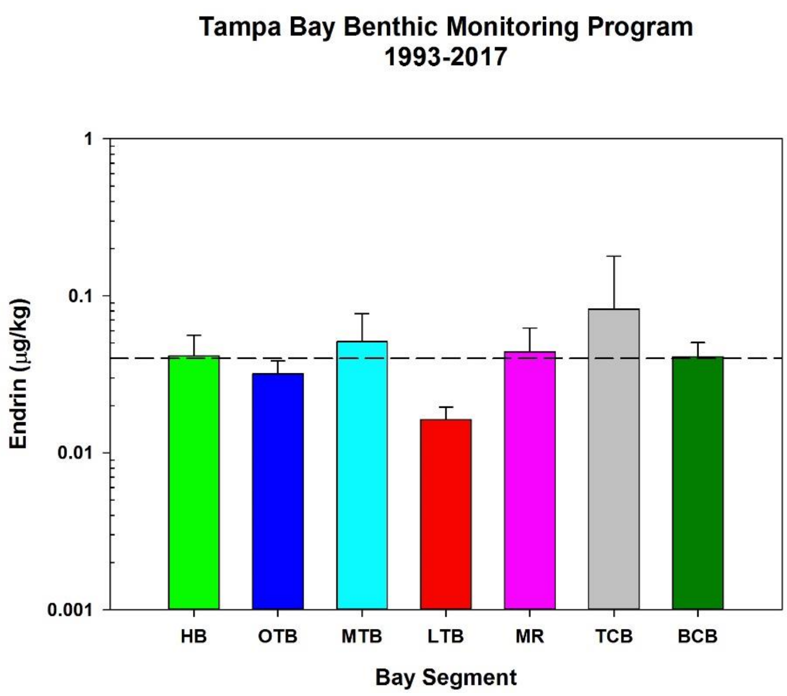

Figure 119. Mean sediment endrin concentrations by bay segment. Error bars = 95% confidence interval, dashed line represents bay-wide mean.

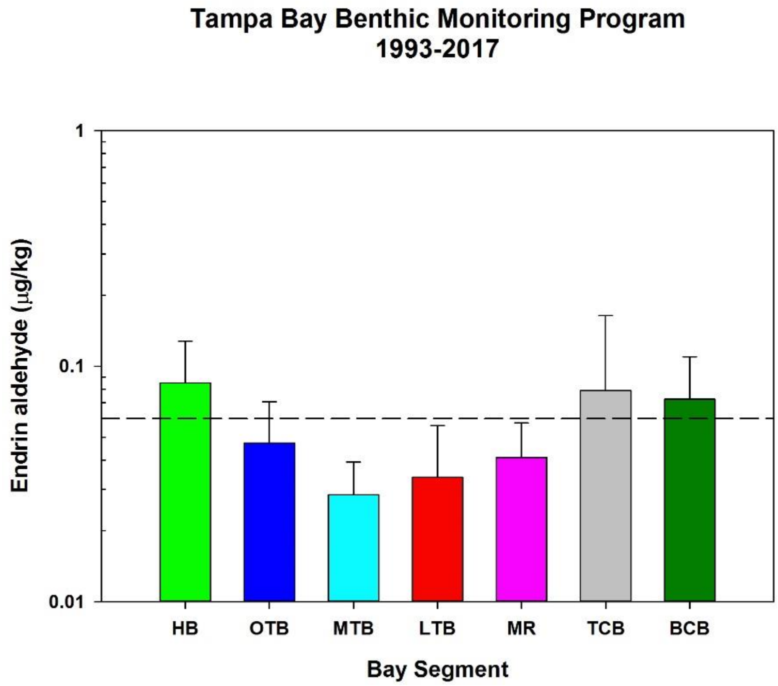

Figure 120. Mean sediment endrin aldehyde concentrations by bay segment. Error bars = 95% confidence interval, dashed line represents bay-wide mean.

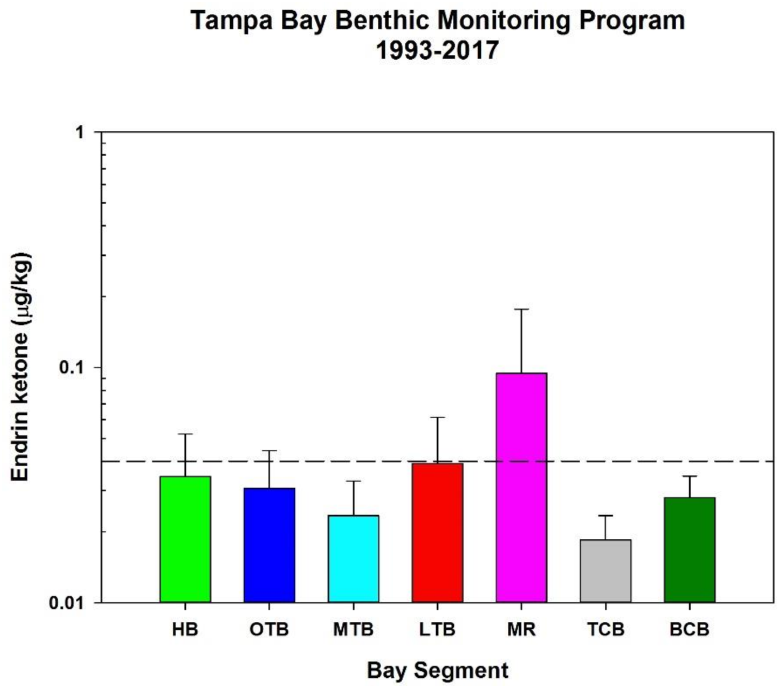

Figure 121. Mean sediment endrin ketone concentrations by bay segment. Error bars = 95% confidence interval, dashed line represents bay-wide mean.

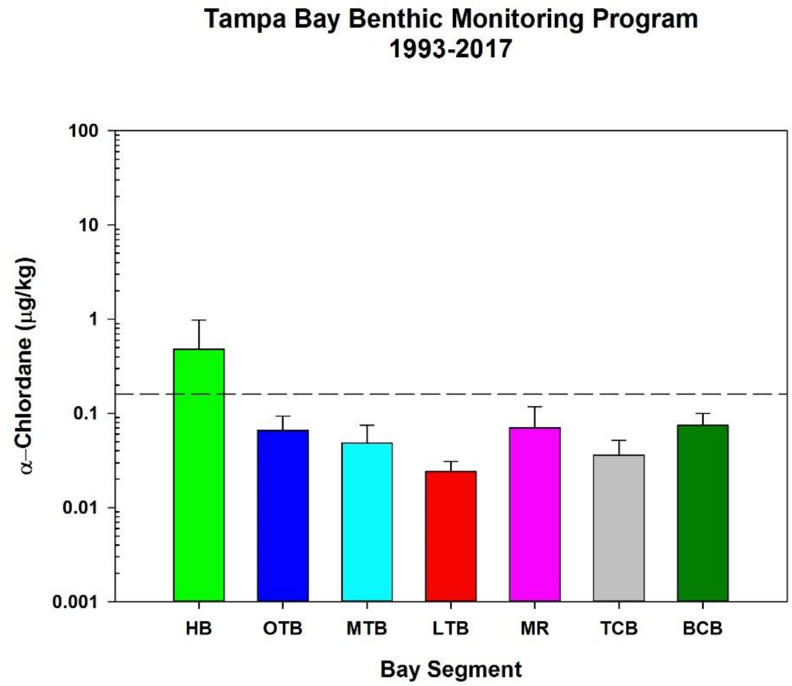

Figure 122. Mean sediment α-chlordane concentrations by bay segment. Error bars = 95% confidence interval, dashed line represents bay-wide mean.

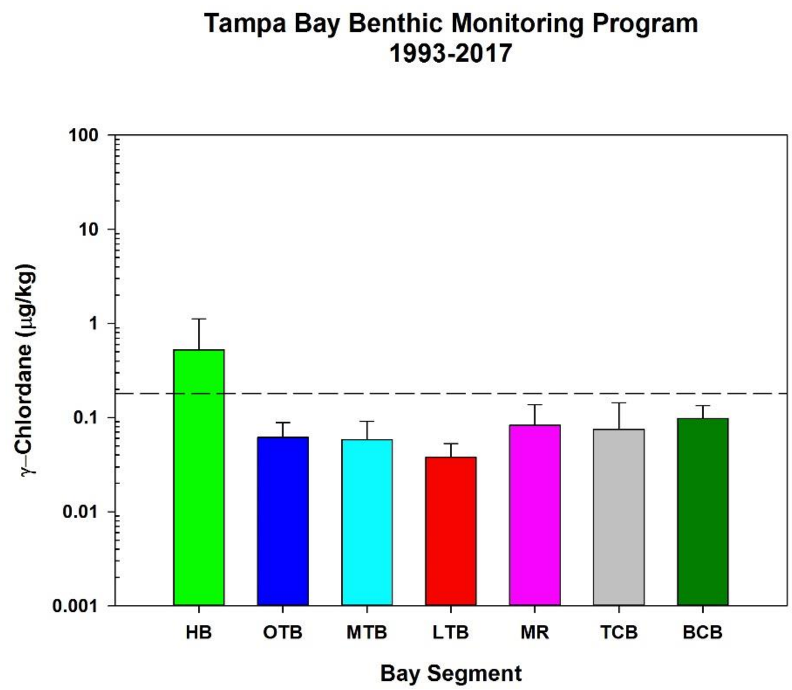

Figure 123. Mean sediment γ-chlordane concentrations by bay segment. Error bars = 95% confidence interval, dashed line represents bay-wide mean.

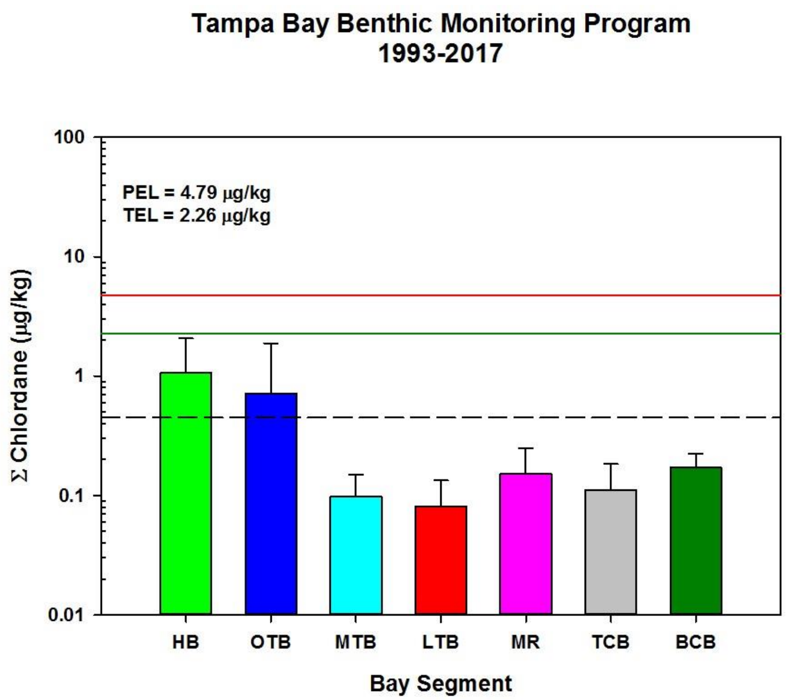

Figure 124. Mean sediment total chlordane concentrations by bay segment. Error bars = 95% confidence interval, dashed line represents bay-wide mean. Solid lines represent PEL (upper; red) and TEL (lower; green) values.

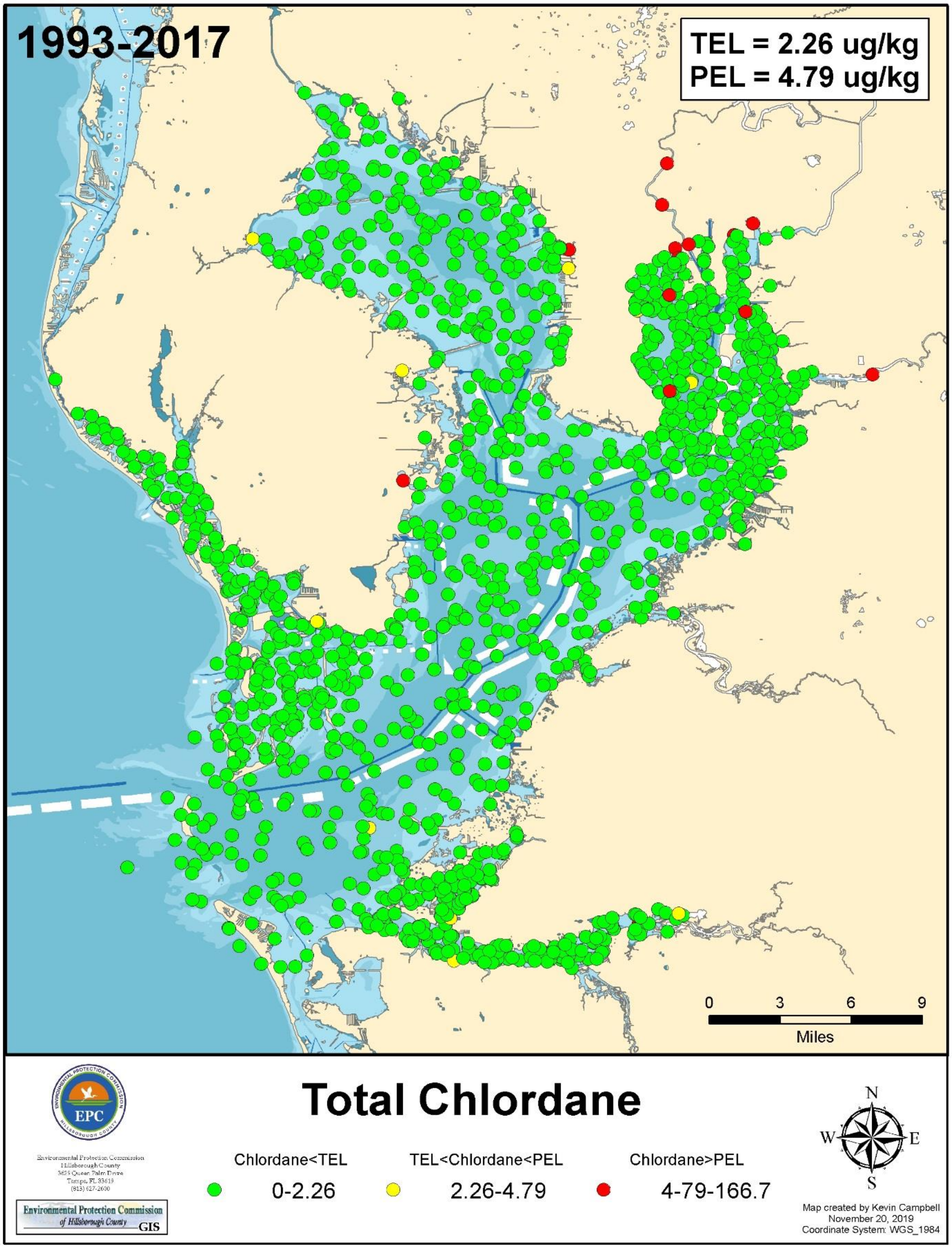

Figure 125. Distribution of total chlordane in Tampa Bay 1993-2017.

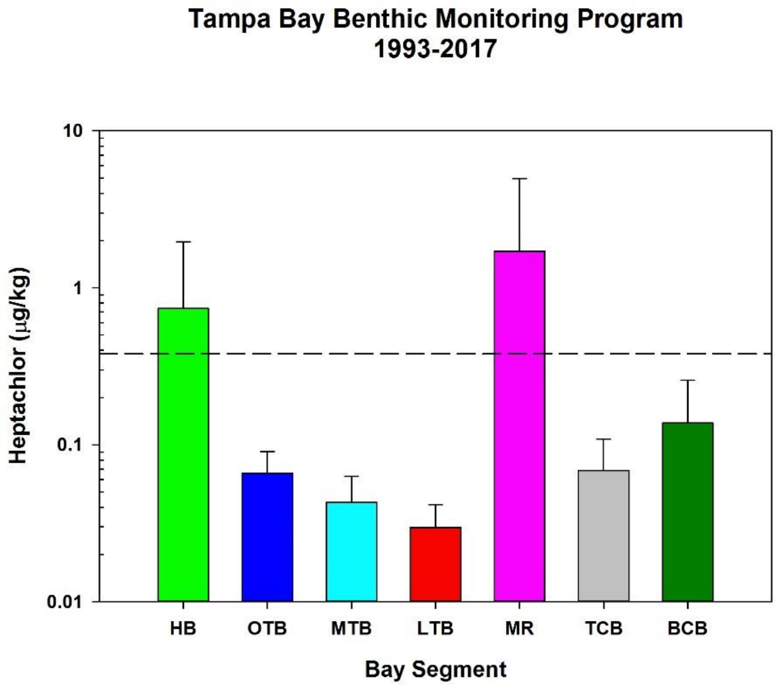

Figure 126. Mean sediment heptachlor concentrations by bay segment. Error bars = 95% confidence interval, dashed line represents bay-wide mean.

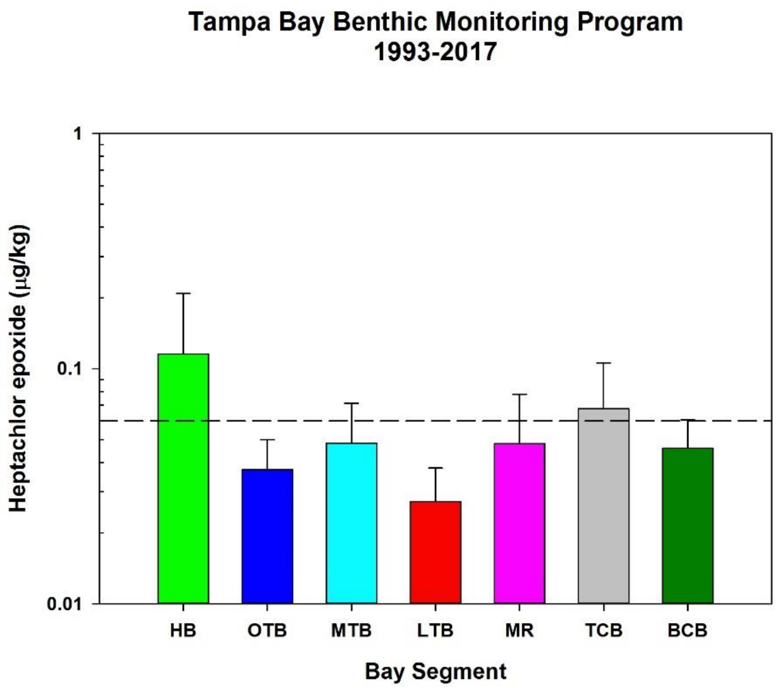

Figure 127. Mean sediment heptachlor epoxide concentrations by bay segment. Error bars = 95% confidence interval, dashed line represents bay-wide mean.

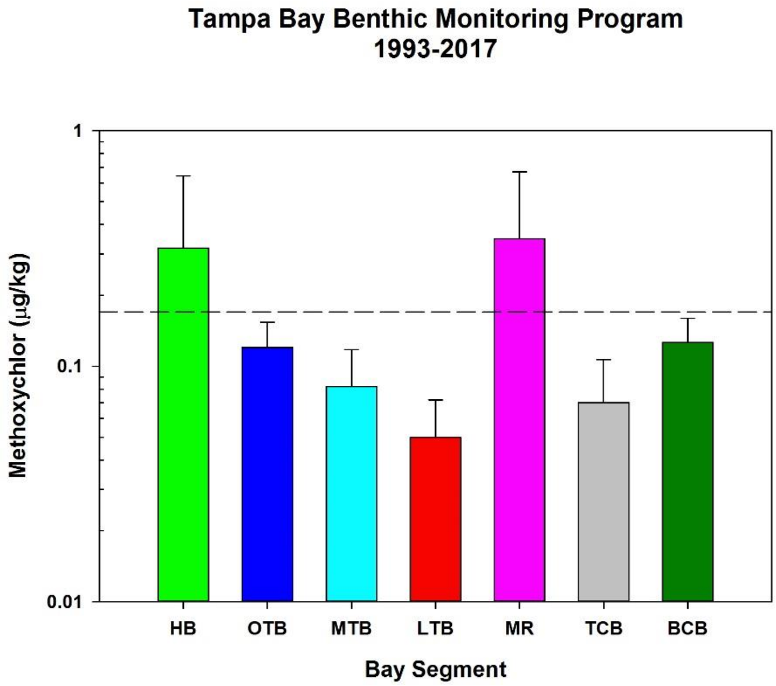

Figure 128. Mean sediment methoxychlor concentrations by bay segment. Error bars = 95% confidence interval, dashed line represents bay-wide mean.

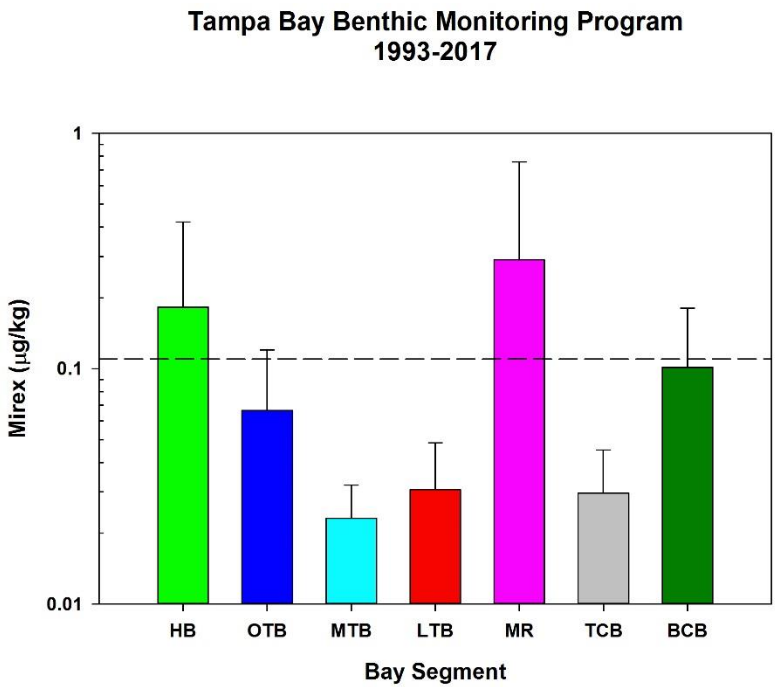

Figure 129. Mean sediment mirex concentrations by bay segment. Error bars = 95% confidence interval, dashed line represents bay-wide mean.

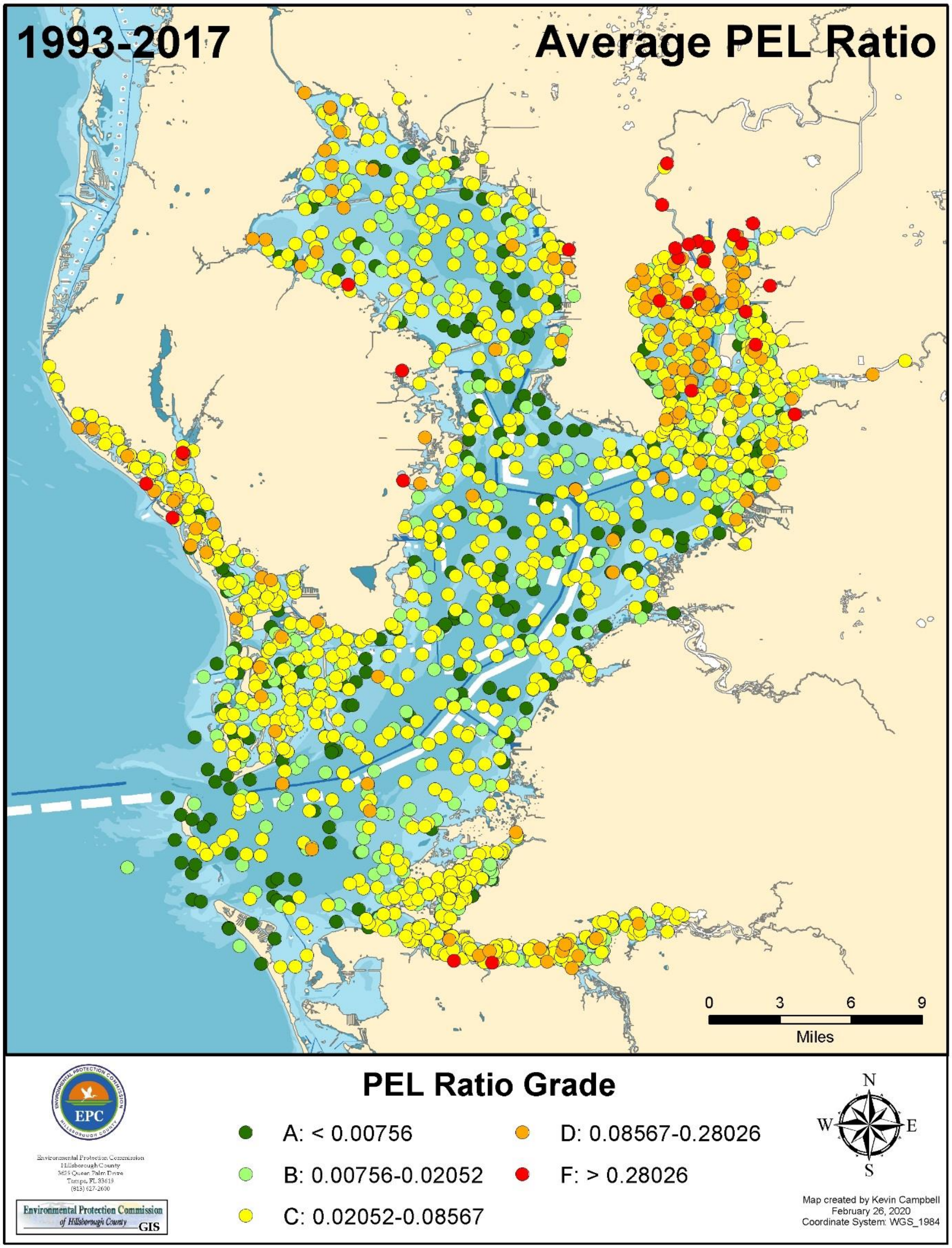

Figure 130. Distribution of Mean PEL ratio Grades 1993-2017.

Benthic Community Structure

Summary Statistics

Table 15 presents the median, minimum, and maximum recorded values for benthic species richness (*S*), abundance (*N*), the Shannon Diversity Index *(H')*, and the Tampa Bay Benthic Index (TBBI) by year. The same summary statistics are presented for each bay segment in Table 16.

The overall median number of taxa per sample was 36, and ranged from 0 to 176 (Tables 15 &16). The highest median number of taxa was found in 2017 (60 taxa), followed by 2016 and 2014 each with a median of 51 taxa. The lowest median numbers of taxa were in 2010 and 2003 (24 and 27 taxa respectively) (Table 15; Figure 131). There was an overall increasing trend in species richness over the monitoring period, with every year since 2012 exceeding the 25-year mean (Figure 131). Species richness trends also appeared to follow similar trends in water quality as indicated by the Tampa Bay Water Quality Index (Figure 131).

There was a general trend of increasing species richness moving towards the lower bay, with the highest number of taxa being recorded in Lower Tampa Bay and Boca Ciega Bay (Table 16; Figure 132). Middle Tampa Bay and Terra Ceia Bay also had relatively high species richness, while fewer taxa were recorded in Hillsborough Bay and the Manatee River (Table 16; Figure 132).

The abundance of benthic organisms ranged from 0 to 183,400 organisms/m^2 , with a median of 6,325 organisms/m^2 (Tables 15 & 16). Abundances were variable between sampling years (Figure 133). Highest abundances were observed in 2017, 2016 and 2014, with an increasing observed over time with every year since 2012 above the 25-year mean (Table 15; Figure 133). Middle Tampa Bay had the highest abundances, while the lowest abundances were in Terra Ceia Bay (Table 16; Figure 134).

The median Shannon Diversity Index was 2.54, and ranged from 0 to 3.97 (Tables 15 & 16). Bay-wide diversity was highest in 2008, and was also above the 25-year mean from 2014-2017 (Figure 135). The diversity increased towards the lower bay (Figure 136), and was highest in Boca Ciega Bay, Terra Ceia Bay, and Lower Tampa Bay, and lowest in Hillsborough Bay (Table 16; Figure 136).

The Tampa Bay Benthic Index (TBBI) had an overall median value of 84.67, which falls within the "Intermediate" category for benthic habitat health (Tables 15 & 16). Yearly mean values tended to fall in the "Intermediate" range with an increasing trend over time, and notably since 2012 (Figure 137). The highest median TBBI score was in 2017 (89.94) and all years from 2013-2017 had TBBI scores above the "Healthy" threshold value of 87 (Table 15). Over the 25-year monitoring period, Lower Tampa Bay and Middle Tampa Bay had median TBBI scores in the "Healthy" range, while Old Tampa Bay had a median TBBI just below 87 (Table 16). There was a spatial trend of increasing TBBI values towards the lower bay segments, with the highest mean TBBI values in Lower Tampa Bay and lowest values in Hillsborough Bay (Figure 138). The areal extents of benthic habitat categories, based on the TBBI averaged over five-year periods and the 25-year monitoring period, are shown in Figure 139. Areas of more “Degraded” benthic habitat were often in portions of Hillsborough Bay, the north and western portions of Old Tampa Bay, as well as the upper portions of the Manatee River (Figure 139). An increase in the extent of “Healthy” benthic habitat is apparent over time, most notably in Middle Tampa Bay and Lower Tampa Bay (Figure 139). Bay-wide, just over 20% of the samples were classified as “Empty” or “Degraded” (1.01% and 19.71% respectively), and just over 40% were classified as “Healthy” (Table 17). Hillsborough Bay had the highest number of empty samples (4.42%), and 30.2% of the sites were classified as “Degraded” (Table 17). The Manatee River had a large percentage of “Degraded” sites (29%), and the highest percentage of “Undefined” samples possibly due to a high number of low salinity sites (Table 17). Over 50% of the sites in Lower Tampa Bay and Middle Tampa Bay, and 47.5% of Old Tampa Bay sites, were classified as “Healthy” (Table 17).

The National Estuary Program Coastal Condition Report, published in 2007, included an evaluation of the estuarine condition in Tampa Bay based on samples collected by the National Coastal Assessment (NCA) monitoring program (USEPA 2007). The NCA collected sediment samples in July 2000 from 25 sites throughout Tampa Bay. These samples were analyzed for benthic invertebrate community structure, and the condition of the benthic community was evaluated at each site using the Gulf Coast Benthic Index (GCBI) developed for the Louisianan Provence EMAP program (Engle et al., 1994; Engle and Summers 1999). The condition of the benthic community at each station was rated as “Good” if the GCBI score was ≥ 5.0, “Fair” if the GCBI score was between 3.0 and 5.0, and “Poor” if the GCBI score was < 3.0 (USEPA 2007). The overall benthic community condition for the estuary was rated based on the following criteria: “Good” if < 10% of the sites had a poor benthic index score and >50% had a good benthic index score; “Fair” if 10% to 20% of the sites had a poor benthic index score or >50% of the sites had a combined poor and fair benthic index score; and “Poor” if >20% of the sites had a poor benthic index score. The overall benthic community condition for Tampa Bay based on these criteria was rated as “Poor”, with 36% of the NCA sites having poor benthic index scores, 20% rated as “Fair”, and 44% as “Good” (USEPA, 2007).

The benthic community condition of the bay-wide monitoring samples was evaluated applying the same criteria for “Good”, “Fair”, and “Poor” as outlined in the Coastal Condition Report (USEPA 2007), but utilizing the Tampa Bay Benthic Index and its scoring criteria for the individual samples. Results from this analysis are presented in Tables 18 &19 by year and bay segment. The bay-wide benthic condition was calculated two ways: initially by evaluating all of the samples equally, and then by proportionally weighing the samples based on their bay segment area in order to compensate for differing sampling densities in the different bay segments. Table 18 shows the bay-wide condition for each bay segment by year, Table 19 reflects the combination of the Manatee River and Terra Ceia Bay into a single reporting unit starting in 2000, and the combination of Middle Tampa Bay and Lower Tampa Bay as a single reporting unit in 2005.

Overall bay-wide results were consistent with the NCA rating of “Poor” for 12 of the 25 years monitoring period (48%), with 10 years (40%) rating as “Fair” and the last three years (2015-2017) rating as “Good” (Table 18). Weighing the samples proportionally by their segment area dropped the number of "Poor" years to 6 (24%), increased the number of "Fair" years to 14 (56%), and increased "Good" ratings to 5 years (20%), including 2015-2017 (Tables 18&19).

Hillsborough Bay, Terra Ceia Bay, the Manatee River, and Boca Ciega Bay generally had "Poor" to "Fair" benthic community conditions for most years (Tables 18 & 19). Terra Ceia Bay had "Good" conditions in 2004 and 2013-2016 (Table 18). Old Tampa Bay, Middle Tampa Bay, and Lower Tampa Bay generally had "Fair" or "Good" benthic community conditions (Tables 18 & 19).

Table 15. Benthic Community Summary Statistics 1993-2017 by Year.

Year	n	Number of taxa		Number per m^2		Diversity (H')		TBBI*		GoM AMBI		TB AMBI	
1993	**91**	39		7975		2.66		79.71		1.8		8.7	
		5	89	250	45500	0.66	3.53	0.34	95.22	0.6	3.1	3.6	10
1994	**90**	33		5863		2.53		75.67		1.7		8.7	
		0	75	0	27800	0.00	3.41	0.00	95.83	0.5	7	0	10
1995	**134**	33		5525		2.49		85.86		1.7		8.6	
		0	99	0	183400	0.00	3.93	0.00	98.19	0.2	7	0	10
1996	**132**	36		7250		2.42		87.42		1.6		8.6	
		0	73	0	91575	0.00	3.62	0.00	97.85	0.8	7	0	10
1997	**123**	41		7175		2.55		85.04		1.8		8.6	
		0	93	0	49450	0.00	3.70	0.00	98.37	0.6	7	0	10
1998	**120**	30		3264		2.55		82.28		1.8		8.4	
		0	89	0	44575	0.00	3.57	0.00	98.28	0.8	7	0	10
1999	**124**	36		6450		2.47		84.43		1.8		8.6	
		0	121	0	54175	0.00	3.79	0.00	100.53	0	7	0	10
2000	**86**	37		7663		2.64		86.02		1.7		8.8	
		2	87	50	43925	0.69	3.61	21.12	95.49	0.4	4.5	3.6	10
2001	**80**	31		3750		2.53		82.63		1.8		8.4	
		0	88	0	21675	0.00	3.61	0.00	94.98	1	7	0	9.9
2002	**83**	38		5850		2.54		84.85		1.9		8.6	
		0	125	0	97075	0.00	3.63	0.00	97.6	0.7	7	0	10
2003	**78**	27		4113		2.40		80.74		2		7.9	
		0	86	0	50376	0.00	3.58	0.00	96.62	0.6	7	0	10
2004	**77**	36		8725		2.33		87.34		1.8		8.4	
		2	101	50	61125	0.51	3.48	46.73	97.27	0.7	4.5	2.6	9.7
2005	**35**	37		10650		2.38		87.41		1.6		8.3	
		1	113	25	51052	0.00	3.98	60.54	98.63	1	3.8	5.1	9.7
2006	**41**	45		7901		2.68		83.52		1.8		8.4	
		5	119	200	70251	1.36	3.63	51.42	96.29	1.2	3.6	3.6	9.7

Year	n	Number of taxa		Number per m^2		Diversity (H')		TBBI*		GoM AMBI		TB AMBI	
2007	**43**	40		5250		2.67		83.85		1.8		8.1	
		1	84	25	46101	0.00	3.56	28.99	94.97	0.3	6	3.6	9.9
2008	**44**	45		7800		2.87		84.82		1.8		8.3	
		4	106	175	36725	1.05	3.76	14	99.76	0.9	4.9	4.1	9.7
2009	**44**	37		5188		2.73		85.86		1.7		8.4	
		0	113	0	45200	0.00	3.72	0.00	98.6	0.7	7	0	9.9
2010	**59**	24		2600		2.55		80.37		1.8		7.9	
		0	136	0	46606	0.00	3.59	0.00	103.79	1.1	7	0	10
2011	**44**	34		2975		2.66		78.27		1.8		8.1	
		0	80	0	18801	0.00	3.76	0.00	91.69	1	7	0	9.3
2012	**44**	34		4050		2.74		86.1		1.8		7.9	
		0	136	0	46451	0.00	3.74	0.00	100.3	0.8	7	0	9.6
2013	**43**	48		9677		2.64		89.81		1.6		8.6	
		0	113	0	38201	0.00	3.79	0.00	99.75	0	7	0	9.7
2014	**44**	51.5		14363.5		2.56		89.705		1.6		8.4	
		5	176	150	41286	1.12	3.89	33.41	104.94	0.8	3.4	4.1	9.7
2015	**44**	39.5		8950		2.50		88.29		1.8		8.6	
		12	121	650	64653	1.56	3.84	63.94	100.5	0.9	2.8	5.7	9.7
2016	**44**	51.5		13600		2.62		88.94		1.7		8.3	
		3	142	100	73552	1.04	3.77	68.30	100.92	0.6	2.6	4.7	9.6
2017	**44**	60		18475.5		2.78		89.935		1.7		8.5	
		0	125	0	122625	0.00	3.90	0.00	98.54	0.9	7	0	9.6
Cumulative	**1791**	**36**		**6325**		**2.54**		**84.67**		**1.8**		**8.4**	
1993-2017		**0**	**176**	**0**	**183425**	**0.00**	**3.97**	**0.00**	**104.94**	**0**	**7**	**0**	**10**

* Negative ("Undefined") TBBI scores omitted.
TBBI: Dark Green = "Healthy"; Yellow = "Intermediate"
GoM AMBI & Adj TB_AMBI: Green = "Unpolluted"; Light Green = "Slightly Polluted"

Table 16. Benthic Community Summary Statistics 1993 - 2017 by Bay Segment.

Segment	n	Number of taxa		Number per m^2		Diversity (H')		TBBI*		GoM AMBI		Adj TB_AMBI	
Hillsborough Bay	**407**	27		5550		2.20		79.62		2		7.3	
		0	87	0	122625	0.00	3.64	0.00	97.27	0	7	0	10
Old Tampa Bay	**269**	35		7676		2.46		86.57		1.7		8.4	
		0	86	0	183425	0.00	3.57	0.00	99.89	0.6	7	0	10
Middle Tampa Bay	**303**	39		8000		2.58		87.88		1.6		9.0	
		0	129	0	102026	0.00	3.84	0.00	100.30	0.2	7	0	10
Lower Tampa Bay	**221**	47		6900		2.92		88.45		1.6		9.3	
		2	176	50	73552	0.68	3.97	38.48	104.94	0.4	2.3	6.9	10
Manatee River	**193**	26		5000		2.32		79.86		1.9		8.1	
		1	117	51	91575	0.00	3.53	8.53	100.92	1.1	4.5	1.4	10
Terra Ceia Bay	**110**	40.5		4887.5		2.91		82.33		1.7		8.4	
		1	97	25	38201	0.00	3.87	27.92	97.85	0.3	6	3.6	10
Boca Ciega Bay	**288**	45		5250		3.03		83.22		1.8		8.6	
		0	135	0	61450	0.00	3.90	0.00	103.77	0	7	0	10
Tampa Bay	**1791**	**36**		**6325**		**2.54**		**84.67**		**1.8**		**8.4**	
		0	**176**	**0**	**183425**	**0.00**	**3.97**	**0**	**104.94**	**0**	**7**	**0**	**10**

* Negative ("Undefined") TBBI scores omitted.
TBBI: Dark Green = "Healthy"; Yellow = "Intermediate"
GoM AMBI & Adj TB_AMBI: Green = "Unpolluted"; Light Green = "Slightly Polluted"

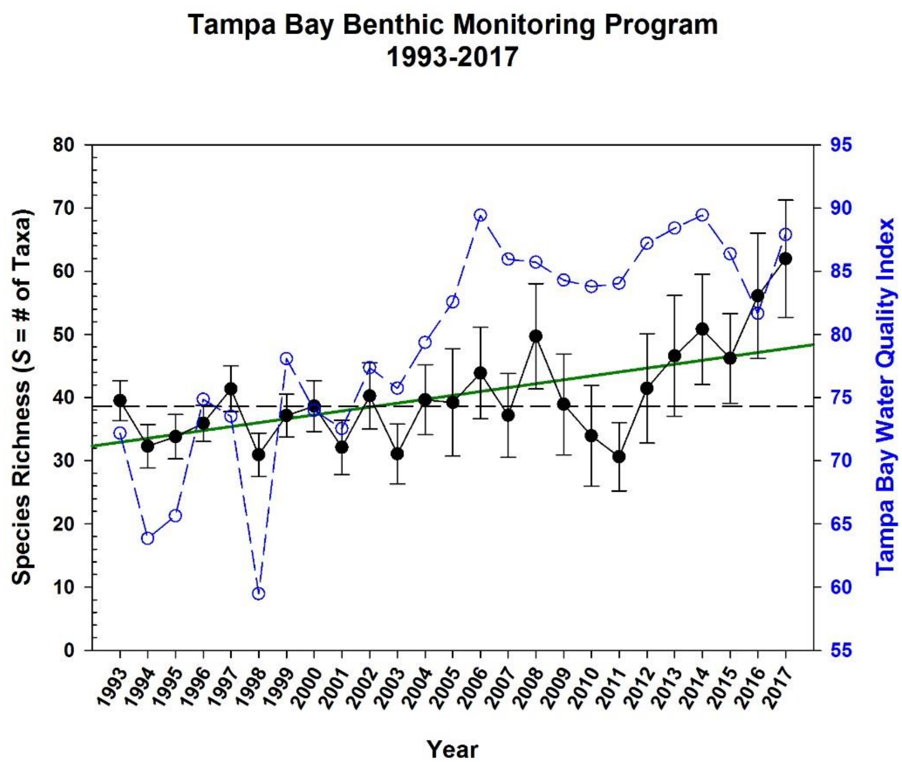

Figure 131. Mean number of benthic taxa by year (black) and Tampa Bay Water Quality Index (blue). Error bars = 95% confidence interval, dashed line represents bay-wide mean.

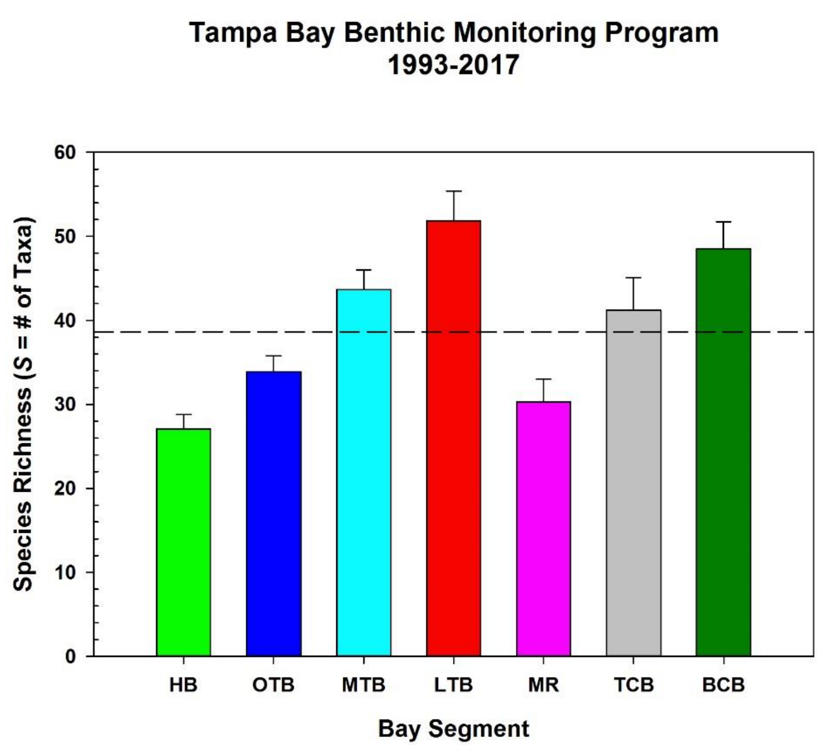

Figure 132. Mean number of benthic taxa by bay segment. Error bars = 95% confidence interval, dashed line represents bay-wide mean.

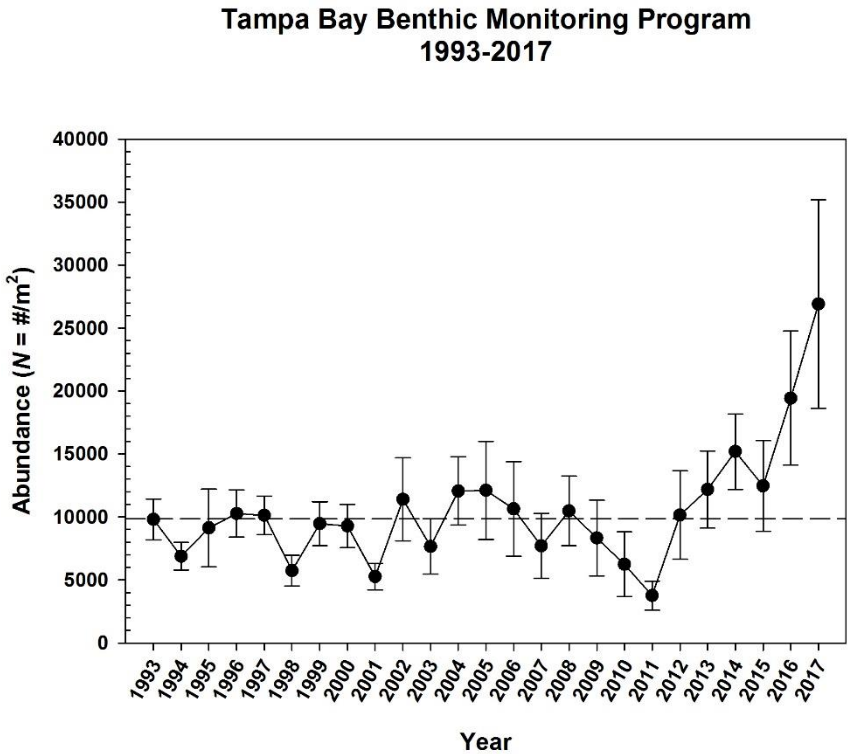

Figure 133. Mean benthic abundance by year. Error bars = 95% confidence interval, dashed line represents bay-wide mean.

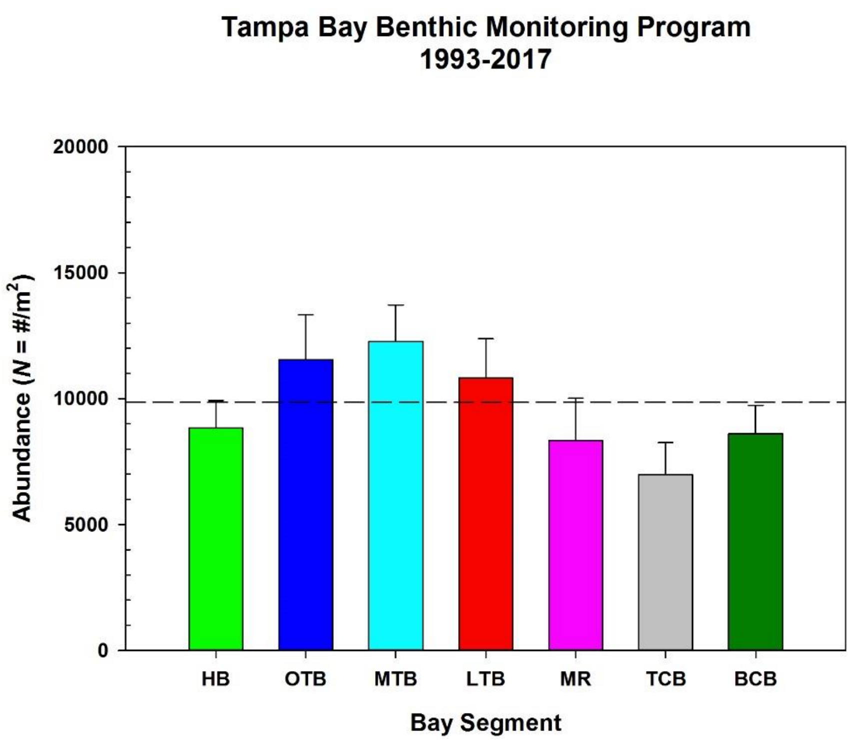

Figure 134. Mean benthic abundance by bay segment. Error bars = 95% confidence interval, dashed line represents bay-wide mean.

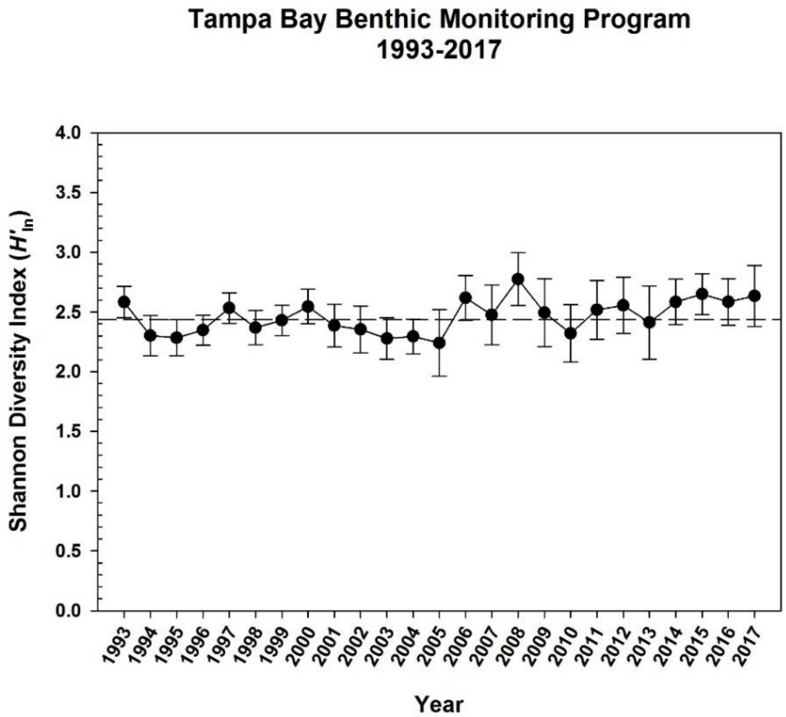

Figure 135. Mean Shannon-Wiener Diversity Index ($\log_e$) by year. Error bars = 95% confidence interval, dashed line represents bay-wide mean.

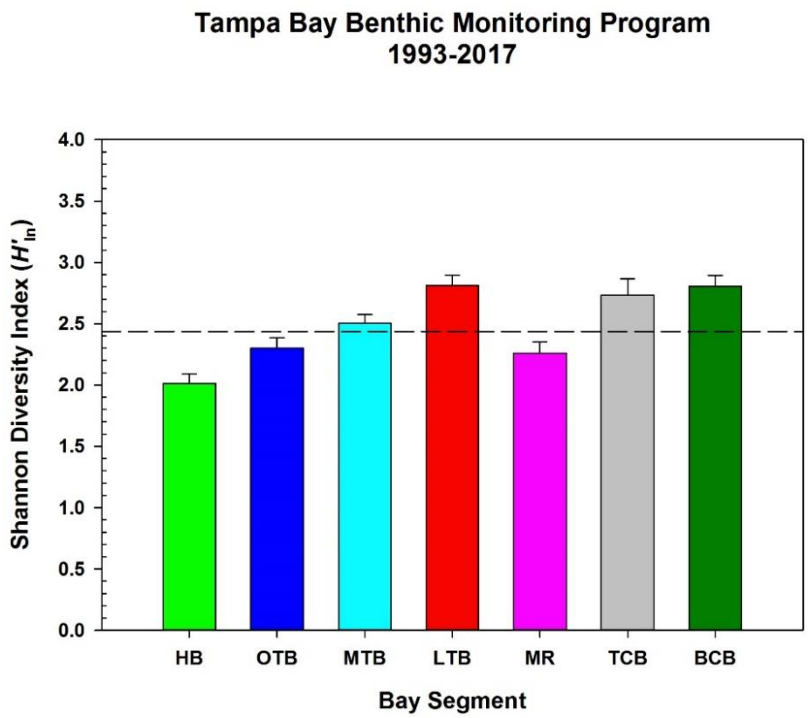

Figure 136. Mean Shannon-Wiener Diversity Index ($\log_e$) by bay segment. Error bars = 95% confidence interval, dashed line represents bay-wide mean.

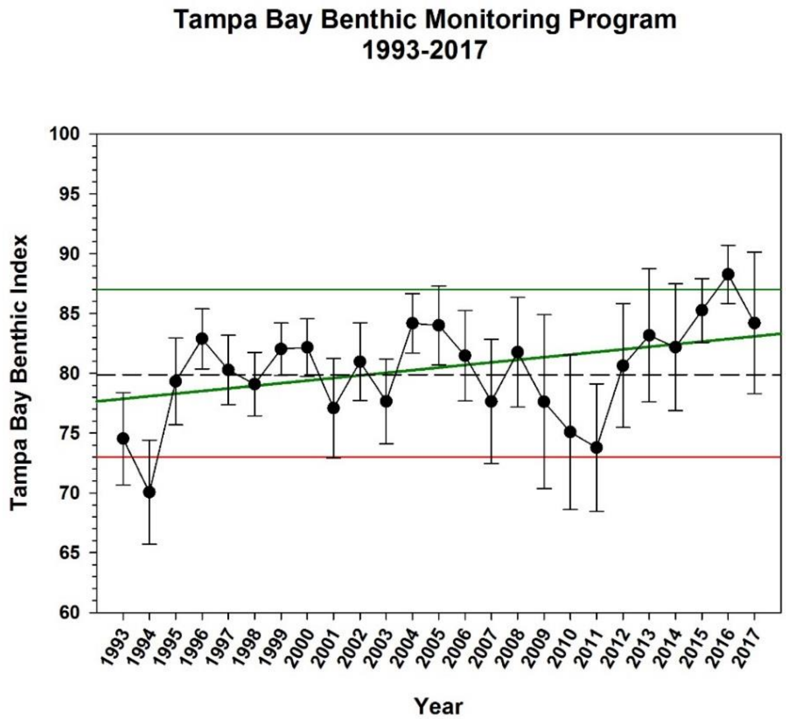

Figure 137. Mean Tampa Bay Benthic Index by year. Error bars = 95% confidence interval, dashed line represents bay-wide mean, solid lines indicate cutoffs for "Degraded" (<73; red) and "Healthy" (>87; green) benthic habitats.

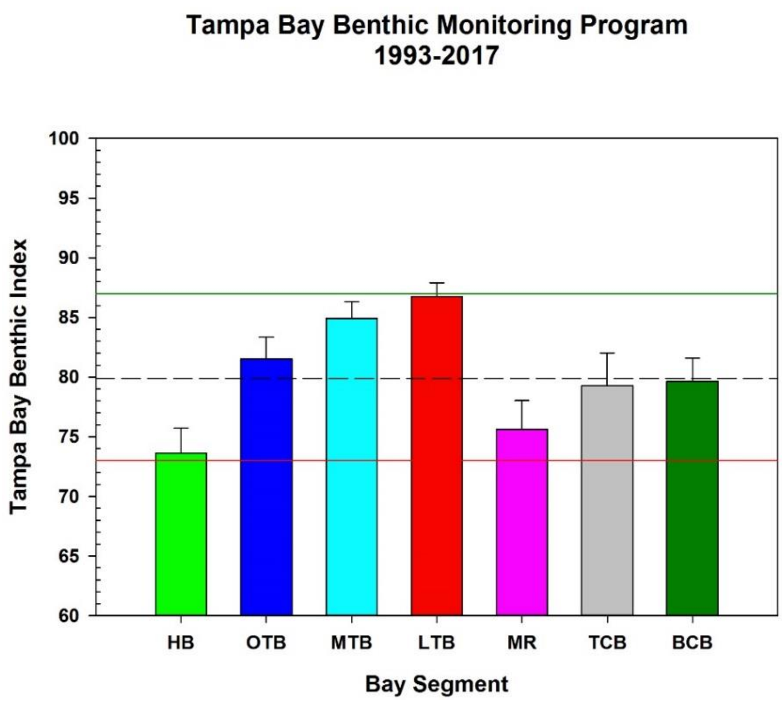

Figure 138. Mean Tampa Bay Benthic Index by bay segment. Error bars = 95% confidence interval, dashed line represents bay-wide mean, solid lines indicate cutoffs for "Degraded" (<73; red) and "Healthy" (>87; green) benthic habitats.

Table 17. Percentage of sites within TBBI categories by bay segment and bay-wide 1993-2017.

Segment	n	Undefined	Empty	Degraded	Intermediate	Healthy
Hillsborough Bay	407	0.25%	4.42%	30.22%	38.57%	26.54%
Old Tampa Bay	269	0.00%	1.49%	16.73%	34.20%	47.58%
Middle Tampa Bay	303	0.33%	0.00%	9.24%	35.97%	54.46%
Lower Tampa Bay	221	0.00%	0.00%	5.43%	35.75%	58.82%
Manatee River	193	3.63%	0.00%	29.02%	41.97%	25.39%
Terra Ceia Bay	110	0.91%	0.00%	21.82%	43.64%	33.64%
Boca Ciega Bay	288	0.35%	1.39%	19.79%	43.40%	35.07%
Tampa Bay (Total)	**1791**	**0.61%**	**1.01%**	**19.71%**	**38.58%**	**40.09%**

Table 18. Condition of Tampa Bay benthic communities 1993-2017 based on the TBBI using the EPA's National Coastal Assessment program criteria by year and segment.

Year	HB	OTB	MTB	LTB	TCB	MR	BCB	Bay-wide	Bay-wide Weighted*
1993	Poor	Poor	Fair	Poor	Fair	Fair		Poor	Poor
1994	Poor	Poor	Poor	Fair	Poor	Poor		Poor	Poor
1995	Poor	Good	Good	Good	Poor	Fair	Fair	Fair	Good
1996	Poor	Good	Fair	Good	Fair/Good	Fair	Fair	Fair	Fair
1997	Poor	Fair/Good	Good	Good	Fair/Good	Poor	Poor	Fair	Fair
1998	Poor	Fair	Fair	Good	Fair	Poor	Poor	Poor	Fair
1999	Fair	Fair	Good	Fair	Poor	Fair	Fair	Fair	Fair
2000	Poor	Good	Fair	Fair	Fair	Poor	Fair	Fair	Fair
2001	Poor	Poor	Fair/Good*	Good	Poor	Fair	Poor	Poor	Fair
2002	Poor	Fair	Good	Fair	Poor	Poor	Poor	Poor	Fair
2003	Poor	Poor	Good	Good	Poor	Poor	Poor	Poor	Poor
2004	Fair	Poor	Good	Good	Good	Poor	Fair	Fair	Fair
2005	Poor	Good	Good	Good	Fair	Fair	Fair/Good	Fair	Good
2006	Poor	Good	Good	Fair	Fair	Poor	Poor	Poor	Fair
2007	Poor	Good	Good	Fair	Poor	Poor	Fair	Poor	Fair
2008	Poor	Fair	Good	Good	Poor	Fair	Fair	Fair	Fair
2009	Fair	Fair	Good	Fair/Good*	Poor	Fair	Poor	Fair	Fair
2010	Fair	Poor	Poor	Good	Fair/Good	Fair	Good	Fair	Poor
2011	Poor	Poor	Fair	Poor	Fair	Poor	Fair	Poor	Poor
2012	Poor	Good	Good	Poor	Poor	Poor	Fair	Poor	Fair
2013	Poor	Fair	Good	Good	Good	Poor	Fair	Poor	Fair
2014	Poor	Poor	Good	Good	Good	Poor	Poor	Poor	Poor
2015	Poor	Fair	Good	Good	Good	Fair	Fair	Good	Good
2016	Good	Poor	Good	Good	Good	Fair	Good	Good	Good
2017	Fair	Fair	Good	Good	Fair	Good	Fair	Good	Good

*Weighted by Bay Segment Area

Table 19. Condition of Tampa Bay benthic communities 1993-2017 based on the TBBI using the EPA's National Coastal Assessment program criteria by year and combined segments.

Year	HB	OTB	MTB	LTB	MTB/LTB	BCB	TCB	MR	TCB/MR	Bay-wide	Bay-wide Weighted*
1993	Poor	Poor	Fair	Poor			Fair	Fair		Poor	Poor
1994	Poor	Poor	Poor	Fair			Poor	Poor		Poor	Poor
1995	Poor	Good	Good	Good		Fair	Poor	Fair		Fair	Good
1996	Poor	Good	Fair	Good		Fair	Fair/Good	Fair		Fair	Fair
1997	Poor	Fair/Good	Good	Good		Poor	Fair/Good	Poor		Fair	Fair
1998	Poor	Fair	Fair	Good		Poor	Fair	Poor		Poor	Fair
1999	Fair	Fair	Good	Fair		Fair	Poor	Fair		Fair	Fair
2000	Poor	Good	Fair	Fair		Fair			Poor	Fair	Fair
2001	Poor	Poor	Fair/Good	Good		Poor			Poor	Poor	Fair
2002	Poor	Fair	Good	Fair		Poor			Poor	Poor	Fair
2003	Poor	Poor	Good	Good		Poor			Poor	Poor	Poor
2004	Fair	Poor	Good	Good		Fair			Poor	Fair	Fair
2005	Poor	Good			Good	Fair/Good			Fair	Fair	Good
2006	Poor	Good			Good	Poor			Poor	Poor	Fair
2007	Poor	Good			Fair/Good	Fair			Poor	Poor	Fair
2008	Poor	Fair			Good	Fair			Poor	Fair	Fair
2009	Fair	Fair			Good	Poor			Poor	Fair	Fair
2010	Fair	Poor			Poor	Good			Fair	Fair	Poor
2011	Poor	Poor			Fair	Fair			Poor	Poor	Poor
2012	Poor	Good			Fair	Fair			Poor	Poor	Fair
2013	Poor	Fair			Good	Fair			Poor	Poor	Fair
2014	Poor	Poor			Good	Poor			Poor	Poor	Poor
2015	Poor	Fair			Good	Fair			Fair	Good	Good
2016	Good	Poor			Good	Good			Fair	Good	Good
2017	Fair	Fair			Good	Fair			Fair	Good	Good

*Weighted by Bay Segment Area

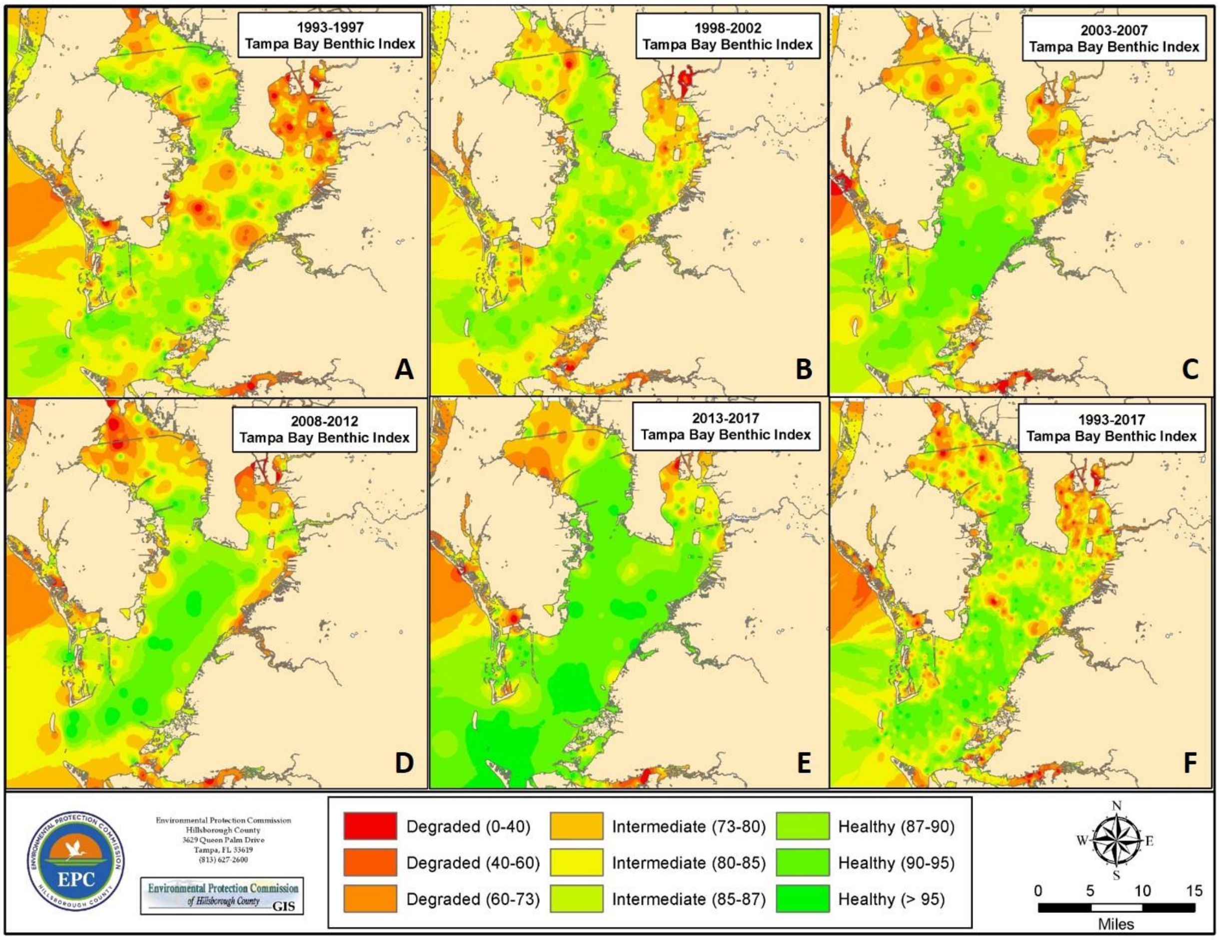

Figure 139. Distribution of Tampa Bay Benthic Index condition 1993-2017 by 5-year periods (A-E) and 25-year composite data (F).

Dominant Taxa

The relative abundance of dominant benthic taxa is presented by sampling year in Table 20, and by Bay Segment in Table 21. Table 21 also summarizes the bay-wide dominant taxa listing the rank order of the top 10 taxa based on relative abundance. The top ten ranked taxa represented over 32% of the total bay-wide abundance, while the top 25 taxa accounted for 50% of the total cumulative abundance.

Branchiostoma floridae Hubbs, 1922

The most abundant species in Tampa Bay was the cephalochordate *Branchiostoma floridae* which accounted for 5.29% of the overall abundance (Table 21) and was present in 40.54% of the samples. The overall mean abundance was $522/m^2$, with a maximum density of $17{,}875/m^2$. The maximum density is higher than reported in previous studies [($1200/m^2$); Stokes, 1996]. It was among the dominant taxa in most years except for 2003, 2005, and 2009-2012. *B. floridae* was the most abundant taxa in 1993, 1997,1998, and 2015 (Table 20). There was a trend of decreasing abundance through 2011, but has increased since 2012. Mean abundances exceeded the 25-year mean from 2013-2017 (Figure 140). *B. floridae* was the most abundant species in Lower Tampa Bay, and among the most dominant taxa in Old Tampa Bay and Middle Tampa Bay (Table 21; Figure 141). Highest densities were seen in Middle Tampa Bay and Lower Tampa Bay (Figures 141 & 142). Similarity percentage analysis (SIMPER), based on salinity, dissolved oxygen, and sediment type indicate that *B. floridae* is found primarily in polyhaline and euhaline salinities, normoxic conditions, and medium to coarse sediments (Tables 30-33). The preference for higher salinities was also shown by Dawson (1965), where a sudden drop in from heavy rainfall resulted in a mass die off. Stokes (1996) evaluated the larval recruitment and post-settlement growth of *B. floridae* in Tampa Bay focusing on a sampling site near the Courtney Campbell Causeway in Old Tampa Bay. Stokes found that reproduction occurred from May to September, with larval settlement from late-May to mid-October. Several earlier studies reported this species as *Branchiostoma caribaeum* (Dawson, 1965; Pierce, 1965; Nelson, 1969; Bloom et al., 1972; Hall and Saloman, 1975).

Glottidia pyramidata (Stimpson, 1860)

The brachiopod *Glottidia pyramidata* was the second most abundant infaunal organism bay-wide, accounting for 4.23% of the total abundance (Table 21). It was found in 30.60% of the samples, with an average density of $417/m^2$ and maximum density of $94{,}375/m^2$. The average density is lower than previously reported by Culter (1979), who found an average of $2{,}275/m^2$ in Old Tampa Bay near the Courtney Campbell Causeway. The relative abundance of *G. pyramidata* was variable over time (Figure 143). It was the most abundant organism in 2001, 2002, and 2005; the second most abundant in 2006 and 2009 (Table 20). The peak abundance was in 2002, when it accounted for 39.5% of the total benthic abundance (Table 20; Figure 143). However, mean abundances have been below the 25-year mean for most years since 2007 (Figure 143). *G. pyramidata* was most abundant in Middle Tampa Bay accounting for nearly 12% of the benthic abundance, and was also among the dominant taxa in Hillsborough Bay and Old Tampa Bay (Table 21; Figures 144 & 145). The SIMPER analysis showed that *G. pyramidata* was found at relatively deeper sites (>2 meters) with fine to medium grained sediments, polyhaline salinities, and normoxic bottom dissolved oxygen levels (Tables 30-33). These findings support previous life-history studies. Paine (1963) studying populations of *G. pyramidata* on the west coast of Florida, found that this species inhabited salinities ranging from 18 – 35 psu, and could tolerate salinities as low 13 psu. Paine also noted that *G. pyramidata* was absent from mud or clay bottoms and from calcareous sediments, preferring sandy habitats. Culter (1979) further showed that *G. pyramidata* cannot burrow in coarse sediments, and that burrowing is inhibited in muddy substrates. Both Paine (1963) and Culter (1979) reported that spawning and recruitment occurred over the summer months. Culter (1979) found that highest densities occurred in August, which corresponds to the time our samples were collected. Culter and Simon (1987) found that a small percentage of *G. pyramidata* in Tampa Bay (< 1%) were hermaphroditic, particularly in areas of low population density.

Kirkegaardia sp. [= *Monticellina cf. dorsobranchialis* (Kirkegaard, 1959)]

The third most abundant species was the cirratulid polychaete *Kirkegaardia* sp. (formerly designated as *Monticellina cf. dorsobranchialis*), representing 3.92% of the total benthic abundance (Table 21). It was the third most frequently occurring taxon, being present in 46.57% of the samples. The average density of *Kirkegaardia sp.* was 387/m^2, with a maximum of 43,250/m^2. It was among the most abundant taxa during all years except for 1995 and 2016 (Table 20). Highest relative abundances occurred in 1994, 1999, 2011, and 2014 (Table 20). The bay-wide annual abundances showed a cyclical pattern, but were consistent throughout the 25-year monitoring period (Figure 146). It was the most abundant taxon in Terra Ceia Bay, and ranked second in Hillsborough Bay and the Manatee River (Table 21). Highest abundances of *Kirkegaardia sp.* were found in Hillsborough Bay and the Manatee River, as well as in Middle Tampa Bay, Terra Ceia Bay, and Boca Ciega Bay (Figures 147 & 148). The SIMPER analysis for the different physical parameters found *Kirkegaardia* sp. occurred at shallow subtidal to deep sites with very fine to medium grained sediments, high mesohaline to euhaline salinities, and dissolved oxygen concentrations ranging from anoxic to normoxic (Tables 30-33). *Kirkegaardia sp.* also appears to be tolerant to sediment contaminants and was found at sites exceeding the PEL for lindane and cadmium, as well as sites above the TEL for several other pesticides (DDTs, dieldrin, lindane), most PAHs, and several trace metals (Karlen et al., 2015).

This polychaete was initially identified as *Tharyx annulosus* during the first year of the program, based on the taxonomic key in Wolf, 1984 and is probably the same as *Tharyx* sp. C of Taylor, 1971 and Hall and Saloman, 1975. Blake (1991) revised the genus *Tharyx* and reinstated the genus *Monticellina* placing several species in this new taxon based on the presence of serrated chaetae. He further synonymized *T. annulosus* with *T. dorsobranchialis* under the new taxon *Monticellina dorsobranchialis*. Blake (1996) further revised this genus, describing several new species from California and mentioned that future revisions were needed. Specifically, Blake mentioned that several taxa he initially synonymized as *Monticellina dorsobranchialis* (including *M. annulosus*) in his 1991 paper were to be reinstated as separate species (Blake 1996). Blake later established the new genus *Kirkegaardia* (Blake, 2016) replacing the genus *Monticellina* because that name was already in use as a genus of turbellarian flatworms. Due to the current revisions of this genus, the identity of the *Kirkegaardia* specimens from Tampa Bay is still uncertain, therefore we are leaving the identification at the genus level as *Kirkegaardia* sp.

***Mysella planulata* (Stimpson, 1851)**

The small bivalve *Mysella planulata* ranked fourth in abundance bay-wide, and was the most abundant species in 1996, 2008, 2009, and 2017; and the second ranked taxa in 1997 and 1998 (Tables 20 & 21). Population trends showed a cyclic pattern over the 25-year monitoring period. Abundance was high in 1996, 2005, and 2008, and the lowest abundance in 2011; maximum mean abundance was in 2017 (Figure 149). *M. planulata* was mainly found in Hillsborough Bay and Old Tampa Bay, where it ranked first and fourth in abundance respectively (Table 21; Figures 150 & 151). SIMPER results indicate that *M. planulata* has a wide depth distribution (intertidal to deep subtidal), was found in fine to medium sediments, high mesohaline to polyhaline salinities, and intermediate to normoxic dissolved oxygen conditions. It was also found at sites that exceeded the PEL for copper and the TEL for cadmium (Karlen et al 2015). *Mysella planulata* is a self-fertilizing hermaphrodite and has larviparous development, where the larvae are brooded within the adult shell during the early larval stages then released into the plankton (Franz 1973).

Naididae

Unidentified oligochaetes in the family Naididae (formerly classified as Tubificinae) ranked fifth overall in relative abundance making up 3.43% of the total abundance (Table 21), with a mean abundance of $338/m^2$ and a maximum of $13,375/m^2$. Naidid oligochaetes were common across all years and bay segments (Tables 20 & 21). They were also the most frequently occurring taxa, found in 62.31% of the samples. This group was composed of immature and/or damaged specimens of multiple species, which could not be identified below the family level. The annual mean abundance trends and mean abundance by bay segment are presented in Figures 152 and 153. Unidentified Naididae were abundant and widespread across all bay segments, but showed lower abundances in the Manatee River and were highest in Boca Ciega Bay (Table 21; Figures 152 & 153). Naididae were among the dominant taxa across all depth and salinity categories. They were abundant in hypoxic to normoxic conditions, and in very fine to medium sediments; they were widely tolerant of sediment contaminants (Karlen et al., 2015).

***Ampelisca holmesi* Pearse, 1908** and ***Ampelisca abdita* Mills, 1964**

The amphipod *Ampelisca holmesi* ranked sixth in overall abundance, accounting for 2.65% (Table 21), and was found at 41% of the sites. It was the most abundant species in 2004 and 2012 (Table 20). Annual abundances exhibited a cyclical trend (Figure 155), and it was among the dominant taxa in Hillsborough Bay, the Manatee River, Terra Ceia Bay, and Old Tampa Bay (Table 21, Figures 156 & 157). The SIMPER analyses showed *A. holmesi* had a wide depth distribution (intertidal to deep subtidal), was found in fine to coarse sediments, high mesohaline to polyhaline salinities, and low to normoxic dissolved oxygen levels. Grabe et al. (2006) reported similar habitat preferences for this specie,s calculating an optimum depth of 0.5 meters, silt + clay of 5.5%, salinity of 21.4 psu, and dissolved oxygen of 8.8 mg/l. *A. holmesi* was present at sites that were above the TEL for arsenic and nickel and exceeded the PEL for cadmium and zinc (Karlen et al., 2015).

The congeneric species *Ampelisca abdita* ranked 13th overall, accounting for 1.45% of the total benthic abundance, and was found at 22.78% of the sites. It was among the top ranked taxa in 1993, 2014 and 2016, and second ranked species in 1996 and 2012 (Table 20). It was the most abundant species in the Manatee River (Table 21 Figure 156). *A. abdita* has a lower salinity preference than *A holmesi*, and was typically found in low mesohaline samples, which is reflected in its spatial distribution in the bay (Figure 158). Grabe et. al. (2006) calculated an optimal depth of 1.5 meters, salinity of 14.4 psu, relatively high silt + clay content (15.6%), and low dissolved oxygen (2.9 mg/l) for this species. *A. abdita* also appeared to have a higher tolerance for sediment contaminants, and was associated with sites that were above the TEL for PCBs, several PAHs and zinc, and above the PEL for DDD and lead (Karlen et al., 2015).

Thoemke (1979) studied the life history and population dynamics of *A. abdita* in Hillsborough Bay over a two-year period (July 1975 – July 1977). His study found that reproduction occurred year-round, but life span of individuals varied seasonally presumably mediated by water temperature. Juvenile *A. abdita* which recruited during March – August had shorter life spans (6-8 weeks), and produced a single generation of offspring, while juveniles which recruited between September – February were longer lived (10-13 weeks) and produced two generations of offspring (Thoemke 1979). The highest population densities were also observed in June/July, followed by a decline in late summer, possibly in response to low dissolved oxygen concentrations (Thoemke, 1979).

Caecum strigosum de Folin, 1868

The gastropod *Caecum strigosum* was the seventh most abundant infaunal animal bay-wide accounting for 2.50% of the relative abundance (Table 21), and was found at 17% of the sites. *C. strigosum* was among the most abundant taxa during all years from 1993-2002, but abundances generally decreased through 2015, peaked in 2007, then increased in 2016-2017 (Table 20; Figure 159). *C. strigosum* was particularly abundant in Middle Tampa Bay, and ranked among the top taxa in Old Tampa Bay and Lower Tampa Bay (Table 21; Figures 160 & 161). The decline observed since 2003 may be due to the program sampling redesign, which reduced the number of samples collected overall and particularly in Middle Tampa Bay and Lower Tampa Bay. The SIMPER analysis indicated that *C. strigosum* was found at deeper sites (>4 meters) with coarse sediments. It was also associated with sites that were above the TEL for lindane and arsenic (Karlen et al., 2015).

Caecum strigosum was recorded in Tampa Bay in the 1960s (Hall and Saloman, 1975), and was initially identified as *Caecum cf. johnsoni* during the early years of the current monitoring program (Mote Marine Laboratory, 1995), as well as in other earlier works (Culter, 1986).

Rudilemboides naglei Bousfield 1973

The amphipod *Rudilemboides naglei* was the eighth most abundant species accounting for 2.49% of the benthic abundance (Table 21), and was present in 19.65% of the samples. It had a mean abundance of 245/m^2, with a maximum of 29,775/m^2 recorded in Old Tampa Bay in 2007 (07OTB25). *R. naglei* was the most abundant species in 2000, 2007, and 2013 (Table 20), and the dominant species in Old Tampa Bay (Table 21). Annual mean abundances showed a cyclical trend with peak abundances in 2000, 2007, 2013, and 2017, and low abundances in 1998, 2001, 2003, and 2010-2012 (Figure 162). Highest mean abundance of *R. naglei* was in Old Tampa Bay, and relatively high abundances were observed in lower Hillsborough Bay and the upper portion and eastern areas of Middle Tampa Bay (Figures 163 & 164).

Grabe et al., (2006) calculated an optimum salinity of 24.4 psu and silt+clay of 2.1% for this species. They also reported an optimum depth of 3.1 meters, and preference for normoxic conditions with an optimum dissolved oxygen concentration of 8.3 mg/L (Grabe et. al., 2006). Thomke (1979) reported *R. naglei* had highest densities in the fall and winter months, which was attributed to lower water temperatures.

Myers (1981) reclassified this species as *Acuminodeutopus naglei,* and it may appear under this name in some studies. The original described name, *Rudilemboides naglei,* is currently accepted as the valid name according to the World Register of Marine Species (WoRMS; www.marinespecies.org; Lowry, 2014).

Fabricinuda trilobata (Fitzhugh, 1983)

The sabellid polychaete *Fabricinuda trilobata* was the ninth most abundant species bay-wide, comprising 1.96% of the benthic abundance (Table 21), and occurring at 20% of the sites. Mean abundance was $193/m^2$, with a maximum of $39{,}825/m^2$ recorded at a Lower Tampa Bay site in 1999 (99LTB2041). *F. trilobata* was among the top five dominant taxa in 1999, all years from 2005-2010, and 2012-2013, 2015, and 2017. It was the most abundant taxon in 2010, and second most abundant in 2005 (Table 20). It was the second most abundant species in Lower Tampa Bay, and among the dominant taxa in the Manatee River and Boca Ciega Bay (Table 21). Annual mean abundances showed an increase through 2005, with peaks in abundance in 1999 and 2005. The lowest abundances were in 1998 and 2011, then peaking again in 2017 (Figure 165). Abundances increased towards the lower portions of the bay, with Lower Tampa Bay having the highest abundance followed by Boca Ciega Bay and the Manatee River (Figures 166 & 167). SIMPER analysis found this species associated with euhaline sites and sites exceeding the TEL for arsenic (Karlen et al., 2015).

Fabricinuda trilobata was originally described as *Fabriciola trilobata* by Fitzhugh (1983), and reclassified by Fitzhugh (1990) in a new genus *Fabricinuda.* Some studies may report this species by its original name (i.e. Ubelacker, 1984) or as another related genus (possibly *Fabricia sabella* in Taylor, 1971).

Uebelacker (1984) documented its occurrence in the Gulf of Mexico (as *Fabriciola trilobata*), reporting it from depths ranging from 10 -189 meters, and across a range of sediment types. Taylor (1971) reported a small sabellid polychaete identified as *Fabricia sabella* in a survey of polychaetes in Tampa Bay. Taylor's description of *F. sabella* closely matches the morphology of *Fabricinuda trilobata*, and may quite possibly be the same. Taylor states that *Fabricia sabella* was the most widely distributed sabellid species, predominantly occurring in Lower Tampa Bay but ranging up to Old Tampa Bay (Taylor, 1971). Taylor further reported that *F. sabella* was found at a salinity range of 23.0 – 35.1 psu (mean = 31.5 psu), a depth of < 4.0 meters (mean = 1.5 meters), and in sand to shell-sand sediments (Taylor, 1971).

Mediomastus spp.; ***Mediomastus ambiseta* (Hartman, 1947);**
***Mediomastus californiensis* Hartman, 1944**

The capitellid polychaete taxon *Mediomastus* spp. is comprised of damaged specimens of two distinct species found in Tampa Bay: *Mediomastus ambiseta* and *Mediomastus californiensis*. Both species are small worms (<25mm length, 0.5 mm width; Ewing, 1984), and are easily fragmented during sample collection and processing, making species level identification difficult. Reexamination of past specimens from this monitoring program has resulted in changing identifications from *M. ambiseta* or *M. californiensis* to *Mediomastus* spp., resulting in some changes in the contribution to the relative abundance of these taxa than previously reported.

These polychaetes are considered to be opportunistic species, and are often associated with disturbed habitats. Neither species were reported by Taylor (1971). Santos and Simon (1980 a&b) found *Mediomastus californiensis* among benthic species recolonizing sediments following defaunation from hypoxia in Hillsborough Bay. Dauer and Simon (1976 a&b) recorded *Mediomastus ambiseta* (as *Capitita ambiseta*) among the dominant polychaetes in the second year following a defaunation event in Old Tampa Bay due to red tide.

Mediomastus spp. ranked 10th overall in abundance accounting for 1.67% of the total benthic abundance (Table 21), and was found in 48% of the samples. It had a mean abundance of 165/m^2, with a maximum of 10,550/m^2. It was among the top 10 dominant taxa in 1993, 1994, 2000, 2007, 2008, and 2017 (Table 20), and in the Manatee River, Middle Tampa Bay, and Boca Ciega Bay (Table 21). The mean annual abundance of *Mediomastus* spp. showed a cyclical trend over time, with peak abundance in 1993, and an increasing trend from 2013-2017 (Figure 168). Highest abundances were found in the Manatee River and Middle Tampa Bay, with the lowest in Old Tampa Bay (Figure 169). It was widespread throughout the bay, with high densities observed in Hillsborough Bay, Middle Tampa Bay, and Boca Ciega Bay, in addition to the Manatee River (Figure 170). SIMPER analysis indicated that *Mediomastus* spp. was associated with depths ranging from 1 to >4 meters, fine to medium sediments, and salinities ranging from low mesohaline to euhaline. *Mediomastus* spp. was also found associated with sites that were above the TELs for lindane, p,p'-DDT, arsenic, and cadmium (Karlen et al., 2015).

Mediomastus ambiseta was originally described from California as *Capitita ambiseta* by Hartman (1947). Earlier studies in Tampa Bay by Dauer and Simon (1976 a&b) use the original name. Hartman (1947) recorded this species from intertidal mud flats. The worms build tubes of mucus and debris, and orient head down vertically in the sediments (Hartman, 1947; Warren et al., 1994).

M. ambiseta ranked 64th overall, accounting for 0.35% of the total benthic abundance, and occurred in 15% of the samples. It had a mean abundance of 35/m^2, with a maximum of 4,550/m^2. It was among the dominant taxa in 1994, with abundances showing a decreasing trend through 2011, then increasing through 2017 (Table 20; Figure 168). The highest abundances were in Hillsborough Bay and the Manatee River (Figure 169). Its overall distribution was more confined to the near shore areas of the bay (Figure171).

Mediomastus californiensis ranked 99th in overall abundance, accounting for 0.20%, and was present at 13.18% of the sites. It had a mean abundance of 19/m^2, and maximum of 2,450/m^2. *M. californiensis* abundance showed a decreasing trend from 1993-2003, then increased to a peak in 2008; most following years were below the 25-year mean abundance (Figure 168). Highest abundances were in Middle Tampa Bay, Old Tampa Bay, and Lower Tampa Bay (Figure 169), but it had a wide distribution throughout the bay (Figure 172). *M. californiensis* has been previously reported from intertidal, muddy sands (Hartman, 1947). The species been found throughout the northern Gulf of Mexico and off the coast of Florida at depths of 18-53 meters in sediments ranging from silt/clay and muddy sands to very fine and medium sands (Ewing, 1984).

Table 20. Top ten benthic taxa (including ties) based on relative abundance by year.

1993	%	1994	%	1995	%	1996	%	1997	%
Branchiostoma floridae (Cephalochordata)	9.60	*Kirkegaardia sp.* (Annelida:Polychaeta)	9.43	CIRRIPEDIA (Crustacea: Cirripedia)	16.01	*Mysella planulata* (Mollusca: Bivalvia)	8.77	*Branchiostoma floridae* (Cephalochordata)	10.17
Mediomastus sp. (Annelida: Polychaeta)	6.09	*Branchiostoma floridae* (Cephalochordata)	7.37	*Neodexiospira) steueri* (Annelida:Polychaeta)	9.86	*Ampelisca abdita* (Crustacea: Amphipoda)	8.37	*Mysella planulata* (Mollusca: Bivalvia)	4.58
Prionospio perkinsi (Annelida: Polychaeta)	3.83	*Caecum strigosum* (Mollusca: Gastropoda)	6.60	NAIDIDAE (Annelida: Oligochaeta)	3.75	*Caecum strigosum* (Mollusca: Gastropoda)	5.22	*Caecum strigosum* (Mollusca: Gastropoda)	4.42
Carazziella hobsonae (Annelida: Polychaeta)	3.44	*Prionospio perkinsi* (Annelida: Polychaeta)	3.99	*Pileolaria rosepigmentata* (Annelida: Polychaeta)	2.52	*Branchiostoma floridae* (Cephalochordata)	4.25	*Kirkegaardia sp.* (Annelida:Polychaeta)	4.00
Ampelisca abdita (Crustacea: Amphipoda)	3.43	NAIDIDAE (Annelida: Oligochaeta)	3.93	*Branchiostoma floridae* (Cephalochordata)	2.42	*Kirkegaardia sp.* (Annelida: Polychaeta)	3.67	*Rudilemboides naglei* (Crustacea: Amphipoda)	3.52
Kirkegaardia sp. (Annelida:Polychaeta)	3.28	*Mediomastus sp.* (Annelida: Polychaeta)	2.79	*Bittiolum varium* (Mollusca: Gastropoda)	2.37	*Rudilemboides naglei* (Crustacea: Amphipoda)	3.57	*Ampelisca holmesi* (Crustacea: Amphipoda)	3.10
Ampelisca holmesi (Crustacea: Amphipoda)	3.02	*Paraprionospio sp.* (Annelida: Polychaeta)	2.72	TELLININAE (Mollusca: Bivalvia)	2.23	*Ampelisca holmesi* (Crustacea: Amphipoda)	3.23	NAIDIDAE (Annelida: Oligochaeta)	2.65
Rudilemboides naglei (Crustacea: Amphipoda)	3.01	*Mediomastus ambiseta* (Annelida: Polychaeta)	2.49	*Amygdalum papyrium* (Mollusca: Bivalvia)	2.21	NAIDIDAE (Annelida: Oligochaeta)	2.99	*Glottidia pyramidata* (Brachiopoda)	2.12
NAIDIDAE (Annelida: Oligochaeta)	2.65	*Metharpinia floridana* (Crustacea: Amphipoda)	2.33	*Caecum strigosum* (Mollusca: Gastropoda)	2.12	*Clymenella mucosa* (Annelida: Polychaeta)	2.84	*Streblospio spp.* (Annelida: Polychaeta)	2.01
Caecum strigosum (Mollusca: Gastropoda)	2.47	*Mysella planulata* (Mollusca: Bivalvia)	2.29	*Ampelisca holmesi* (Crustacea: Amphipoda)	2.10	*Leptochelia sp.* (Crustacea: Tanaidacea)	2.31	*Phascolion cryptum* (Sipuncula)	1.94

Table 20. (Continued)

1998	%	1999	%	2000	%	2001	%	2002	%
Branchiostoma floridae (Cephalochordata)	9.34	*Kirkegaardia sp.* (Annelida:Polychaeta)	7.83	*Rudilemboides naglei* (Crustacea: Amphipoda)	6.24	*Glottidia pyramidata* (Brachiopoda)	9.13	*Glottidia pyramidata* (Brachiopoda)	39.42
Mysella planulata (Mollusca: Bivalvia)	6.01	*Branchiostoma floridae* (Cephalochordata)	6.54	*Mulinia lateralis* (Mollusca: Bivalvia)	5.47	*Kirkegaardia sp.* (Annelida:Polychaeta)	6.36	*Branchiostoma floridae* (Cephalochordata)	3.23
Caecum strigosum (Mollusca: Gastropoda)	6.00	*Glottidia pyramidata* (Brachiopoda)	5.35	*Ampelisca holmesi* (Crustacea: Amphipoda)	4.69	NAIDIDAE (Annelida: Oligochaeta)	5.04	NAIDIDAE (Annelida: Oligochaeta)	2.07
Kirkegaardia sp. (Annelida:Polychaeta)	5.86	*Caecum strigosum* (Mollusca: Gastropoda)	4.12	*Kirkegaardia sp.* (Annelida:Polychaeta)	4.09	*Caecum strigosum* (Mollusca: Gastropoda)	4.93	*Caecum strigosum* (Mollusca: Gastropoda)	1.58
Prionospio perkinsi (Annelida: Polychaeta)	4.75	*Fabricinuda trilobata* (Annelida: Polychaeta)	3.82	*Cyclaspis varians* (Crustacea: Cumacea)	4.04	*Ampelisca holmesi* (Crustacea: Amphipoda)	4.30	*Prionospio perkinsi* (Annelida: Polychaeta)	1.47
Mulinia lateralis (Mollusca: Bivalvia)	3.91	*Prionospio perkinsi* (Annelida: Polychaeta)	2.74	*Tubificoides wasselli* (Annelida: Oligochaeta)	3.72	*Branchiostoma floridae* (Cephalochordata)	3.43	*Mysella planulata* (Mollusca: Bivalvia)	1.34
NAIDIDAE (Annelida: Oligochaeta)	3.61	*Mulinia lateralis* (Mollusca: Bivalvia)	2.62	*Branchiostoma floridae* (Cephalochordata)	3.01	TELLININAE (Mollusca: Bivalvia)	2.39	ENTEROPNEUSTA (Hemichordata)	1.29
Neodexiospira) steueri (Annelida:Polychaeta)	3.04	NAIDIDAE (Annelida: Oligochaeta)	2.27	*Aricidea philbinae* (Annelida: Polychaeta)	2.80	*Paraprionospio sp.* (Annelida: Polychaeta)	1.82	CIRRIPEDIA (Crustacea: Cirripedia)	1.26
Amygdalum papyrium (Mollusca: Bivalvia)	2.47	*Pinnixa spp.* (Crustacea: Decapoda)	2.06	*Leptochelia sp.* (Crustacea: Tanaidacea)	2.68	*Carazziella hobsonae* (Annelida: Polychaeta)	1.67	*Clymenella mucosa* (Annelida: Polychaeta)	1.25
Ampelisca holmesi (Crustacea: Amphipoda)	1.85	*Pomatoceros americanus* (Annelida: Polychaeta)	1.99	*Mediomastus sp.* (Annelida: Polychaeta)	2.22	*Inanidrilus sp.* (Annelida: Oligochaeta)	1.42	*Kirkegaardia sp.* (Annelida:Polychaeta)	1.10

Table 20. (Continued)

2003	%	2004	%	2005	%	2006	%	2007	%
Polydora cornuta (Annelida: Polychaeta)	7.23	*Ampelisca holmesi* (Crustacea: Amphipoda)	7.42	*Glottidia pyramidata* (Brachiopoda)	12.26	*Exogone dispar* (Annelida: Polychaeta)	14.68	*Rudilemboides naglei* (Crustacea: Amphipoda)	11.98
NAIDIDAE (Annelida: Oligochaeta)	5.18	*Branchiostoma floridae* (Cephalochordata)	5.91	*Fabricinuda trilobata* (Annelida: Polychaeta)	8.45	*Glottidia pyramidata* (Brachiopoda)	7.02	*Kirkegaardia sp.* (Annelida:Polychaeta)	4.73
Amygdalum papyrium (Mollusca: Bivalvia)	4.92	*Glottidia pyramidata* (Brachiopoda)	3.84	*Bittiolum varium* (Mollusca: Gastropoda)	5.70	NAIDIDAE (Annelida: Oligochaeta)	6.27	*Caecum strigosum* (Mollusca: Gastropoda)	4.06
Kirkegaardia sp. (Annelida:Polychaeta)	4.85	NAIDIDAE (Annelida: Oligochaeta)	3.78	*Ampelisca holmesi* (Crustacea: Amphipoda)	5.65	*Rudilemboides naglei* (Crustacea: Amphipoda)	3.74	*Fabricinuda trilobata* (Annelida: Polychaeta)	3.72
Paraprionospio sp. (Annelida: Polychaeta)	4.21	*Kirkegaardia sp.* (Annelida:Polychaeta)	3.63	*Mysella planulata* (Mollusca: Bivalvia)	4.16	*Kirkegaardia sp.* (Annelida:Polychaeta)	3.61	*Branchiostoma floridae* (Cephalochordata)	3.44
Amphibalanus improvisus (Crustacea: Cirripedia)	3.71	*Mesokalliapseudes macsweenyi* (Crustacea: Tanaidacea)	3.22	*Amygdalum papyrium* (Mollusca: Bivalvia)	2.64	*Mysella planulata* (Mollusca: Bivalvia)	3.37	*Clymenella mucosa* (Annelida: Polychaeta)	3.38
Glottidia pyramidata (Brachiopoda)	2.88	*Parastarte triquetra* (Mollusca: Bivalvia)	3.09	*Grandidierella bonnieroides* (Crustacea: Amphipoda)	2.38	*Branchiostoma floridae* (Cephalochordata)	2.52	*Carazziella hobsonae* (Annelida: Polychaeta)	3.29
Augeneriella hummelincki (Annelida: Polychaeta)	2.63	BALANIDAE (Crustacea: Cirripedia)	2.77	NAIDIDAE (Annelida: Oligochaeta)	2.26	*Fabricinuda trilobata* (Annelida: Polychaeta)	2.35	*Prionospio perkinsi* (Annelida: Polychaeta)	
Streblospio spp. (Annelida: Polychaeta)	2.09	*Rudilemboides naglei* (Crustacea: Amphipoda)	2.51	*Kirkegaardia sp.* (Annelida:Polychaeta)	2.25	*Amygdalum papyrium* (Mollusca: Bivalvia)	2.14	*Exogone dispar* (Annelida: Polychaeta)	3.02
Aspidosiphon cf. muelleri (Sipuncula)	2.01	*Cerapus sp. C* (Crustacea: Amphipoda)	2.27	*Paraprionospio sp.* (Annelida: Polychaeta)	1.70	*Tubificoides brownae* (Annelida: Oligochaeta)	2.04	NAIDIDAE (Annelida: Oligochaeta)	
								Ampelisca holmesi (Crustacea: Amphipoda)	2.93
								Mediomastus sp. (Annelida: Polychaeta)	2.12

Table 20. (Continued)

2008	%	2009	%	2010	%	2011	%	2012	%
Mysella planulata (Mollusca: Bivalvia)	12.89	*Mysella planulata* (Mollusca: Bivalvia)	7.71	*Fabricinuda trilobata* (Mollusca:Bivalvia)	5.43	*Kirkegaardia sp.* (Annelida:Polychaeta)	11.73	*Ampelisca holmesi* (Crustacea: Amphipoda)	6.62
NAIDIDAE (Annelida: Oligochaeta)	4.97	*Glottidia pyramidata* (Brachiopoda)	4.59	NAIDIDAE (Annelida: Oligochaeta)	5.40	NAIDIDAE (Annelida: Oligochaeta)	8.34	*Mesokalliapseudes macsweenyi* (Crustacea: Tanaidacea)	4.49
Mesokalliapseudes macsweenyi (Crustacea: Tanaidacea)	3.60	*Amygdalum papyrium* (Mollusca: Bivalvia)	4.53	*Caecum pulchellum* (Mollusca: Gastropoda)	4.11	*Bittiolum varium* (Mollusca: Gastropoda)	4.57	*Ampelisca abdita* (Crustacea: Amphipoda)	
Fabricinuda trilobata (Annelida: Polychaeta)	3.57	*Mesokalliapseudes macsweenyi* (Crustacea: Tanaidacea)	3.60	*Exogone dispar* (Annelida: Polychaeta)	4.10	*Parastarte triquetra* (Mollusca:Bivalvia)	3.01	*Amygdalum papyrium* (Mollusca: Bivalvia)	4.45
Mulinia lateralis (Mollusca: Bivalvia)	3.12	NAIDIDAE (Annelida: Oligochaeta)	3.09	*Mesokalliapseudes macsweenyi* (Crustacea: Tanaidacea)	2.49	*Heteromastus filiformis* Annelida: Polychaeta)	2.85	*Fabricinuda trilobata* (Annelida: Polychaeta)	3.82
Branchiostoma floridae (Cephalochordata)	2.51	*Rudilemboides naglei* (Crustacea: Amphipoda)	2.63	*Bittiolum varium* (Mollusca: Gastropoda)	2.45	*Paraprionospio sp.* (Annelida: Polychaeta)	2.63	NAIDIDAE (Annelida: Oligochaeta)	3.38
Kirkegaardia sp. (Annelida:Polychaeta)	2.29	*Fabricinuda trilobata* (Annelida: Polychaeta)	2.40	Balanidae (Crustacea: Cirripedia)	2.32	*Aricidea philbinae* (Annelida: Polychaeta)	2.45	*Clymenella mucosa* (Annelida: Polychaeta)	3.13
Mediomastus sp. (Annelida: Polychaeta)	2.01	*Prionospio perkinsi* (Annelida: Polychaeta)	1.85	*Glottidia pyramidata* (Brachiopoda)	2.31	*Ampelisca holmesi* (Crustacea: Amphipoda)	2.44	*Bittiolum varium* (Mollusca: Gastropoda)	2.87
Exogone lourei (Annelida: Polychaeta)	1.98	*Boguea enigmatica* (Annelida: Polychaeta)	1.80	*Acteocina canaliculata* (Mollusca: Gastropoda)	2.26	*Acteocina canaliculata* (Mollusca: Gastropoda)	1.88	*Paraprionospio sp.* (Annelida: Polychaeta)	2.86
Clymenella mucosa (Annelida: Polychaeta)	1.75	*Kirkegaardia sp.* (Annelida:Polychaeta)		TELLININAE *(Mollusca:Bivalvia)*	2.10	*Haminoea succinea* (Mollusca: Gastropoda)	1.77	*Tubificoides wasselli* (Annelida: Oligochaeta)	2.67
		TELLININAE *(Mollusca:Bivalvia)*	1.74					*Kirkegaardia sp.* (Annelida:Polychaeta)	2.58

Table 20. (Continued)

2013	%	2014	%	2015	%	2016	%	2017	%
Rudilemboides naglei (Crustacea: Amphipoda)	6.79	*Kirkegaardia sp.* (Annelida:Polychaeta)	7.92	*Branchiostoma floridae* (Cephalochordata)	8.54	*Caecum pulchellum* (Mollusca: Gastropoda)	9.41	*Mysella planulata* (Mollusca: Bivalvia)	13.20
Branchiostoma floridae (Cephalochordata)	5.53	*Branchiostoma floridae* (Cephalochordata)	7.26	NAIDIDAE (Annelida: Oligochaeta)	5.91	NAIDIDAE (Annelida: Oligochaeta)	4.15	*Branchiostoma floridae* (Cephalochordata)	9.29
Ampelisca holmesi (Crustacea: Amphipoda)	3.83	NAIDIDAE (Annelida: Oligochaeta)	3.68	*Caecum pulchellum* (Mollusca: Gastropoda)	4.68	*Dipolydora cf. tetrabranchia* (Annelida: Polychaeta)	3.72	*Rudilemboides naglei* (Crustacea: Amphipoda)	4.87
Parastarte triquetra (Mollusca:Bivalvia)	3.79	*Caecum pulchellum* (Mollusca: Gastropoda)	2.60	*Bittiolum varium* (Mollusca: Gastropoda)	3.39	*Aricidea philbinae* (Annelida: Polychaeta)	3.49	*Fabricinuda trilobata* (Annelida: Polychaeta)	4.62
Clymenella mucosa (Annelida: Polychaeta)		*Rudilemboides naglei* (Crustacea: Amphipoda)	2.58	*Kirkegaardia sp.* (Annelida:Polychaeta)	3.28	*Branchiostoma floridae* (Cephalochordata)	3.16	*Caecum pulchellum* (Mollusca: Gastropoda)	4.43
NAIDIDAE (Annelida: Oligochaeta)	3.36	*Clymenella mucosa* (Annelida: Polychaeta)	2.32	*Caecum imbricatum* (Mollusca: Gastropoda)	2.93	*Mysella planulata* (Mollusca: Bivalvia)	2.85	*Clymenella mucosa* (Annelida: Polychaeta)	3.78
Travisia hobsonae (Annelida:Polychaeta)	3.17	*Littoridinops sp.* (Mollusca: Gastropoda)	2.21	*Pileolaria rosepigmentata* (Annelida: Polychaeta)	2.47	*Glottidia pyramidata* (Brachiopoda)	2.73	*Mediomastus sp.* (Annelida: Polychaeta)	2.52
Caecum pulchellum (Mollusca: Gastropoda)	2.72	*Aricidea philbinae* (Annelida: Polychaeta)	2.11	*Fabricinuda trilobata* (Annelida: Polychaeta)	2.25	*Ampelisca abdita* (Crustacea: Amphipoda)	2.63	*Caecum imbricatum* (Mollusca: Gastropoda)	2.49
Fabricinuda trilobata (Annelida: Polychaeta)	2.45	*Ampelisca abdita* (Crustacea: Amphipoda)	2.08	*Tubificoides brownae* (Annelida: Oligochaeta)	2.15	SPIRORBINAE (Annelida: Polychaeta)	2.57	*Kirkegaardia sp.* (Annelida:Polychaeta)	2.32
Kirkegaardia sp. (Annelida:Polychaeta)	2.09	*Caecum imbricatum* (Mollusca: Gastropoda)	1.97	*Phascolion caupo* (Sipuncula)	1.97	*Mesokalliapseudes macsweenyi* (Crustacea: Tanaidacea)	2.44	NAIDIDAE (Annelida: Oligochaeta)	2.20
Tubificoides brownae (Annelida: Oligochaeta)	1.89								

Table 21. Dominant benthic taxa (Relative Abundance) by Bay Segment 1993-2017.

Hillsborough Bay	%	Old Tampa Bay	%	Middle Tampa Bay	%	Lower Tampa Bay	%
Mysella planulata (Mollusca: Bivalvia)	12.29	*Rudilemboides naglei* (Crustacea: Amphipoda)	8.77	*Glottidia pyramidata* (Brachiopoda)	11.93	*Branchiostoma floridae* (Cephalochordata)	11.39
Kirkegaardia sp. (Annelida:Polychaeta)	8.14	CIRRIPEDIA (Crustacea: Cirripedia)	5.72	*Branchiostoma floridae* (Cephalochordata)	10.15	*Fabricinuda trilobata* (Annelida:Polychaeta)	5.14
Glottidia pyramidata (Brachiopoda)	5.65	*Branchiostoma floridae* (Cephalochordata)	5.20	*Caecum strigosum* (Mollusca: Gastropoda)	6.68	*Caecum strigosum* (Mollusca: Gastropoda)	3.53
Ampelisca holmesi (Crustacea: Amphipoda)	5.12	*Mysella planulata* (Mollusca: Bivalvia)	4.97	*Kirkegaardia sp.* (Annelida:Polychaeta)	2.83	*Mesokalliapseudes macsweenyi* (Crustacea: Tanaidacea)	2.74
NAIDIDAE (Annelida: Oligochaeta)	3.44	*Ampelisca holmesi* (Crustacea: Amphipoda)	4.42	NAIDIDAE (Annelida: Oligochaeta)	2.62	*Leptochelia sp.* (Crustacea: Tanaidacea)	2.55
Amygdalum papyrium (Mollusca: Bivalvia)	3.21	*Glottidia pyramidata* (Brachiopoda)	2.81	*Rudilemboides naglei* (Crustacea: Amphipoda)	2.57	NAIDIDAE (Annelida: Oligochaeta)	2.50
Prionospio perkinsi (Annelida: Polychaeta)	3.12	*Caecum strigosum* (Mollusca: Gastropoda)	2.63	*Clymenella mucosa* (Annelida: Polychaeta)	1.89	*Phascolion caupo* (Sipuncula)	2.32
Paraprionospio pinnata (Annelida: Polychaeta)	2.95	*Exogone dispar* (Annelida: Polychaeta)	2.58	*Prionospio perkinsi* (Annelida: Polychaeta)	1.85	*Clymenella mucosa* (Annelida: Polychaeta)	2.14
Carazziella hobsonae (Annelida: Polychaeta)	2.81	NAIDIDAE (Annelida: Oligochaeta)	2.52	*Neodexiospira steueri* (Annelida:Polychaeta)	1.67	*Neodexiospira steueri* (Annelida:Polychaeta)	1.87
Aricidea philbinae (Annelida: Polychaeta)	2.58	*Tubificoides wasselli* (Annelida: Oligochaeta)	2.30	*Mediomastus spp.* (Annelida: Polychaeta)	1.51	*Acanthohaustorius uncinus* (Crustacea: Amphipoda)	1.76

Table 21. Continued

Manatee River	%	Terra Ceia Bay	%	Boca Ciega Bay	%	Tampa Bay	%
Ampelisca abdita (Crustacea: Amphipoda)	9.55	*Kirkegaardia sp.* (Annelida:Polychaeta)	5.38	NAIDIDAE (Annelida: Oligochaeta)	7.96	*Branchiostoma floridae* (Cephalochordata)	5.29
Kirkegaardia sp. (Annelida:Polychaeta)	7.03	NAIDIDAE (Annelida: Oligochaeta)	4.88	*Neodexiospira steueri* (Annelida:Polychaeta)	3.63	*Glottidia pyramidata* (Brachiopoda)	4.23
Caecum pulchellum (Mollusca: Gastropoda)	5.68	*Caecum pulchellum* (Mollusca: Gastropoda)	4.43	*Kirkegaardia sp.* (Annelida:Polychaeta)	2.90	*Kirkegaardia sp.* (Annelida:Polychaeta)	3.92
Mulinia lateralis (Mollusca: Bivalvia)	5.24	*Ampelisca holmesi* (Crustacea: Amphipoda)	4.39	*Fabricinuda trilobata* (Annelida:Polychaeta)	2.44	*Mysella planulata* (Mollusca: Bivalvia)	3.91
Amygdalum papyrium (Mollusca: Bivalvia)	4.16	*Paraprionospio sp.* (Annelida: Polychaeta)	3.08	*Clymenella mucosa* (Annelida: Polychaeta)	2.31	NAIDIDAE (Annelida: Oligochaeta)	3.43
Ampelisca holmesi (Crustacea: Amphipoda)	4.01	*Caecum cf. bipartitum* (Mollusca: Gastropoda)	2.92	*Pileolaria rosepigmentata* (Annelida: Polychaeta)	2.22	*Ampelisca holmesi* (Crustacea: Amphipoda)	2.65
Mediomastus spp. (Annelida: Polychaeta)	4.00	*Caecum imbricatum* (Mollusca: Gastropoda)	2.59	*Exogone dispar* (Annelida: Polychaeta)	1.97	*Caecum strigosum* (Mollusca: Gastropoda)	2.50
Grandidierella bonnieroides (Crustacea: Amphipoda)	3.96	*Clymenella mucosa* (Annelida: Polychaeta)	2.50	TELLININAE (Mollusca:Bivalvia)	1.92	*Rudilemboides naglei* (Crustacea: Amphipoda)	2.49
Fabricinuda trilobata (Annelida:Polychaeta)	3.45	*Acteocina canaliculata* (Mollusca: Gastropoda)	2.42	*Mediomastus spp.* (Annelida: Polychaeta)	1.89	*Fabricinuda trilobata* (Annelida:Polychaeta)	1.96
Cyclaspis varians (Crustacea:Cumacea)	3.05	*Mulinia lateralis* (Mollusca: Bivalvia)	2.20	SPIRORBINAE	1.86	*Mediomastus spp.* (Annelida: Polychaeta)	1.67

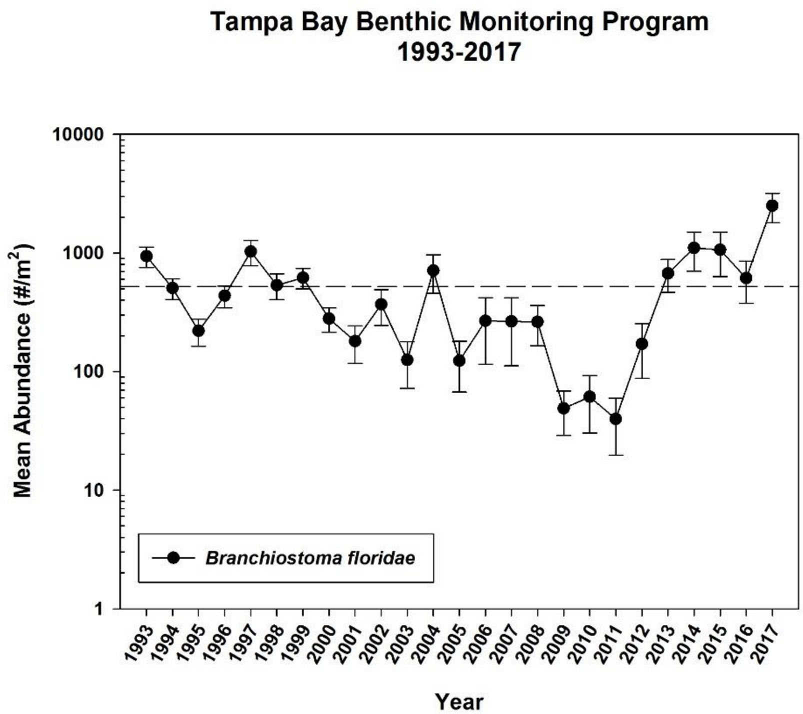

Figure 140. Mean abundance of *Branchiostoma floridae* by year. Error bars = 1 standard error, dashed line represents bay-wide mean value.

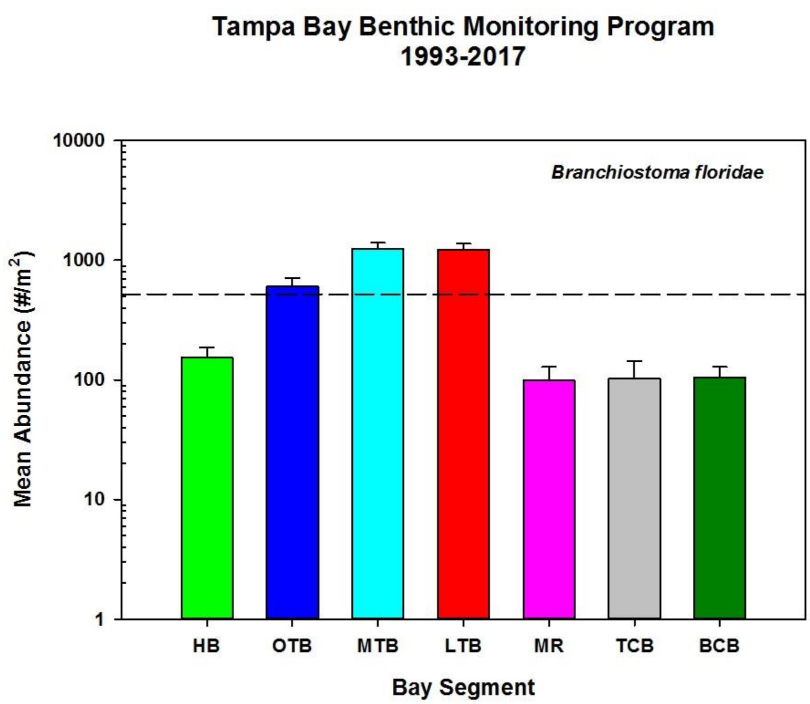

Figure 141. Mean abundance of *Branchiostoma floridae* by bay segment. Error bars = 1 standard error, dashed line represents bay-wide mean value.

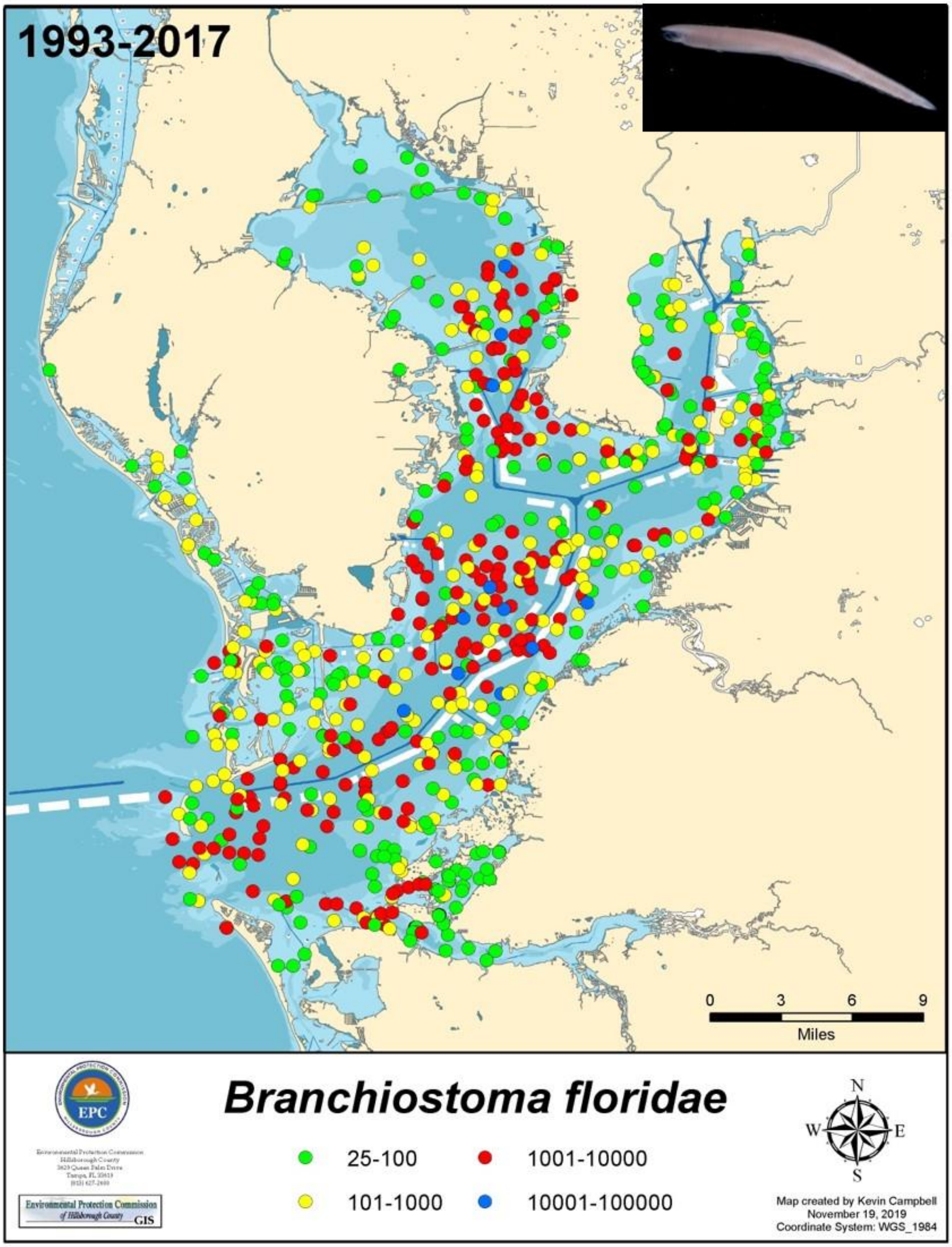

Figure 142. Late-Summer distribution of *Branchiostoma floridae* in Tampa Bay 1993-2017.

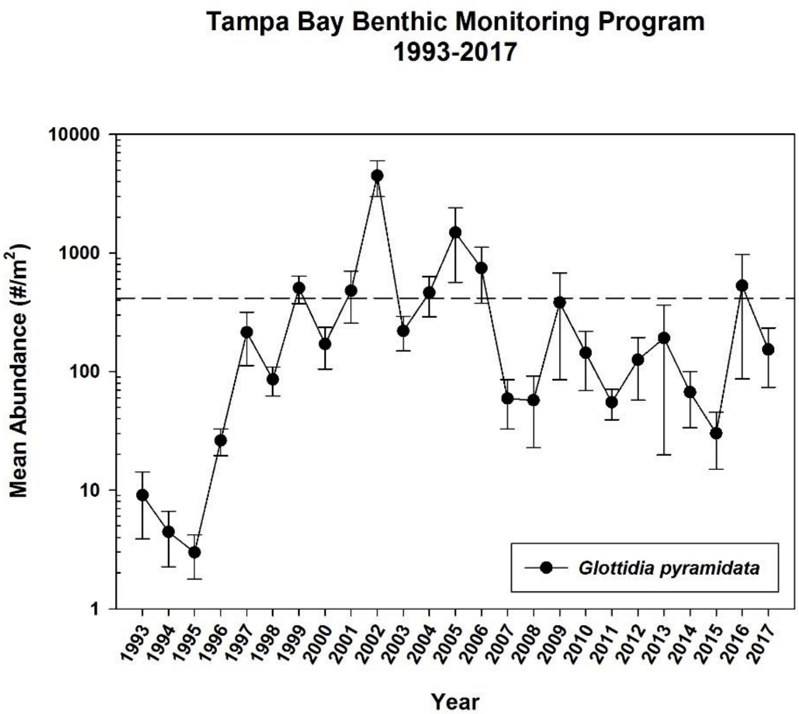

Figure 143. Mean abundance of *Glottidia pyramidata* by year. Error bars = 1 standard error, dashed line represents bay-wide mean value.

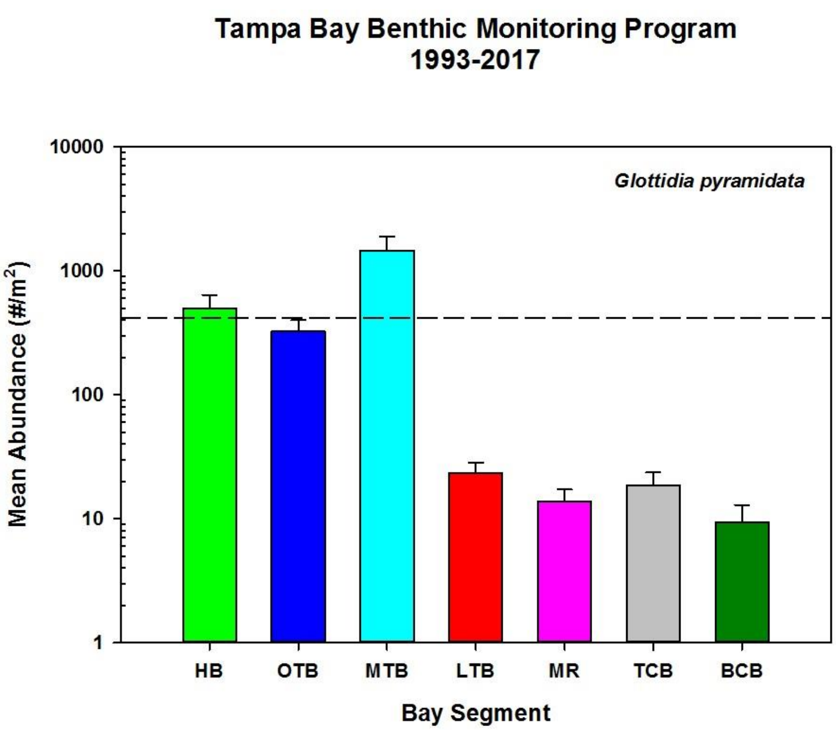

Figure 144. Mean abundance of *Glottidia pyramidata* by bay segment. Error bars = 1 standard error, dashed line represents bay-wide mean value.

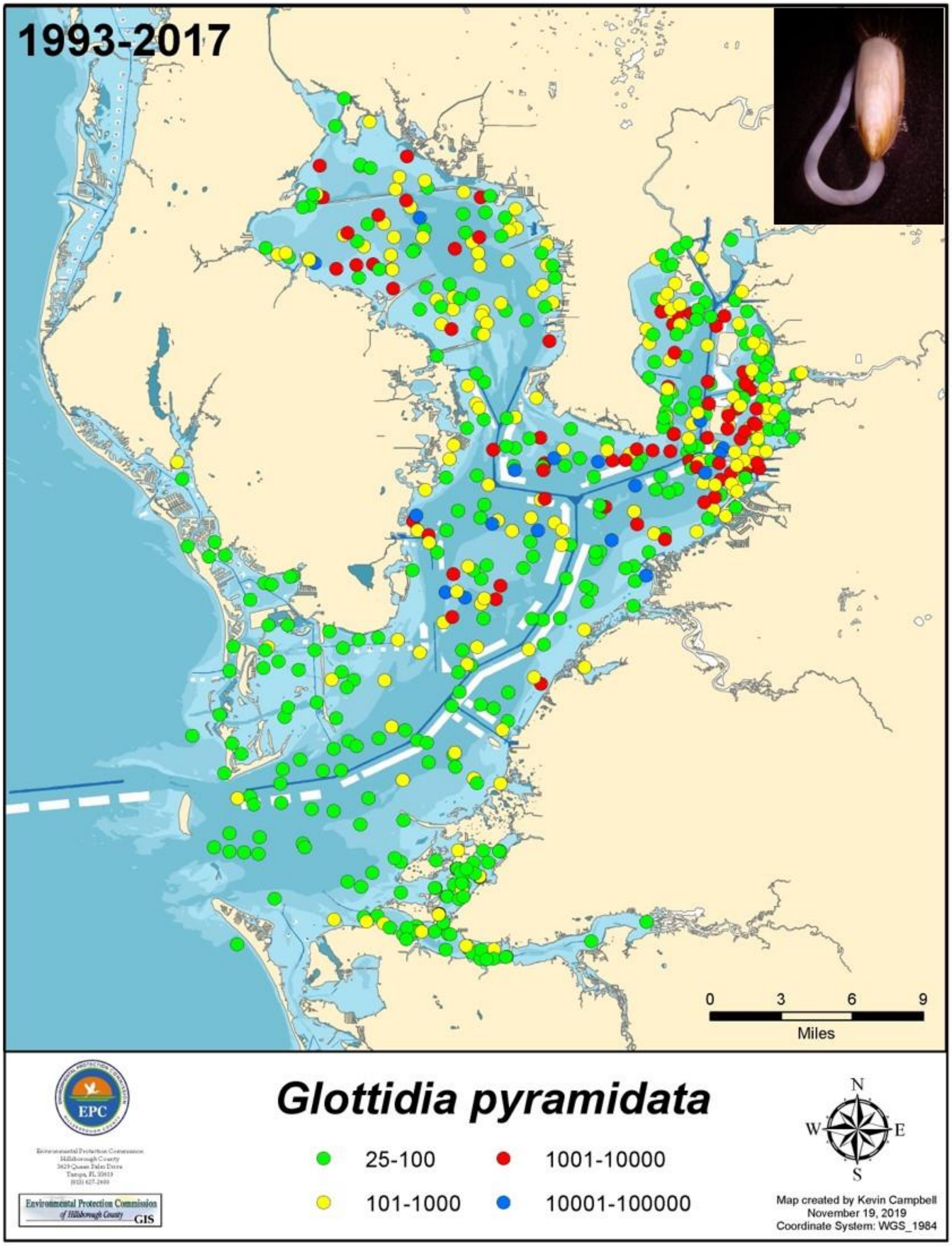

Figure 145. Late-Summer distribution of *Glottidia pyramidata* in Tampa Bay 1993-2017.

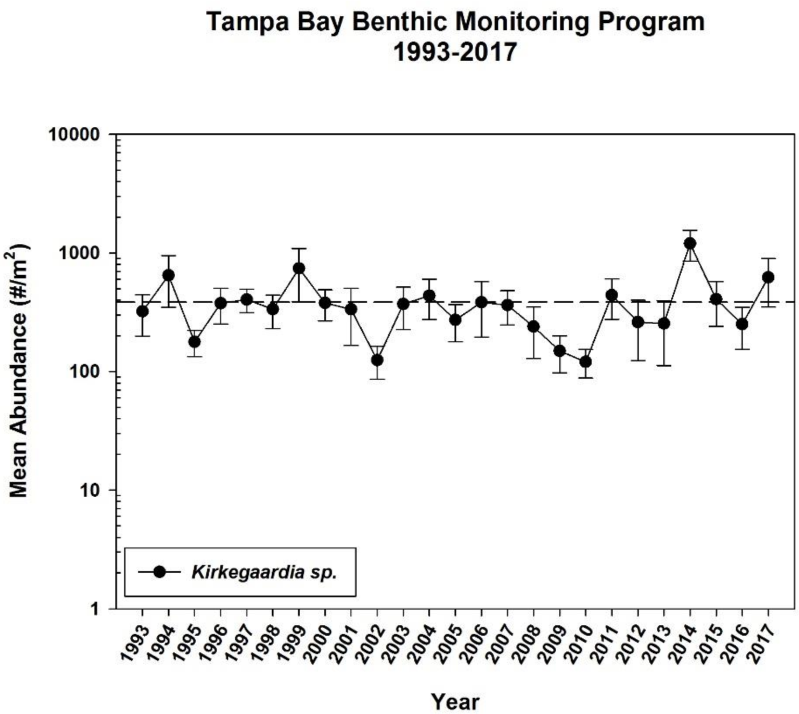

Figure 146. Mean abundance of *Kirkegaardia* sp. (=*Monticellina cf. dorsobranchialis)* by year. Error bars = 1 standard error, dashed line represents bay-wide mean value.

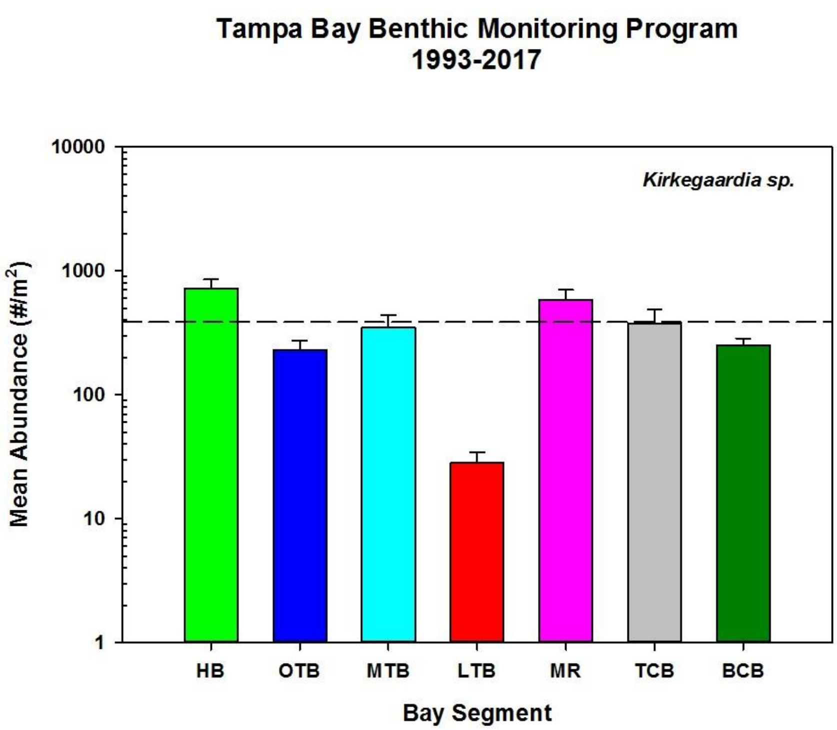

Figure 147. Mean abundance of *Kirkegaardia* sp. (=*Monticellina cf. dorsobranchialis* by bay segment. Error bars = 1 standard error, dashed line represents bay-wide mean value.

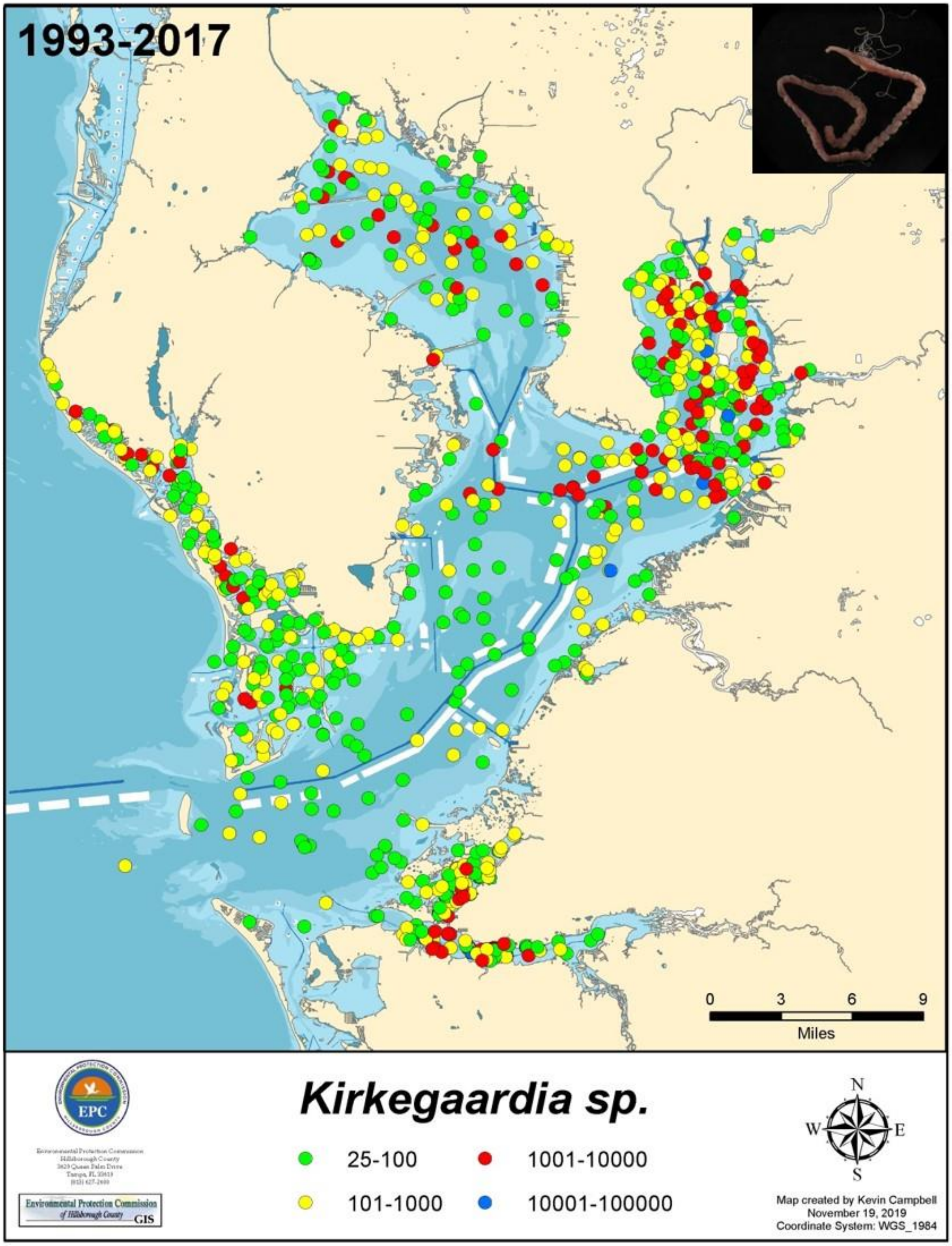

Figure 148. Late-Summer distribution of *Kirkegaardia* sp. (= *Monticellina cf. dorsobranchialis*) in Tampa Bay 1993-2017.

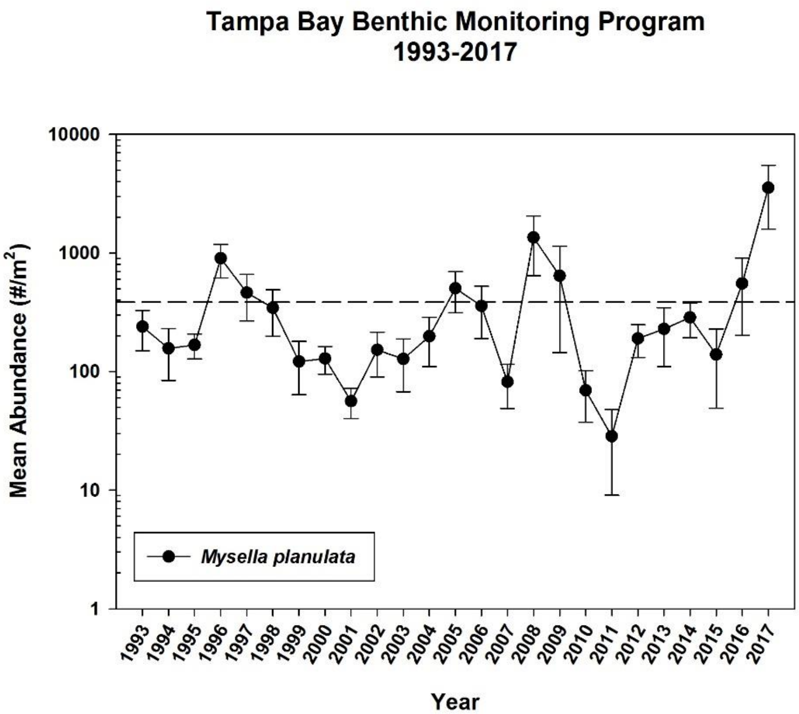

Figure 149. Mean abundance of *Mysella planulata* by year. Error bars = 1 standard error, dashed line represents bay-wide mean value.

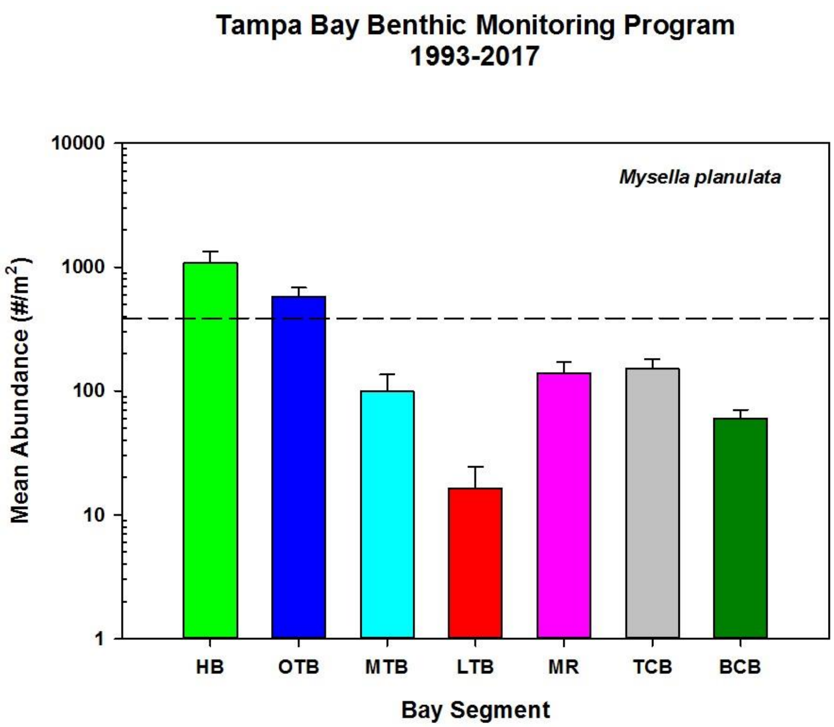

Figure 150. Mean abundance of *Mysella planulata* by bay segment. Error bars = 1 standard error, dashed line represents bay-wide mean value.

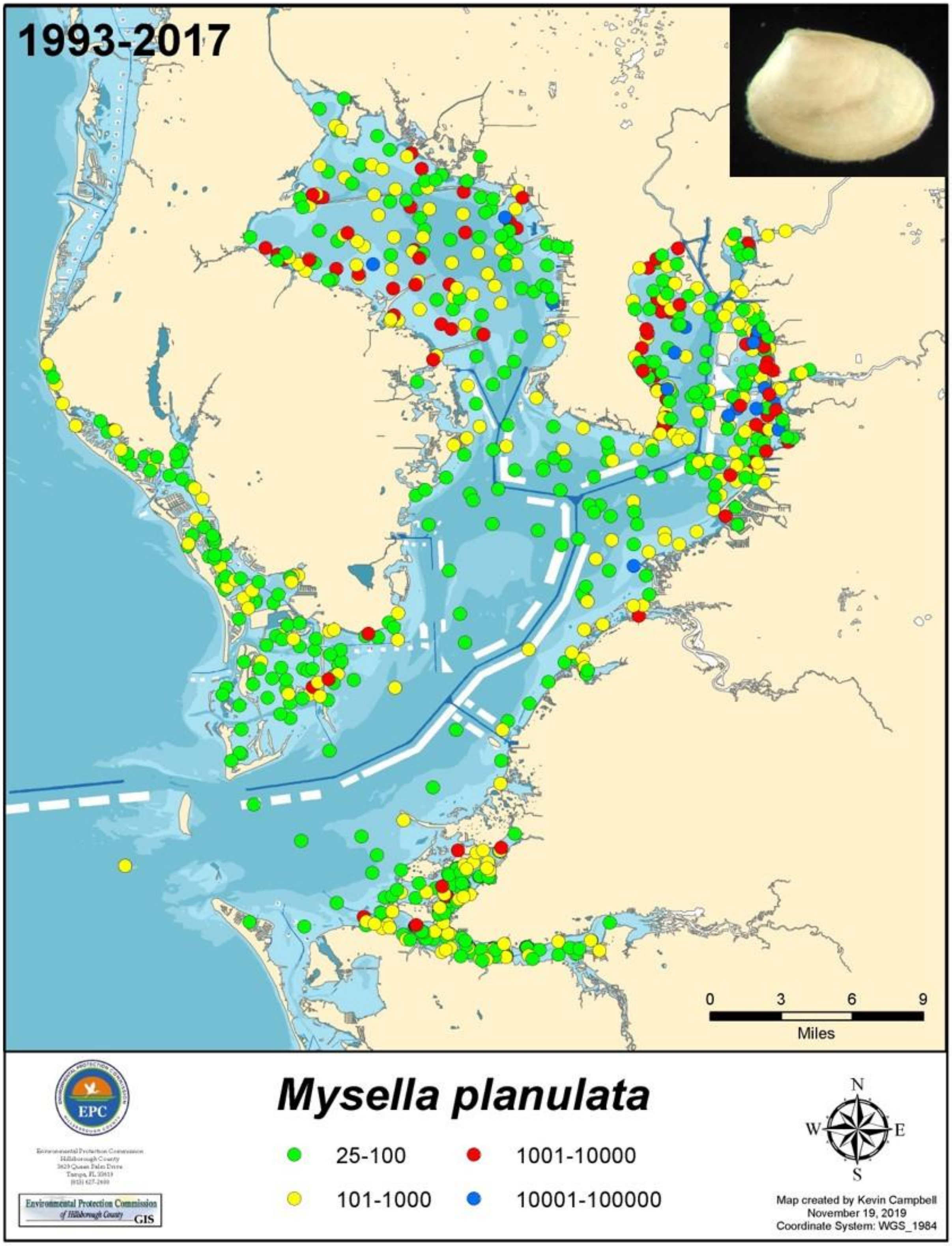

Figure 151. Late-Summer distribution of *Mysella planulata* in Tampa Bay 1993-2017.

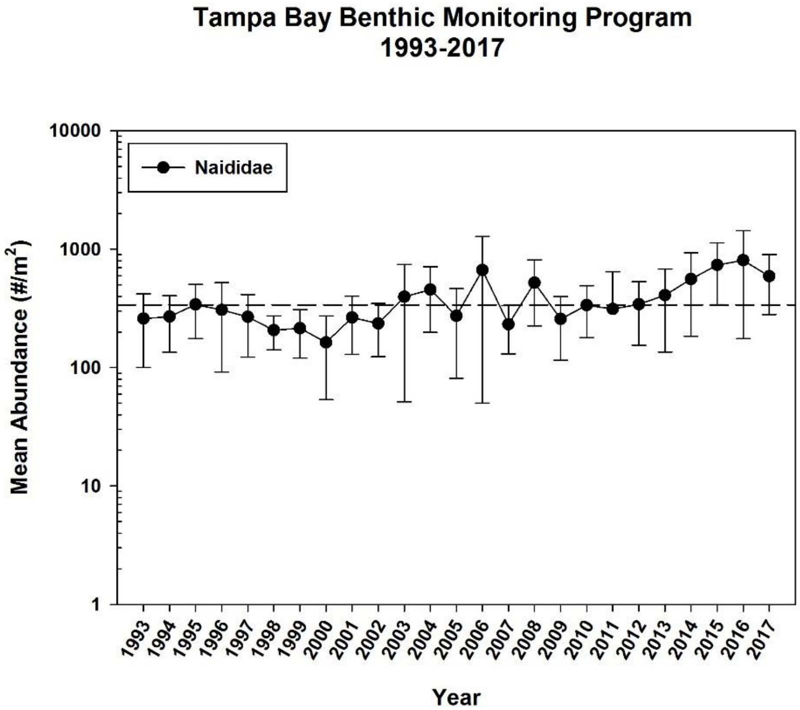

Figure 152. Mean abundance of unidentified Naididae (=Tubificinae) by year. Error bars = 1 standard error, dashed line represents bay-wide mean value.

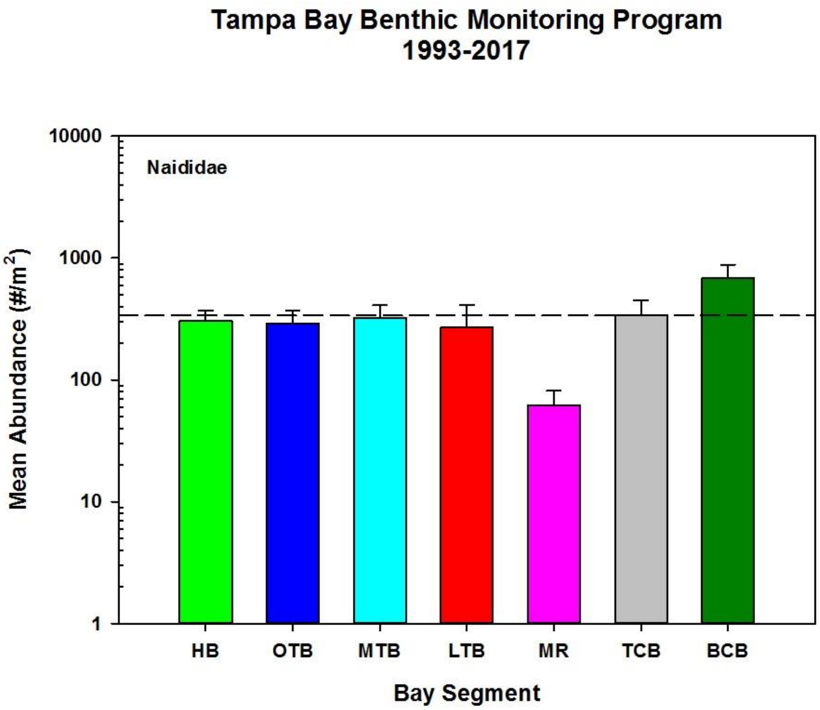

Figure 153. Mean abundance of unidentified Naididae (=Tubificinae) by bay segment. Error bars = 1 standard error, dashed line represents bay-wide mean value.

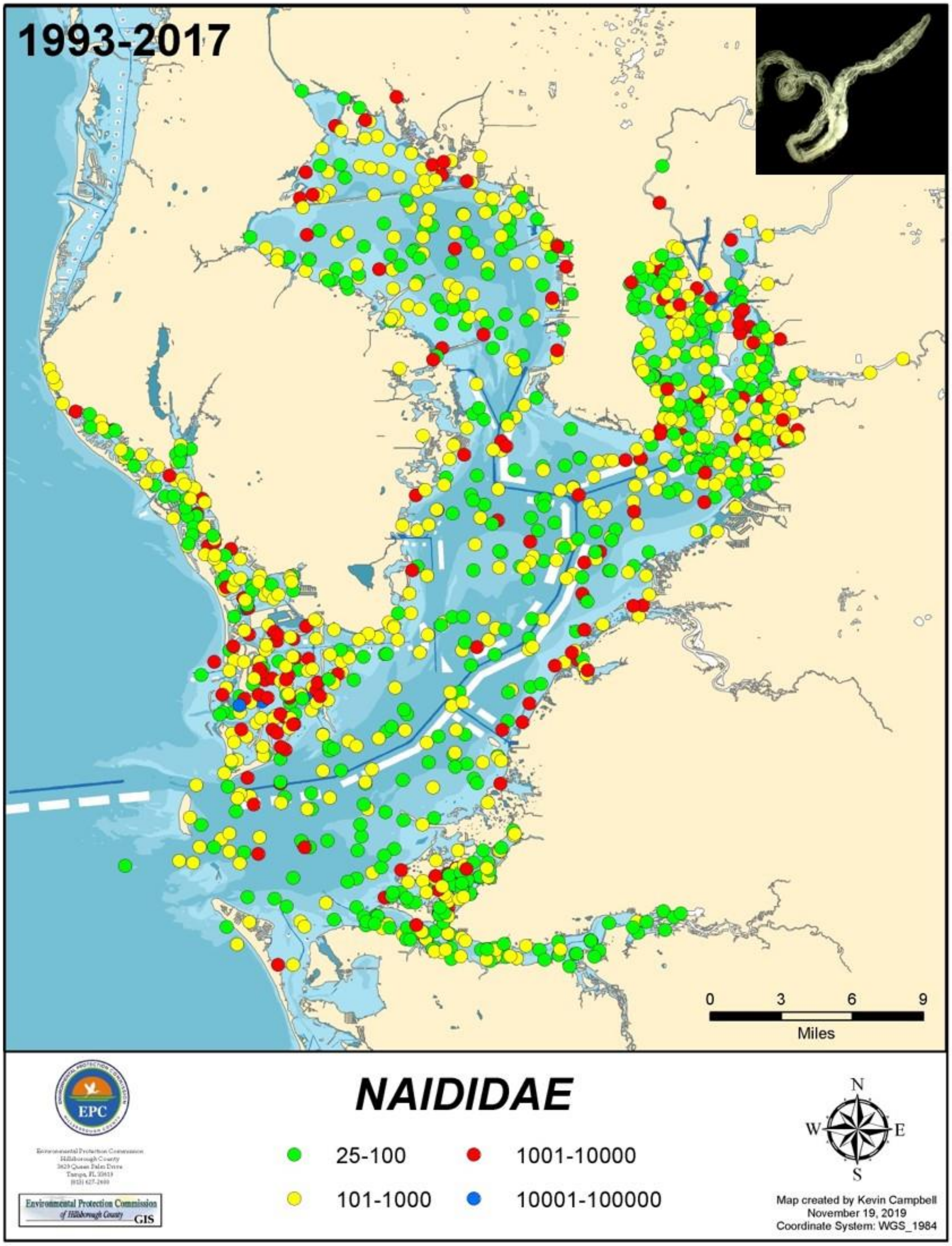

Figure 154. Late-Summer distribution of unidentified Naididae in Tampa Bay 1993-2017.

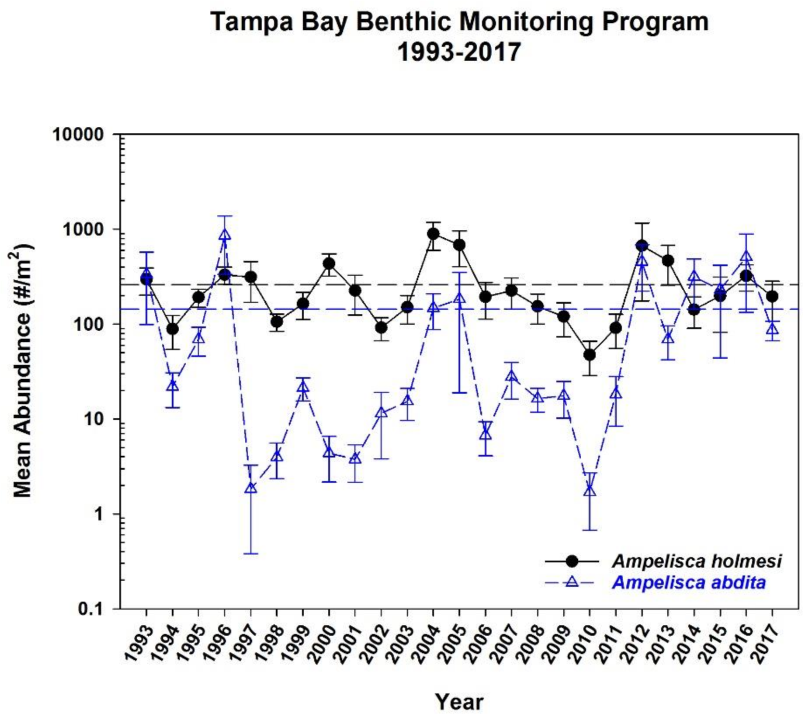

Figure 155. Mean abundance of *Ampelisca holmesi* (black dots) and *Ampelisca abdita* (blue open triangles) by year. Error bars = 1 standard error, black and blue dashed lines represent bay-wide mean values for *A. holmesi* and *A. abdita* respectively.

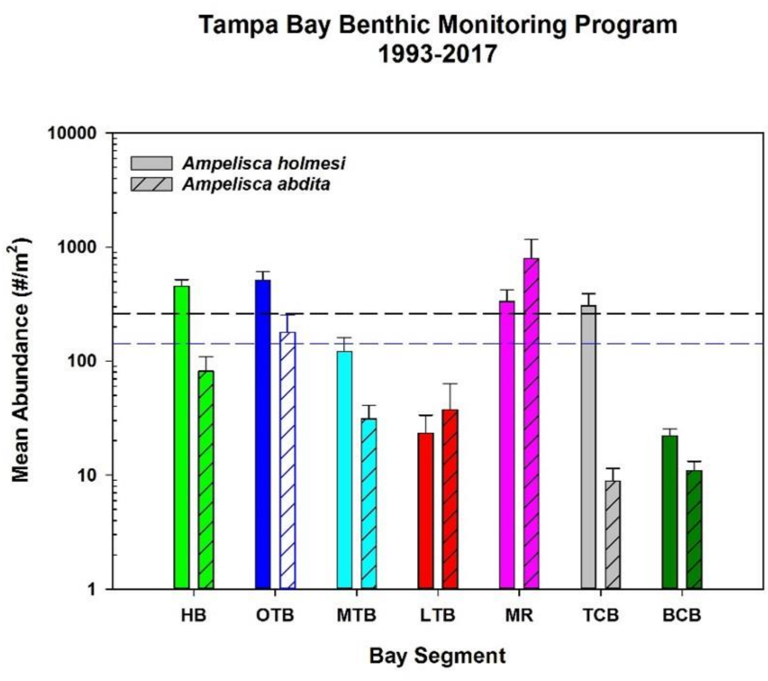

Figure 156. Mean abundance of *Ampelisca holmesi* and *Ampelisca abdita* by bay segment. Error bars = 1 standard error, black and blue dashed lines represent bay-wide mean values for *A. holmesi* and *A. abdita* respectively.

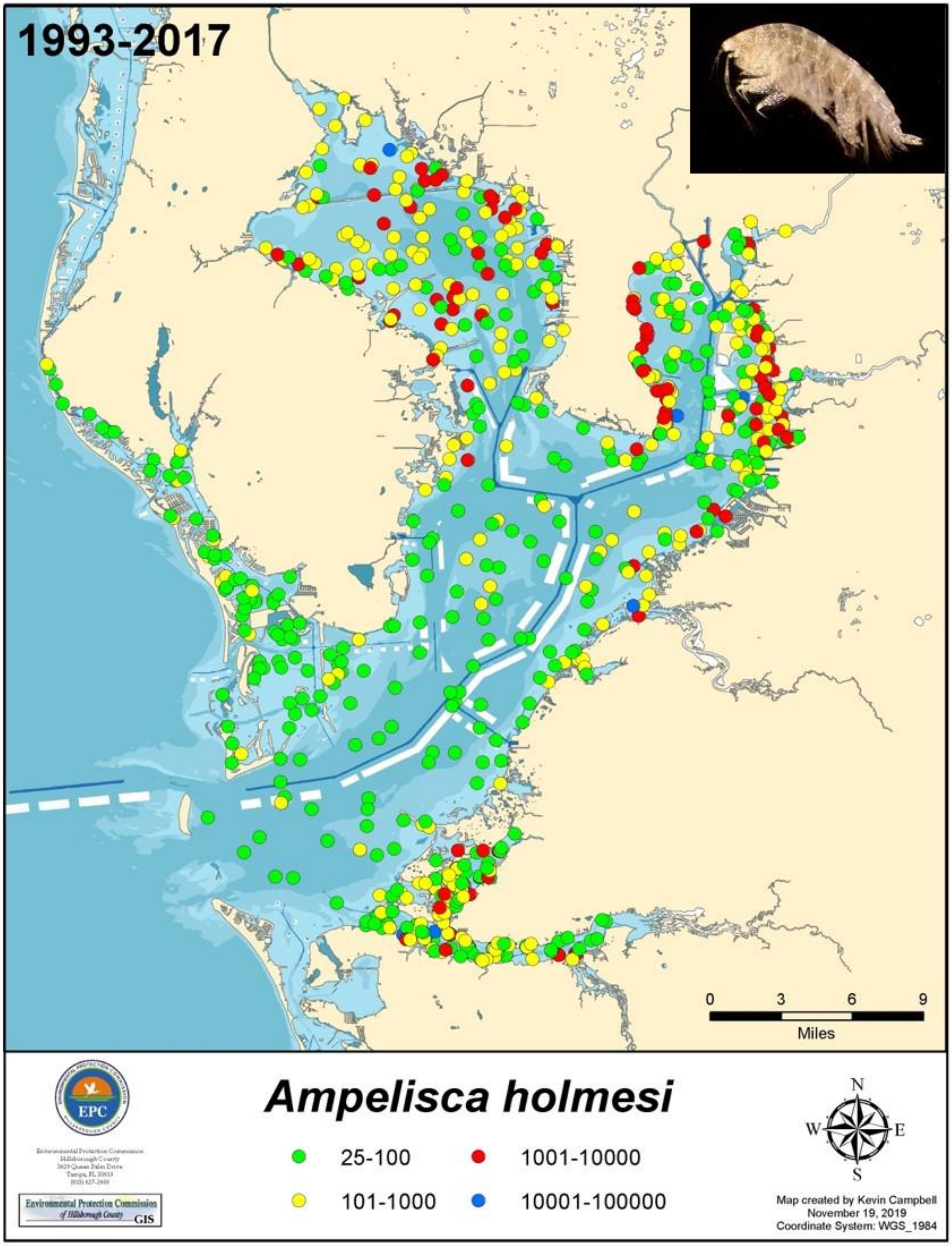

Figure 157. Late-Summer distribution of *Ampelisca holmesi* in Tampa Bay 1993-2017.

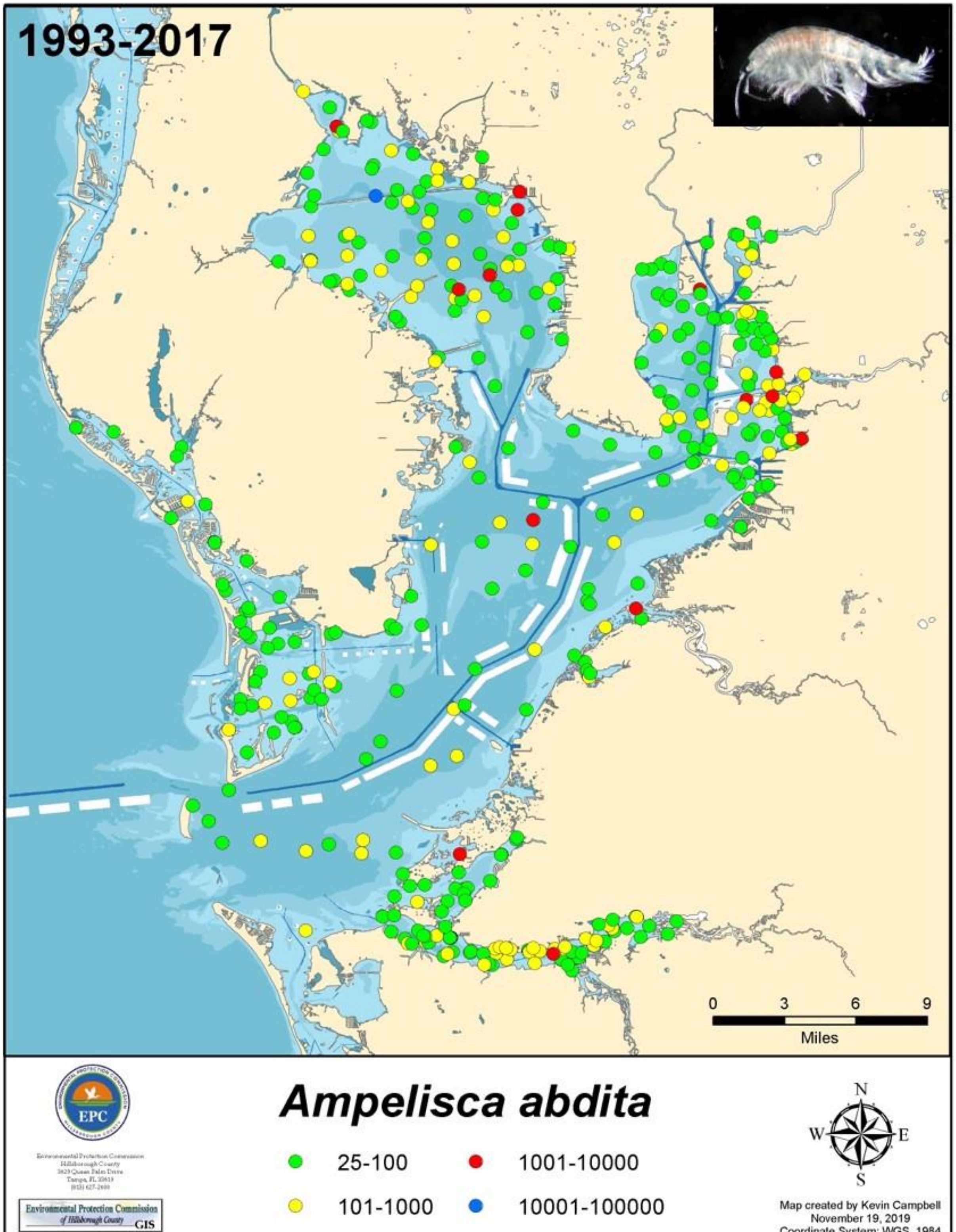

Figure 158. Late-Summer distribution of *Ampelisca abdita* in Tampa Bay 1993-2017.

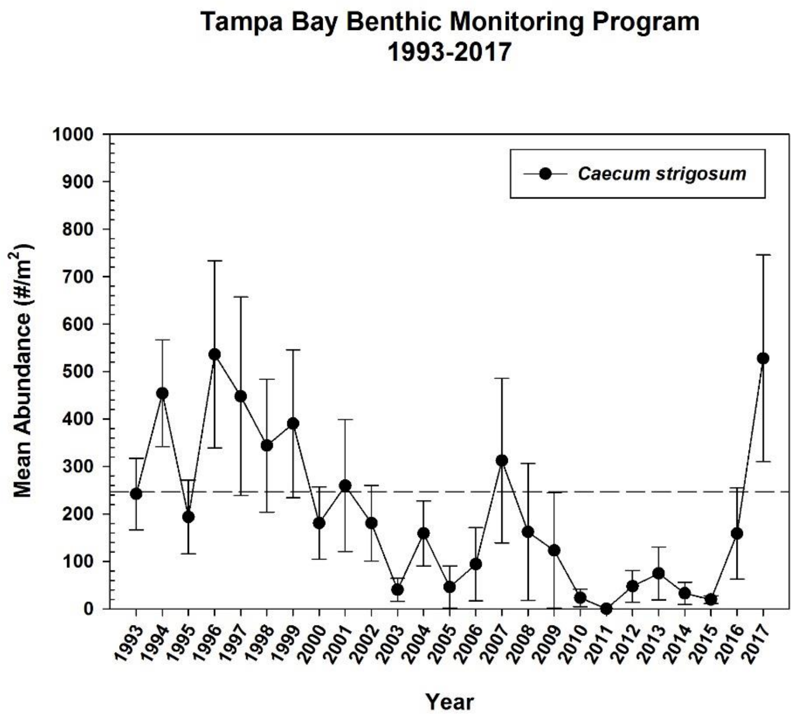

Figure 159. Mean abundance of *Caecum strigosum* by year. Error bars = 1 standard error, dashed line represents bay-wide mean value.

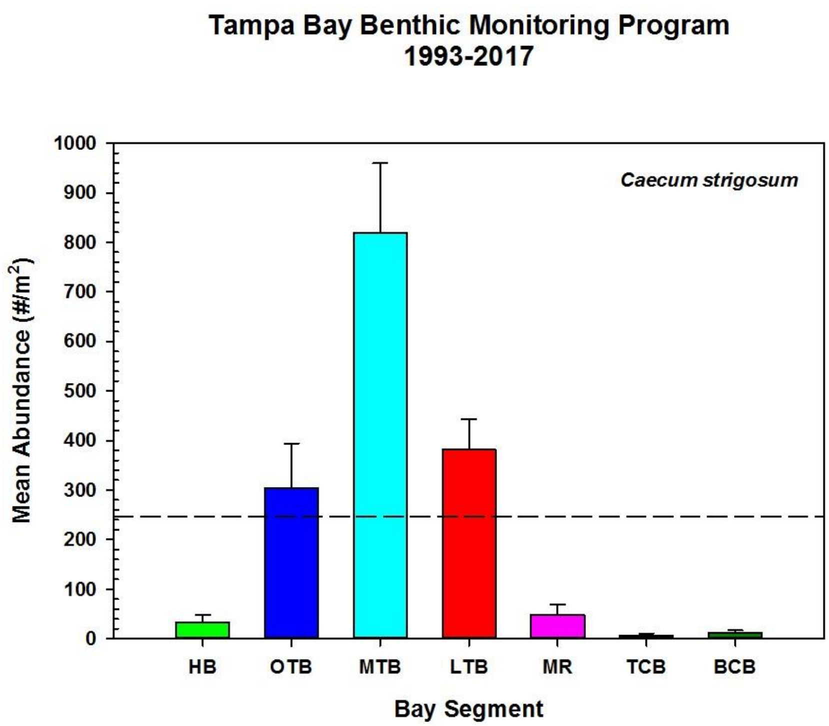

Figure 160. Mean abundance of *Caecum strigosum* by bay segment. Error bars = 1 standard error, dashed line represents bay-wide mean value.

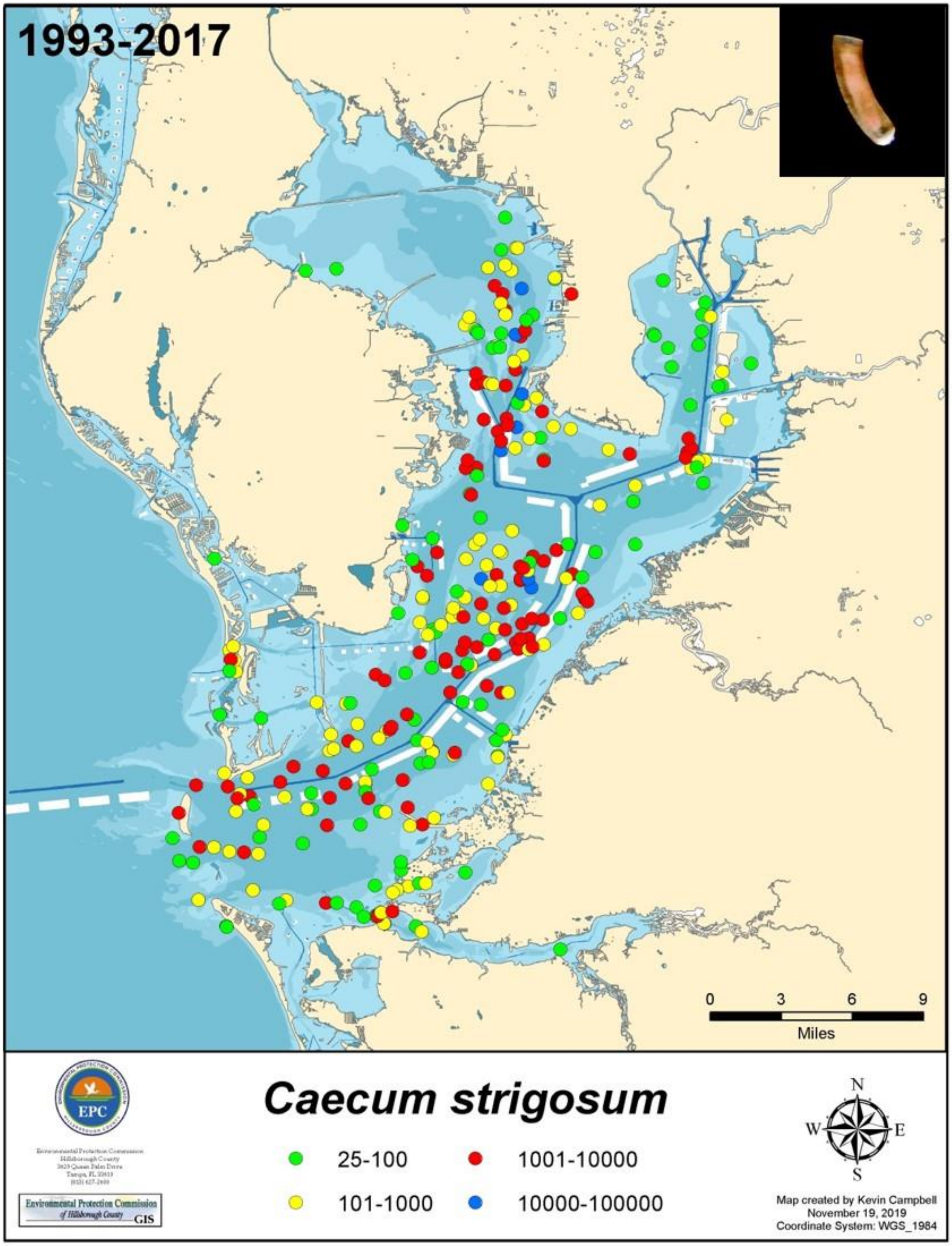

Figure 161. Late-Summer distribution of *Caecum strigosum* in Tampa Bay 1993-2017.

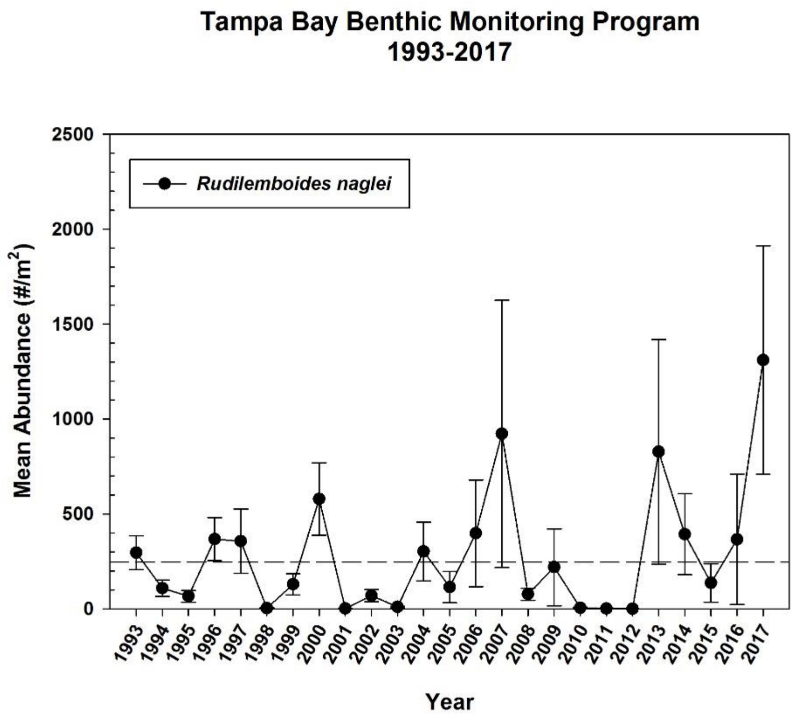

Figure 162. Mean abundance of *Rudilemboides naglei* by year. Error bars = 1 standard error, dashed line represents bay-wide mean value.

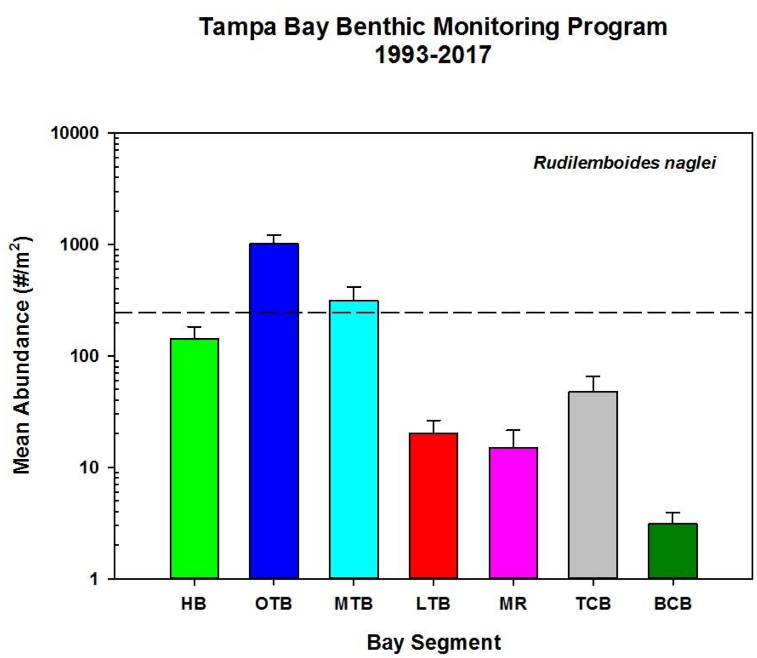

Figure 163. Mean abundance of *Rudilemboides naglei* by bay segment. Error bars = 1 standard error, dashed line represents bay-wide mean value.

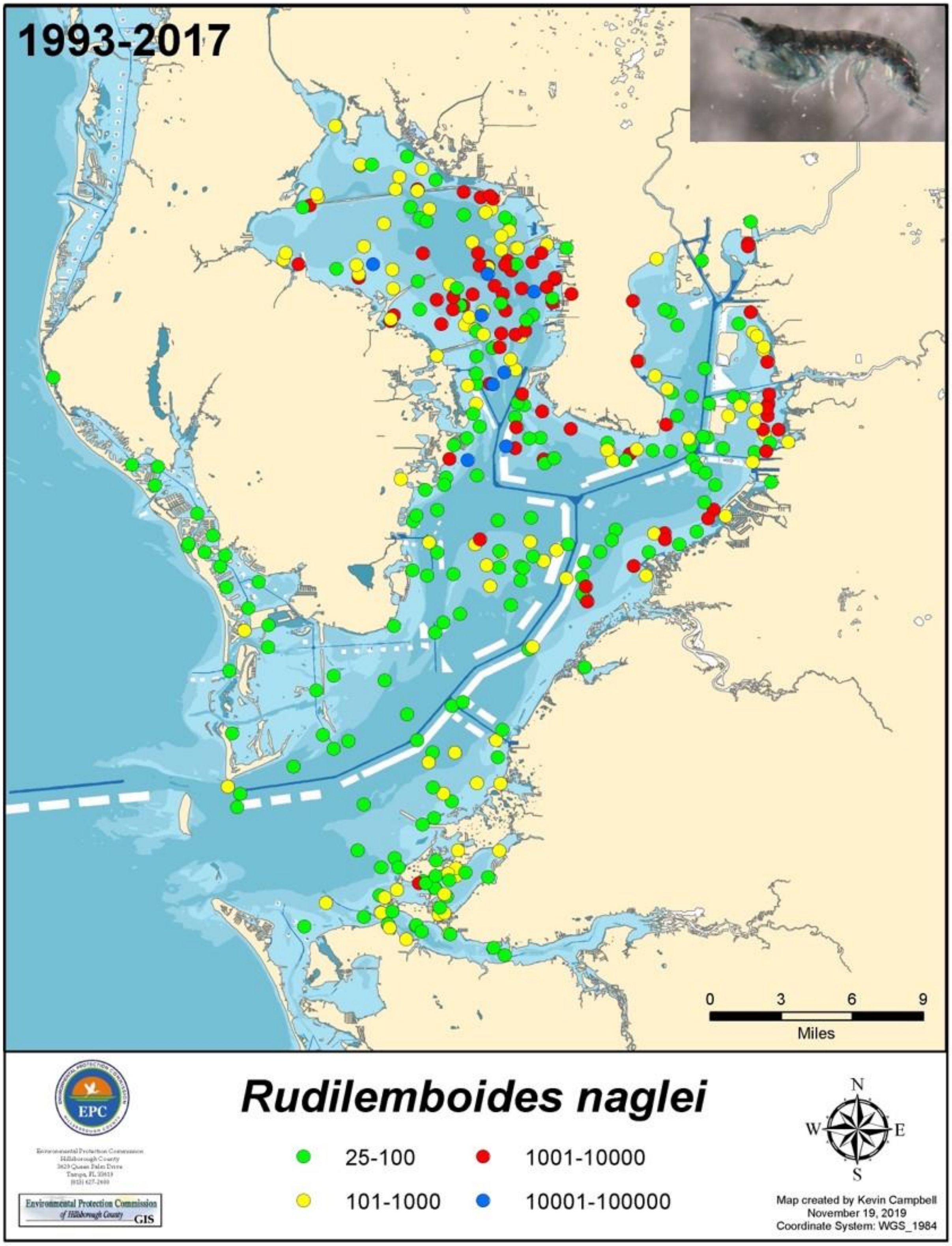

Figure 164. Late-Summer distribution of *Rudilemboides naglei* in Tampa Bay 1993-2017.

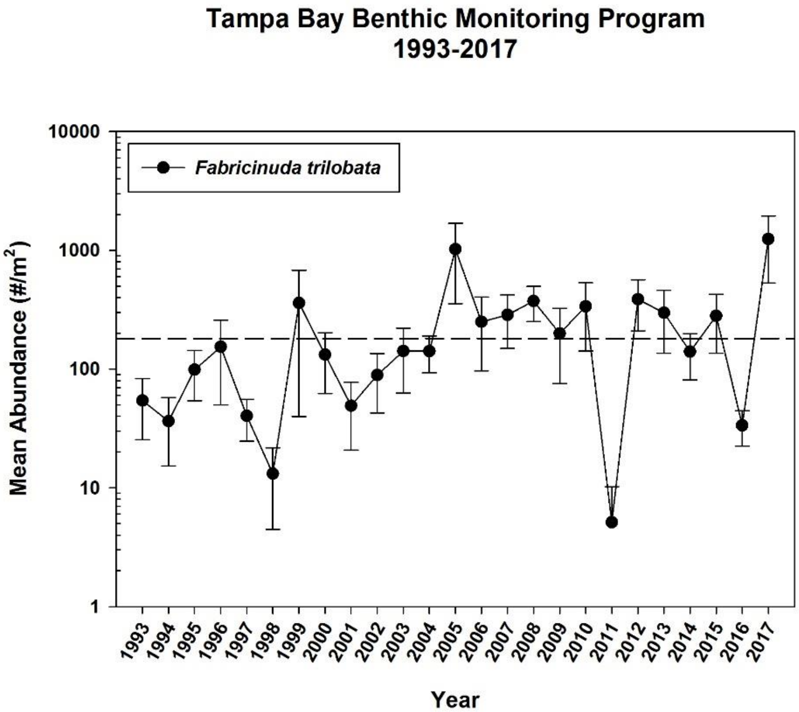

Figure 165. Mean abundance of *Fabricinuda trilobata* by year. Error bars = 1 standard error, dashed line represents bay-wide mean value.

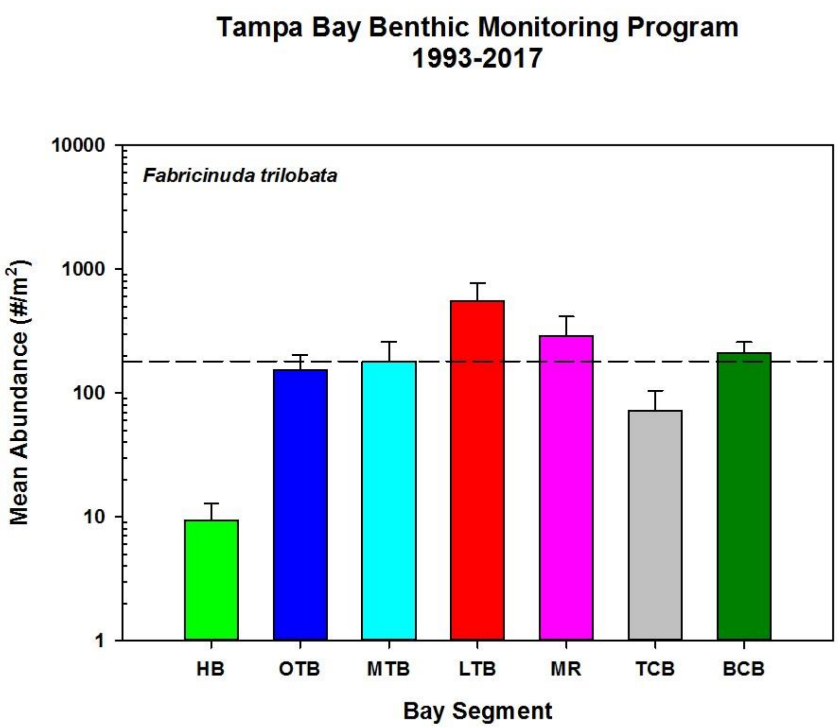

Figure 166. Mean abundance of *Fabricinuda trilobata* by bay segment. Error bars = 1 standard error, dashed line represents bay-wide mean value.

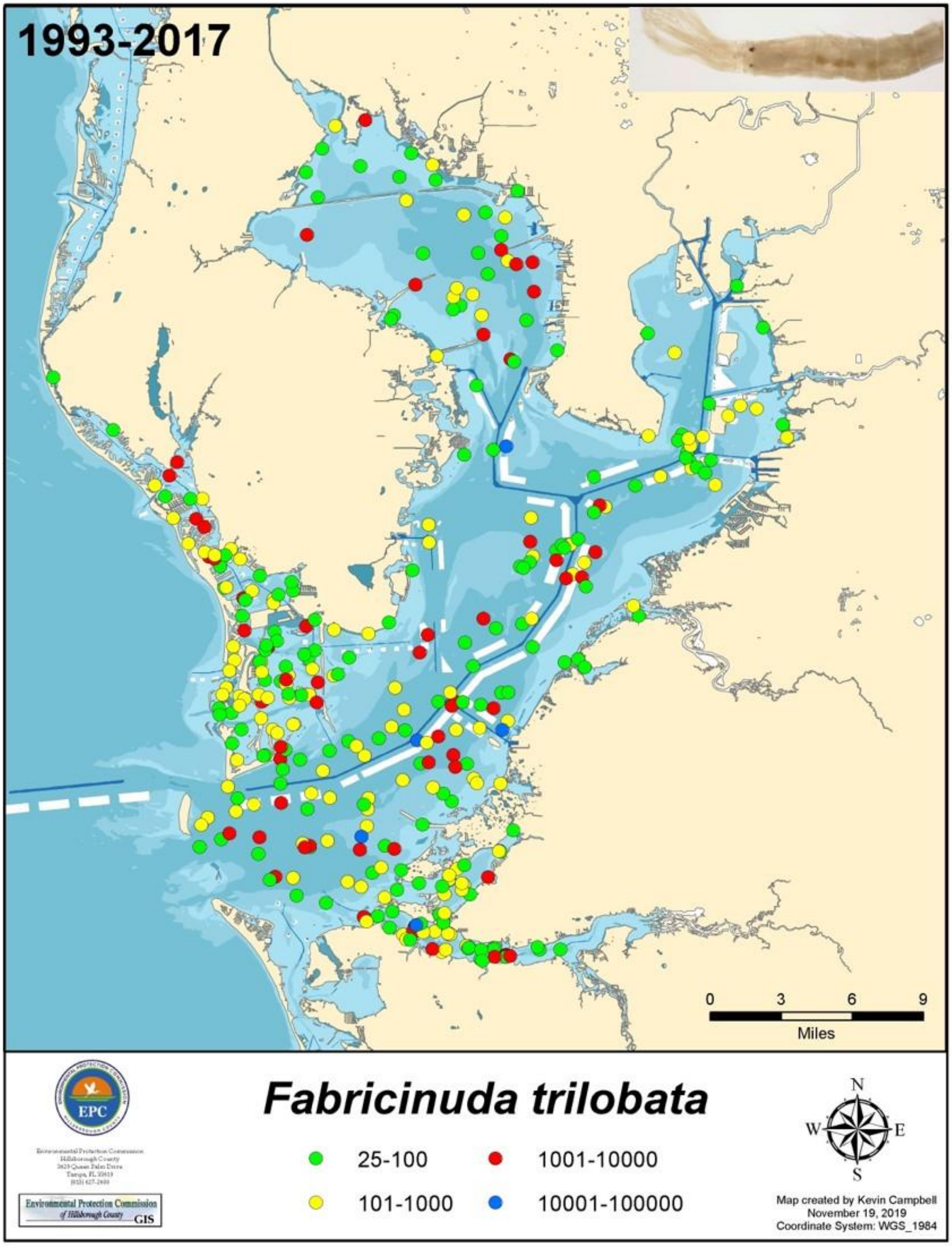

Figure 167. Late-Summer distribution of *Fabricinuda trilobata* in Tampa Bay 1993-2017.

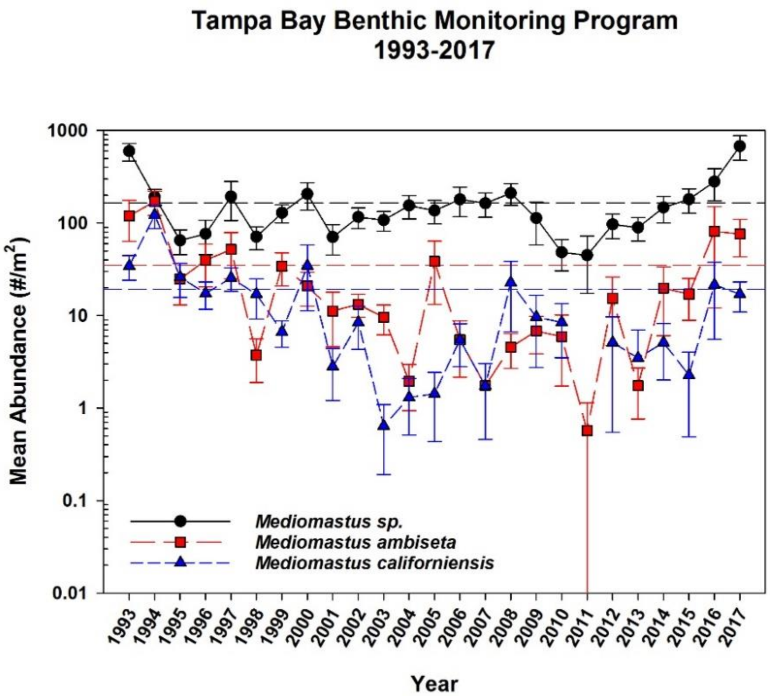

Figure 168. Mean abundance of unidentified *Mediomastus* sp. (black circles), *Mediomastus ambiseta* (red squares) and *Mediomastus californiensis* (blue triangles) by year. Error bars = 1 standard error, dashed lines represent bay-wide mean values for each respective taxon.

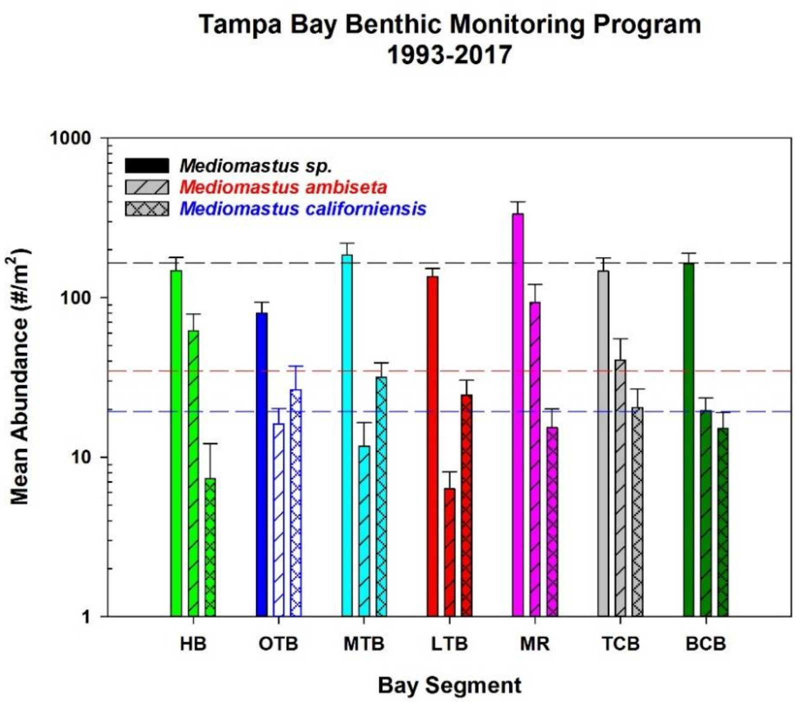

Figure 169. Mean abundance of unidentified *Mediomastus* spp. (solid bars), *Mediomastus ambiseta* (diagonal hash) and *Mediomastus californiensis* (cross hash) by bay segment. Error bars = 1 standard error, dashed lines represent bay-wide mean value for each respective taxon.

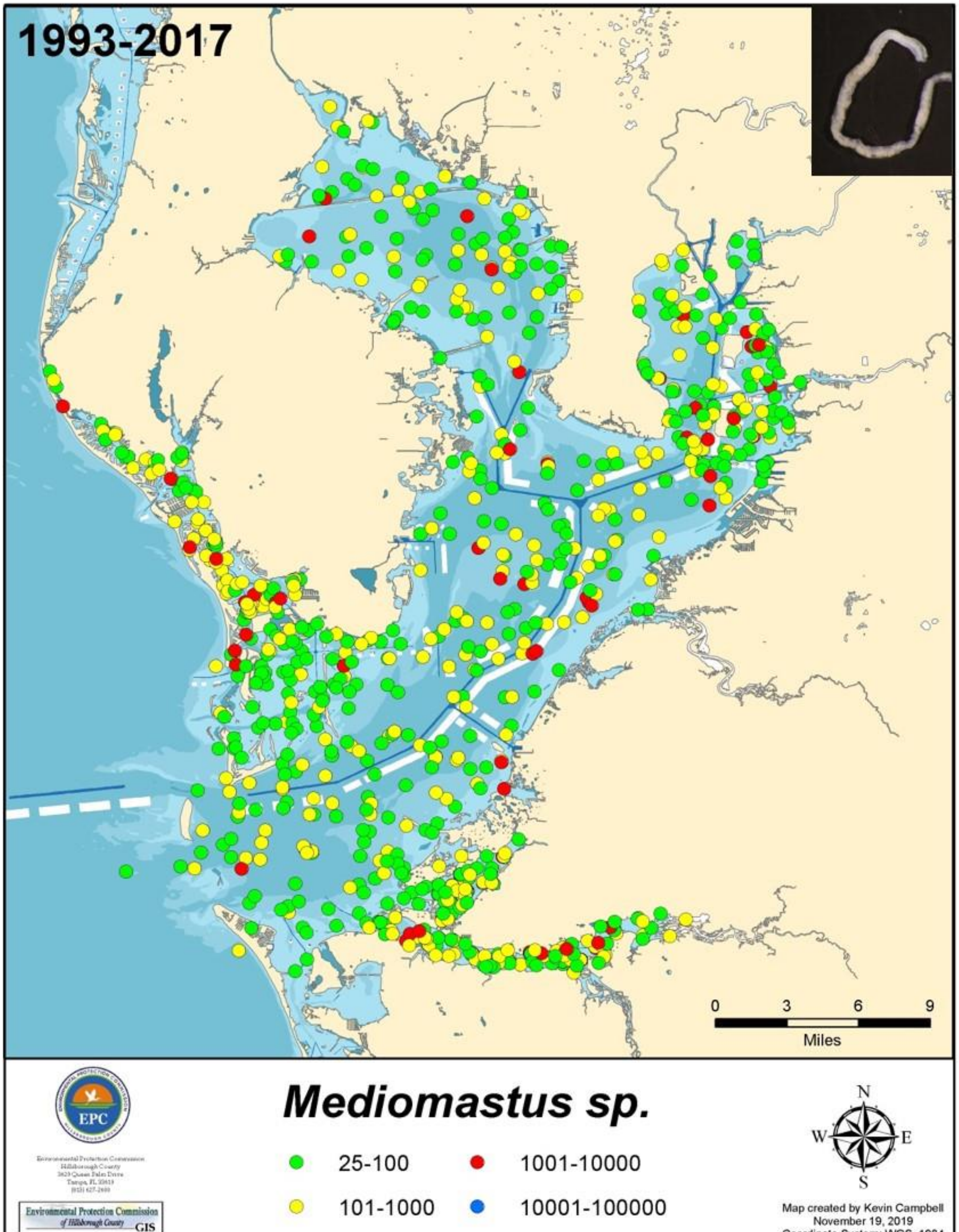

Figure 170. Late-Summer distribution of unidentified *Mediomastus spp.* in Tampa Bay 1993-2017.

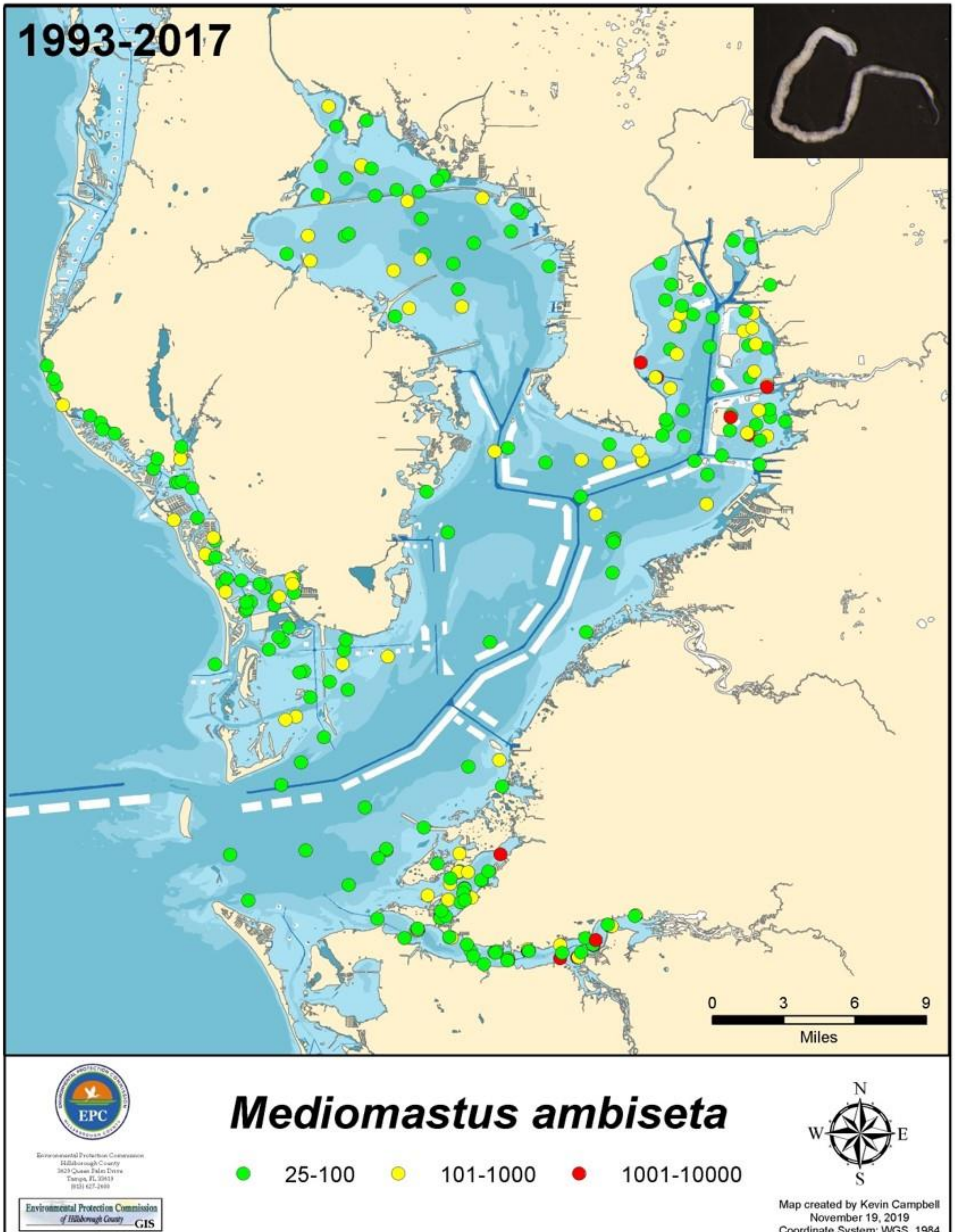

Figure 171. Late-Summer distribution of *Mediomastus ambiseta* in Tampa Bay 1993-2017.

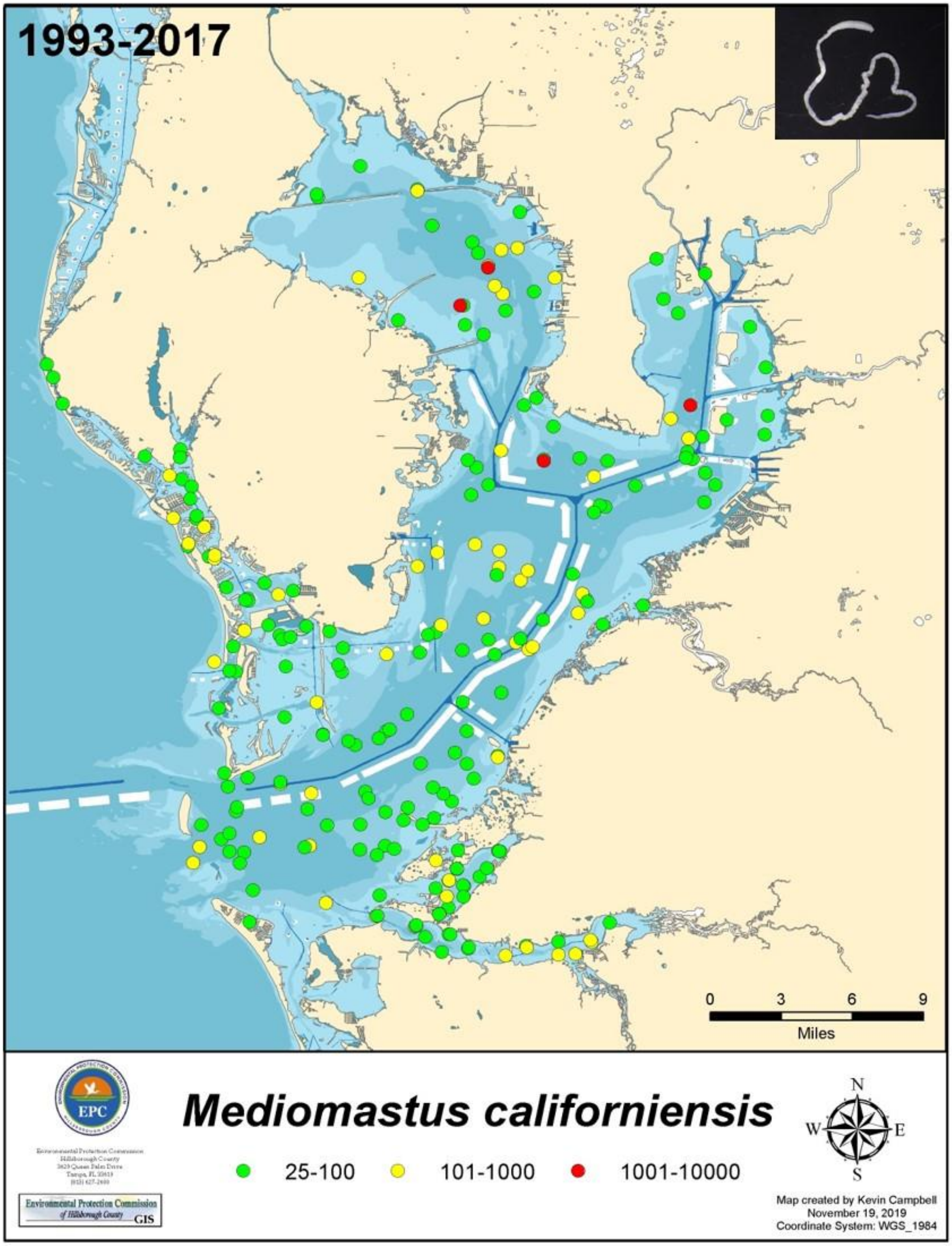

Figure 172. Late-Summer distribution of *Mediomastus californiensis* in Tampa Bay 1993-2017.

Benthic Community Similarity Analysis

Cluster analysis of sampling years (Figure 173) indicated that the Tampa Bay benthic community fell into five main temporal groupings: 1993 - 2002 (Group A); 2004 + 2006-2009 (Group B); 2003+2005 (Group C); 2012-2017 (Group D); and 2010+2011 (Group E). SIMPER analysis found the Group A years had an average Bray-Curtis similarity of 63.64%, with *Branchiostoma floridae*, *Kirkegaardia sp.,* and *Caecum strigosum* contributing to the similarity among those years. Group B had and average similarity of 60.64%, with Naididae, *Kirkegaardia sp.*, *Mysella planulata,* and *Fabricinuda trilobata* contributing to the similarity among years. Group C had an average similarity of 57.83% among years, with the bivalve *Amygdalum papyrium,* Naididae, *Kirkegaardia sp,* and *Glottidia pyramidata* contributing to the similarity. Group D had an average similarity of 62.15% among years, with *Branchiostoma floridae*, Naididae, *Kirkegaardia sp*., *Caecum pulchellum,* and *Ampelisca holmesi* contributing to the similarity. Group E had an average similarity of 56.91%, with Naididae, the gastropod *Bittiolum varium*, *Kirkegaardia sp*. and the polychaetes *Paraprionospio* sp. and *Aricidea philbinae* to the similarity among years.

The similarity profile test (SIMPROF) divided Group A into four sub-groupings: A1 (1993 +1994); A2 (1995+1996); A3 (1998+2001); and A4 (1997+1999 with 2000 as an outlier); additionally, 2002 was an outlier for groups A3 and A4 combined (Figure 173). SIMPER analysis showed that A1 had an average similarity of 66.99%, and was characterized by high abundances of *Branchiostoma floridae, Kirkegaardia sp.,* and *Prionospio perkinsi*. The A2 group had an average similarity of 67.23%, and was characterized by Naididae, *Branchiostoma floridae, Caecum strigosum,* and *Ampelisca holmesi*. Group A3 had an average similarity of 67.85%, with *Kirkegaardia sp*, *Caecum strigosum,* and Naididae contributing to the similarity. Group A4 was characterized by *Branchiostoma floridae, Kirkegaardia sp., Caecum strigosum,* Naididae, as well as *Glottidia pyramidata*.

Within Group B, sampling years 2004+2006, and 2007 formed subgroup (B1), while 2008+2009 formed subgroup (B2) (Figure 173). The B1 group had an average similarity of 61.56%, with *Kirkegaardia sp*., *Rudilemboides naglei*, Naididae, and *Branchiostoma floridae* contributing to the similarity. The B2 group had an average similarity of 63.95%, with *Mysella planulata*, the tanaid crustacean *Mesokalliapseudes macsweenyi*, Naididae, and *Fabricinuda trilobata*.

Within Group D, 2013, 2014, and 2015 formed one group and 2016 and 2017 formed another subgroup, designated D1 and D2 respectively, with 2012 as an outlier (Figure 173). The D1 group had an average similarity of 66.19%, with *Branchiostoma floridae,* Naididae, *Caecum pulchellum*, *Kirkegaardia sp*., and *Rudilemboides naglei* contributing to the similarity. The D2 group had an average similarity of 65.8%, with *Caecum pulchellum*, *Branchiostoma floridae*, Naididae, *Mysella planulata,* and spirorbid polychaetes (Spirorbidae) contributing to the similarity among years.

The cluster analysis performed on the average species assemblage by bay segment (Figure 174) showed that the Tampa Bay benthic community fell into two main spatial groupings; with the upper segments (Hillsborough Bay and Old Tampa Bay) plus Terra Ceia Bay and the Manatee River forming one group (Group A), and the lower segments of the bay (Middle Tampa Bay, Lower Tampa Bay, and Boca Ciega Bay) forming the second group (Group B). Group A bay segments had an average Bray-Curtis similarity of 61.68%, and were characterized by high abundances of *Ampelisca holmesi, Kirkegaardia sp.*, *Mysella planulata,* Naididae, and the bivalve *Mulinia lateralis.* The Group B segments had an average similarity of 64.92%, and were characterized by *Branchiostoma floridae*, Naididae oligochaetes, the maldanid polychaete (“bamboo worm”) *Clymenella mucosa*, the spirorbid polychaete *Neodexiospira steueri,* and *Fabricinuda trilobata*.

Within Group A, Hillsborough Bay and Old Tampa Bay were more similar and form a subgroup designated Group A1, whereas the Manatee River and Terra Ceia Bay formed a subgroup designated A2 (Figure 174). Group A1 had an average similarity of 65.65%, with *Mysella planulata*, *Ampelisca holmesi,* and *Glottidia pyramidata* contributing to the similarity within that group. Group A2 had an average similarity of 64.97%, with *Kirkegaardia sp., Caecum pulchellum*, *Ampelisca holmesi*, and *Mulinia lateralis* contributing to the similarity within that group.

Within Group B, the Middle Tampa Bay and Lower Tampa Bay segments formed a distinct subgroup; designated B1 in Figure 174. The B1 subgroup had an average similarity of 69.98%, and had high abundances of *Branchiostoma floridae* and *Caecum strigosum*. Boca Ciega Bay (designated B2 in Figure 174) had higher abundances of the spirorbid polychaetes *Pileolaria rosepigmentata*, unidentified Spirorbinae, and the sabellid polychaete *Augeneriella hummelincki*.

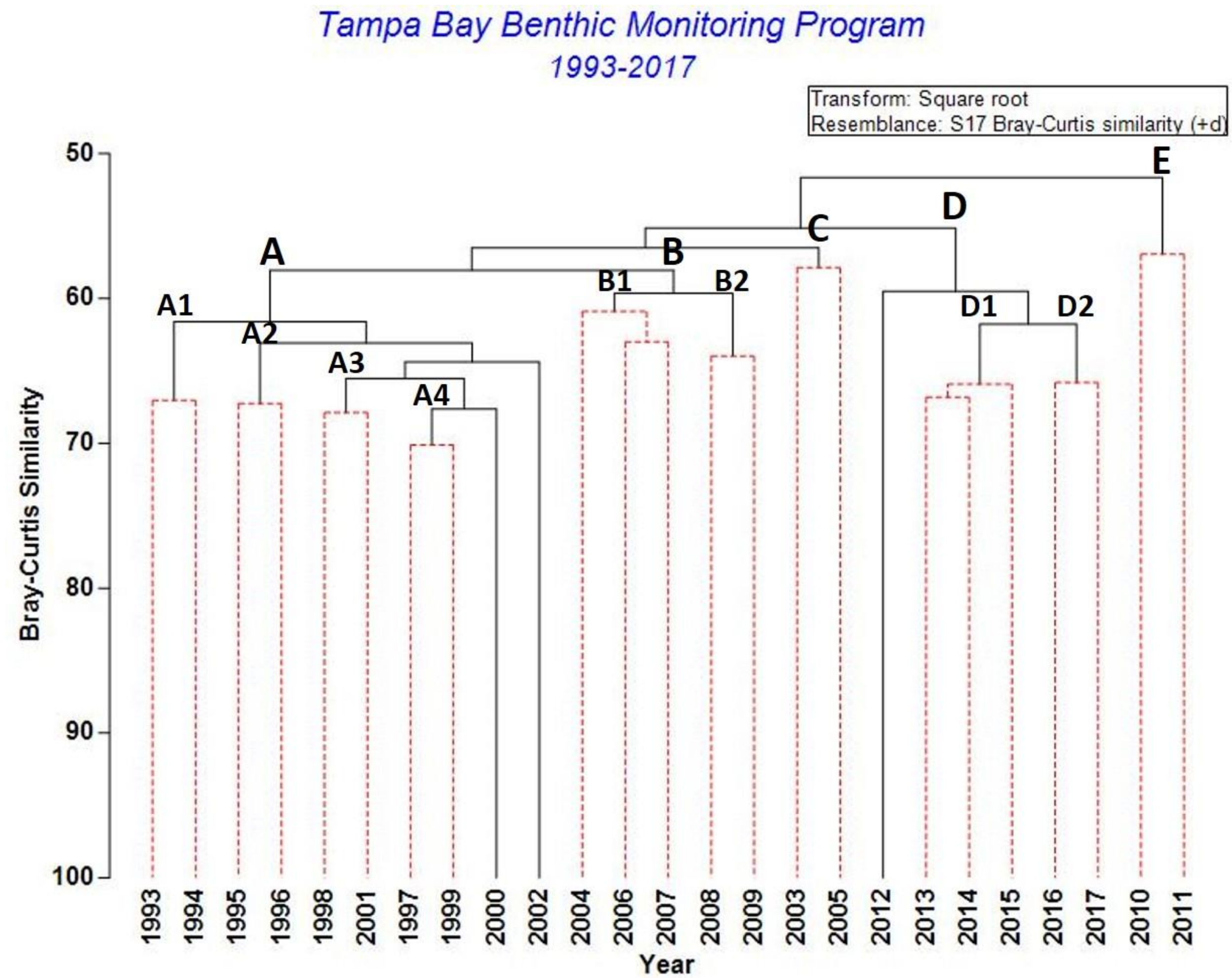

Figure 173. Cluster Analysis: Benthic community averaged by year.

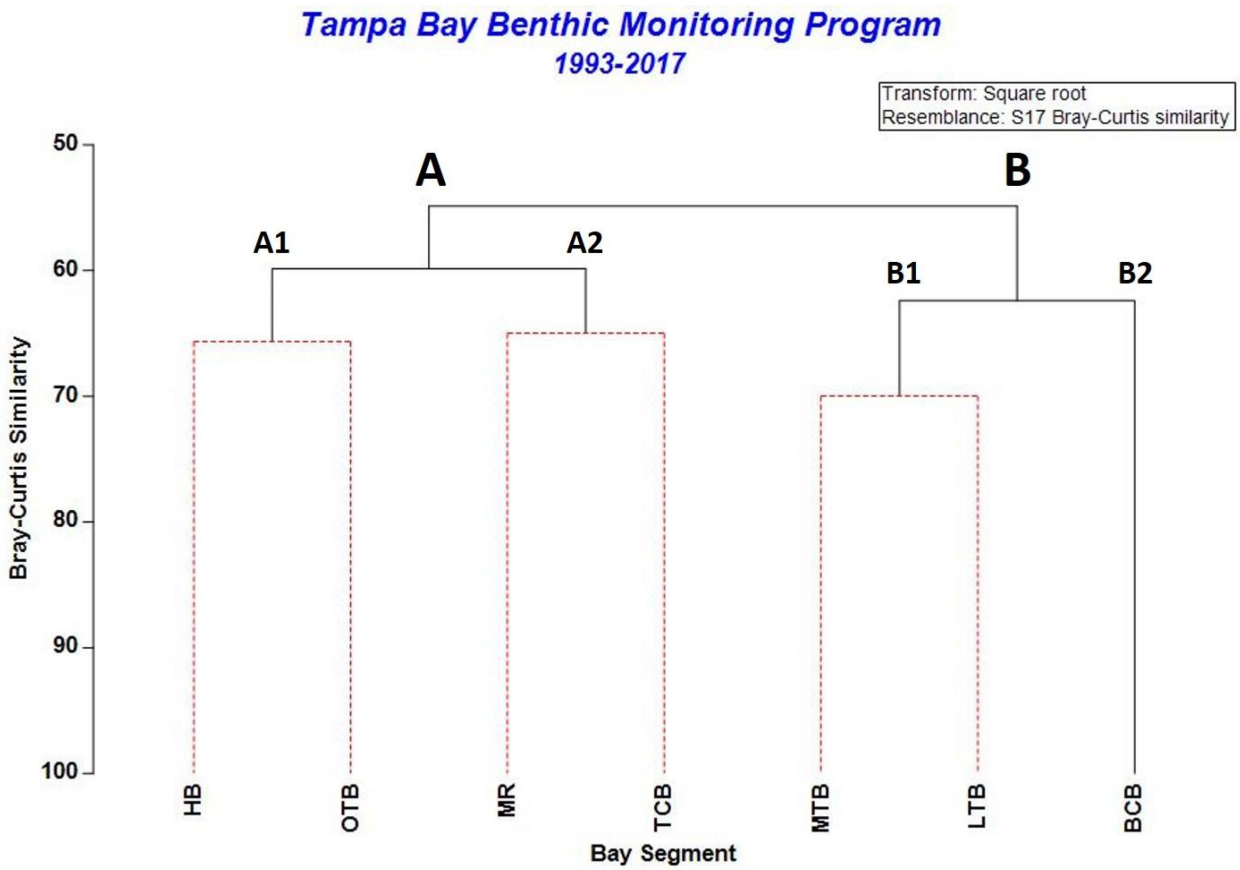

Figure 174. Cluster Analysis; Benthic community averaged by bay segment.

Relating Biological and Environmental data

Table 22 presents multiple linear regression analysis of the benthic community indices compared with the six measured hydrographic and sediment parameters and the mean sediment contaminant PEL ratio. Depth and bottom temperature had a positive correlation with species richness (*S*). Salinity was positively correlated with species richness, abundance (*N*), Shannon Diversity (*H'*), Pielou's evenness *(J'*), and the adjusted Tampa Bay AMBI (Adj. TB_AMBI) index, however it was negatively correlated with the Gulf of Mexico AMBI (GoM_AMBI) index, because this index is on an opposite scale. Bottom dissolved oxygen was positively correlated with species richness, abundance, Shannon diversity, the Tampa Bay Benthic Index (TBBI), and Adj. TB_AMBI, and negatively with the GoM AMBI. Bottom pH had a negative correlation with abundance. The percent silt+clay was negatively correlated with species richness, abundance, Shannon diversity, the TBBI, and Adj. TB_AMBI, but positively with evenness and the GoM_AMBI. The mean PEL Ratio was not significantly correlated to any of the benthic community indices except for a positive relationship with the GoM_AMBI.

Spearman Rank Order correlations between the benthic community indices and the hydrographic and sediment parameters are presented in Table 23. Species richness had a positive correlation with salinity, bottom dissolved oxygen, and pH; but was negatively correlated with percent silt+clay and the PEL ratio. Abundance and Shannon diversity were both positively correlated with salinity, dissolved oxygen, and pH, but negatively with the % silt+clay and PEL ratio. Evenness was positively correlated with salinity, and with the % silt+clay and PEL ratio. The Tampa Bay Benthic Index showed positive correlations with depth, salinity, dissolved oxygen, and pH, but was negatively correlated with % silt+clay and PEL Ratio. The GoM AMBI and the Adj. TB_AMBI indices were both correlated with all of the measured physical parameters, except depth. The GoM AMBI was negatively correlated with salinity, dissolved oxygen, and pH, but positively with temperature, % silt+clay and PEL. The Adj. TB_AMBI has the opposite correlation with the same parameters. Higher salinities and dissolved oxygen corresponded to less polluted habitats, and higher silt+clay and PEL ratios indicated more polluted habits with both indices.

Table 22. Multiple linear regression results of benthic community indices vs. physical parameters.

	Adj. R^2	n	Depth	Temp	Salinity	DO	pH	Silt+Clay	PEL Ratio
Species Richness (*S*)	**0.460**	**1619**	**+ (p=0.007)**	**+ (p=0.012)**	**+ (p<0.001)**	**+ (p<0.001)**	**NS (p=0.128)**	**- (p<0.001)**	**NS (p=0.200)**
Abundance (*N*)	**0.351**	**1619**	**NS (p=0.244)**	**+ (p=0.002)**	**+ (p=0.003)**	**+ (p<0.001)**	**- (p=0.039)**	**- (p<0.001)**	**NS (p=0.358)**
Shannon Diversity (*H'*)	**0.349**	**1619**	**NS (p=0.484)**	**NS (p=0.483)**	**+ (p<0.001)**	**+ (p<0.001)**	**NS (p=0.440)**	**- (p<0.001)**	**NS (0.273)**
Pielou's Evenness (*J'*)	**0.019**	**1579**	**- (p=0.038)**	**NS (p=0.361)**	**+ (p<0.001)**	**NS (p=0.334)**	**NS (p=0.620)**	**+ (p<0.001)**	**NS (p=0.737)**
TBBI	**0.224**	**1608**	**NS (p=0.668)**	**NS (p=0.836)**	**NS (p=0.301)**	**+ (p<0.001)**	**NS (p=0.542)**	**- (p<0.001)**	**NS (p=0.548)**
GoM_AMBI	**0.357**	**1618**	**NS (p=0.491)**	**NS (p=0.638)**	**- (p<0.001)**	**- (p<0.001)**	**NS (p=0.841)**	**+ (p<0.001)**	**+ (p=0.028)**
Adj TB_AMBI	**0.462**	**1619**	**NS (p=0.851)**	**NS (p=0.624)**	**+ (p<0.001)**	**+ (p<0.001)**	**NS (p-0.059)**	**- (p<0.001)**	**NS (p=0.476)**

Note: All parameters were log(n+1) transformed for analysis except J' and Silt+Clay, which were arcsin(√) transformed for analysis

Table 23. Spearman correlation coefficients (ρ) and statistical p-values for benthic community indices vs. environmental parameters and mean sediment PEL ratio.

		Depth	Temp	Salinity	DO	pH	Silt+Clay	PEL Ratio
Species Richness (*S*)	ρ	0.053	0.014	0.354	0.292	0.242	-0.312	-0.255
	p	0.025	0.570	<0.001	<0.001	<0.001	<0.001	<0.001
	n	1790	1779	1788	1774	1732	1780	1671
Abundance (*N*)	ρ	0.005	0.051	0.067	0.173	0.097	-0.294	-0.228
	p	0.833	0.031	0.005	<0.001	<0.001	<0.001	<0.001
	n	1790	1779	1788	1774	1732	1780	1671
Shannon Diversity (*H'*)	ρ	-0.005	-0.022	0.376	0.277	0.240	-0.228	-0.211
	p	0.818	0.347	<0.001	<0.001	<0.001	<0.001	<0.001
	n	1790	1779	1788	1774	1732	1780	1671
Pielou's Evenness (*J'*)	ρ	-0.017	-0.031	0.172	0.031	0.038	0.110	0.075
	p	0.484	0.204	<0.001	0.196	0.119	<0.001	0.002
	n	1749	1738	1747	1733	1691	1739	1631
TBBI	ρ	0.087	-0.020	0.168	0.253	0.201	-0.377	-0.280
	p	<0.001	0.406	<0.001	<0.001	<0.001	<0.001	<0.001
	n	1779	1768	1777	1763	1721	1769	1660
GoM_AMBI	ρ	0.020	0.069	-0.203	-0.372	-0.245	0.509	0.336
	p	0.401	0.003	<0.001	<0.001	<0.001	<0.001	<0.001
	n	1789	1778	1787	1773	1731	1779	1670
Adj TB_AMBI	ρ	0.058	-0.131	0.377	0.478	0.283	-0.669	-0.434
	p	0.015	<0.001	<0.001	<0.001	<0.001	<0.001	<0.001
	n	1790	1779	1788	1774	1732	1780	1671

Non-metric Multi-Dimensional Scaling (MDS) indicates that the benthic communities within individual bay segments were relatively distinct and consistent over time (Figure 175), and this trend is even more apparent when the data are averaged by segment and year (Figure 176). There is an apparent gradation in the species composition from the upper to the lower segments of the Bay, with little overlap in species composition between Hillsborough Bay and Lower Tampa Bay. Boca Ciega Bay appeared to have a unique benthic community. The Manatee River and Terra Ceia Bay benthic communities were more variable, which may be a result of the smaller number of samples collected in these two segments.

Coding the sample points for descriptive categories of the different physical parameters illustrates that the benthic community composition is structured in part by depth (Figure 177), salinity (Figure 178), dissolved oxygen (Figure 179), and sediment type (Figure 180).
The MDS plot coded by the PEL grade indicates a general relationship between the benthic community composition and level of sediment contamination, with the higher contaminated "F" and "D" samples grouping together and separately from the lower contaminated "A" and "B"

samples (Figure 181). The MDS plots coded by the TBBI (Figure 182), the Gulf of Mexico AMBI (Figure 183), and Tampa Bay AMBI (Figure 184) pollution classification all show similar trends, with the more polluted/degraded sites grouping towards the right side of the plot and unpolluted/healthy sites grouping together on the left side of the plot.

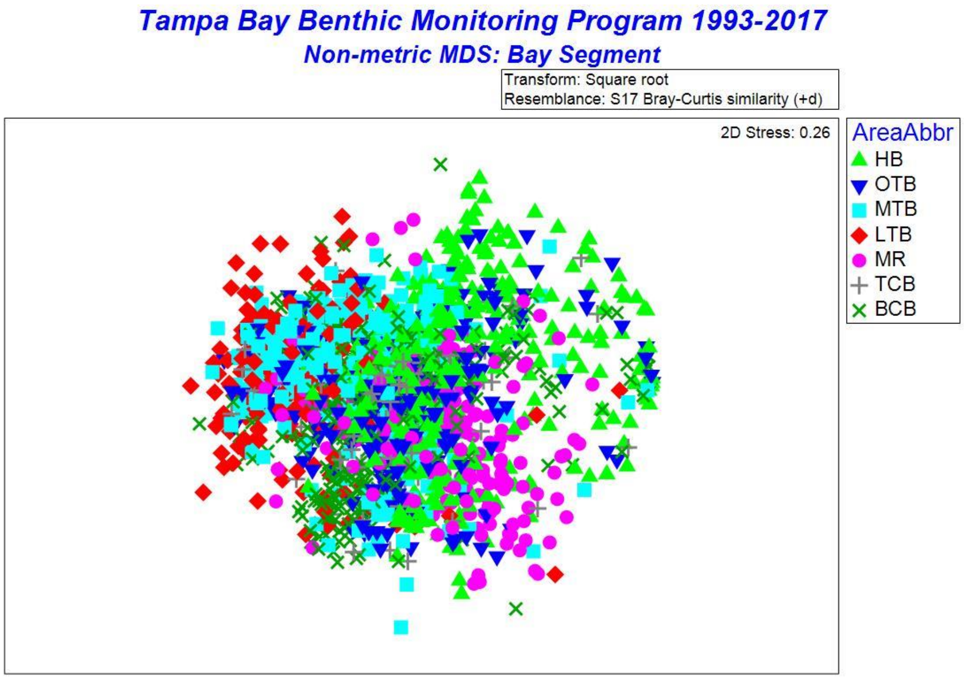

Figure 175. MDS plot of benthic species composition by bay segment - all samples shown.

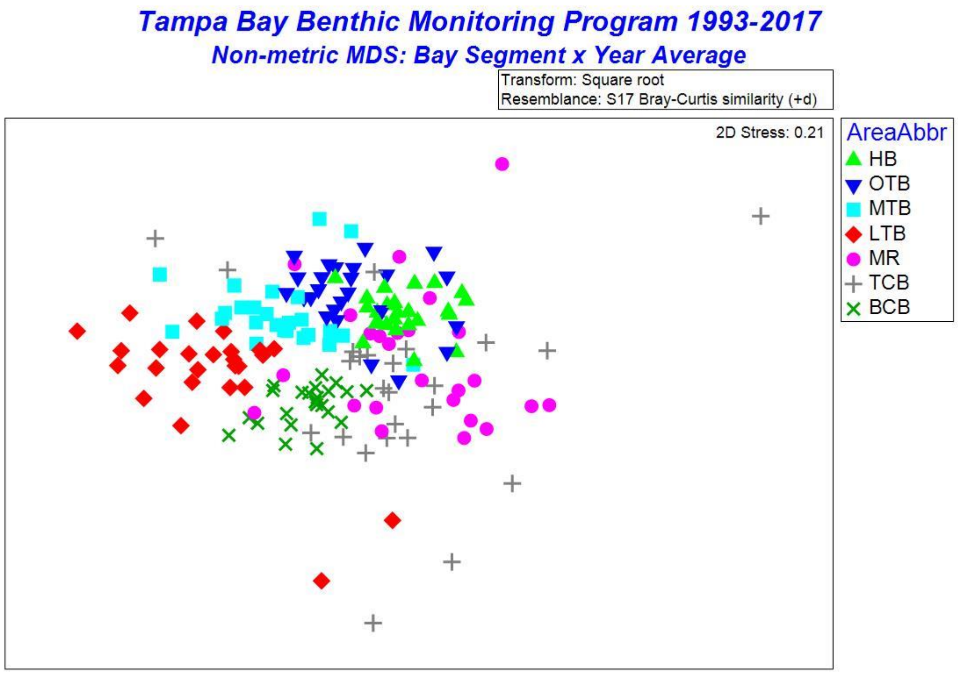

Figure 176. MDS plot of benthic species composition by year and bay segment averaged.

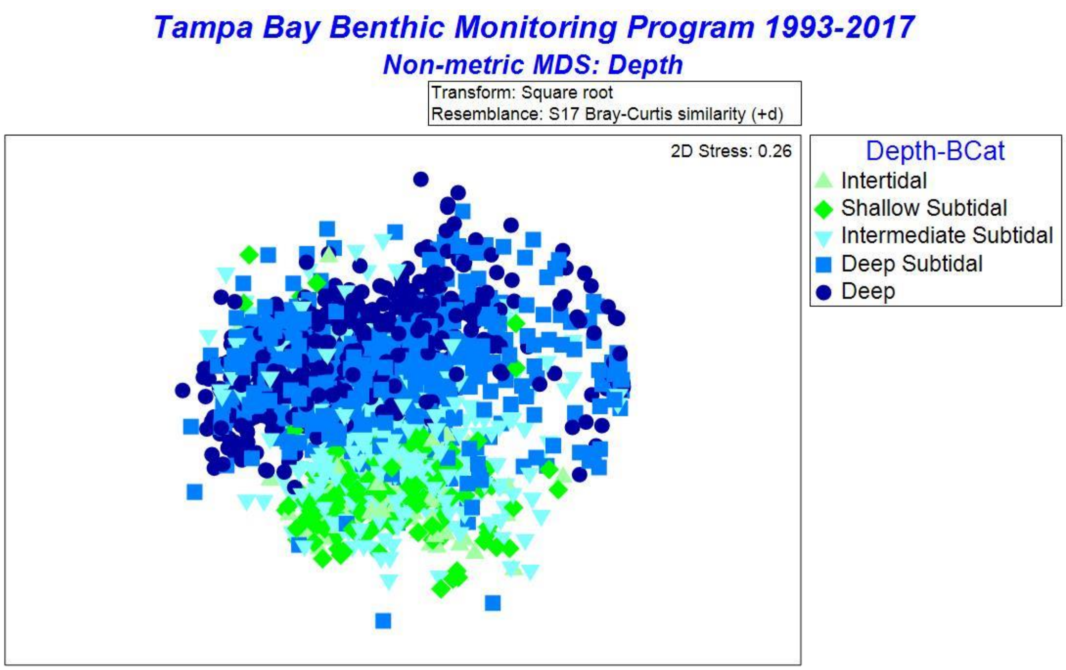

Figure 177. MDS plot data coded by sample depth category - all samples shown.

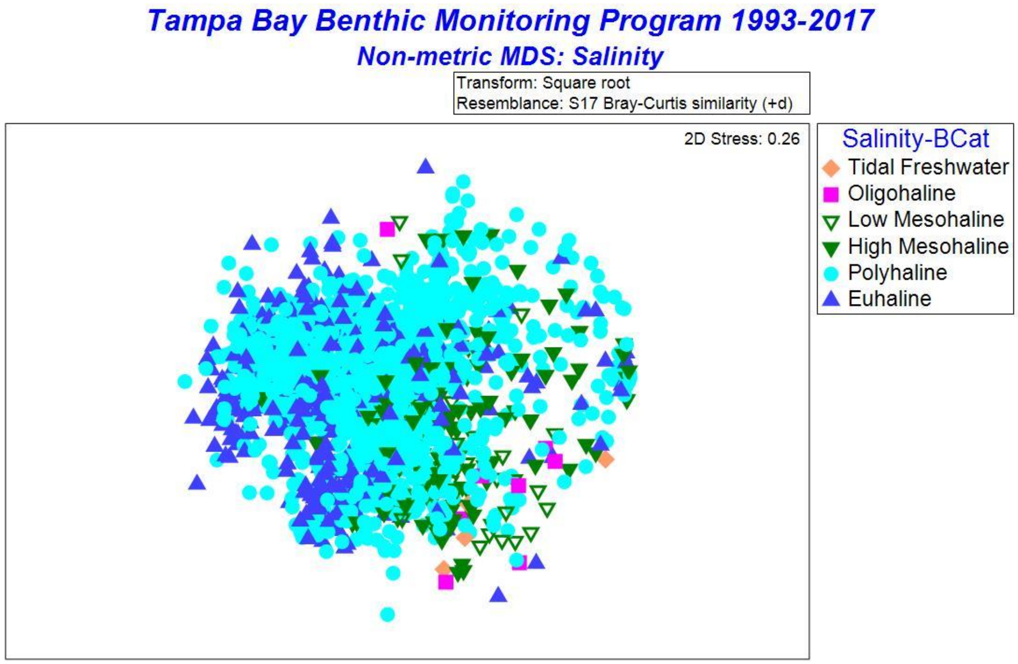

Figure 178. MDS plot data coded by salinity category - all samples shown.

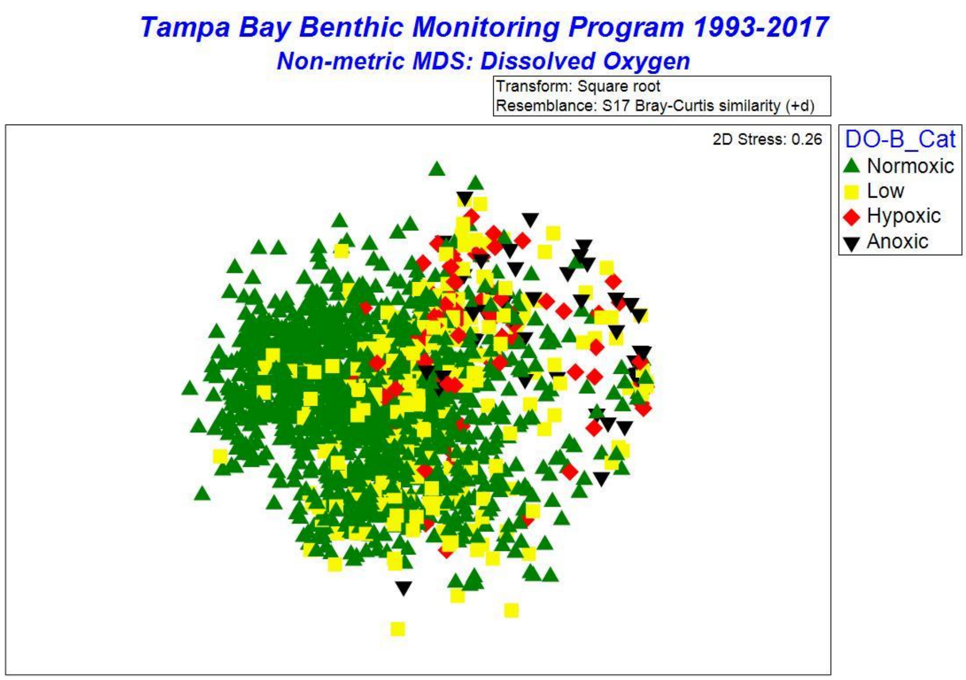

Figure 179. MDS plot data coded by dissolved oxygen category - all samples shown.

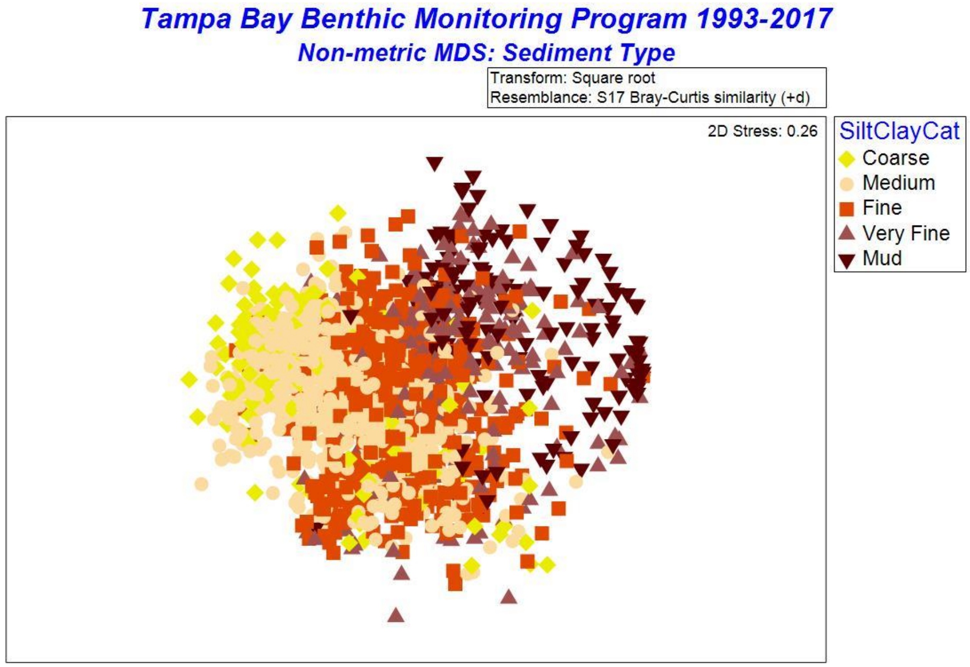

Figure 180. MDS plot data coded by sediment category - all samples shown.

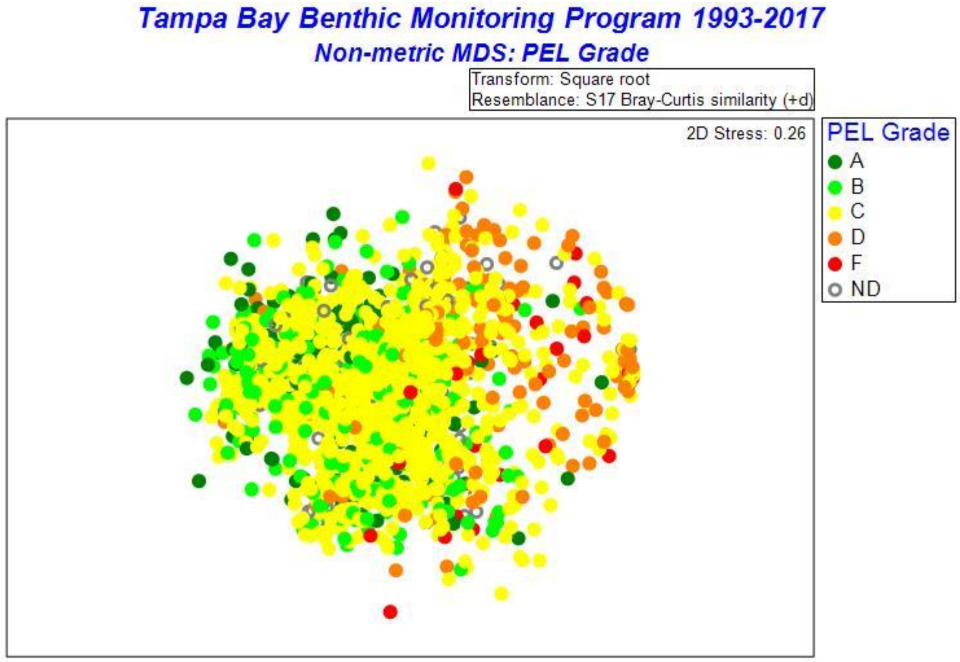

Figure 181. MDS plot data coded by PEL grade - all samples shown.

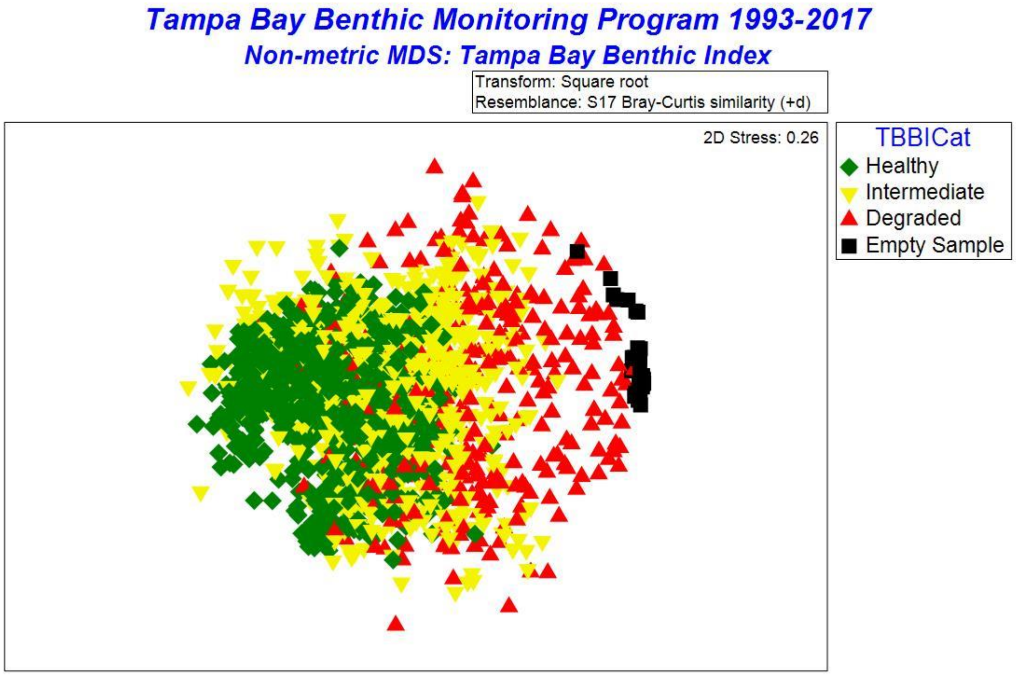

Figure 182. MDS plot data coded by TBBI category - all samples shown.

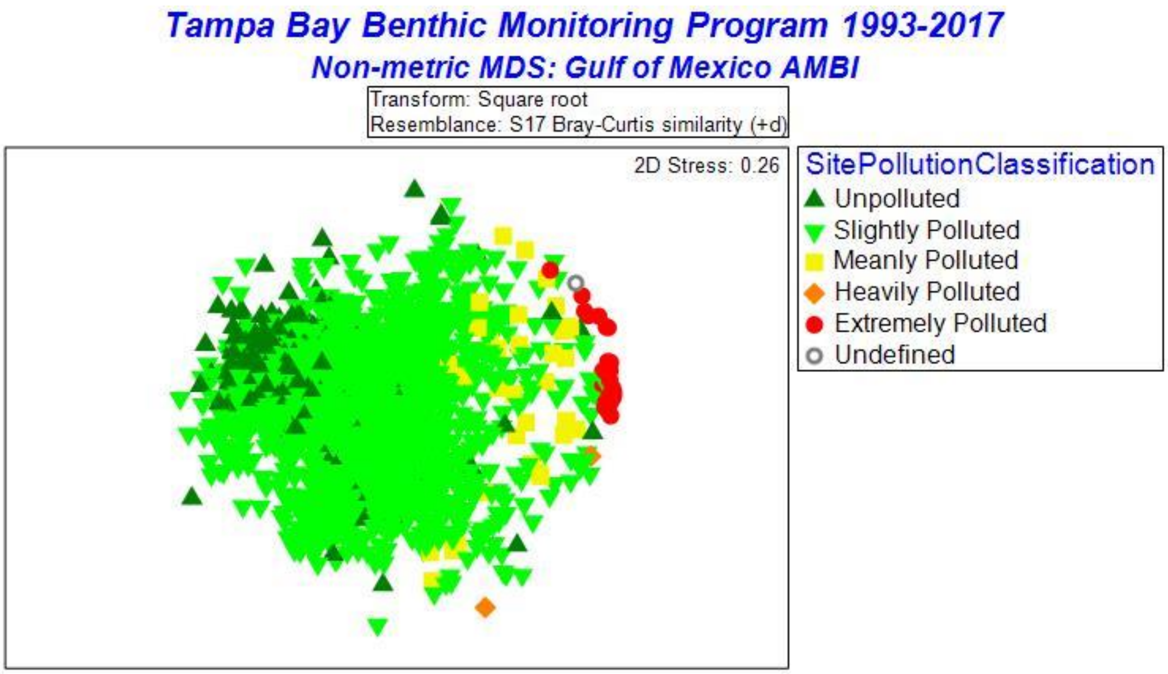

Figure 183. MDS plot data coded by Gulf of Mexico AMBI pollution classification.

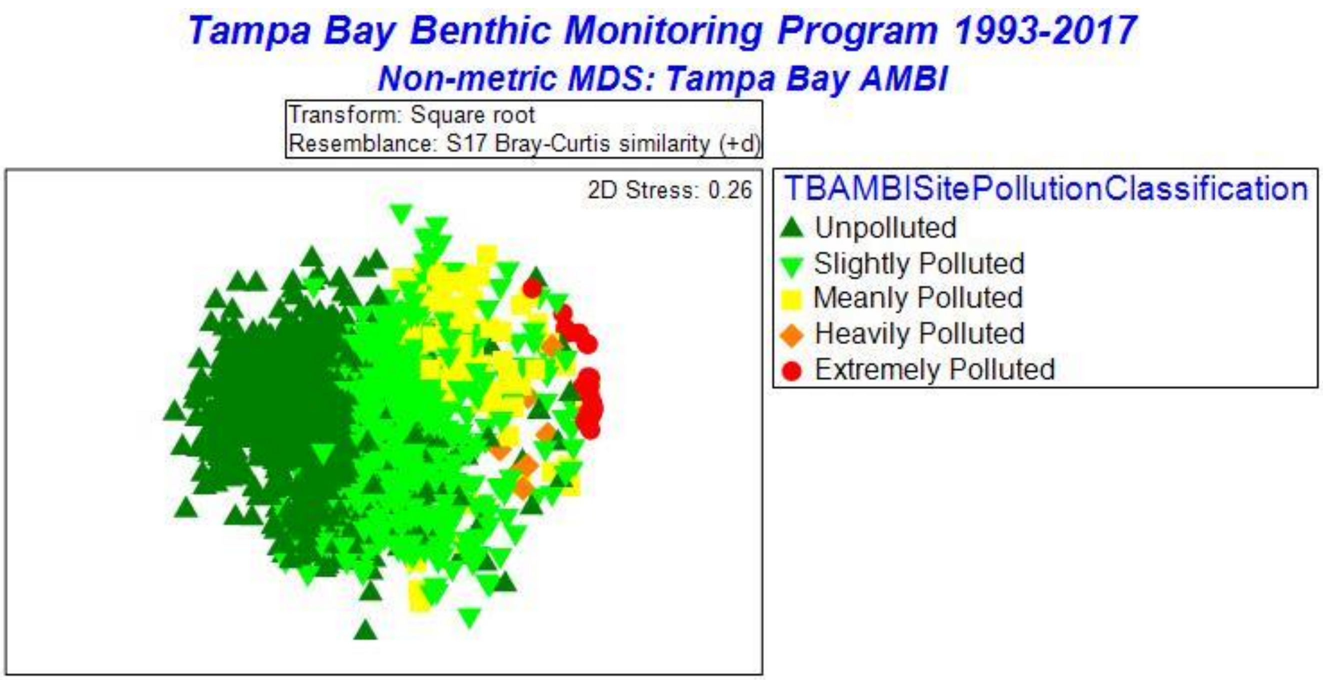

Figure 184. MDS plot data coded by Gulf of Mexico AMBI pollution classification.

The BIO-ENV analysis between the environmental factors and the benthic species composition indicated that the strongest correlation was with a combination of depth, percent bottom dissolved oxygen saturation, bottom salinity, and percent silt+clay (ρ_s = 0.488). The single variable with the highest correlation was percent silt+clay (ρ_s = 0.396), followed by bottom dissolved oxygen saturation (ρ_s = 0.218), and bottom dissolved oxygen concentration (ρ_s = 0.213).

Table 24 shows the SIMPER analysis results indicating which taxa contributed to the similarity among sites within each depth category, and reflects the depth distribution for some of the dominant taxa. Naididae were among the top taxa across all depths. Among the other dominant species, *Ampelisca holmesi* and *Mysella planulata* were more prominent at the Intertidal to Intermediate Subtidal sites (< 2 meters), while *Glottidia pyramidata* and *Branchiostoma floridae* were associated with Intermediate Subtidal to Deep sites.

Table 25 shows the SIMPER analysis results for the different salinity categories. The results reflect the trend of increasing diversity and species richness with increasing salinity, and the salinity ranges for some of the dominant taxa. Naididae were the top taxa across most salinity zones with the exception of the Freshwater sites (where they ranked second) and the Low Mesohaline sites. There were very few freshwater and oligohaline sites overall, which is reflected in the few taxa and high percent contributions of the individual taxa in those salinity categories. The Freshwater sites were characterized by the presence of larval chironomid insects (*Polypedilum scalaenum* group), the nereid polychaete *Laeonereis culveri,* and the amphipod *Grandidierella bonnieroides.* The Oligohaline sites were characterized by the isopod *Cyathura polita* and the ribbon worm (nemertean) Palaeonemertea sp. A of EPC. *Mediomastus* spp. were found across a wide range of salinities ranging from Low Mesohaline to Euhaline sites. This may be because this taxon is a composite of two distinct species, which individually may have different optimal salinity ranges (as discussed previously). Other dominant taxa exhibited more restricted salinity preferences. *Branchiostoma floridae* was associated with Polyhaline and Euhaline sites, while *Glottidia pyramidata* was predominantly associated with Polyhaline sites. *Ampelisca holmesi* was associated with High Mesohaline and Polyhaline sites, while the congeneric *Ampelisca abdita* was associated with Low Mesohaline habitats.

Table 26 reflects the trend of increasing species richness and diversity with increasing dissolved oxygen. The polychaetes *Paraprionospio* sp*. and Kirkegaardia* sp. along with Naididae were among the dominant taxa across all dissolved oxygen categories. The polychaete *Sigambra tentaculata* was associated with anoxic sites, while the unidentified hemichordate Enteropneusta was dominant at both anoxic and hypoxic sites. Other dominant taxa including *Prionospio perkinsi* ranged from hypoxic to normoxic sites, while *Ampelisca holmesi* and *Mysella planulata* ranged from low to normoxic sites; both *Branchiostoma floridae* and *Glottidia pyramidata* were characteristic of normoxic sites.

Dissolved oxygen can affect the benthic community structure by decreasing the abundance and diversity of infaunal organisms during periods of hypoxia (Harper et al., 1981; Gaston 1985), or through the complete defaunation of areas impacted by periods of severe hypoxia or anoxia

(Santos and Simon, 1980 a&b). Hypoxia can affect individual organisms by decreasing feeding and growth rates, or inhibiting their immune systems resulting in higher mortality (Burnett and Stickle, 2001). Tolerance for low dissolved oxygen conditions is variable across different taxonomic groups and ecological niches, which influences the species composition in habitats impacted by hypoxia. Several studies have shown that crustaceans are more sensitive to hypoxia (Harper et al., 1981; Winn and Knott, 1992). Polychaetes tend to dominate under hypoxic conditions with burrowing species being more tolerant than tube dwelling taxa (Harper et al., 1981; Gaston, 1985). Some benthic organisms can exhibit physiological adaptations to hypoxic conditions, such as increased production of respiratory pigments and switching from aerobic to anaerobic respiration (Burnett and Stickle, 2001). Low dissolved oxygen can also influence behavioral responses in infaunal organisms, including movement out of burrows or movement closer to the sediment surface, which in turn can result in increased predation by fish (Diaz et al., 1992; Nestlerode and Diaz, 1998).

Table 27 presents the SIMPER analysis results for sediment categories, and reflects the trend of increasing species richness and diversity with decreasing percent silt+clay and increasing sediment grain size from muds to median grained sands. Coarse sediments had fewer taxa contributing to the similarity within that category, with *Branchiostoma floridae* largely dominating that sediment type. The Mud and Very Fine sediments were primarily dominated by polychaetes, Naididae, and Enteropneusta. Most of the taxa characteristic of these sediment types were associated with sites that were anoxic or hypoxic (Table 27). The spionid polychaetes *Paraprionospio* sp. and *Prionospio perkinsi* were found in sediments ranging from Mud to Medium grained sands, and the cirratulid polychaete *Kirkegaardia* sp. ranged from Very Fine to Medium grain sediments. Other dominant taxa such as *Mysella planulata* and *Glottidia pyramidata* were associated with Fine to Medium sediments, while *Branchiostoma floridae* was associated with Medium to Coarse sediments.

The relationship between sediments and benthic infaunal communities over small and large spatial scales has been well established (Zajac 2001). Factors such as sediment grain size and organic content can affect the species present based on their feeding mode (Bloom et al., 1972). Within Tampa Bay, the distribution of dominant taxa is largely influenced by the sediment type as indicated by the high abundances of filter feeding organisms (*Branchiostoma floridae*, *Glottidia pyramidata*) in areas of low percent silt +clay, while deposit feeding species such as *Kirkegaardia sp.* dominated in areas with high silt+clay content.

Sediment contaminants can have adverse effects on the structure of benthic infaunal communities. Long et al., (2001), in a review of several data sets, found a relationship between increasing sediment toxicity and reduced measures of benthic diversity and abundance, particularly with amphipods. Table 28 presents the SIMPER results for the sediment contaminant categories (PEL Grade), and highlights the decrease in taxonomic diversity with increasing levels of sediment contamination. Naididae were among the dominant taxa across all sediment contamination categories. The least contaminated sediments (“A” and” B”) were dominated by *Branchiostoma floridae*, and were more taxonomically diverse overall with several crustacean and molluscan taxa contributing to the similarity among those groups. The most contaminated sites (“D” and “F”) were dominated by annelids with *Paraprionospio* sp. contributing the most to the similarity.

Table 29 presents the SIMPER results for the Tampa Bay Benthic Index categories. The "Healthy" sites were dominated by *Branchiostoma floridae,* and had a higher number of taxa contributing to the similarity among sites and greater taxonomic diversity overall. The "Intermediate" sites had a relatively high taxonomic diversity, but were dominated by annelid taxa including Naididae and the polychaetes *Kirkegaardia* sp. and *Paraprionospio* sp. The "Degraded" sites were primarily dominated by annelids with Naididae contributing the most to the similarity among samples.

Table 30 presents the SIMPER results for the Gulf of Mexico AMBI pollution categories. The "Unpolluted" sites were dominated by *Branchiostoma floridae,* and several crustacean and molluscan taxa. The "Slightly Polluted" sites had more taxa contributing to the similarity among sites, but annelids comprised the top five taxa. "Meanly Polluted" and "Heavily Polluted" sites were strongly dominated by Naididae and the polychaete *Capitella capitata,* respectively, and the "Extremely Polluted" category comprised the depauperate sites.

Table 31 presents the SIMPER results for the proposed Tampa Bay AMBI pollution categories. The "Unpolluted" sites had the most taxa and greatest taxonomic diversity contributing to the similarity, with *Branchiostoma floridae* dominating. The "Slightly Polluted" sites were largely dominated by annelids with *Kirkegaardia sp.* and Naididae contributing the most to the similarity among sites. Five taxa (four polychaetes and Enteropneusta) contributed over 50% to the similarity among the "Meanly Polluted" sites, with *Paraprionospio* sp. and *Kirkegaardia* sp. dominating. Naididae contributed over 90% to the similarity among the "Heavily Polluted" sites.

Table 24. SIMPER analysis by depth category; values = percent contribution to similarity. Taxa contributing 50% to similarity within category listed.

Intertidal		Shallow Subtidal		Intermediate Subtidal		Deep Subtidal		Deep	
Naididae	16.05	Naididae	14.04	Naididae	7.98	*Kirkegaardia sp.*	6.86	*Branchiostoma floridae*	7.06
Aric idea (Acmira) philbinae	6.09	*Ampelisca holmesi*	5.62	*Ampelisca holmesi*	6.36	*Paraprionospio sp.*	6.56	*Pinnixa spp.*	6.04
Laeonereis culveri	4.13	*Aricidea (Acmira) philbinae*	5.26	*Mysella planulata*	5.16	Naididae	5.59	*Prionospio perkinsi*	5.49
Ampelisca holmesi	3.94	*Capitella capitata complex*	4.60	*Acteocina canaliculata*	4.01	*Prionospio perkinsi*	4.73	Naididae	5.13
Capitella capitata complex	3.89	*Mysella planulata*	3.68	Tellininae	3.61	*Mediomastus sp.*	4.26	*Kirkegaardia sp.*	5.09
Prionospio heterobranchia	3.69	*Laeonereis culveri*	3.26	*Mediomastus sp.*	3.37	Tellininae	3.82	*Mediomastus sp.*	3.16
Acteocina canaliculata	2.77	*Prionospio heterobranchia*	3.02	*Kirkegaardia sp.*	3.13	*Branchiostoma floridae*	3.67	*Paraprionospio sp.*	2.90
Cymadusa compta	2.41	*Acteocina canaliculata*	2.75	*Paraprionospio sp.*	2.82	*Mysella planulata*	2.82	*Nucula proxima*	2.52
Mysella planulata	2.37	*Cymadusa compta*	1.99	*Glycinde solitaria*	2.43	*Ampelisca holmesi*	2.68	*Caecum strigosum*	2.27
Amygdalum papyrium	2.27	*Amygdalum papyrium*	1.99	*Branchiostoma floridae*	2.33	*Pinnixa spp.*	2.64	*Phlyctiderma semiaspera*	2.15
Heteromastus filiformis	2.23	*Prunum apicinum*	1.88	*Haminoea succinea*	2.01	*Nucula proxima*	2.39	Tellininae	2.08
Leitoscoloplos sp.	2.21	*Magelona pettiboneae*	1.78	*Amakusanthura magnifica*	1.98	*Glottidia pyramidata*	2.14	*Amakusanthura magnifica*	2.05
		Kirkegaardia sp.	1.73	*Prunum apicinum*	1.97	*Amakusanthura magnifica*	1.99	*Glottidia pyramidata*	2.04
				Amygdalum papyrium	1.81			*Sigambra tentaculata*	1.98
				Aricidea (Acmira) philbinae	1.69			Ophiuroidea	1.87

Table 25. SIMPER analysis by salinity category; values = percent contribution to similarity. Taxa contributing 50% to similarity within category listed.

Freshwater		Oligohaline		Low Mesohaline		High Mesohaline		Polyhaline		Euhaline	
Polypedilum scalaenum grp.	15.84	Naididae	23.05	*Mediomastus sp.*	11.87	Naididae	9.67	Naididae	7.11	Naididae	7.92
Naididae	15.15	*Cyathura polita*	15.36	*Amygdalum papyrium*	7.59	*Ampelisca holmesi*	8.33	*Kirkegaardia sp.*	5.53	*Mediomastus sp.*	4.76
Laeonereis culveri	14.72	*Palaeonemertea sp. A of EPC*	12.48	*Xenanthura brevitelson*	6.45	*Paraprionospio sp.*	7.76	*Prionospio perkinsi*	4.80	*Branchiostoma floridae*	4.75
Grandidierella bonnieroides	14.57			*Cyathura polita*	6.13	*Kirkegaardia sp.*	5.18	*Branchiostoma floridae*	4.46	Tellininae	4.34
				Streblospio spp.	5.24	*Mysella planulata*	4.53	*Paraprionospio sp.*	4.07	*Clymenella mucosa*	3.70
				Mulinia lateralis	5.22	*Amygdalum papyrium*	4.48	*Ampelisca holmesi*	3.70	*Kirkegaardia sp.*	3.58
				Tellininae	5.11	*Mulinia lateralis*	4.14	*Pinnixa spp.*	3.66	*Parvilucina crenella*	2.60
				Ampelisca abdita	4.82	*Mediomastus sp.*	3.51	*Mysella planulata*	3.30	*Jaspidella blanesi*	2.14
						Glycinde solitaria	3.24	*Mediomastus sp.*	2.70	*Idunella barnardi*	2.08
								Tellininae	2.65	*Exogone dispar*	1.91
								Glottidia pyramidata	2.47	*Nucula proxima*	1.89
								Amakusanthura magnifica	2.38	*Paraprionospio sp.*	1.62
								Nucula proxima	1.76	*Phascolion (Lesenka) cryptum*	1.58
								Kirsteueriella cf. biocellata	1.75	*Angulus cf. versicolor*	1.58
										Fabricinuda trilobata	1.44
										Pinnixa spp.	1.43
										Amakusanthura magnifica	1.42
										Acteocina canaliculata	1.26
										Phlyctiderma semiaspera	1.26

Table 26. SIMPER analysis by dissolved oxygen category; values = percent contribution to similarity. Taxa contributing 50% to similarity within category listed.

Anoxic		Hypoxic		Low		Normoxic	
Paraprionospio sp.	14.96	*Kirkegaardia sp.*	15.46	Naididae	13.60	Naididae	6.96
Kirkegaardia sp.	14.56	*Prionospio perkinsi*	8.89	*Kirkegaardia sp.*	8.99	*Branchiostoma floridae*	5.24
Sigambra tentaculata	10.08	*Paraprionospio sp.*	8.14	*Paraprionospio sp.*	6.70	*Mediomastus sp.*	4.05
Enteropneusta	9.14	Enteropneusta	7.30	*Prionospio perkinsi*	5.96	*Kirkegaardia sp.*	3.88
Naididae	7.81	Naididae	6.91	*Mysella planulata*	4.16	Tellininae	3.68
		Carazziella hobsonae	5.93	*Ampelisca holmesi*	2.95	*Ampelisca holmesi*	3.36
				Carazziella hobsonae	2.76	*Pinnixa spp.*	2.98
				Podarkeopsis levifuscina	2.57	*Paraprionospio sp.*	2.95
				Pinnixa spp.	2.28	*Prionospio perkinsi*	2.84
				Sigambra tentaculata	2.21	*Mysella planulata*	2.70
						Amakusanthura magnifica	2.55
						Nucula proxima	1.92
						Idunella barnardi	1.76
						Acteocina canaliculata	1.73
						Kirsteueriella cf. biocellata	1.60
						Glottidia pyramidata	1.53
						Glycinde solitaria	1.42

Table 27. SIMPER analysis by sediment category; values = percent contribution to similarity. Taxa contributing 50% to similarity within category listed.

Coarse		Medium		Fine		Very Fine		Mud	
Branchiostoma floridae	19.08	*Branchiostoma floridae*	7.27	Naididae	9.41	*Kirkegaardia sp.*	17.08	*Paraprionospio sp.*	12.73
Metharpinia floridana	5.42	Naididae	6.37	*Kirkegaardia sp.*	9.37	Naididae	10.60	*Carazziella hobsonae*	10.40
Amakusanthura magnifica	5.34	*Ampelisca holmesi*	4.43	*Paraprionospio sp.*	5.16	*Paraprionospio sp.*	8.38	Enteropneusta	9.47
Caecum strigosum	5.17	*Mediomastus sp.*	3.46	*Mediomastus sp.*	4.47	*Prionospio perkinsi*	7.75	*Prionospio perkinsi*	8.76
Eudevenopus honduranus	3.24	Tellininae	3.34	*Prionospio perkinsi*	3.87	*Carazziella hobsonae*	4.95	*Sigambra tentaculata*	8.59
Acanthohaustorius uncinus	3.22	*Amakusanthura magnifica*	2.95	Tellininae	3.39	*Podarkeopsis levifuscina*	4.00	Naididae	8.16
Travisia hobsonae	2.96	*Pinnixa spp.*	2.80	*Mysella planulata*	3.24				
Ampelisca holmesi	2.84	*Mysella planulata*	2.79	*Ampelisca holmesi*	2.51				
Pinnixa spp.	2.66	*Glottidia pyramidata*	2.04	*Pinnixa spp.*	2.25				
Tellininae	2.27	*Nucula proxima*	2.01	*Angulus cf. versicolor*	2.09				
		Kirkegaardia sp.	1.89	*Podarkeopsis levifuscina*	2.01				
		Kirsteueriella cf. biocellata	1.88	*Acteocina canaliculata*	1.98				
		Prionospio perkinsi	1.88	*Glottidia pyramidata*	1.65				
		Idunella barnardi	1.85						
		Acteocina canaliculata	1.81						
		Paraprionospio sp.	1.69						
		Prunum apicinum	1.48						
		Ampelisca sp. C of LeCroy, 2002	1.45						

Table 28. SIMPER analysis by sediment PEL Grade; values = percent contribution to similarity. Taxa contributing 50% to similarity within category listed.

A		B		C		D		F	
Branchiostoma floridae	12.62	Naididae	6.44	Naididae	9.35	*Paraprionospio sp.*	12.66	*Paraprionospio sp.*	23.63
Pinnixa spp.	5.11	*Branchiostoma floridae*	6.41	*Kirkegaardia sp.*	5.95	Naididae	11.69	Naididae	23.04
Naididae	3.68	*Kirkegaardia sp.*	4.92	*Paraprionospio sp.*	3.99	*Carazziella hobsonae*	10.43	*Streblospio spp.*	10.64
Ampelisca holmesi	3.32	*Mediomastus sp.*	3.47	*Mediomastus sp.*	3.88	*Kirkegaardia sp.*	9.93		
Tellininae	3.23	*Mysella planulata*	3.45	Tellininae	3.46	*Prionospio perkinsi*	6.69		
Amakusanthura magnifica	2.99	*Ampelisca holmesi*	3.26	*Prionospio perkinsi*	3.32				
Metharpinia floridana	2.91	*Pinnixa spp.*	3.05	*Ampelisca holmesi*	3.24				
Caecum strigosum	2.82	Tellininae	2.99	*Mysella planulata*	2.95				
Kirsteueriella cf. biocellata	2.44	*Prionospio perkinsi*	2.99	*Branchiostoma floridae*	2.47				
Prionospio perkinsi	2.33	*Amakusanthura magnifica*	2.59	*Pinnixa spp.*	2.24				
Prunum apicinum	2.21	*Nucula proxima*	2.17	*Acteocina canaliculata*	1.98				
Mediomastus sp.	2.19	*Paraprionospio sp.*	2.10	*Amakusanthura magnifica*	1.97				
Nucula proxima	2.12	*Idunella barnardi*	1.67	*Glottidia pyramidata*	1.92				
Mysella planulata	2.11	*Glottidia pyramidata*	1.65	*Glycinde solitaria*	1.53				
		Kirsteueriella cf. biocellata	1.49	*Nucula proxima*	1.51				
		Podarkeopsis levifuscina	1.44	*Idunella barnardi*	1.50				

Table 29. SIMPER analysis by TBBI category; values = percent contribution to similarity. Taxa contributing 50% to similarity within category listed.

Healthy		Intermediate		Degraded	
Branchiostoma floridae	6.96	Naididae	8.49	Naididae	13.63
Naididae	5.42	*Kirkegaardia sp.*	8.47	*Paraprionospio sp.*	9.72
Ampelisca holmesi	3.59	*Paraprionospio sp.*	5.84	*Mediomastus sp.*	9.64
Mysella planulata	3.27	*Prionospio perkinsi*	4.49	*Kirkegaardia sp.*	6.35
Amakusanthura magnifica	3.08	*Mediomastus sp.*	3.71	*Prionospio perkinsi*	4.81
Tellininae	3.03	Tellininae	3.17	*Carazziella hobsonae*	3.92
Pinnixa spp.	2.94	*Pinnixa spp.*	3.09	Tellininae	2.62
Nucula proxima	2.43	*Ampelisca holmesi*	2.91		
Kirkegaardia sp.	2.35	*Branchiostoma floridae*	2.80		
Glottidia pyramidata	2.09	*Mysella planulata*	2.71		
Prionospio perkinsi	2.00	*Podarkeopsis levifuscina*	1.99		
Mediomastus sp.	1.80	*Idunella barnardi*	1.73		
Kirsteueriella cf. biocellata	1.79	*Glycinde solitaria*	1.59		
Idunella barnardi	1.70				
Clymenella mucosa	1.65				
Acteocina canaliculata	1.54				
Prunum apicinum	1.51				
Phyllodoce arenae	1.41				
Ampelisca sp. C of LeCroy, 2002	1.36				
Metharpinia floridana	1.34				

Table 30. . SIMPER analysis by Gulf of Mexico AMBI Pollution category; values = percent contribution to similarity. Taxa contributing 50% to similarity within category listed.

Unpolluted		Slightly Polluted		Meanly Polluted		Heavily Polluted		Extremely Polluted	
Branchiostoma floridae	16.27	Naididae	8.81	Naididae	54.42	*Capitella capitata complex*	100.00	**Empty samples**	
Metharpinia floridana	7.63	*Kirkegaardia sp.*	6.05						
Eudevenopus honduranus	5.34	*Paraprionospio sp.*	4.37						
Pinnixa spp.	4.49	*Mediomastus sp.*	4.03						
Nucula proxima	4.41	*Prionospio perkinsi*	3.85						
Acanthohaustorius uncinus	3.89	*Ampelisca holmesi*	3.27						
Tellininae	3.49	*Mysella planulata*	3.23						
Amakusanthura magnifica	3.48	Tellininae	3.06						
Travisia hobsonae	3.12	*Branchiostoma floridae*	2.93						
		Pinnixa spp.	2.60						
		Amakusanthura magnifica	1.90						
		Acteocina canaliculata	1.80						
		Podarkeopsis levifuscina	1.79						
		Glottidia pyramidata	1.66						
		Glycinde solitaria	1.50						

Table 31. SIMPER analysis by proposed Tampa Bay AMBI Pollution category; values = percent contribution to similarity. Taxa contributing 50% to similarity within category listed.

Unpolluted		Slightly Polluted		Meanly Polluted		Heavily Polluted		Extremely Polluted	
Branchiostoma floridae	8.19	*Kirkegaardia sp.*	12.94	*Paraprionospio sp.*	14.30	Naididae	90.79	**Empty samples**	
Naididae	4.59	Naididae	11.19	*Kirkegaardia sp.*	10.76				
Tellininae	4.09	*Paraprionospio sp.*	7.85	*Sigambra tentaculata*	10.66				
Mediomastus sp.	3.87	*Prionospio perkinsi*	5.82	*Carazziella hobsonae*	9.71				
Amakusanthura magnifica	3.42	*Mysella planulata*	3.76	Enteropneusta	9.38				
Ampelisca holmesi	3.17	*Podarkeopsis levifuscina*	2.87						
Pinnixa spp.	2.98	*Ampelisca holmesi*	2.69						
Nucula proxima	2.58	*Mediomastus sp.*	2.40						
Idunella barnardi	2.21	*Carazziella hobsonae*	2.10						
Mysella planulata	2.06								
Prionospio perkinsi	1.67								
Ampelisca sp. C of LeCroy, 2002	1.60								
Kirsteueriella cf. biocellata	1.60								
Prunum apicinum	1.59								
Metharpinia floridana	1.56								
Clymenella mucosa	1.56								
Glottidia pyramidata	1.49								
Kirkegaardia sp.	1.46								
Caecum strigosum	1.42								

Conclusions and Recommendations

The recommendation of this report is to maintain the current sampling design that has been in place since 2005, with the possibility of increasing the number of special study sites as needed to evaluate areas and issues of special concern to the Tampa Bay Estuary Program and regional bay managers. Our last report made several recommendations, including revisiting some of our past special study sites and since then we have resampled Clam Bayou in 2016 (Karlen et al., 2017) and East Bay in 2019. We should continue dedicating a set number of annual samples to special studies, consider revisiting past sites, as well as possibly sampling the major tributaries (Hillsborough River, Alafia River, etc.) as special study sites in the upcoming monitoring cycle. Several additional parameters were also recommended for consideration in our previous report. Of those, microplastics has gained recent attention. A recent study of microplastics in Tampa Bay found an average of 280 microplastic particles/kg of sediment, with the highest concentration (790 particles/kg) in Ybor Channel (McEachern et al., 2019). The methods used in that study could easily be adapted for our current monitoring program and could establish the beginning of a long-term dataset on this pollutant of concern.

Tampa Bay has shown tremendous improvements in water quality since the early 1980s (Sherwood et al., 2016). Seagrasses have also experienced a remarkable recovery in Tampa Bay, increasing from a total coverage of 8,761 ha in 1982 to 16,451 ha in 2018, exceeding the Tampa Bay Estuary Program's restoration goal of 1950s seagrass coverage of 16,357 ha (Sherwood et al., 2017; Tomasko et al., 2018). The benthic community is now also showing healthier conditions, with increasing trends in overall species richness and abundance, which tracks with improvements in water quality and seagrass recovery (Figure 131). The Tampa Bay Benthic Index indicates an improving benthic community over time, most notably since 2013, when the median bay-wide TBBI score exceeded 87 every year through 2017 (Table 15). Population growth and development, however, continue to strain the environmental resources of the region, and monitoring efforts such as the Bay-wide Benthic Monitoring Program are essential to assess the current environmental conditions in the bay, track long term environmental trends, and identify areas in need of remediation.

Literature Cited

Adams, D.H., and Onorato, G.V. 2005. Mercury concentrations in red drum, *Sciaenops ocellatus*, from estuarine and offshore waters of Florida. Marine Pollution Bulletin 50, 291-300.

AISN Software. 2000. *Table Curve 2D ver.5.0*, SPSS, Chicago, IL.

Amezcua-Allieri, M., and Salazar-Coria, L. 2008. Nickel and vanadium concentrations and its relation with sediment acute toxicity. Bulletin of Environmental Contamination and Toxicology 80(6), 555-560.

Anderson, M.J., Gorley, R.N., Clarke, K.R. 2008. PERMANOVA+ for PRIMER: Guide to Software and Statistical Methods. PRIMER-E. Plymouth, U.K. 214pp.

ATSDR. 1990. Toxicological Profile for Silver. Agency for Toxic Substances and Disease Registry, U.S. Public Health Service. 145 pp.

ATSDR. 1992. Toxicological Profile for Antimony and Compounds. Agency for Toxic Substances and Disease Registry, U.S. Public Health Service. 136 pp.

ATSDR. 1994. Toxicological Profile for Chlordane. Agency for Toxic Substances and Disease Registry, U.S. Public Health Service. 234 pp.

ATSDR. 1995a. Toxicological Profile for Polycyclic Aromatic Hydrocarbons. Agency for Toxic Substances and Disease Registry, U.S. Public Health Service. 136 pp.

ATSDR. 1995b. Toxicological Profile for Mirex and Chlordecone. Agency for Toxic Substances and Disease Registry, U.S. Public Health Service. 333 pp.

ATSDR. 1996. Toxicological Profile for Endrin. Agency for Toxic Substances and Disease Registry, U.S. Public Health Service. 191 pp.

ATSDR. 1999. Toxicological Profile for Mercury. Agency for Toxic Substances and Disease Registry, U.S. Public Health Service. 617 pp.

ATSDR. 2000. Toxicological Profile for Polychlorinated Biphenyls (PCBs). Agency for Toxic Substances and Disease Registry, U.S. Public Health Service. 765 pp.

ATSDR. 2002a. Toxicological Profile for Aldrin/Dieldrin. Agency for Toxic Substances and Disease Registry, U.S. Public Health Service. 303 pp.

ATSDR. 2002b. Toxicological Profile for DDT, DDE, and DDD. Agency for Toxic Substances and Disease Registry, U.S. Public Health Service. 403 pp.

ATSDR. 2002c. Toxicological Profile for Methoxychlor. Agency for Toxic Substances and Disease Registry, U.S. Public Health Service. 244 pp.

ATSDR. 2003. Toxicological Profile for Selenium. Agency for Toxic Substances and Disease Registry, U.S. Public Health Service. 418 pp.

ATSDR. 2004. Toxicological Profile for Copper. Agency for Toxic Substances and Disease Registry, U.S. Public Health Service. 272 pp.

ATSDR. 2005a. Toxicological Profile for Nickel. Agency for Toxic Substances and Disease Registry, U.S. Public Health Service. 351 pp.

ATSDR. 2005b. Toxicological Profile for Tin and Tin Compounds. Agency for Toxic Substances and Disease Registry, U.S. Public Health Service. 376 pp.

ATSDR. 2005c. Toxicological Profile for Zinc. Agency for Toxic Substances and Disease Registry, U.S. Public Health Service. 307 pp.

ATSDR. 2005d. Toxicological Profile for Naphthalene, 1-methylnaphthalene, and 2-Methylnaphthalene. Agency for Toxic Substances and Disease Registry, U.S. Public Health Service. 291 pp.

ATSDR. 2005e. Toxicological Profile for Alpha-, Beta-, Gamma-, and Delta-hexachlorocyclohexane. Agency for Toxic Substances and Disease Registry, U.S. Public Health Service. 325 pp.

ATSDR. 2007a. Toxicological Profile for Arsenic. Agency for Toxic Substances and Disease Registry, U.S. Public Health Service. 500 pp.

ATSDR. 2007b. Toxicological Profile for Lead. Agency for Toxic Substances and Disease Registry, U.S. Public Health Service. 528 pp.

ATSDR. 2011. Addendum to the Toxicological Profile for Polychlorinated Biphenyls. Agency for Toxic Substances and Disease Registry, U.S. Public Health Service. 39 pp.

ATSDR. 2012. Toxicological Profile for Manganese. Agency for Toxic Substances and Disease Registry, U.S. Public Health Service. 506 pp.

ATSDR. 2013. Toxicological Profile for Endosulfan [Draft]. Agency for Toxic Substances and Disease Registry, U.S. Public Health Service. 342 pp.

Austen, M.C., and McEvoy, A.J. 1997. Experimental effects of tributyltin (TBT) contaminated sediments on a range of meiobenthic communities. Environmental Pollution 96, 435-444.

Bakir, A., Rowland, S.J., Thompson, R.C. 2014. Transport of persistent organic pollutants by microplastics in estuarine conditions. Estuarine, Coastal and Shelf Science 140, 14-21.

Balckmore, G. 2000. Imposex in Thais clavigera (Neogastropoda) as an indicator of TBT (Tributyltin) bioavailability in coastal waters of Hong Kong. Journal of Molluscan Studies 66, 1-8.

Bannon, D.I., Drexler, J.W., Fent, G.M., Casteel, S.W., Hunter, P.J., Brattin, W.J., Major, M.A. 2009. Evaluation of Small Arms Range Soils for Metal Contamination and Lead Bioavailability. Environmental Science & Technology 43, 9071-9076.

Barwick, M., and Maher, W. 2003. Biotransference and biomagnification of selenium copper, cadmium, zinc, arsenic and lead in a temperate seagrass ecosystem from Lake Macquarie Estuary, NSW, Australia. Marine Environmental Research 56, 471-502.

Bauer, M., and Blodau, C. 2006. Mobilization of arsenic by dissolved organic matter from iron oxides, soils and sediments. The Science of the Total Environment 354, 179-190.

Benson, R.F., Saraceno, J.A., Lowell, D.R., Brett, D.W. 1994. Selenium levels in the Palm River and MacKay Bay region of Tampa Bay. Florida Scientist 57(4), 177-184.

Beyer, W.N., Spalding, M., Morrison, D. 1997. Mercury concentrations in feathers of wading birds from Florida. Ambio 26, 97-100.

Billiard, S.M., Querbach, K., Hodson, P.V. 1999. Toxicity of retene to early life stages of two freshwater fish species. Environmental Toxicology and Chemistry 18, 2070-2077.

Birchenough, S.N.R., Reiss, H., Degraer, S., Mieszkowska, N., Borja, Á., Buhl-Mortensen, L., Braeckman, U., Craeymeersch, J., De Mesel, I., Kerckhof, F., Kröncke, I., Parra, S., Rabaut, M., Schröder, A., Van Colen, C., Van Hoey, G., Vincx, M., Wätjen, K. 2015. Climate change and marine benthos: a review of existing research and future directions in the North Atlantic. WIREs Climate Change 2015. doi: 10.1002/wcc.330

Bjork, M., and Gilek, M. 1996. Uptake and Elimination of 14C-Phenanthrene by the Blue Mussel *Mytilus edulis* L. at different algal concentrations. Bulletin of Environmental Contamination and Toxicology 56, 151-158.

Blackmore, G. 2000. Field evidence of metal transfer from invertebrate prey to an intertidal predator, *Thais clavigera* (Gastropoda: Muricidae). Estuarine, Coastal and Shelf Science 51, 127-139.

Blackmore, G. 2000. Imposex in *Thais clavigera* (Neogastropoda) as an indicator of TBT (Tributyltin) bioavailability in coastal waters of Hong Kong. Journal of Molluscan Studies 66, 1-8.

Blake, J.A. 1991. Revision of some genera and species of Cirratulidae (Polychaeta) from the Western North Atlantic. Ophelia Suppl 5, 17-30.

Blake, J.A. 1996. Chapter 8. Family Cirratulidae Ryckholdt, 1851: Including a revision of the genera and species from the Eastern North Pacific. Pp. 263-384 in J.A. Blake, B. Hilbig and P.H. Scott (eds). Taxonomic Atlas of the benthic fauna of the Santa Maria Basin and the Western Santa Barbara Channel Volume 6: The Annelida Part 3 Polychaeta: Orbiniidae to Cossuridae. Santa Barbara Museum of Natural History, Santa Barbara, CA.

Blake, J.A. 2016. *Kirkegaardia* (Polychaeta, Cirratulidae), new name for *Monticellina* Laubier, preoccupied in the Rhabdocoela, together with new records and descriptions of eight previously known and sixteen new species from the Atlantic, Pacific, and Southern Oceans. Zootaxa 4166 (1), 1-93. http://doi.org/10.11646/zootaxa.4166.1.1

Bloom, S.A., Simon, J.L. and Hunter, V.D. 1972. Animal-sediment relations and community analysis of a Florida estuary. Marine Biology 13, 43-56.

Boese, B.L., Lamberson, J.O., Swartz, R.C., Ozretich, R.J. 1997. Photoinduced Toxicity of Fluoranthene to Seven Marine Benthic Crustaceans. Archives of Environmental Contamination and Toxicology 32, 389-393.

Borgert, C.J., Gross, T.S., Guiney, P.D., Osimitz, T.G., Price, B., Wells, C. 2004. Interactive effects of p,p′-dichlorodiphenyldichloroethylene and methoxychlor on hormone synthesis in largemouth bass ovarian cultures. Environmental Toxicology and Chemistry 23, 1947-1956.

Borja, A., Franco, J., Pérez, V. 2000. A marine biotic index to establish the ecological quality of soft-botttom benthos within European estuarine and coastal environments. Marine Pollution Bulletin 40(12), 1100-1114.

Boulajfene, W., Boukhicha, J., Deidun, A., Berto, D., Romeo, T., Ben Hassine, O.K., Tlig-Zouari, S. 2015. Biomonitoring of the environmental contamination by organotins in the Gulf of Tunis: occurrence of imposex in Stramonita haemastoma (Linnaeus, 1767). Marine and Freshwater Research 66(9), 778-785.

Brinkmann, R. 1994. Lead pollution in soils adjacent to homes in Tampa, Florida. Environmental Geochemistry and Health 16, 59-64.

Brooks, G.R. and Doyle, L.J. 1991. Distribution of sediments and sedimentary contaminants in Tampa Bay. In: Treat, S.F. and P.A. Clark (Eds.). Proceedings, Tampa Bay Area Scientific Information Symposium 2 (February 27 – March 1, 1991). Tampa, FL.

Brooks, G.R. and Doyle, L.J. 1992. A characterization of Tampa Bay Sediments. Phase III: Distribution of sediments and sedimentary contaminants. Final Report Submitted to SWFWMD.

Brown, M.J., and Margolis, S. 2012. Lead in drinking water and human blood levels in the United States. Centers for Disease Control and Prevention, Morbidity and Mortality Weekly Report (August 10, 2012) Supplement/Vol. 61, 1-9.

Burreau, S., Zebühr, Y., Broman, D., and Ishaq, R. 2006. Biomagnification of PBDEs and PCBs in food webs from the Baltic Sea and the northern Atlantic Ocean. Science of the Total Environment 366, 659-672.

Burnett, L.E. and Stickle, W.B. 2001. Physiological responses to hypoxia. Chapter 6 pp. 101-114 in N.N. Rabalais and R.E. Turner (eds.) Coastal Hypoxia: Consequences for Living Resources and Ecosystems. American Geophysical Union, Washington D.C.

Butkus, M.A., and Johnson, M.C. 2011. Reevaluation of Phosphate as a Means of Retarding Lead Transport from Sandy Firing Ranges. Soil and Sediment Contamination: An International Journal 20, 172 - 187.

Calbet, A., Saiz, E., Barata, C. 2007. Lethal and sublethal effects of naphthalene and 1,2-dimethylnaphthalene on the marine copepod *Paracartia grani*. Marine Biology 151, 195-204.

Cao, X., Ma, L.Q., Chen, M., Hardison, D.W., Harris, W.G. 2003. Lead transformation and distribution in the soils of shooting ranges in Florida, USA. The Science of the Total Environment 307, 179-189.

Chen, Y.W., Deng, T.L., Filella, M., Belzile, N. 2003. Distribution and early diagenesis of antimony species in sediments and porewaters of freshwater lakes. Environmental Science & Technology 37, 1163-1168.

Cheney, D., Logan, J.M., Gardner, K., Sly, E., Wysor, B. Greenwood, S. 2019. Bioaccumulation of PCBs by a seaweed bloom (*Ulva rigida*) and transfer to higher trophic levels in an estuarine food web. Marine Ecology Progress Series 611, 75-93. https://doi.org/10.3354/meps12840

Cheney, M.A., Liu, J., Amei, A., Zhao, X., Joo, S.W., Qian, S. 2009. A comparative study on the uptake of polycyclic aromatic hydrocarbons by *Anodonta californiensis*. Environmental Pollution 157, 601-608.

Christensen, M., Banta, G.T., Andersen, O. 2002. Effects of the polychaetes Nereis diversicolor and Arenicola marina on the fate and distribution of pyrene in sediments. Marine Ecology Progress Series 237, 159-172.

Clarke, R.K and Ainsworth, M. 1993. A method of linking multivariate community structure to environmental variables. Marine Ecology Progress Series 92, 205-219.

Clarke, K.R., and Gorley, R.N. 2015. *PRIMER v7: User Manual/Tutorial* PRIMER-E: Plymouth, U.K.

Clarke, K.R., Gorley, R.N., Somerfield, P.J., Warwick, R.M. 2014. *Change in marine communities: an approach to statistical analysis and interpretation, 3nd edition.* PRIMER-E: Plymouth, U.K.

Clarke, K.R., Somerfield, P.J. and Chapman, M.G. 2006. On resemblance measures for ecological studies, including taxonomic dissimilarities and a zero-adjusted Bray-Curtis coefficient for denuded assemblages. Journal of Experimental Marine Biology and Ecology 330, 55-80.

Clausen, J.L., Bostick, B., Korte, N. 2011. Migration of Lead in Surface Water, Pore Water, and Groundwater With a Focus on Firing Ranges. Critical Reviews in Environmental Science and Technology 41, 1397-1448.

Cleckner, L.B., Garrison, P.J., Hurley, J.P., Olson, M.L., Krabbenhoft, D.P. 1998. Trophic transfer of methyl mercury in the northern Florida Everglades. Biogeochemistry 40, 347-361.

Coastal Environmental, Inc. 1994. A monitoring program to assess environmental changes in Tampa Bay Florida. Prepared for: Tampa Bay National Estuary Program. TBNEP Tech. Pub #02-93.

Conradi, M., and Depledge, M.H. 1999. Effects of zinc on the life-cycle, growth and reproduction of the marine amphipod *Corophium volutator*. Marine Ecology Progress Series 176, 131-138.

Courtney, C.M., Grabe, S.A., Karlen, D.J., Brown, R. and Heimbuch, D. 1995. Field operations manual for a synoptic survey of benthic macroinvertebrates of the Tampa Bay estuaries. EPCHC Technical Document. November 1995. 55 pp.

Culter, J.K. 1979. A population study of the inarticulate brachiopod *Glottidia pyramidata* (Stimpson). M.A. Thesis, Department of Biology, University of South Florida. Tampa, FL.

Culter, J.K. 1986. Manual for identification of marine invertebrates: A guide to some common estuarine macroinvertebrates of the Big Bend region, Tampa Bay, Florida. USEPA Document EPA/600/4-86/002.

Culter, J.K. and Simon, J.L. 1987. Sex ratios and the occurrence of hermaphrodites in the inarticulate brachiopod, *Glottidia pyramidata* (Stimpson) in Tampa Bay, Florida. Bulletin of Marine Science 40(2), 193-197.

Dahllof, I., Agrenius, S., Blanck, H., Hall, P., Magnusson, K., Molander, S. 2001. The Effect of TBT on the Structure of a Marine Sediment Community - a Boxcosm Study. Marine Pollution Bulletin 42, 689-695.

Dauer, D.M., and Simon, J.L. 1976a. Repopulation of the Polychaete Fauna of an Intertidal Habitat Following Natural Defaunation: Species Equilibrium. Oecologia 22, 99-117.

Dauer, D.M., and Simon, J.L. 1976b. Habitat Expanson among Polychaetous Annelids Repopulating a Defaunated Marine Habitat. Marine Biology 37, 169-177.

Davis, A.P., Shokouhian, M., Ni, S. 2001. Loading estimates of lead, copper, cadmium, and zinc in urban runoff from specific sources. Chemosphere 44, 997-1009.

Dawson, C.E. 1965. Rainstorm induced mortality of lancelets, Branchiostoma, in Mississippi Sound. Copeia 1965 (1), 505-506.

Delile, H., Blichert-Toft, J., Goiran, J.-P., Keay, S., Albarède, F. 2014. Lead in ancient Rome's city waters. PNAS 111, 6594-6599.

Diaz, R.J., Neubauer, R.J., Schaffner, L.C., Pihl, L., Baden, S.P. 1992. Continuous monitoring of dissolved oxygen in an estuary experiencing periodic hypoxia and the effect of hypoxia on macrobenthos and fish. Science of the Total Environment Suppl. 1992, 1055-1068.

Di Toro, D.M., Mahony, J.D., Hansen, D.J., Scott, K.J., Hicks, M.B., Mayr, S.M., Redmond, M.S. 1990. Toxicity of cadmium in sediments: the role of acid volatile sulfide. Environmental Toxicity and Chemistry 9, 1487-1502.

Dijkstra, J.A., Westerman, E.L., Harris, L.G. 2010. The effects of climate change on species composition, succession and phenology: a case study. Global Change Biology (2010), doi: 10.1111/j.1365-2486.2010.02371.x.

Din, Z.B., 1992. Use of aluminum to normalize heavy-metal data from estuarine and coastal sediments of Straits of Melaka. Marine Pollution Bulletin 24, 484-491.

Dix, T.L., Karlen, D.J., Grabe, S.A., Goetting, B.K., Holden, C.M., Markham, S.E. 2005. Spionid Polychaetes as Environmental Indicators: An Example from Tampa bay, Florida. Chapter 18 in S.A. Bortone (ed.). Estuarine Indicators CRC Press. Boca Raton, Florida. 277-296.

Egeler, P., Römbke, J., Meller, M., Knacker, Th., Franke, C., Studinger, G. and Nagel, R. 1997. Bioaccumulation of lindane and hexachlorobenzene by tubificid sludgeworms (Oligochaeta) under standardized laboratory conditions. Chemosphere 35(4), 835-852.

Ellis-Tabanor, M., Hyslop, E. 2005. Effect of Sublethal Concentrations of Endosulfan on Growth and Fecundity of Two Species of Snails. Bulletin of Environmental Contamination and Toxicology 74, 1173-1178.

Engle, V.D., and Summers, J.K. 1999. Refinement, validation, and application of a benthic condition index for Northern Gulf of Mexico Estuaries. Estuaries 22(3A), 624-635.

Engle, V.D., Summers, J.K., and Gaston, G.R. 1994. A benthic index of environmental condition of Gulf of Mexico estuaries. Estuaries 17(2), 372-384.

ESRI. (2012) ArcGIS 10.1. Redlands, CA.

Eun Jung, C., Qtae, J., Hyo-Bang, M., Chang-Keun, K., Ju-Chan, K. 2007. Time-course uptake and elimination of benzo(a)pyrene and its damage to reproduction and ensuing reproductive outputs of Pacific oyster, *Crassostrea gigas*. Marine Biology 151, 157-165.

Fair, P.A., Adams, J., Mitchum, G., Hulsey, T.C., Reif, J.S., Houde, M., Muir, D., Wirth, E., Wetzel, D., Zolman, E., McFee, W., Bossart, G.D. 2010. Contaminant blubber burdens in Atlantic bottlenose dolphins (*Tursiops truncatus*) from two southeastern US estuarine areas: Concentrations and patterns of PCBs, pesticides, PBDEs, PFCs, and PAHs. Science of the Total Environment 408, 1577-1597.

Fattorini, D., Notti, A., Halt, M.N., Gambi, M.C., Regoli, F. 2005. Levels and chemical speciation of arsenic in polychaetes: a review. Marine Ecology 26, 255-264.

FDEP. 2012 Mercury TMDL for the State of Florida Appendix B: Complete list of Florida Water Segments Verified as Impaired for Mercury (In Fish Tissue). 33 pp.

FDEP. 2013. Mercury TMDL for the State of Florida: Final Report. 104 pp.

Ferguson, P.L. and Chandler, G.T. 1998. A laboratory and field comparison of sediment polycyclic aromatic hydrocarbon bioaccumulation by the cosmopolitan estuarine polychaete *Streblospio benedicti* (Webster). Marine Environmental Research 45, 387-401.

Ferraro, S.P. and Cole, F.A. 1997. Effects of DDT sediment contamination on macrofaunal community structure and composition in San Francisco Bay. Marine Biology 130, 323-334.

Filella, M., Belzile, N., Chen, Y.-W. 2002. Antimony in the environment: a review focused on natural waters: I. Occurrence. Earth-Science Reviews 57, 125-176.

Fitzhugh, K. 1983. New species of Fabriciola and Fabricia (Polychaeta:Sabellidae) from Belize. Proceedings of the Biological Society of Washington. 96, 276-290.

Fitzhugh, K. 1990. *Fabricinuda*, A New Genus of Fabriciinae (Polychaeta:Sabellidae). Proceedings of the Biological Society of Washington. 103(1), 161-178.

Fliedner, A. and Klein, W. 1996. Effects of Lindane on the Planktonic Community in Freshwater Microcosms. Ecotoxicology and Environmental Safety 33, 228–235.

Franz, D.R. 1973. The ecology and reproduction of a marine bivalve, *Mysella planulata* (Erycinacea). Biological Bulletin 144, 93-106.

Frithsen, J.B., Schreiner, S.P., Strebel, D.E., Lalijani, R.M., Logan, D.T., and Zarbock, H.W. 1995. Chemical contaminants in the Tampa Bay Estuary: A summary of distributions and inputs. TBNEP Tech. Pub. #01-95.

Gaston, G.R. 1985. Effects of hypoxia on macrobenthos of the inner shelf off Cameron, Louisiana. Estuarine, Coastal and Shelf Science 20, 603-613.

Gillett, D.J., Weisberg, S.B., Grayson, T., Hamilton, A., Hansen, V., Leppo, E.W., Pelletier, M.C., Borja, A., Cadien, D., Dauer, D., Diaz, R., Dutch, M., Hyland, J.L., Kellogg, M., Larsen, P.F., Levinton, J.S., Llansó, R., Lovell, L.L., Montagna, P.A., Pasko, D., Phillips, C.A., Rakocinski, C., Ranasinghe, J.A., Sanger, D.M., Teixeira, H., Van Dolah, R.F., Velarde, R.G., Welch, K.I. 2015. Effect of ecological group classification schemes on performance of the AMBI benthic index in US coastal waters. Ecological Indicators 50, 99-107. http://dx.doi.org/10.1016/j.ecolind.2014.11.005

Grabe, S.A. and Barron, J. 2002. Status of Tampa Bay sediments: Polycyclic aromatic hydrocarbons, organochlorine pesticides, and polychlorinated biphenyls (1993 and 1995-1999). Environmental Protection Commission of Hillsborough County Technical Report.

Grabe, S.A. and Barron, J. 2004. Sediment contamination, by habitat, in the Tampa Bay estuarine system (1993-1999): PAHs, Pesticides and PCBs. Environmental Monitoring and Assessment 91, 105-144.

Grabe, S.A., Courtney, C.M., Lin, Z., Alberdi, D., Wilson, H.T., and Blanchard, G. 1996. Environmental Monitoring and Assessment Program – Estuaries West Indian Province 1993 Sampling Volume III Technical Report: A synoptic survey of the benthic macroinvertebrates and demersal fishes of the Tampa Bay estuarine system. TBNEP Tech. Pub. #95-12.

Grabe, S.A., Karlen, D.J., Holden, C., Goetting, B., Markham, S. Dix, T. 2005. Ecological assessment of selected dredge holes in Tampa Bay: hydrographic conditions, sediment contamination and benthic macroinvertebrates. Environmental Protection Commission of Hillsborough County Technical Report. 104 pp.

Grabe, S.A., Karlen, D.J., Holden, C.M., Goetting, B.K., Markham, S.E. and Dix, T.L. 2006. Gammaridean Amphipoda of Tampa Bay, Florida (Gulf of Mexico): Distribution and association with abiotic variables. EPCHC Technical Report prepared for the Tampa Bay Estuary Program.

Grall, J., Glémarec, M. 1997. Using biotic indices to estimate macrobenthic community perturations in the Bay of Brest. Estuarine, Coastal and Shelf Science 44 (Supp. A), 43-53.

Guo, T., DeLaune, R.D., Patrick, J.W.H. 1997. The influence of sediment redox chemistry on chemically active forms of arsenic, cadmium, chromium, and zinc in estuarine sediment. Environment International 23, 305-316.

Hafen, M.R. and Brinkmann, R. 1996. Analysis of lead in soils adjacent to an interstate highway in Tampa, Florida. Environmental Geochemistry and Health 18(4), 171-179.

Hall, J.R. and Saloman, C.H. 1975. Distribution and abundance of macroinvertebrate species of six phyla in Tampa Bay, Florida, 1963-64 and 1969. NMFS Data Report 100. USDOC/NOAA/NMFS Seattle WA. 505 pp.

Harper, D.E. Jr., McKinney, L.D., Salzer, R.R., and Case, R.J. 1981. The occurrence of hypoxic bottom water off the upper Texas coast and its effects on the benthic biota. Contributions in Marine Science 24, 53-79.

Hartman, O. 1947. Polychaetous Annelids Part VII. Capitellidae. Allan Hancock Pacific Expeditions. 10 (4), 391 -481.

Hatje, V., Macedo, S.M., de Jesus, R.M., Cotrim, G., Garcia, K.S., de Queiroz, A.F., Ferreira, S.L.C. 2010. Inorganic As speciation and bioavailability in estuarine sediments of Todos os Santos Bay, BA, Brazil. Marine Pollution Bulletin 60, 2225-2232.

Hochberg, R.J., Weisberg, S.B., Frithsen, J.B., Janicki, A.J., Heimbuch, D.H., and Wilson, H.T. 1992. Design of a basin wide monitoring program for the Tampa Bay estuary. TBNEP Technical Publication #09-92.

Jamieson, A.J., Malkocs, T., Piertney, S.B., Fujii, T., Zhang, Z. 2017. Bioaccumulation of persisent organic pollutants in the deepest ocean fauna. Nature Ecology & Evolution 1, 0051 DOI: 10.1038/s41559-016-0051

Janicki Environmental, Inc. 2003. Tampa Bay Benthic Monitoring Program redesign assessment Final Report. TBEP Tech. Pub #06-03. 11 pp.

Janicki Environmental, Inc. 2005. Development of a benthic index to establish sediment quality targets for the Tampa Bay estuary. Final Report. TBEP Tech. Pub. #01-06.

Julian, P., II. 2013. Mercury Bio-concentration Factor in Mosquito Fish (*Gambusia* spp.) in the Florida Everglades. Bulletin of Environmental Contamination and Toxicology 90, 329-332.

Karlen, D.J. 2014. Surface Water Quality 2001-2010 Hillsborough County, Florida. Environmental Protection Commission of Hillsborough County Technical Report.

Karlen, D.J., Dix, T., Goetting, B.K., Markham, S.E., Meyer, C., Flock, M., Blanchard, G. 2008. Tampa Bay Benthic Monitoring Program Interpretive Report: 1993-2004. Tampa Bay Estuary Program Technical Publication #05-08. 133 pp.

Karlen D.J., Dix, T.L., Goetting, B.K., Markham, S.E. 2009 . The Benthic Macrofaunal Community and Sediment Quality Conditions in Clam Bayou, Pinellas County, Florida. Tampa Bay Estuary Program Technical Publication # 05-09. 50 pp.

Karlen, D.J., Dix, T.L., Goetting, B.K., Markham, S.E., Campbell, K.W., Jernigan, J..M. 2015. Twenty-year Trends in the Benthic Community and Sediment Quality of Tampa Bay 1993-2012. Tampa Bay Benthic Monitoring Program Interpretive Report Prepared for: Tampa Bay Estuary Program. TBEP Technical Publication #04-15. 238 pp.

Karlen, D.J., Dix, T.L., Goetting, B.K., Markham, S.E., Campbell, K.W., Jernigan, J.M. 2017. A Reassessment of the Benthic Macrofaunal Community and Sediment Quality Conditions in Clam Bayou, Pinellas County, Florida: 2008 vs. 2016. Report Prepred for the Florida Department of Environmental Protection and Tampa Bay Estuary Program. 62 pp.

Karlen, D.J., Goetting, B.K., Dix, T.L., Markham, S.E., Campbell, K. Jernigan, J., Christian, J., Chacour, A. Martinez, K., Grossmann, L., LaMonica, L. 2018. Tampa Bay Dredged Hole Habitat Assessment: Status of Benthic Macrofauna and Sediment Contaminants. TBEP Technical Report #03-18. 105 pp.

Kamrin, M.A. (ed.). 1997. Pesticide profiles: toxicity, environmental impact and fate. CRC Press. Boca Raton. 676 pp.

Kane Driscoll, S. and Mc Elroy, A.E. 1996. Bioaccumulation and Metabolism of Benzo[a]Pyrene in Three Species of Polychaete Worms. Environmental Toxicology and Chemistry 15, 1401-1410.

Kang, H., Gye, M., Kim, M. 2008. Effects of Endosulfan on Survival and Development of *Bombina orientalis* (Boulenger) Embryos. Bulletin of Environmental Contamination and Toxicology 81, 262-265.

Keilty, T.J., White, D.S., Landrum, P.F. 1988. Sublethal responses to endrin in sediment by *Limnodrilus hoffmeisteri* (Tubificidae), and in mixed-culture with *Stylodrilus heringianus* (Lumbriculidae). Aquatic Toxicology 13, 227-249.

Kelly, L.D., McGuinness, L.R., Hughes, J.E., Wainright, S.C. 1999. Effects of Phenanthrene on Primary Production of Phytoplankton in Two New Jersey Estuaries. Bulletin of Environmental Contamination and Toxicology 63, 646-653.

Kennish, M.J. 1998. Pollution impacts on marine biotic communities. CRC Press, Boca Raton. 310 pp.

Kennish, M.J. and Ruppel, B.F. 1996. Chlordane contamination in selected estuarine and coastal marine finfish and shellfish of New Jersey, USA. Environmental Pollution 94(1), 75-81.

Kennish, M.J., and Ruppel, B.F. 1997. Chlordane contamination in selected freshwater finfish of New Jersey. Bulletin of Environmental Contamination and Toxicology 58, 142-149.

Kirby, J., Maher, W., Krikowa, F. 2001. Selenium, Cadmium, Copper, and Zinc Concentrations in Sediments and Mullet (*Mugil cephalus*) from the Southern Basin of Lake Macquarie, NSW, Australia. Archives of Environmental Contamination and Toxicology 40, 246-256.

Klerks, P.L., Felder, D.L., Strasser, K., and Swarzenski, P.W. 2007. Effects of ghost shrimp on zinc and cadmium in sediments from Tampa Bay, FL. Marine Chemistry 104, 17-26.

Kukkonen, J.V.K., Landrum, P.F. 1998. Effect of particle-xenobiotic contact time on bioavailability of sediment-associated benzo(a)pyrene to benthic amphipod, Diporeia spp. Aquatic Toxicology 42, 229-242.

Kuzyk, Z.A., Stow, J.P., Burgesss, N.M., Solomon, S.M., and Reimer, K.J. 2005. PCBs in sediments and the coastal food web near a local contaminant source in Saglek Bay, Labrador. Science of the Total Environment 351-352, 264-284.

Labare, M.P., Butkus, M.A., Riegner, D., Schommer, N., Atkinson, J. 2004. Evaluation of lead movement from the abiotic to biotic at a small-arms firing range. Environmental Geology 46, 750-754.

Larsen, M.H. and Mouritsen, K.N. 2014. Temperature-parasitism synergy alters intertidal soft-bottom community structure. Journal of Experimental Marine Biology and Ecology 460, 109-119.

Lee, C.-H., Ryu, T.-K., Chang, M., and Choi, J.-W. 2004. Effect of silver, cadmium, chromium, copper, and zinc on the fertilization of the Northern Pacific asteroid, *Asterias amurensis*. Bulletin of Environmental Contamination and Toxicology 73, 613-619.

Leppanen, M.T. and Kukkonen, J.V.K. 2000. Effect of sediment-chemical contact time on availability of sediment-associated pyrene and benzo[a]pyrene to oligochaete worms and semi-permeable membrane devices. Aquatic Toxicology 49, 227-241.

Lesen, A.E. 2006. Sediment organic matter composition and dynamics in San Francisco Bay, California, USA: Seasonal variation and interactions between water column chlorophyll and the benthos. Estuarine, Coastal and Shelf Science 66, 501-512.

Lewis, R.R. and Whitman, R.L. 1985. A new geographic description of the boundaries and subdivisions of Tampa Bay. In: Treat, S.F., Simon, J.L., Lewis, R.R., Whitman, R.L. (Eds.). Proceedings, Tampa Bay Area Scientific Information Symposium (May 1982). Burgess Publishing Co., Inc., Minneapolis, MN.

Lewis, R.R., III and Estevez, E.D. 1988. The ecology of Tampa Bay, Florida: an estuarine profile. U.S. Fish and Wildlife Service Biological Report 85(7.18), 132 pp.

Long, E.R., Hong, C.B., Severn, CG. 2001. Relationships between acute sediment toxicity in laboratory tests and abundance and diversity of benthic Infauna in marine sediments: A review. Environmental Toxicology and Chemistry 20(1), 46-60.

Long, E.R., Wolfe, D.A., Carr, R.S., Scott, K.J., Thursby, G.A., Windom, H.L., Lee, R., Calder, F.D. Slone, G.M. and Seal, T. 1994. Magnitude and Extent of Sediment Toxicity in Tampa Bay, Florida. NOAA Tech. Mem. NOS ORCA 78. NOAA Silver Spring, MD.

Longman, J., Veres, D., Finsinger, W., Ersek, V. 2018. Exceptionally high levels of lead pollution in the Balkans from the Early Bronze Age to the Industrial Revolution. Proceedings of the National Academy of Sciences 115 (25), E5661-E5668. www.pnas.org/cgi/doi/10.1073/pnas.1721546115

Lotufo, G.R. and Fleeger, J.W. 1996. Toxicity of Sediment Associated Pyrene and Phenanthrene to *Limnodrilus hoffmeisteri* (Oligochaeta: Tubificidae). Environmental Toxicology and Chemistry 15, 1508-1516.

Lotufo, G.R. and Fleeger, J.W. 1997. Effects of sediment-associated phenanthrene on survival, development and reproduction of two species of meiobenthic copepods. Marine Ecology Progress Series 151, 91-102.

Lowry, J. (2014). Acuminodeutopus naglei (Bousfield, 1973). In: Horton, T.; Lowry, J. & De Broyer, C. (2013 onwards) World Amphipoda Database. Accessed through: World Register of Marine Species at http://www.marinespecies.org/aphia.php?p=taxdetails&id=421566 on 2015-02-12

Luoma, S.N., Ho, Y.B, and Bryan, G.W. 1995. Fate, bioavailability and toxicity of silver in estuarine environments. Marine Pollution Bulletin 31(1-3), 44-54.

Macauley, J.M. 1993. Environmental Monitoring and Assessment Program Estuaries – Louisianian Province: 1993 Sampling. Field Operations Manual. United States Environmental Protection Agency ERL/GB NO SR119. [DRAFT 4/22/93].

MacDonald, D.D. 1994. Approach to the Assessment of Sediment Quality in Florida Coastal Waters Volume 1 - Development and Evaluation of Sediment Quality Assessment Guidelines. Florida Department of Environmental Protection. 124 pp.

MacDonald, D.D., Carr, R.S., Calder, F.D., Long, E.R., and Ingersoll, C.G. 1996. Development and evaluation of sediment quality guidelines for Florida coastal waters. Ecotoxicology 5, 253-278.

MacDonald, D.D., Carr, R.S., Eckenrod, D., Greening, H., Grabe, S., Ingersoll, C.G., Janicki, S., Janicki, T., Lindskoog, R.A., Long, E.R., Pribble, R., Sloane, G., and Smorong, D.E. 2004. Development, evaluation and application of sediment quality targets for assessing and managing contaminated sediments in Tampa Bay, Florida. Archives of Environmental Contamination and Toxicology. 46, 147-161.

Magni, P., Tagliapietra, D., Lardicci, C., Balthis, L., Castelli, A., Como, S., Frangipane, G., Giordani, G., Hyland, J., Maltagliati, F., Pessa, G., Rismondo, A., Tataranni, M., Tomassetti, P., Viaroli, P. 2009. Animal-sediment relationships: Evaluating the [`]Pearson-Rosenberg paradigm' in Mediterranean coastal lagoons. Marine Pollution Bulletin 58, 478-486.

Mahler, B.J., Metre, P.C.V., Wilson, J.T., Musgrove, M., Burbank, T.L., Ennis, T.E., Bashara, T.J. 2010. Coal tar-Based Parking Lot Sealcoat: An Unrecognized Source of PAH to Settled House Dust. Environmental Science & Technology 44, 894-900.

Magnusson, K., Ekelund, R., Grabic, R. and Bergqvist, P.-A. 2006. Bioaccumulation of PCB congeners in marine benthic infauna. Marine Environmental Research 61, 379-395.

Malloy, J.C., Meade, M.L., Olsen, E.W. 1999. Small scale spatial variation of selenium concentrations in chironomid larvae. Bulletin of Environmental Contamination and Toxicology 62, 122-129.

Malloy, K.J., Wade, D. Janicki, A. Grabe, S.A., and Nijbroek, R. 2007. Development of a benthic index to assess sediment quality in the Tampa Bay Estuary. Marine Pollution Bulletin 54, 22-31.

Manning, L.M., Peterson, C.H., Bishop, M.J. 2014. Dominant macrobenthic populations experience sustained impacts from annual disposal of fine sediments on sandy beaches. Marine Ecology Progress Series 508, 1-15.

Martinez, E.A., Moore, B.C., Schaumloffel, J., Dasgupta, N. 2001. Induction of morphological deformities in Chironomus tentans exposed to Zinc- and Lead- spiked sediments. Environmental Toxicology and Chemistry 20, 2475-2481.

Masscheleyn, P.H., Delaune, R.D., Patrick, W.H. 1990. Transformations of selenium as affected by sediment oxidation-reduction potential and pH. Environmental Science and Technology 24, 91-96.

Masscheleyn, P.H., Delaune, R.D., Patrick, W.H. 1991. Effect of redox potential and pH on arsenic speciation and solubility in a contaminated soil. Environmental Science and Technology 25, 1414-1419.

McConnell, J.R., Wilson, A.I., Stohl, A. Arienzo, M.M., Chellman, N.J., Eckhardt, S., Thompson, E.M., Pollard, A.M., Steffensen, J.P. 2018. Lead pollution recorded in Greenland ice indicates European emissions tracked plagues, wars, and imperial expansion during antiquity. Proceedings of the National Academy of Sciences 115 (22), 5726-5731.

McConnell, R., and Brink, T. 1997. Toxic contamination assessment: sources of sediment contaminants of concern and recommendations for prioritization of Hillsborough and Boca Ciega sub-basins. TBNEP Tech. Pub. #03-97. 119 pp.

McConnell, R., DeMott, R., and Schulten, J. 1996. Toxic contamination sources assessment: risk assessment for chemicals of potential concern and methods for identification of specific sources. TBNEP Tech. Pub. #09-96. 265 pp.

McEachern, K., Alegria, H., Kalagher, A.L., Hansen, C. Morrison, S., Hastings, D. 2019. Microplastics in Tampa Bay, Florida: Abundance and variability in estuarine waters and sediments. Marine Pollution Bulletin 148, 97-106. https://doi.org/10.1016/j.marpolbul.2019.07.068

McLeese, D.W., Burridge, L.E., Van Dinter, J. 1982. Toxicities of five organochlorine compounds in water and sediment to *Nereis virens*. Bulletin of Environmental Contamination and Toxicology 28(2), 216-220.

Mirlean, N, Baisch, P., Machado, I. Shumilin, E. 2008. Mercury contamination of soil as the result of long-term phosphate fertilizer production. Bulletin of Environmental Contamination and Toxicology 81(3), 305-308.

Moore, M.T., Huggett, D.B., Gillspie W.B. Jr., Rodgers, J.H. Jr, and Cooper, C.M. 1998. Comparative toxicity of chlordane, chlorpyrifos, and aldicarb to four aquatic testing organisms. Archives of Environmental Contamination and Toxicology 34, 152-157.

Mote Marine Laboratory. 1995. Benthic Infauna of Tampa Bay Summer 1993. TBEP Tech. Pub. #02-95. 142 pp.

Mühling, M., Bradford, A., Readman, J.W., Somerfield, P.J., Handy, R.D. 2009. An investigation into the effects of silver nanoparticles on antibiotic resistance of naturally occurring bacteria in an estuarine sediment. Marine Environmental Research 68, 278-283.

Muller, J.K., Johnson, K.G., SepÃºlveda, M.S., Borgert, C.J., Gross, T.S. 2004. Accumulation of dietary DDE and dieldrin by Largemouth Bass, *Micropterus salmoides floridanus*. Bulletin of Environmental Contamination and Toxicology 73, 1078-1085.

Myers, A.A. 1981. Amphipod Crustacea I. Family Aoridae. Memoirs of the Hourglass Cruises. Florida Department of Natural Resources Marine Research Laboroatory. St. Petersburg, FL 75 pp.

Naqvi, S.M, and de la Cruz, A.A. 1973. Mirex incorporation in the environment: Toxicity in selected freshwater organisms. Bulletin of Environmental Contamination and Toxicology 10(5), 305-308.

Neff, J.M. 1997. Ecotoxicology of arsenic in the marine environment. Environmental Toxicology and Chemistry 16, 917-927.

Negro, C., Senkman, L., Vierling, J., Repetti, M., García, S., Collins, P. 2012. Bioaccumulation in Freshwater Crabs. Endosulfan Accumulation in Different Tissues of *Zilchiopsis collastinensis* P. (Decapoda: Trichodactylidae). Bulletin of Environmental Contamination and Toxicology 89, 1000-1003.

Nelson, G.E. 1969. Amphioxus in Old Tampa Bay, Florida. Quarterly Journal of the Florida Academy of Sciences 31, 93-100.

Nestlerode, J.A. and Diaz, R.J. 1998. Effects of periodic environmental hypoxia on predation of a tethered polychaete, *Glycera americana*: implications fro trophic dynamics. Marine Ecology Progress Series 172, 185-195.

Newsome, T., Aranguren, F., Brinkman, R. 1997. Lead contamination adjacent to roadways in Trujillo, Venezuela. The Professional Geographer 49(3), 331-341.

Ngabe, B., Bidleman, T.F., and Scott, G.I. 2000. Polycyclic aromatic hydrocarbons in storm runoff from urban and coastal South Carolina. The Science of the Total Environment 255, 1-9.

Nikolaou, M., Neofitou, N., Skordas, K., Castritsi-Catharios, I., Tziantziou, L. 2014. Fish farming and anti-fouling paints: a potential source of Cu and Zn in farmed fish. Aquaculture Environment Interactions 5, 163-171.

Oberdorster, E., Brouwer, M., Hoexum-Brouwer, T., Manning, S., McLachlan, J.A. 2000. Long-Term Pyrene Exposure of Grass Shrimp, *Palaemonetes pugio*, Affects Molting and Reproduction of Exposed Males and Offspring of Exposed Females. Enviromental Health Perspectives 108, 641-646.

Oikari, A., Fragoso, N., Leppänen, H., Chan, T., Hodson, P.V. 2002. Bioavailability to juvenile rainbow trout (Oncorynchus mykiss) of retene and other mixed-function oxygenase-active compounds from sediments. Environmental Toxicology and Chemistry 21, 121-128.

Oliva, M., Perales, J.A., Gravato, C., Guilhermino, L., Galindo-Riaño, M.D. 2012. Biomarkers responses in muscle of Senegal sole (Solea senegalensis) from a heavy metals and PAHs polluted estuary. Marine Pollution Bulletin 64, 2097-2108.

Olsgard, F. 1999. Effects of copper contamination on recolonization of subtidal marine soft sediments – an experimental field study. Marine Pollution Bulletin 38(6), 448-462.

Paine, R.T. 1963. Ecology of the brachiopod *Glottidia pyramidata.* Ecological Monographs 33(3), 187-213.

Palanikumar, L., Kumaraguru, A.K., Ramakritinan, C.M., Anand, M. 2013. Toxicity, Feeding Rate and Growth Rate Response to Sub-lethal Concentrations of Anthracene and Benzo [a] Pyrene in Milkfish *Chanos chanos* (Forskkal). Bulletin of Environmental Contamination and Toxicology 90, 60-68.

Pan, L., Ren, J., Liu, J. 2005. Effects of benzo(k)fluoranthene exposure on the biomarkers of scallop Chlamys farreri. Comparative Biochemistry and Physiology Part C: Toxicology & Pharmacology 141, 248-256.

Pardue, J.H., DeLanune, R.D., Patrick, W.H., Jr. 1992. Metal to aluminum correlation in Louisiana coastal wetlands: identification of elevated metal concentrations. Journal of Environmental Quality 21, 539-545.

Pelletier, M.C., Burgess, R.M., Ho, K.T., Kuhn, A., McKinney, R.A., Ryba, S.A. 1997. Phototoxicity of individual polycyclic aromatic hydrocarbons and petroleum to marine invertebrate larvae and juveniles. Environmental Toxicology and Chemistry 16 (10), 2190-2199.

Percival, J. B. and Lindsay, P. J. 1997. Measurement of physical properties of sediments, in A. Mudroch, J. M. Azcue and P. Mudroch (eds), *Manual of Physico-chemical Analysis of Aquatic Sediments,* Lewis Publ. Boca Raton, pp. 7-46.

Pichler, T., Brinkmann, R., Scarzella, G.I. 2008. Arsenic abundance and variation in golf course lakes. Science of the total environment 394, 313-320.

Pierce, E. L. 1965. The distribution of lancelets (Amphioxi) along the coasts of Florida. Bulletin of Marine Science 15 (2), 480-494.

Price, R.E., London, J., Wallschläger, D., Ruiz-Chancho, M.J., Pichler, T. 2013. Enhanced bioaccumulation and biotransformation of As in coral reef organisms surrounding a marine shallow-water hydrothermal vent system. Chemical Geology 348, 48-55.

PRIMER-E Ltd. 2017. PRIMER v7. Plymouth, U.K.

Przeslawski, R., Zhu, Q., Aller, R. 2009. Effects of abiotic stresssors on infaunal burrowing and associated sediment characteristics. Marine Ecology Progress Series 392, 33-42.

Purcell, T.W. and Peters, J.J. 1998. Sources of silver in the environment. Environmental Toxicology and Chemistry 17(4), 539-546.

Rainbow, P.S., Smith, B.D., Casado-Martinez, M.C. 2011. Biodynamic modelling of the bioaccumulation of arsenic by the polychaete Nereis diversicolor. Environmental Chemistry 8, 1-8.

Rainbow, P.S., Wang, W.-X. 2001. Comparative assimilation of Cd, Cr, Se, and Zn by the barnacle Elminius modestus from phytoplankton and zooplankton diets. Marine Ecology Progress Series 218, 239-248.

Ramdahl, T. 1983. Retene - a molecular marker of wood combustion in ambient air. NATURE 306, 580-582.

Rasmussen, A.D., Banta, G.T., and Andersen, O. 1998. Effects of Bioturbation by the lugworm *Arenicola marina* on cadmium uptake and distribution in sandy sediments. Marine Ecology Progress Series 164, 179-188.

Rees, A.B., Turner, A., Comber, S. 2014. Metal contamination of sediment by paint peeling from abandoned boats, with particular reference to lead. Science of the Total Environment 494 & 495, 313-319.

Ruelas-Inzunza, J., and Páez-Osuna, F. 2008. Trophic distribution of Cd, Pb, and Zn in a food web from Altata-Ensenada del Pabellón subtropical lagoon, SE Gulf of California. Archives of Environmental Contamination and Toxicology 54, 584-596.

Santos, S.L. and Simon, J.L. 1980a. Marine soft-bottom community establishment following annual defaunation: larval or adult recruitment? Marine Ecology Progress Series, 235 – 241.

Santos, S.L. and Simon, J.L. 1980b. Response of soft-bottom benthos to annual catastrophic disturbance in a South Florida estuary. Marine Ecology Progress Series 3, 347 – 355.

SAS Institute, Inc. 2003. Statistical Analysis Software v. 9.1.3 Service Pack 4. Cary, NC.

Scheuhammer, A.M. and Norris, S.L. 1996. The ecotoxicology of lead shot and lead fishing weights. Ecotoxicology 5, 279-295.

Schiff, K.C. and Weisberg, S.B. 1999. Iron as a reference element for determining trace metal enrichment in Southern California coastal shelf sediments. Marine Environmental Research 48, 161-176.

Schropp, S.J., Lewis, F.G., Windom, H.L., Ryan, J.D., Calder, F.D., Burney, L.C. 1990. Interpretation of Metal Concentrations in Estuarine Sediments of Florida Using Aluminum as a Reference Element. Estuaries 13, 227-235.

Schultz, A.G., Boyle, D., Chamot, D., Ong, K.J., Wilkinson, K.J., McGeer, J.C., Sunahara, G., Goss, G.G. 2014. Aquatic toxicity of manufactured nanomaterials: challenges and recommendations for future toxicity testing. Environmental Chemistry 11, 207-226.

Scoggins, M., McClintock, N.L., Gosselink, L., Bryer, P. 2007. Occurrence of polycyclic aromatic hydrocarbons below coal tar-sealed parking lots and effects on stream benthic macroinvertebrate communities. Journal of the North American Benthological Society 26, 694-707.

Seebaugh, D.R., Estephan, A., and Wallace, W.G. 2006. Relationship between dietary cadmium adsorption by grass shrimp (*Palaemonetes pugio*) and trophically available cadmium in amphipod (*Gammarus lawrencianus*) prey. Bulletin of Environmental Contamination and Toxicology 76, 16-23.

Sherwood, E.T., Karlen, D.J., Dix, T.L., Goetting, B.K., Markham, S.E., Chacour, A. Miller, M. 2007. Tidal Tributary Study Summary Report: Water Quality, Sediment Chemistry, Benthic Macrofauna, and Watershed Characterization. Environmental Protection Commission of Hillsborough County Technical Report. 241 pp.

Sherwood, E.T., Greening, H.S., Janicki, A.J., Karlen, D.J. 2016. Tampa Bay estuary: Monitoring long-term recovery through regional partnerships. Regional Studies in Marine Science. 4, 1-11. http://dx.doi.org/10.1016/j.rsma.2015.05.005

Sherwood, E.T., Greening, H.S., Johansson, J.R., Kaufman, K., & Raulerson, G.E. 2017. Tampa Bay (Florida, USA): Documenting Seagrass Recovery since the 1980's and Reviewing the Benefits. Southeastern Geographer 57(3), 294-319. doi:10.1353/sgo.2017.0026.

Singh, N. and Turner, A. 2009a. Leaching of copper and zinc from spent antifouling paint particles. Environmental Pollution 157, 371-376.

Singh, N. and Turner, A. 2009b. Trace metals in antifouling paint particles and their heterogeneous contamination of coastal sediments. Marine Pollution Bulletin 58, 559-564.

Sizmur, T., Canário, J., Gerwing, T.G., Mallory, M.L., O'Driscoll, N.J. 2013. Mercury and methylmercury bioaccumulation by polychaete worms is governed by both feeding ecology and mercury bioavailability in coastal mudflats. Environmental Pollution 176, 18-25.

Stokes, M.D. 1996. Larval settlement, post-settlement growth and secondary production of the Florida lancelet (= amphioxus) *Branchiostoma floridae*. Marine Ecology Progress Series 130, 71-84.

Straub, C.L., Maul, J.D., Halbrook, R.S., Spears, B. and Lydy, M.J. 2007. Trophic transfer of polychlorinated biphenyls in great blue heron (*Ardea herodias*) at Crab Orchard National Wildlife Refuge, Illinois, United States. Archives of Environmental Contamination and Toxicology 52, 572-579.

Street, J.H., Paytan, A. 2005. Iron, phytoplankton growth, and the carbon cycle, in: Sigel, A., Sigel, H., Sigel, R.K.O. (Eds.), Metal Ions in Biologial Systems, Volume 43 - Biogeochemical Cycles of Elements. CRC Press, Tayor and Francis Group, pp. 153-193.

Suryavanshi, U., Sreepada, R.A., Ansari, Z.A., Nigam, S., Badesab, S. 2009. A study on biochemical changes in the penaeid shrimp, Metapenaeus monoceros (Fabricius) following exposure to sublethal doses of organochlorine pesticide (endosulfan). Chemosphere 77, 1540-1550.

Swartz, R.C., Schults, D.W., Dewitt, T.H., Ditsworth, G.R., Lamberson, J.O. 1990. Toxicity of fluoranthene in sediment to marine amphipods: a test of the equilibrium partitioning approach to sediment quality criteria. Environmental Toxicology and Chemistry 9, 1071-1080.

Swartz, R.C., Cole, F.A., Lamberson, J.O., Ferraro, S.P., Schults, D.W., DeBen, W.A., Lee II, H., Ozretich, R.J. 1994. Sediment Toxicity, Contamination and Amphipod Abundance at a DDT- and Dieldrin-Contaminated Site in San Francisco Bay. Environmental Toxicology and Chemistry 13, 949-962.

Syracuse Research Corporation (SRC). 2007. Toxicological Profile for Heptachlor and Heptachlor epoxide. Agency for Toxic Substances and Disease Registry, U.S. Public Health Service. 158 pp.

SYSTAT Software, Inc. 2004. SYSTAT® 11. Richmond, CA.

SYSTAT Software, Inc. 2006a. SigmaStat® 3.5. Richmond, CA.

SYSTAT Software, Inc. 2006b. SigmaPlot 10.0. Richmond CA.

Taylor, J.L. 1971. Polychaetous annelids and benthic environments in Tampa Bay, Florida. Doctoral Dissertation. University of Florida, Gainesville FL. Facsimile copy, UMI Dissertation Services Ann Arbor, MI.

Taylor, J.L., Hall, J.R. and Saloman, C.H. 1970. Mollusks and benthic environments in Hillsborough Bay, Florida. Fishery Bulletin 68 (2), 191-202.

Terlizzi, A., Geraci, S., Gibbs, P.E. 1999. Tributyltin (TBT)-induced imposex in the Neogastropod *Hexaplex trunculus* in Italian coastal waters: morphological aspects and ecological implications. Italian Journal of Zoolology 66, 141-146.

Teta, C., Naik, Y.S. 2018. Endosulfan reduces fertilization success and causes abnormal embryo development to zebrafish. Toxicological & Environmental Chemistry 100(4), 452-464. https://doi.org/10.1080/02772248.2018.1530777

Thoemke, K.W. 1979. The life histories and population dynamics of four subtidal amphipods from Tampa Bay, Florida. Doctoral Dissertation. University of South Florida, Tampa, FL. Facsimile copy, UMI Dissertation Services Ann Arbor, MI.

TBNEP 1996. Charting the course: The Comprehensive Conservation and Management Plan for Tampa Bay.

Tomasko, D., Alderson, M., Burnes, R., Hecker, J., Leverone, J., Raulerson, G. Sherwood, E. 2018. Widespread recovery of seagrass coverage in Southwest Florida (USA): Temporal and spatial trends and management actions responsible for success. Marine Pollution Bulletin 135, 1128-1137. https://doi.org/10.1016/j.marpolbul.2018.08.049.

Trannum, H.C., Olsgard, F., Skei, J.M., Indrehus, J., Øverås, and Eriksen, J. 2004. Effects of copper, cadmium, and contaminated harbour sediments on recolonization of soft-bottom communities. Journal of Experimental Marine Biology and Ecology 310, 87-114.

Trefry, J.H., Metz, S., Trocine, R.P., Nelsen, T.A. 1985. A Decline in Lead Transport by the Mississippi River. Science 230, 439-441.

Turner, A., Pollock, H., Brown, M.T. 2009. Accumulation of Cu and Zn from antifouling paint particles by the marine macroalga, Ulva lactuca. Environmental Pollution 157, 2314-2319.

Uebelacker, J.M. 1984. Chapter 54. Family Sabellidae Malmgren, 1867, pp. 54-1:54-43 in J.M. Uebelacker and P.G. Johnson eds., Taconomic Guide to the Polychaetes of the Northern Gulf of Mexico. Vol. VII. Final Report to the Mineral Management Service, contract 14-12-001-29091. Barry A. Vittor & Associates, Inc., Mobile, Alabama.

U.S. Census Bureau (2015) http://quickfacts.census.gov/qfd/states/12000.html

U.S. Environmental Protection Agency. 2007. National Estuary Program Coastal Condition Report. http://www.epa.gov/owow/oceans/nepccr/index.html

Van Derveer, W.D. and Canton, S.P , 1997. Selenium Sediment Toxicity Thresholds and Derivation of Water Quality Criteria for Freshwater Biota of Western Streams. Environmental Toxicology and Chemistry 16, 1260-1268.

Van Dolah, R.F, Riekerk, G.H.M., Levisen, M.V., Scott, G.I., Fulton, M.H., Bearden, D., Sivertsen, S., Chung, K.W., and Sanger, D.M. 2005. An evaluation of polycyclic aromatic hydrocarbon (PAH) runoff from highways into estuarine wetlads of South Carolina. Archives of Environmental Contamination and Toxicology. 49, 362-370.

Van Metre, P.C. and Mahler, B.J. 2010. Contribution of PAHs from coal tar pavement sealcoat and other sources to 40 U.S. lakes. Science of the total environment 409, 334-344.

Velzeboer, I., Kwadijk, C.J.A.F., Koelmans, A.A. 2014. Strong sorption of PCBs to nanoplastics, microplastics, carbon nanotubes, and fullerenes. Environmental Science & Technology 48, 4869-4876. dx.doi.org/10.1021/es405721v

Venice Symposium. 1959. Final Resolution: The Venice System for the Classification of Marine Waters According to Salinity. Archivio di Oceanografia e Limnologia 11 (Suppl), 243-248.

Versar, Inc. 1993. Tampa Bay National Estuary Program Benthic Project Field and Laboratory Methods manual. Technical Document prepared for TBNEP March 1993. 32 pp.

Virnstein, R.W. 1977. The importance of predation by crabs and fishes on benthic infauna in Chesapeake Bay. Ecology 58(6), 1199-1217.

Walker, R.L. and Tenore, K.R. 1984. Growth and production of the Dwarf Surf Clam *Mulinia lateralis* (Say 1822) in a Georgia Estuary. Gulf Research Reports 7(4), 357-363.

Wang, W.-X. and Rainbow, P.S. 2000. Dietary uptake of Cd, Cr, and Zn by the barnacle *Balanus trigonus*: influence of diet composition. Marine Ecology Progress Series 204, 159-168.

Wang, X. and Wang, W.-X. 2005. Uptake, absorption efficiency and elimination of DDT in marine phytoplankton, copepods and fish. Environmental Pollution 136(3), 453-464.

Watson, G.J., Pini, J.M., Richir, J. 2018. Chronic exposure to copper and zinc induces DNA damage in the polychaete *Alitta virens* and the implications for future toxicity of coastal sites. Environmental Pollution 243, 1498-1508.

Watts, A.W., Ballestero, T.P., Roseen, R.M., Houle, J.P. 2010. Polycyclic Aromatic Hydrocarbons in Stormwater Runoff from Sealcoated Pavements. Environmental Science & Technology. 44, 8849-8854.

Watzin, M.C. and Roscigno, P.R. 1997. The Effects of Zinc Concentration on the Recruitment and Early Survival of Benthic Invertebrates in an Estuary. Marine Pollution Bulletin 34, 443-455.

Weis, P., Weis, J.S., Lores, E. 1993. Uptake of metals from chromated-copper-arsenate (CCA)-treated lumber by epibiota. Marine Pollution Bulletin 26, 428-430.

Whitmore, T., Riedinger-Whitmore, M., Smoak, J., Kolasa, K., Goddard, E., Bindler, R. 2008. Arsenic contamination of lake sediments in Florida: evidence of herbicide mobility from watershed soils. Journal of Paleolimnology 40, 869-884.

Wilcoxen, S.E., Meier, P.G., Landrum, P.F. 2003. The toxicity of fluoranthene to Hyalella azteca in sediment and water-only exposures under varying light spectra. Ecotoxicology and Environmental Safety 54, 105-117.

Winn, R.N. and Knott, D.M. 1992. An evaluation of the survival of experimental populations exposed to hypoxia in the Savannah River estuary. Marine Ecology Progress Series 88, 161-179.

Wirth, E.F., Lund, S.A., Fulton, M.H., Scott, G.I. 2001. Determination of acute mortality in adults and sublethal embryo responses of *Palaemonetes pugio* to endosulfan and methoprene exposure. Aquatic Toxicology 53, 9-18.

Wirth, E.F., Lund, S.A., Fulton, M.H., Scott, G.I. 2002. Reproductive alterations in adult grass shrimp, *Palaemonetes pugio*, following sublethal, chronic endosulfan exposure. Aquatic Toxicology 59, 93-99.

Witter, A.E., Nguyen, M.H., Baidar, S., Sak, P.B. 2014. Coal tar-based sealcoated pavement: A major PAH source to urban stream sediments. Environmental Pollution 185, 59-68.

Wolf, P.S. 1984. Chapter 12. Family Cirratulidae Carus, 1863. pp 12.1-12.30 in J.M. Uebelacker and P.G. Johnson (eds): Taxonomic Guide to the Polychaetes of the Northern Gulf of Mexico Vol. II. Final Report to the Minerals Management Service, Contract No 14-12-001-29091.

Yang, Y., Metre, P.C.V., Mahler, B.J., Wilson, J.T., Ligouis, B., Razzaque, M.M., Schaeffer, D.J., Werth, C.J. 2010. Influence of Coal tar Sealcoat and Other Carbonaceous Materials on Polycyclic Aromatic Hydrocarbon Loading in an Urban Watershed. Environmental Science & Technology 44, 1217-1223.

Yogui, G.T., de Oliveira Santos, M.C., Montone, R.C. 2003. Chlorinated pesticides and polychlorinated biphenyls in marine tucuxi dolphins (*Sotalia fluviatilis*) from the Cananéia estuary, southeastern Brazil. The Science of the Total Environment 312, 67-78.

You, J., Schuler, L.J., Lydy, M.J. 2004. Acute Toxicity of Sediment-Sorbed Endrin, Methoxychlor, and Endosulfan to Hyalella azteca and Chironomus tentans. Bulletin of Environmental Contamination and Toxicology 73, 457-464.

Zajac, R.N. 2001. Organism-sediment relations at multiple spatial scales: implications for community structure and successional dynamics. pp. 119-139 in J.Y. Aller, S.A. Woodin, and R.C. Aller (eds.) Organism-sediment Interactions. University of South Carolina Press Columbia SC.